Substrate Specificity and Mapping of Residues Critical For Transport in the Yeast Glutathione Transporter, Hgt1p.

A thesis

Submitted for the degree of

Doctor of Philosophy

By

M. Zulkifli

Department of Biological Sciences

Indian Institute of Science Education and Research (IISER)

Mohali- 140306

September 2016

INDIAN INSTITUTE OF SCIENCE EDUCATION AND RESEARCH MOHALI

Sector 81, SAS Nagar, Mohali

PO Manauli, Punjab 140306, India

DECLARATION

The work presented in this thesis entitled "Substrate Specificity and Mapping of Residues Critical for Transport in the Yeast Glutathione Transporter, Hgt1p" has been carried out by me under the supervision of Prof. Anand Kumar Bachhawat at the Department of Biological Sciences, Indian Institute of Science Education and Research (IISER) Mohali.

This work has not been submitted in part or full for a degree, a diploma, or a fellowship to any other university or institute. Whenever contributions of others are involved, every effort is made to indicate this clearly, with due acknowledgment of collaborative research and discussions. This thesis is a bonafide record of original work done by me and all sources listed within have been detailed in the bibliography

(M. Zulkifli)

Date:

Place:

In my capacity as supervisor of the candidate's doctoral thesis work, I certify that above statements by the candidate are true to the best of my knowledge.

(Prof. Anand Kumar Bachhawat)

Department of Biological Sciences

Indian Institute of Science Education and Research Mohali

Dedicated To My Family

TABLE OF CONTENTS

Acknowledgements

"In the name of God, the creator and sustainer of the world who bestowed upon us this wonderful life to learn and to share what we have learned."

Looking back to the journey of my Ph.D., I am surprised and at the same time highly grateful for all that I received and achieved. It certainly shaped me as a student as well as a person and led me where I am now. I feel evolved. I can appreciate the maturity and understand the alphabets of science. It would have never been possible for me to complete my Ph.D. thesis without the support and help of people around me. I would like to take this opportunity to express my deepest gratitude and regards for all of them who have aided me in this journey of mine.

First and foremost I owe my greatest debt and heartfelt gratitude to my Ph.D. supervisor Prof. Anand Kumar Bachhawat who has been the soul behind every effort that I have put forth in this thesis. In spite of my shortcomings, he always continued his support and guidance to me. It was under his tutelage that I developed a focus and became interested in research. His understanding of the subjects, mind boggling logics, and suggestions, extraordinary patience, encouraging words and confidence in me have shaped my personality to a large extent. I admire and respect him for his loving and caring behavior, valuable feedback and amount of freedom he renders to each of his students. His exceptional dedication, guidance, and enthusiasm helped me to expand my knowledge and horizon throughout the journey of my thesis work. He has been a great mentor, always willing to extend help in all spheres of life.

I would like to thank Prof. N. Sathymurthy, Director, IISER Mohali, for giving me the opportunity to work at this premier research institute and to avail the opportunity to use the excellent infrastructure to carry out research work. I am also thankful for the arrangements he made for the travel on the daily basis to go to IMTECH during the initial years of my Ph.D. work. I must also thank Dr. Girish Sahni, former Director, IMTECH, Chandigarh, to allow me to work and use all the core research facilities during the first year of my Ph.D.

I express my immense gratitude to my doctoral committee members, Dr. Sudip Mondal and Dr. Samarjit Bhattacharya for their helpful suggestions and timely review of the progress of my work.

I am thankful to Dr. Monica and Dr. Shashi Bhushan Pandit for giving their precious time and effort for the development of Hgt1p, ab initio model. I am also grateful to Rivi Verma for teaching me the basics of PyMol and helping me understand the model.

I express my immense gratitude to Dr. Shravan Mishra, Dr. Samrat Mukhopadhyay, Dr. Mehak Sharma and Dr. Kausik Chattopadhyay and their lab members for providing me access to their lab facilities and for many fruitful discussions during my Ph.D. work.

I am grateful to Dr. Ram Yadav and Shikha for teaching me how to handle confocal microscope. I would also like to put on record a special word of thanks for Dr. Sudip Mondal, Dr. Lolotika Mondal, and their lab members especially Satish and Saikat for their valuable time and help in taking the confocal images, which formed a crucial part of my study.

I express my gratitude to Prof. P. Guptasarma for his continuous support while lab establishment and after that. His lengthy discussion and advice on several occasion helped me to overcome many barriers.

I would also like to thank Dr. Ganesan and lab members, IMTECH Chandigarh for providing me access to their lab reagents and yeast strains. Special thanks go to Alfatah and Vinay who have been a tremendous support both as a friend and senior on both personal and professional front.

I am highly grateful to Dr. Nandita madam with whom I always enjoyed talking. She always guided me at professional and personal front. Her company was always cherished in lab parties.

Thanks are due to the entire IISER family, administration, library, instrumentation, store and purchase sections, mess staff, canteen staff and hostel caretakers for their cooperation in the smooth running of my mind and Ph.D.

I am extremely grateful to have incredible lab members. Their active interest in my work, useful suggestions, and constructive criticism during lab seminars and in general provided a cordial environment in the lab. Thanks to my wonderful lab seniors Dr. Anil Thakur, Dr. Shailesh Kumar, Dr. Anup Deshpande, Dr. Banani, Dr. Akhilesh Kumar, Dr. Hardeep Kaur, Dr. Amit Yadav and Prashant Desai

for their great help and support in and out of the lab. I received due care and affection from them which helped me to settle down in a new "research" environment. Anil sir, an elder brother, friend and mentor to me was very considerate. He was very helpful, always around and gave me sound training of the different lab techniques. My sincere thanks to Amandeep Kaur Deol, a cooperative lab mate and nice friend. She has been a tremendous support on both personal and professional front. I enjoyed her company and learned some Punjabi and bhangra from her. Special thanks to Shambhu Yadav, with whom I literally started my Ph.D. work. His hard work and dedication always astonished me. We worked together 24×7 to pull the project to the finish line. I am thankful to Avinash, Anuj, and Shambhu for the fantastic night sessions, leg-pulling sessions, and discussion on different topics which were full of fun. I am also indebted to Manisha and Muskan for their help when needed. Muskan was sometimes life saver for me. She always arranged the credit cards for me when I needed the most. I am also thankful to my lovable juniors, Sriharsha, Ankita, Thoi, Krishna, Bindya and Tejaswani for their help and co-operation when needed. Thanks to Vidya who works hard to maintain the lab and arrange things on time. I will always cherish the moments I shared with you all.

I consider myself lucky to have a large friend circle. I am thankful to Aman, Avinash, Anand, Anwar, Ashish, Dominic, Gulia, Karan, Kanika, Prabhat, Shruti, Satish, Swati and Saurav for being wonderful and extending their help whenever needed. Special thanks go to Rivi and Aastha for taking care of me when I was low, for their home made food, fruit sessions, outing, stupid fights, and leg pulling. Deepest thanks to my IMTECH friends, Bhagi Raj, Rehan, Zeeshan, Salman, Faraz and Sajid for their love, support and Saturday parties. I would also like to thank my juniors (no names, as the list is too long, and space is short) for the great time we had. You all directly or indirectly contributed a lot in my personal and professional life.

A prominent acknowledgment goes to the IISER Mohali basketball team members Agastya, Manu, Rohit, Yashpal, Sunil, Rohan, Prashant, Pranshu, and Bhatt. Without you guys stay at IISER would have been lot difficult. I will always remember you guys for your support, occasional outing and after the game massage and fun-filled discussions.

Words are never enough to describe the gratitude one feels towards their family. As always, I fell short of words to describe what I feel for them. They have been my strong pillar of support-understanding and encouraging during all my trials in life. All of my achievements in life till date have been and will always be because of their love, prayers, support, encouragement, sacrifices for me and the values instilled in me. Their immense unwavering faith in me and my abilities, greater than my own, has always driven me to aspire for the pinnacle of success and this thesis is dedicated to them.

I owe my deepest gratitude to my wife Suby for her eternal support and understanding of my goals and aspirations. She has been through the thick and thin of my life. Her love, support, care and encouragement have always been my strength. Without her help, I would not have been able to complete much of what I am. My appreciation for her is endless, and continuing to grow with each passing day. Last but by no means least, I wish to thank all whose names could not be included but are fondly remembered.

M. Zulkifli

List of Publications

1) **Zulkifli M.,** Yadav S., Thakur A., Singla S., Sharma M. and Bachhawat A.K.(2016). Substrate Specificity and Mapping of Residues Critical for Transport in the High Affinity Glutathione Transporter, Hgt1p. *Biochem J.* 10.1042/BCJ20160231
2) Singh K, **Zulkifli M**, Prasad N. Identification and characterization of novel natural pathogen of *Drosophila melanogaster* isolated from wild captured *Drosophila* spp. *Microbes and Infection*, doi:10.1016/j.micinf.2016.07.008
3) Bachhawat A. K., Thakur, A., Kaur, J., and **Zulkifli, M. (2013).** Glutathione transporters. *Biochim.Biophys.Acta (General Subjects)* 1830, 3154–164.
4) **Zulkifli M.** and Bachhawat A.K. Identification of residues involved in pH / proton coupled glutathione translocation in yeast high affinity glutathione transporter, Hgt1p. **(Manuscript under preparation)**

Gene sequences submitted at GenBank:

Singh K, **Zulkifli M** and Prasad NG (2014). Staphylococcus succinus subsp. Succinus strain

PK-1 heat shock protein 60 gene sequence. GenBank: KM516055.

Poster Presentations / Conferences Attended

1) Attended and presented poster at the "Mechanisms of Membrane Transport" seminar and conference organized by Gordon Research Conferences at Bates College, Lewiston, Maine, USA from July 27th to 3rd Aug 2015.

2) Attended and presented a poster at the "20-Years of CDR1, Research" at Hotel Crown Plaza, Rohini, New Delhi, India from December 4th to 8th Jan 2014.

3) Attended and received **best poster award** at the "International Conference on Yeast Biology (ICYB)", CSIR- Institute of Microbial Technology (IMTECH), Chandigarh, India from December 4th to 7th, 2013.

4) Attended Mini-Symposium on " Ubiquitin Systems and Cellular Processes" organized by Dept. of Biological Sciences, IISER Mohali, India from 17^{h} to 18th October 2013.

5) Attended three days' workshop " Advanced Microscopy and Imaging Technique" organized by DSS Imagetech Tech Pvt. Ltd. Olympus (Japan) at IISER Mohali, Mohali, India in May 28^{h} to 30th, 2013.

6) Attended the "International Conference on Yeast Biology (ICYB) Indian Institute of Technology Bombay, Mumbai, India from December 10$^{th\ to}$ 13th, 2011.

ABBREVIATION

WEIGHTS AND MEASURES	
O.D.	Optical density
mol, nmoles, mmoles	micromole, nanomoles, millimoles
RT	Room temperature
bp, kb	Base pair, kilobase
kDa	Kilodalton
°C	Degree centigrade
Psi	Pounds per square inch
%	Percent
sec, min, h	Second, minute, hour
rpm	Revolutions per minute
µM, mM, M	micromolar, millimolar, molar
µg, mg, g	microgram, milligram, gram
µl, ml, L	Microliter, milliliter, liter
µCi, Ci	Microcurie, curie
Symbols	
~	Approximately
=	Equal to
α	Alpha
β	Beta
γ	Gamma
Δ	Delta
CHEMICALS	
Amp	Ampicillin
APS	Ammonium persulfate
ATP	Adenosine Triphosphate
BSA	Bovine Serum Albumin
CCCP	Carbonyl cyanide *3*-chlorophenylhydrazone
dNTPs	2'-deoxyadenosine 5'-triphosphate
EDTA	Ethylenediamine-tetra-acetic acid
GSH	Reduced glutathione
GS-NEM	S-(N-Ethylsuccinimido)glutathione
GSSG	Oxidized glutathione
HEPES	N-[2-Hydroxyethyl] piperazine-N'-[2ethanesulfonic acid]
PEG	Poly Ethylene Glycol
PMSF	Phenylmethylsulfonyl fluoride
SDS	Sodium Dodecyl Sulphate
TEMED	N, N, N', N'-tetramethylethylenediamine
Tris	Tris (hydroxymethyl) amino methane
β-ME	β-Metcaptoethanol
AMINO ACIDS	
Asn (N)	Asparagine
Arg (R)	Arginine
Asp (D)	Aspartic acid
Cys (C)	Cysteine

Gln (Q)	Glutamine
Glu (E)	Glutamate
Gly (G)	Glycine
His (H)	Histidine
Ile (I)	Isoleucine
Leu (L)	Leucine
Lys (K)	Lysine
Met (M)	Methionine
Phe (F)	Phenylalanine
Pro (P)	Proline
Ser (S)	Serine
Thr (T)	Threonine
Trp (W)	Tryptophan
Tyr (Y)	Tyrosine
Val (V)	Valine
Miscellaneous	
NCBI	National Center for Biotechnology Information
BLAST	Basic Local Alignment Search Tool
PSI-BLAST	Position-Specific Iterated BLAST
ORF	Open Reading Frame
ER	Endoplasmic Reticulum
GFP	Green Fluorescent Protein
HA	Hemagglutinin
HRP	Horseradish peroxidase
LB	Luria Bertani
MFS	Major Facilitator Superfamily
MRPs	Multidrug Resistance associated Proteins
ABC	ATP Binding Cassette
SCAM	Substituted Cysteine Accessibility Method
TMD	Transmembrane domain
S.E.	Standard error

SYNOPSIS

Introduction and Background

Glutathione (GSH) or L-γ-glutamyl-L-cysteinyl-glycine is a low molecular weight non-protein thiol compound present in almost all eukaryotes barring a few amitochondrial protozoans (Fahey and Sundquist, 1991; Meister and Anderson, 1983). Intracellular glutathione concentrations typically range between 1-10 mM. Glutathione acts as the major redox buffer inside the cell. It is involved in the biosynthesis of iron–sulphur proteins and in the detoxification of heavy metals and xenobiotics, and is important in apoptosis, redox signaling, and sulphur storage. Glutathione is essential for normal growth in eukaryotes. Disruption of glutathione biosynthesis leads to embryonic lethality in plants and mice, and glutathione auxotrophy in yeast. Altered glutathione levels have been associated with diseases and different pathologies. Thus, maintenance of glutathione homeostasis is very important both in terms of its concentration and in the ratio of the reduced form (GSH) to the oxidized form (GSSG). The concentrations and the ratios are regulated by various processes such as biosynthesis, degradation, distribution, consumption in different reactions and influx or efflux mediated by transporters.

Hgt1p (Opt1p) of *Saccharomyces cerevisiae* was the first reported high-affinity glutathione transporter in any organism (Bourbouloux et al., 2000). It belongs to the oligopeptide transporter family with homologs restricted to bacteria, fungi and plants (Gomolplitinant and Saier Jr, 2011; Yen et al., 2001). Hgt1p is present on the plasma membrane and is required for the uptake of GSH from the extracellular medium. Hgt1p, a protein of 799 amino acids, is currently predicted to have 12 transmembrane domains (TMDs) although some prediction tools have suggested 13 or 14 TMDs (Wiles et al., 2006). Transport of GSH by Hgt1p is both electrogenic and proton-dependent (Osawa et al., 2006). The expression of HGT1 gene is under strong sulphur regulation (Miyake et al., 1998; Srikanth et al., 2005) and its constitutive overexpression leads to glutathione dependent toxicity (Kumar et al., 2011; Srikanth et al., 2005). Kinetic analysis of this transporter has demonstrated it to be a high affinity glutathione transporter. Significant inhibition of radioactive glutathione uptake was observed with oxidized glutathione (GSSG), and glutathione conjugate (GS-NEM) (Bourbouloux et al., 2000). Hgt1p was initially also described as an oligopeptide transporter (Opt1p), owing to its ability to transport tetra/pentapeptides and Leu-enkephalin (Hauser et al., 2000). Subsequent studies using two-electrode voltage clamp experiments in *Xenopus laevis* oocytes revealed that Hgt1p produces inward currents in oocytes in response to GSH, GSSG, the glutathione derivative

phytochelatin (PC) and the tetrapeptide GGFL, but not KLGL (Osawa et al., 2006). This suggested a preference for glutathione and glutathione-derived peptides. It is interesting that with the exception of Hgt1p, all reported eukaryotic GSH transporters are shown to transport GSH-conjugates with higher affinity rather than reduced glutathione. Detailed kinetic studies with other glutathione conjugates have not been undertaken with Hgt1p.

Hgt1p has been the subject of several structure-function studies. Alanine scanning mutagenesis of polar and charged residues in the putative transmembrane domains of Hgt1p revealed the transmembrane domains, TMD1 (Asn124), TMD4 (Gln222) and TMD9 (Gln526) important for glutathione transport (Kaur and Bachhawat, 2009). Based on these results a subsequent alanine scanning of TMD9 revealed that in addition to earlier identified Gln526, the residue Phe523 played a critical role in substrate recognition (Thakur and Bachhawat, 2010). Absence of any structural data on Hgt1p, or any member of the OPT family limits our understanding of the mechanism of transport by this relatively uncharacterized OPT family. With the goal to carry out a detailed and more thorough investigation by targeting all the predicted TMDs of the Hgt1 protein, a subsequent study targeted the TMDs 1, 5, 7, 8, 11 for alanine scanning mutagenesis. However the mutants were not analyzed in detail (Shambhu Yadav, MS thesis, IISER Mohali).In the current thesis, I have attempted to consolidate and extend these studies. In addition to focusing on substrate binding sites, I have also tried to examine the proton binding sites.

With this background, the objectives of the current thesis have been framed as follows:

1. Determination of the substrate specificity of Hgt1p towards different glutathione conjugates and glutathione analogs.
2. Alanine scanning mutagenesis of TMD2, TMD3, TMD4, TMD6, TMD10, TMD12 and TMD13 of Hgt1p and evaluation of all the 269 TMD mutants for their role in glutathione transport.
3. Identification of residues involved in proton binding and transport by Hgt1p.

Results and Conclusions

Determination of the substrate specificity of Hgt1p towards different glutathione conjugates and glutathione analogs:

Since a quantitative comparison of reduced glutathione and glutathione-conjugate transport by Hgt1p was never undertaken, we have revisited the substrate specificity of Hgt1p. Comparative inhibition studies using [^{35}S]-GSH uptake by Hgt1p revealed significant inhibition of glutathione uptake by GSH (85%), S-decyl-GSH (87%), S-hexyl-GSH (86%) and S-methyl-GSH (83%). Slightly lower levels of inhibition were observed

with S-lactoyl-GSH (76%) and GSSG (72%), but very little inhibition was observed in the case of glutathione sulphonate (<5%) suggesting that although Hgt1p can possibly transport a wide variety of GSH conjugates, not all GSH-conjugates are recognized. The apparent *Km* of WT Hgt1p for glutathione was estimated to be 27.8 ± 1.2 µM and the *Vmax* was found to be 54.0 ± 0.8 nmol of glutathione.mg of protein^{-1}.min^{-1}. The *Km* determination of the other compounds, however, was not possible owing to the lack of availability of these radio-labelled conjugates. We, therefore, determined the *Ki* of a few selected inhibitors showing significant inhibition. Our results indicated that these ligands were competitive inhibitors as the *Vmax* remained constant but the effective *Km* increased with increasing inhibitor concentrations. The *Ki* of GSH was also determined for comparisons and was found to be 24.2 ± 6.5µM. The *Ki* for GSSG (92.5 ± 9.8 µM) was significantly higher than GSH suggesting a significantly lower affinity of Hgt1p for GSSG as compared to GSH. The *Ki* for S-hexyl-GSH (34.2 ± 8.0 µM) was found to be close to that of reduced glutathione followed by S-lactoyl-GSH (51.2 ± 3.3 µM) and S-methyl-GSH (65.4 ± 4.2 µM). These results suggest that Hgt1p preferentially binds GSH but also binds to a broad range of GSH derivatives, apparently preferring those with a hydrophobic group linked to the sulfhydryl group of glutathione. We also examined the importance of each amino acid of the tripeptide glutathione, governing recognition and transport by Hgt1p using custom synthesized analogs and could demonstrate the critical requirement for the γ-glutamyl and cysteine residues for recognition by Hgt1p.

Re-evaluation of topology of Hgt1p.

In the current study, one of the goals was to comprehensively map the residues that are important for substrate binding and translocation. For this, a reasonably reliable topology model is a pre-requisite before targeting the residues in the transmembrane domains (TMDs). Although the currently accepted topology is a 12 TMD protein (Kaur and Bachhawat, 2009), various predictions have indicated 13 and 14 TMDs as well (Wiles et al., 2006). To resolve this issue, we re-evaluated the topology using different softwares in a consensus approach. Our analysis suggested a topological model consisting of 13 TMDs with the N-terminus outside and C-terminus inside. The new predicted TMD appears after the 11th TMD; thus the nomenclature of the first 11 TMDs remains unchanged with previous studies. To experimentally validate this topology we used an HGT1 construct with a hexahistidine epitope at the N-terminus and an HA-tag at the C-terminus. The localization of N- and C-terminus was verified by indirect immunofluorescence using peptide directed antibodies against these epitopes in permeabilized and non-permeabilized spheroplasts.

The His-tag was detected in both permeabilized and non-permeabilized spheroplasts suggesting extracellular localization. However, the HA-tag was not detected in non-permeabilized spheroplasts but was detected in permeabilized spheroplasts confirming its intracellular localization. This demonstrates that the N- and C–termini are oriented at opposite sides of the membrane as predicted by computational methods, hence strengthening the currently predicted topology model.

Alanine scanning mutagenesis of TMD2, TMD3, TMD4, TMD6, TMD10, TMD12 and TMD13 of Hgt1p and evaluation of all the 269 TMD mutants for their role in glutathione transport.

In this chapter efforts are described to comprehensively map the residues in the transmembrane domains for their involvement in glutathione binding and translocation through alanine scanning mutagenesis. As TMD1, TMD5, TMD7, TMD8, TMD9, and TMD11 were previously subjected to alanine scanning mutagenesis, in the current study TMD2, TMD3, TMD4, TMD6, TMD10, TMD12 and TMD13 were targeted for mutagenesis, thus completing the set of 13 TMDs to be studied. A total of 269 amino acid residues comprising 13 predicted TMDs were included in the functional study. After eliminating mutants defective in either protein sorting or expression, the TMDs and the residues that were identified were TMD1 (N124), TMD3 (V185, L187, Y193, I197), TMD4 (Q222, G225, Y226), TMD5 (P292), TMD6 (L373, Y374), TMD7 (L429), and TMD9 (F523, Q526). To further characterize these mutants we carried out a detailed kinetic characterization of each of the severely defective mutants to determine the *Km* and *Vmax*. This kinetic characterization of the new mutants revealed interesting insights into the role of these residues in the functional activity of the transporter. Y226A showed the highest increase (~ ten-fold higher compared to WT) in *Km* followed by P292A (~ seven-fold higher), L429A (~ four-fold higher), V185A and G225A (~ three-fold higher). This significant decrease in the glutathione affinity of V185A, G225A, Y226A, P292A and L429A suggest that these residues play a critical role in interacting with the substrate. Kinetic analysis of Y374A revealed that although this mutant showed a drastic loss in transport efficiency, it also displayed about a two-fold increase in *Km*, placing it as a residue also possibly involved in substrate binding and translocation.

The kinetic analysis of P704A and P705A revealed a drastic loss (sixteen and eight-fold decrease) in the catalytic activity without affecting the *Km*. The significant decrease in *V*max values obtained for the mutants V185A, L429A, P704A and P705A which could not be attributed to the decreased protein levels or mislocalization of the mutant proteins,

suggest that these residues might play some important role in the conformation changes in Hgt1p during translocation of the substrate. However, the mutants L187A, Y193A, I197A and L373A which expressed well and localized properly on the plasma membrane showed very little uptake thus making it difficult to obtain reliable kinetic parameters. Nevertheless, these mutants clearly have a role in glutathione transport and are also strong candidates for being involved in substrate binding, although the precise role has not been determined. An *ab initio* based computational approach was further developed to derive a structural model for Hgt1p. This model building was facilitated by the detailed, comprehensive map of residues likely to form the substrate channel. Thus, this study which investigates the role of every residue in all the predicted TMDs provides new insights in substrate transport by this high affinity glutathione transporter.

Identification of residues involved in proton binding and transport by Hgt1p:

Transport mediated by Hgt1p is proton-dependent, and the identification of residues involved in proton transport becomes critical if we wish to understand the mechanism of active transport by Hgt1p. A pH profiling of the Hgt1p transporter revealed that transport is optimal at pH 5.5 and falls drastically with increasing pH. We have used this property (of low or no transport at high pH) as an initial strategy towards identifying the residues involved in proton binding and transport in Hgt1p. In this strategy, mutants that allowed growth at higher pH were identified. The logical basis for isolating such mutants has been that those residues which upon mutation can lead to growth at high pH, would be likely to play a role in proton binding/proton transport. In the absence of any structural data for the entire OPT family, we carried out an exhaustive analysis to screen all the 269 mutants (alanine mutants of all TMDs) showing pH independent growth based on a pH based plate assay. A genetic selection by random mutagenesis was also carried out. Evaluation of all alanine mutants of the 13 predicted TMDs in combination with *in vitro* random mutagenesis identified E135 and N710 to be important for pH dependent transport. Biochemical and kinetic characterization of these mutants by radioactive substrate studies also showed increased uptake at higher pH as compared to the WT Hgt1p, but the transport was not completely pH independent. To examine if these mutants were capable of transporting protons, we used yeast cells expressing pHluorin (a fluorescent ratiometric probe for pH measurement *in vivo*) (Maresova et al., 2010) in the cytosol to check cellular acidification in response to GSH transport by these mutants and found that substrate transport by E135 and N710 mutants did not abrogate cellular acidification, although they showed pH independent growth phenotype and more transport at higher pH.

To follow up these studies further (based on previous knowledge of proton-coupled transporters), we targeted 31 amino acid residues (Asp, Glu, His, Arg, Lys, or Tyr) for mutagenesis depending on their conservation pattern and their location in the predicted topology model. Alanine mutants of these residues were subjected to plate based assay and after eliminating mutants defective in protein expression or their sorting to cell surface we identified residues specifically defective in GSH transport. Measurement of cellular acidification *in vivo* using pHluorin identified D335A, Y374A, H445A and R554 as specifically defective in proton transport as no cytoplasmic acidification was observed in response to GSH transport even at high substrate concentration (1mM) or increased time intervals (1 hour) as compared to mutants showing similar or low levels of transport. This suggested an uncoupling of substrate-proton transport in these mutants. Further kinetic characterization of these mutants revealed that the residues D335A, Y374A and H445A showed no significant increase in *Km* compared to WT Hgt1p but were severely compromised in their translocation rate. A possible explanation for these results is that the mutant transporters are protonated so that the substrate can bind with high affinity and hence these residues are not involved in direct protonation but are probably required for its release. In contrast, R554A showed a drastic increase in the *Km* with a two-fold decrease in the *Vmax* and are present in the long interconnecting loop. Being most likely outside the substrate channel, the positively charged Arg may not be directly involved in binding of protons. The study has thus enabled us to identify several different residues that are likely to be involved in different stages of the proton binding and translocation by Hgt1p

Overall these studies have yielded new insights on this proton-coupled high affinity glutathione transporter, Hgt1p.

CHAPTER 1:

Review Of Literature

1.1. INTRODUCTION

Glutathione (GSH) or L-γ-glutamyl-L-cysteinyl-glycine is a low molecular weight non-protein thiol compound present in many bacteria and almost all the eukaryotes except for a few amitochondrial parasitic protozoans (Fahey and Sanduist, 1991). Intracellular glutathione concentrations typically range between 1-10 mM and exist as thiol reduced (GSH) and disulphide oxidized (GSSG) forms. It is synthesized from its constituent amino acids- glutamate, cysteine and glycine, by a two-step pathway, which is found to be similar in all the glutathione producing organisms examined so far (reviewed in (Griffith & Mulcahy 1999; Noctor *et al.* 2002). The presence of the unusual γ-glutamyl bond between the Glu and Cys residues prevents its proteolytic degradation by general peptidases (Meister and Anderson, 1983). In addition the sulphydryl group of the cysteine residue allows glutathione to participate in several redox dependent reactions inside the cell depending on the cellular conditions. The sulphydryl group of glutathione serves as an electron donor empowering glutathione with its reducing properties. The high intracellular concentration, presence of a reactive thiol group and the ability of this reduced form of glutathione to be in equilibrium with its oxidized form makes glutathione the predominant redox buffer inside the cell.

When the cell encounters a stress from outside, glutathione biosynthesis is upregulated and the elevated levels of glutathione combats the stress either by direct reaction (ROS), conjugation (xenobiotics) or sequestration (heavy metals) (Stephen & Jamieson 1996; Xiang & Oliver 1998; Cummins *et al.* 2011; Mohsenzadeh *et al.* 2011). In addition, glutathione protects the cell from exposures to ionizing radiations (Jaruga *et al.* 1995; Prasad 2014), osmotic stress and heat shock (Krems *et al.* 1995; Sugiyama *et al.* 2000; Wang *et al.* 2015). It also acts as a cofactor for some enzymes (Meister & Anderson 1983). GSH is also required for iron-sulphur metabolism, protein and DNA biosynthesis (Arrigo 1999; Mühlenhoff *et al.* 2003; Circu & Yee Aw 2008). In addition to these functions, GSH also acts as a sulphur or nitrogen storage compound inside the cell (Elskens *et al.* 1991). Glutathione deficiency and/or alteration in the redox ratio changes the oxidizing state of the cell and induces apoptosis (Circu & Yee Aw 2008). A disturbance in glutathione homeostasis has been associated with aging and is implicated in the etiology and progression of many diseases including cancer, cardiovascular, neurodegenerative, inflammatory and

immune diseases, cystic fibrosis, liver diseases, diabetes, sickle cell anemia, heart attack and AIDS (Wu *et al.* 2004; Franco *et al.* 2008). GSH also participates in the regulation of various cellular processes such as glutathione mediated signaling through glutathionylation of the target proteins (Arrigo 1999; Fratelli *et al.* 2005; Shackelford *et al.* 2005; Michelet *et al.* 2006; Rouhier *et al.* 2008).

Glutathione is essential for growth in eukaryotes. Disruption of glutathione biosynthesis in the yeasts *Saccharomyces cerevisiae, Schizosaccharomyces pombe* and *Candida albicans* leads to glutathione auxotrophy phenotype and growth arrest in the absence of glutathione (Wu & Moye-Rowley 1994; Grant *et al.* 1996; Chaudhuri *et al.* 1997; Baek *et al.* 2004). Disruption of glutathione biosynthesis in plants and mice leads to embryonic lethality (Dalton *et al.* 2000; Shi *et al.* 2000; Cairns *et al.* 2006). However in contrast to eukaryotes, growth in *Escherichia coli* mutants defective in glutathione biosynthesis were unaffected but these mutants were more susceptible to oxidative stress, certain chemicals and osmotic stress (Smirnova *et al.* 2001). Further, in *Listeria monocytogenes*, a pathogenic bacteria, a defect in glutathione biosynthesis affected its virulence in macrophage like cell lines and also led to impaired growth and high susceptibility to oxidative stress under culture conditions (Gopal *et al.* 2005).

Thus, maintenance of glutathione homeostasis is very important and this depends on its concentration and ratio of reduced (GSH) to oxidized (GSSG) forms. The levels and GSH/GSSG ratio is regulated by various processes such as biosynthesis, degradation, spatio-temporal distribution, consumption in different reactions and influx or efflux mediated by different transporters.

1.2. COMPARTMENTALIZATION OF GLUTATHIONE:

Glutathione biosynthesis is carried out by the sequential action of two ATP dependent enzymes. Although the bulk of glutathione is retained in the cytoplasm, it is also found in other compartments of the cell, such as, the mitochondria, nucleus, endoplasmic reticulum (ER), vacuole, chloroplast (in plants) and the extracellular milieu. Each organelle differs in the absolute concentrations of glutathione and redox ratios (*i.e.* GSH: GSSG). This compartmentalization of glutathione within different organelles creates distinct redox environments, which shows dynamic spatial and temporal variations depending on cells physiological conditions or in stress (Noctor *et*

al. 2002; Meyer & Hell 2005; Circu & Yee Aw 2008). The use of different methodology, techniques and cell types to estimate the levels of GSH and its redox ratio have led to conclusions that are contradictory. Until recently majority of the reports were based on cell fractionation techniques which are reliable only for mitochondrial studies, however their usefulness in nuclear and ER GSH estimation is controversial (Pollardo et al., 2009). In addition, these indirect procedures may affect the results and may not very well reflect the *in vivo* conditions.

The introduction of redox sensitive GFP (roGFP) based probes have been instrumental in determination of redox status in compartment specific manner. roGFPs have a cysteine pair in the vicinity of the fluorophore which can undergo reversible oxidation/reduction in a redox dependent manner and influence the spectral properties of GFP (Østergaard *et al.* 2001; Østergaard *et al.* 2004). The roGFP have been genetically modified and targeted to different compartments of the cells allowing the estimation of the redox status of specific organelles (Björnberg *et al.* 2006). In addition, these sensors in combination with confocal microscopy and fluorometery, have been optimized to measure real time redox potential in live cells in a non-destructive manner. However, these conventional redox-sensitive GFPs (roGFP1 and roGFP2) were limited by undefined specificity and a slow response to dynamic changes in redox potential. In addition these sensors have midpoint potentials between −280 to −290 mV rendering them almost fully reduced in the cytosol, mitochondria, plastids, and peroxisomes and fully oxidized in the ER (Meyer & Dick 2010). To overcome these lacunae, these biosensors were equipped with an enzyme, glutaredoxin-1 (Grx1) to specifically catalyze the equilibration between the GSH: GSSG redox couple allowing a direct measurement of glutathione redox potential (E_{GSH}). Grx1-roGFP2 sensor can detect nanomolar to millimolar changes in GSSG or GSH on a scale of seconds to minutes (Gutscher *et al.* 2008; Aller *et al.* 2015).

The cytoplasm being the primary site of glutathione biosynthesis, comprises the largest reservoir of glutathione (80% of the total glutathione) and its concentrations have been estimated to be in the range of 5-14 mM. In addition, the glutathione redox potential (E_{GSH}) in cultured human cell line was estimated to be in the range of -320 to -240 mV (Gutscher *et al.* 2008).Whole-cell measurements which were believed to represent the cytosolic glutathione pool indicated the redox ratios to be in the range of 30:1 to 100:1 depending upon the cell's physiological status. However by using

genetically encoded sensors, the cytosolic GSH:GSSG ratio was found to be much higher and was estimated to be in the order of 10,000:1 in the yeast cytosol (Winther & Jakob 2013).

This high GSH:GSSG ratio in the cytosol appeared to be controversial because of the lack of a satisfactory explanation for where the missing GSSG could be. The glutathione-conjugate transporters of the vacuole, YCF1 and BPT1 that preferentially transport glutathione-conjugates seems a possible saver of oxidized glutathione (Chaudhuri *et al.* 1997; Sharma *et al.* 2002). Recently Morgan and coworkers have demonstrated that the yeast cells actively sequester oxidized glutathione in its vacuole, using Ycf1p transporter hence maintaining a highly reducing environment in the cytosol even under extreme conditions of oxidative stress (Morgan *et al.* 2013; Winther & Jakob 2013). In addition vacuoles are considered as store house in plants and yeast cells which can store glutathione that can serve as source of amino acids, nitrogen or carbon under starvation conditions (Mehdi & Penninckx 1997). Further they are also involved in detoxification of cytosol from toxic metabolites and heavy metals as glutathione conjugates (Rebbeor *et al.* 1998a; Rebbeor *et al.* 1998b).

The mitochondria lacks the glutathione biosynthesis machinery and its glutathione pool is derived from the cytosol (Griffith & Meister 1985). Mitochondria are a major source of reactive oxygen species (ROS), thus high glutathione levels are maintained within this organelle. Mitochondria has been suggested to possess a discrete glutathione pool as compared to the cytosol in a sense of being more reducing than the cytosol. The redox potential of the mitochondrial matrix in mammalian cells has been estimated to be -360 mV (Circu & Yee Aw 2008). Mitochondrial glutathione levels represents a minor fraction (10-15%) of the total GSH pool. However taking into account the volume of the mitochondrial matrix, glutathione concentrations were found to be similar to that of cytosol (10-14mM) (Marí *et al.* 2013).

The chloroplast is also involved in electron transfer reactions and oxidative metabolism and has been estimated to have glutathione concentrations ranging from 1 to 4.5 mM (Wachter *et al.* 2005). Recently chloroplast glutathione levels were estimated to be 1.4 mM using immunogold labelling of glutathione followed by direct and simultaneous determination of reduced and oxidized glutathione by liquid chromatography-electrospray and mass spectrometry (Koffler *et al.* 2013).

Chloroplast also have glutathione biosynthesis ability but there is a significant compartmentalization of glutathione biosynthesis between chloroplast and cytosol and regulation of this is not very clear (Noctor *et al.* 2002). Differences in glutathione concentrations between chloroplast and cytosol have been implicated in redox signaling and regulation of different enzymes by glutathionlyation in response to light and dark cycles in chloroplast (Noctor *et al.* 2002; Meyer & Hell 2005).

In contrast to the cytosol and other compartments, the ER is relatively more oxidizing as this is important for the formation and maintenance of native disulphide bonds during protein folding where GSH provides reducing equivalents to prevent hyper oxidation of the ER during this process (Jessop & Bulleid 2004; Lohman & Remington 2008). E_{GSH} in the ER of HeLa cell was found to be less reducing (−208 mV at pH 7.0) than the cytosol (-320mV) (Birk *et al.* 2013) and the GSH:GSSG ratio in the ER of intact cell was found to be less than 7:1 (Montero *et al.* 2013). Surprisingly the total concentration of glutathione (GSH + GSSG) in the ER was found to be higher (>15mM) than that of cytosol suggesting that a relatively high total GSH concentration constitutes a general characteristic of ER physiology which is an adjustable and homeostatic parameter (Montero *et al.* 2013).

In contrast to other organelles, nuclear glutathione is more controversial and the existence of a separate and distinct pool of glutathione in the nucleus is disputed. GSH level in the nucleus is very dynamic in nature and tends to fluctuate with the different phases of the cell cycle (Söderdahl *et al.* 2003; Green *et al.* 2006; Markovic *et al.* 2010). In mammalian cells, glutathione is recruited in the nucleus during early proliferation cycle (G1 and S phase), suggesting that the process of DNA replication is protected from oxidative damage (Markovic *et al.* 2007; Vivancos *et al.* 2010). However the mechanism of GSH transport and sequestration in the nucleus is yet unknown.

1.3. GLUTATHIONE TRANSPORTERS:

The existence of glutathione transporters has been known for many years and play a major role in cellular glutathione homeostasis. Many glutathione transporters from bacteria to humans have been reported. These transporters belong to varied families having different substrate specificities transporting glutathione or its conjugates as one of the substrates (reviewed in Bachhawat *et al*. 2013). Schematic representation

of the different transporters implicated in GSH transport in a yeast and mammalian cell have been summarized in Fig 1.1A and 1.1B. The first transporters identified to be capable of transporting glutathione was the multidrug resistance associated proteins (MRPs) belonging to the ABC superfamily. These were involved in efflux of glutathione at the plasma membrane in mammalian cells and at the vacuolar membrane of *S. cerevisiae*. These MRPs displayed a broad substrate specificity and showed higher affinity for glutathione conjugates (*Km* in µM range) rather than reduced glutathione (*Km* in mM range). Thus, these appeared to be primarily glutathione-conjugate efflux pumps that were also able to efflux reduced glutathione with low affinity. In contrast to MRPs the yeast Hgt1p/ Opt1p was discovered as a high-affinity glutathione transporter belonging to the oligopeptide transporter family as it displayed a low *Km* (54 µM) for reduced glutathione (Bourbouloux *et al.* 2000). The discovery of this transporter has paved the way for the discovery of many other glutathione transporters (Bachhawat *et al.* 2013).

The majority of the glutathione transporters ranging from bacteria to human belong to the ATP binding cassette (ABC) superfamily followed by the oligopeptide transporter (OPT) family. A few glutathione transporters belong to the major facilitator (MFS) superfamily, solute carrier (SLC) family and mitochondrial carrier family.

Here, I review the different glutathione transporter and what is currently known in terms of mechanism of transport. As the yeast high affinity glutathione transporter Hgt1p has been investigated in this thesis, the oligopeptide transporter family of which Hgt1p is a member will be reviewed first followed by the review of other glutathione transporters belonging to other different families.

1.3.1. Glutathione Transporters in the Oligopeptide Transporter Family (Table 1.1):

The "**O**ligo**p**eptide **t**ransporter" (OPT) family includes members that transport a variety of different peptides, metal chelates, metal siderophores or glutathione and are thought to contribute in many biological functions (Lubkowitz *et al.* 1997). The acronym OPT is sometimes confusing as it is also used to represent the members of the peptide transporter (PTR) superfamily also known as the Proton coupled oligopeptide transporter (POT) family . After the initial identification of fungal OPT

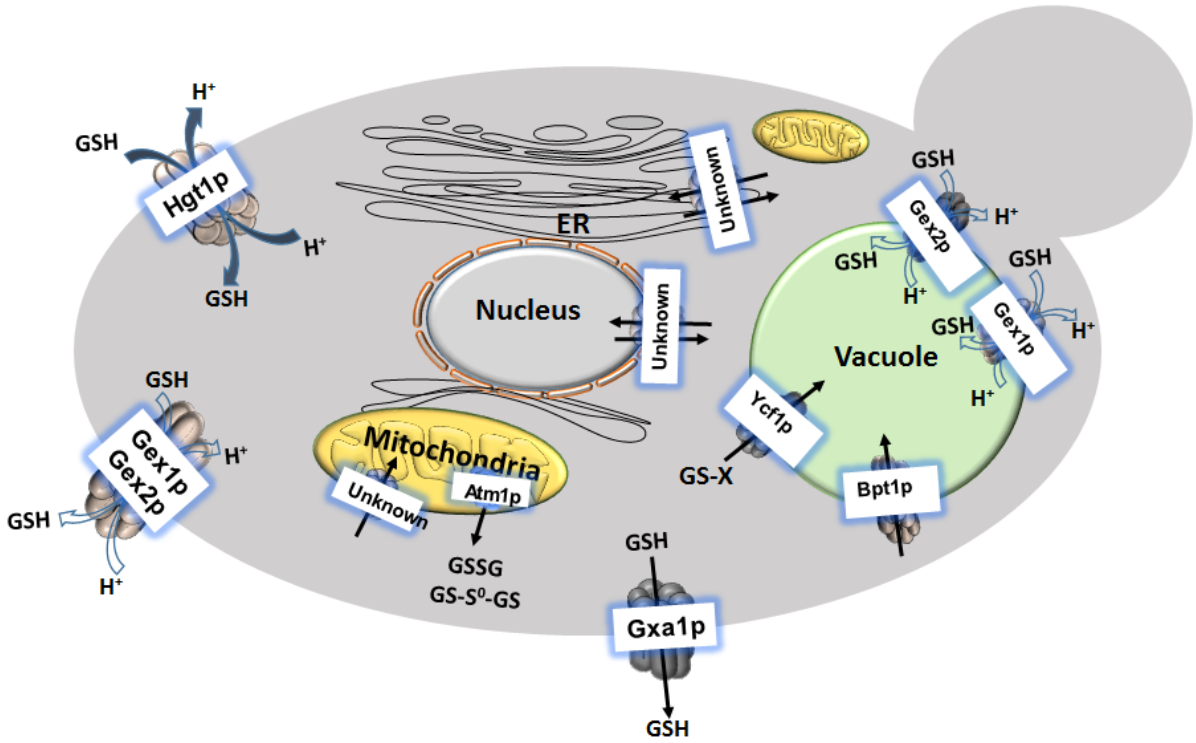

Fig 1.1A Schematic representation of the known GSH transporters in the budding yeast (*S. cerevisiae*): High affinity glutathione transporter (Hgt1p) mediates the uptake of glutathione (or oxidized glutathione and its conjugates) from the extracellular medium into the cytosol. The MRP family members (Ycf1p and Bpt1p) and ABC family members (Gex1p and Gex2p) mediate uptake of glutathione and its various forms into the vacuoles. Atm1p export GS-sulphides from mitochondrial matrix to the cytosol. Gex1p, Gex2p and Gxa1p are involved in efflux of GSH from plasma membrane. The yeast mitochondrial, nucleus and endoplasmic reticulum glutathione transporters are not yet identified.

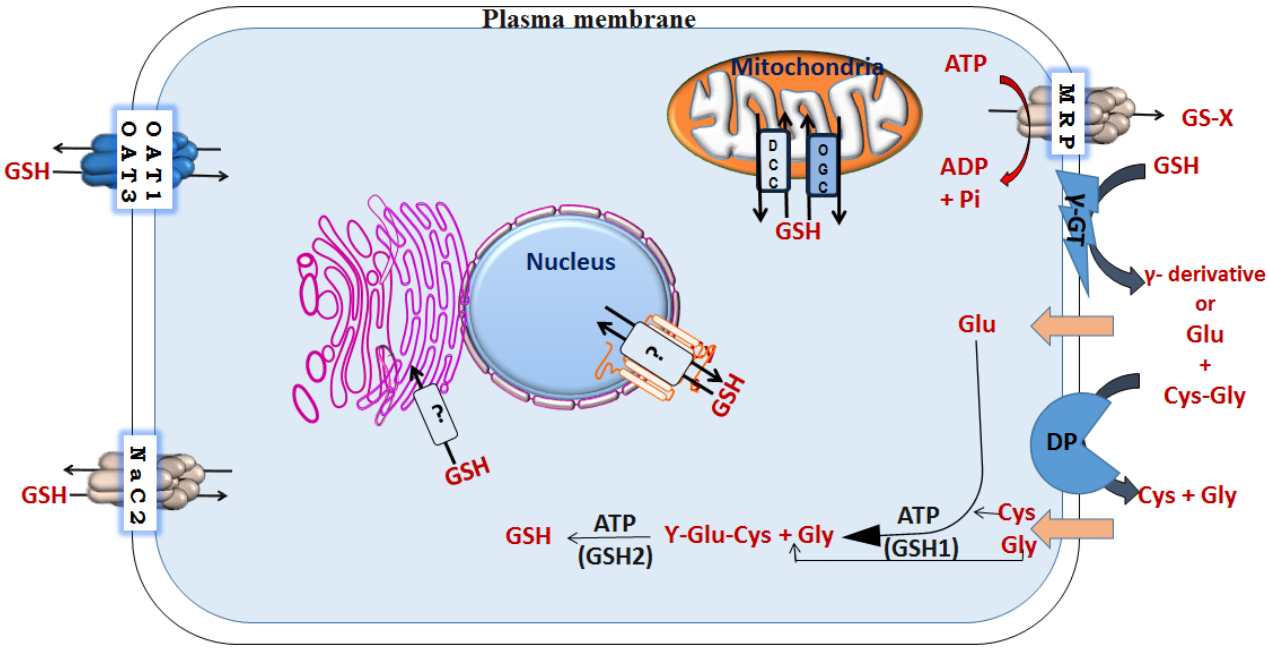

Fig 1.1B. Schematic representation of the different GSH transport mechanism in a mammalian cell. Glutathione uptake in a cell can be mediated by 1) the membrane anchored γ-glutamyl transpeptidase (γ- GT) and a dipeptidase (DP) catalyze degradation of extracellular glutathione into constituent amino acids, which are taken up by the cell, followed by *de novo* synthesis of glutathione by the action of GSH1 and GSH2 enzymes; 2) by direct uptake of the intact glutathione molecule *via* organic anion transport (OAT) systems such as sodium independent organic anion transporters 1 and 3 (OAT1/3) and sodium–dicarboxylate transporter 2 (SDCT-2). 3) Glutathione efflux is mediated by ATP pumps –MRP family members (MRP) and members of organic anion transporting polypeptide family (OATP), which catalyze exchange of GSH for an organic anion (OA^-). 4) Glutathione transport across the inner mitochondria membrane is mediated by the anion carrier members – Dicarboxylate carrier (DCC), which catalyzes exchange of glutathione molecule for an inorganic phosphate and 2-oxoglutarate carrier (OGC), which drives glutathione uptake using 2-deoxyglutatrate gradient across the membrane.

Table 1.1 List of glutathione transporters of OPT family

Transporter	Organism	Known substrates
Yeast		
Hgt1p/Opt1p	*S. cerevisiae*	GSH *Km* = 54 µM GSSG *Km* = 91 µM GS-Conjugates ✓ PC *Km* = 35 µM Oligopeptides ✓ GGFL *Km* = 211 µM ✓ Leu-Enk *Km* = 310 µM
Opt2p	*S. cerevisiae*	GSSG Oligopeptides
Pgt1p	*S. pombe*	GSH *Km* = 62.3 µM
Sj-Hgt1p	*S. japonicus*	GSH *Km* = 204.1 µM
Kl-Hgt1p	*K. lactis*	GSH *Km* = 64.3 µM
Pg-Hgt1p	*P. guilliermondii*	GSH
Cn-Hgt1p	*C. neoformans*	GSH *Km* = 82.5 µM
Ca-Opt7p	*C. albicans*	GSH *Km* = 204 µM
Plants		
At-Opt4p	*A. thaliana*	GSH *Km* = 1.4 mM
At-Opt6p	*A. thaliana*	GSH *Km* = 566 µM GSSG *Km* = 91 µM KLLG *Km* = 10.1 µM AtCLE *Km* = 91 µM
BjGt1p	*B. juneja*	GSH
OsGt1p	*O. sativa*	GSH *Km* = 400 µM, 23mM GS-Conjugates Oligopeptides
ZmGT1	*Z. mays*	GSH, GS-NEM

homologues, a more extensive sequence comparison using the existing database of sequences led to the finding that members of the OPT family belong to a plethora of organisms, ranging from archaea and bacteria to plants and fungi, however no apparent homologue was found in higher animals (Yen *et al.* 2001; Gomolplitinant & Saier Jr 2011).

Functional characterization of only few selected members of the OPT family have been done so far, however these studies have paved the way to understand the relationship between the different clusters and functions of the different homologues within the clusters. By imposing functional information on the phylogenetic tree of the OPT family, two distinct clades can be defined within the OPT family- a) peptide transport (PT) clade, that mediate uptake of oligopeptides, glutathione and metal chelates (Koh *et al.* 2002; Bogs *et al.* 2003; Vasconcelos *et al.* 2008) and are restricted to plants and fungi and b) Yellow strip (YS) clade, that mediate uptake of metal-secondary amino acid derivatives and have homologues in prokaryotes, fungi and plants (Curie *et al.* 2001; Wintz *et al.* 2003; DiDonato *et al.* 2004; Murata *et al.* 2006). Both these clades derive their names from the substrate specificity of the first member characterized in each group (Lubkowitz 2006).

An initial phylogenetic analysis of the homologues of OPT family revealed that they form 5 distinct clusters. The prokaryotes form a separate cluster from the eukaryotes (Cluster 1). Among the eukaryotes, four distinct clusters were observed – two well defined clusters for the plant homologues (Clusters 2 and 5) and two well defined fungi clusters (Clusters 3 and 4) (Yen *et al.* 2001; Lubkowitz 2006). However with the sequencing of new genomes, additional OPT family members have been identified. A subsequent phylogenetic analysis identified three different cluster for the PT clade- two for the fungal homologs and one cluster for plant homologs (Fig 1.2.). As compared to the previous analysis the plant cluster was found to be present between the two fungal PT clade clusters. In the YS clade also three different clusters were observed. One cluster for the fungal homologs, one for plant homologs and another one for bacterial homologs (Thakur & Bachhawat 2010). A recent phylogenetic analysis also yielded 5 different clusters but the clustering pattern varied with respect to the previous analysis as these clusters were not restricted to organismal level. The five different clusters were further subdivided into different

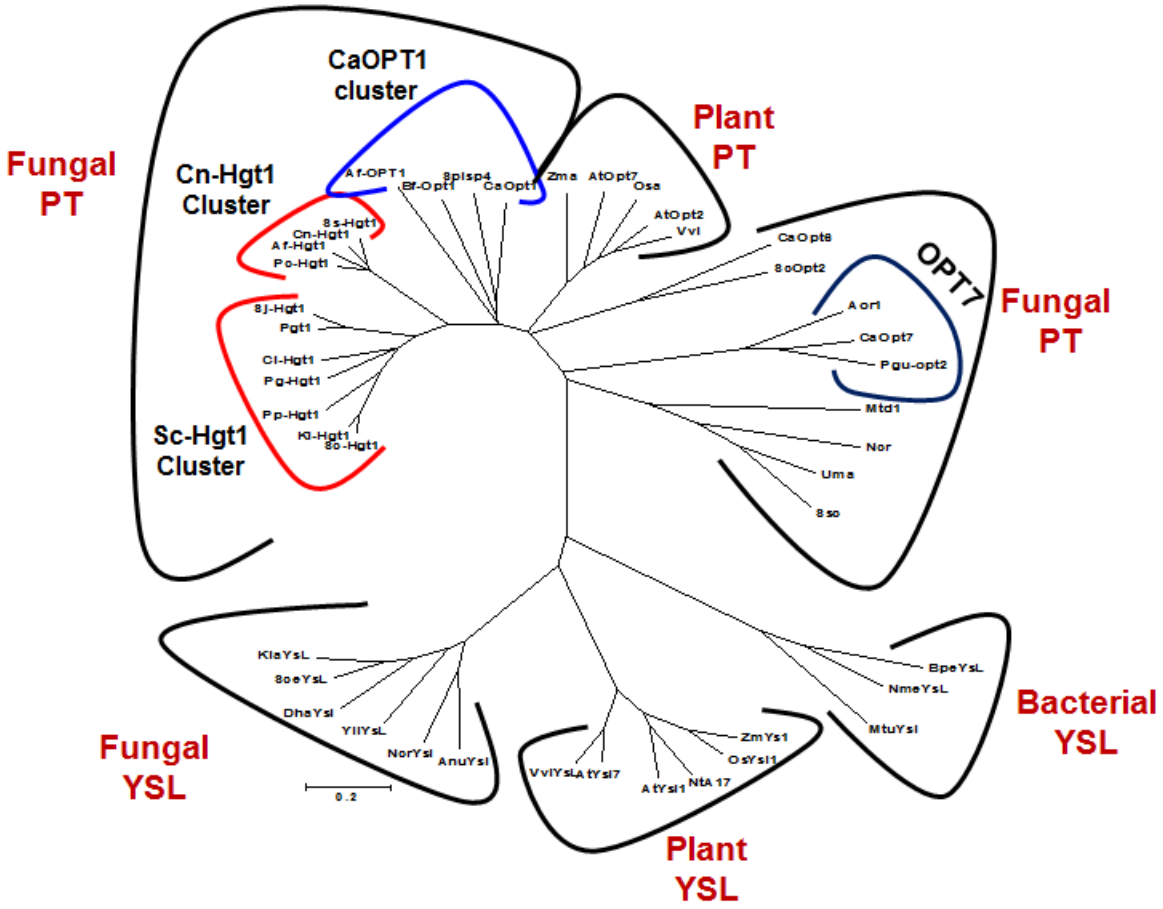

Fig 1.2: Unrooted phylogenetic tree of the OPT family: Phylogenetic analysis identified six different groups in the OPT family. In the fungal PT clusters, homologs having the corresponding functionally important residues, Phe523 and Gln526 of Hgt1p (a glutathione transporter) were found to transport glutathione and form a sub-cluster named as "*Sc-HGT1* cluster". The orthologs with the Iso523 and Glu526 residues also transport glutathione, cluster together and was named "*CnHGT1* cluster". *CaOPT1*, a non-glutathione transporter, lack these residues and form a distinct "*CaOPT1* cluster". *CaOPT7* also a glutathione transporter, clustered in the second fungal PT cluster and was named "*CaOPT7* cluster". Other OPT members have their own branch are marked accordingly. This figure has been adapted from Thakur et al., 2010.

sub-clusters depending on the organism and protein size (Gomolplitinant & Saier Jr 2011).

1.3.1.1. The *Saccharomyces cerevisiae* High Affinity Glutathione Transporter (*HGT1*):

Biochemical studies had suggested the presence of glutathione uptake systems in yeast (Miyake *et al.* 1998). Based upon genetic and biochemical evidences, a high-affinity glutathione transporter was discovered in *S. cerevisiae*, that was encoded by ORF *YJL212*, and was named as *HGT1* (Bourbouloux *et al.* 2000). Disruption of this gene led to a complete loss in glutathione uptake ability of the yeast cells. In addition the *hgt1Δ* mutants were non-viable in a glutathione biosynthetic mutant (*gsh1Δ*) background. The kinetic analysis of the transporter demonstrated a high affinity (*Km*= 54 μM) glutathione transporter having high specificity, as significant inhibition in glutathione uptake was observed only with reduced glutathione (GSH), oxidized glutathione (GSSG), and glutathione conjugate (GS-NEM). Interestingly *HGT1* was also described as an oligopeptide transporter based on the ability to transport tetra/penta peptides (Hauser *et al.* 2000), leading to confusion about the true substrates for this transporter. In subsequent studies using two-electrode voltage clamp experiments in *Xenopus laevis* oocytes, Hgt1p was shown to produce inward currents in oocytes in response to GSH, GSSG, glutathione derivatives phytochelatin (PC) and tetra peptide GGFL, but not by KLGL. Kinetic analysis in these studies revealed that the *Km* for GSH was 76 μM, for GSSG was 91 μM versus 211 μM for GGFL suggesting a preference for glutathione and glutathione derived peptides (Osawa *et al.* 2006).

The study by Osawa et al., 2006 also demonstrated that the uptake of substrate by Hgt1p is electrogenic since oocytes injected with *ScHGT1* cRNA exhibited an inward current in the presence of GSH, GSSG, tetra peptide (GGFL) or the phytochelatin (PC), PC2. Since these substrates have a net negative charge, it was concluded that Hgt1p transport is coupled with a cation. To check for the possibility of proton coupled symport, steady-state currents were measured in the presence of these substrates at different pH and found that the currents increased with increase in proton concentrations and these currents were largely saturable. This pH dependent currents and positive shifts of the reversal potentials at higher extracellular proton concentrations suggested that protons are co-transported with substrates in

stoichiometries that lead to a net positive charge per transport cycle irrespective of the negative charges of the substrates. However at lower pH, proton leak currents were observed in absence of GSH or other substrates, suggesting proton slippage, making it difficult to determine the coupling ratio. Together these result suggests that Hgt1p is a proton coupled symporter where the coupling of substrate and proton is loose (Osawa *et al.* 2006).

1.3.1.1.1. Hgt1p is regulated by Sulphur Regulatory Network:

The HGT1 promoter lacks the known motifs involved in sulphur regulation. Despite this, HGT1 gene was found to be under strong sulphur regulation. Studies using promoter deletion analysis identified a novel 9 bp *cis*-regulatory motif, CCGCCACAC, located at the -356 to -364 region of the promoter required for expression of *HGT1* gene (Miyake *et al.* 2003). A subsequent study suggested that this gene is under classical sulphur regulatory network involving the suphur regulatory transcription factor Met4p. Promoter deletion analysis in combination with phylogenetic footprinting and mutational analysis revealed that the previously described 9-bp *cis* element CCGCCACAC located at -356 to -364 region of the promoter can be refined to a 7-bp CGCCACA motif which is also present at -333 to -340 region and both copies of this cis-motifs are required for the expression of the gene in response to sulphur levels (Srikanth *et al.* 2005). In addition to the strong regulation by the sulphur status of the medium, *HGT1* expression is also regulated to some extent by the levels of few non-sulphur amino acids such as leucine and tryptophan (Wiles *et al.* 2006a). However the principal regulation is by the sulphur status with a strong repression seen by either cysteine or methionine. These studies by different groups led to the common conclusion that the expression of *HGT1* gene is under strong sulphur regulation and therefore its physiological role might be more in scavenging glutathione as a sulphur source from the medium to recover cysteine which is often limiting in the cell. It further suggests its role as a glutathione transporter rather than a general oligopeptide transporter.

1.3.1.1.2. *HGT1* Constitutive Overexpression Leads to Glutathione Dependent Toxicity:

HGT1 expression is normally tightly regulated by the levels of sulphur in the medium. However when *HGT1* gene was overexpressed under the strong constitutive TEF promoter, the GSH transport activity was severely inhibited in a medium containing 250 µM GSH (Bourbouloux *et al.* 2000). This observation was studied in

detail (Srikanth *et al.* 2005) and it was found that the yeast cells overexpressing *HGT1* were able to grow at 15 µM GSH and unable to grow on ≥ 50µM GSH concentrations. The latter had glutathione levels several fold higher than the corresponding WT strain suggesting that the observed toxicity is a consequence of over accumulation of glutathione in these cells (Srikanth *et al.* 2005). This phenotype has been exploited for the development of a functional assay for *HGT1* (Srikanth *et al.* 2005; Kaur & Bachhawat 2009).

Glutathione toxicity was examined in detail by a genome wide analysis as a consequence of toxic levels of GSH. This study found two major group of genes to be induced (Kumar *et al.* 2011). The first group was highly similar to the response of iron-starved cells and also similar to that of *atm1Δ*, an inner mitochondrial membrane ABC transporter required for extra-mitochondrial iron sulphur cluster (ISC) assembly. This response comprised of 25 genes of the iron regulon controlled by transcription factor "activator of ferrous transport" *Aft1* and *Aft2*, which regulate the uptake, metabolism, compartmentalization and use of iron. The second major groups of genes upregulated in response to high GSH levels included the UPR pathway, regulated by *Hac1* (homologous to *Atf*) transcription factor and *Ire1* kinase. These results showed that the GSH toxicity in *HGT1* overexpressing cells is due to disruption of iron metabolism and persistent high levels of the UPR (Kumar *et al.* 2011).

1.3.1.1.3. 2D Topology Model of Hgt1p:

Hgt1p was predicted to have 12-14 transmembrane domains (TMDs) using five different topology prediction softwares, including HMMTOP (Tusnady & Simon 2001), TMHMM (Krogh *et al.* 2001), MEMSAT (Jones *et al.* 1994), PHDHTM (Rost 1996), TopPRED II (CIaros & von Heijne 1994) along with multiple sequence alignment (MSA) of the functionally characterized OPT family members (Wiles *et al.* 2006b). The Hgt1p protein sequence was submitted as query and predictions were made using default parameters. However two of the predicted TMDs, corresponding to the regions 537-568 and 707-724 had proline rich motifs (EXIXGYX2PG[R/K]PXAX4KX2G and PPX[N/T]P) in proximity to glycine residue which theoretically disfavors the region to form a helix. These regions were thought to be unlikely to form TMDs and were predicted to form loops. Hence the final topology model of Hgt1p thus predicted previously consisted of twelve transmembrane domains with N- and C-terminal facing the extra-cellular matrix

(Wiles *et al.* 2006b). However the absence of any experimental evidence for omitting the two likely TMDs, was a major drawback to the predicted topology model of Hgt1p.

A subsequent topological study on the OPT family members, including Hgt1p suggested that the members have sixteen or occasionally seventeen TMDs. However this report was based on the average topological analysis of 325 members using only two software programs, WHAT (Zhai & Saier 2001) and TMHMM (Käll *et al.* 2007). The AveHAS program (Zhai & Saier Jr 2001) was further used to generate the average hydropathy plots, which revealed 16 TMDs. The TMDs 1-4 cluster loosely followed by clustering of TMDs 5-8. In contrast TMDs 9-16 were found to cluster tightly together (Gomolplitinant & Saier Jr 2011). However peak 3 (TMD3) and peak 11 (TMD11) in the hydropathy plot was divided into two small peaks with gaps suggesting a contradictory topology of 14 TMDs.

The number of transmembrane domains and their exact topology thus still remains a controversial point, and it has been examined more rigorously in this thesis.

1.3.1.1.4 Structure-Function Characterization of Hgt1p:

Structure-function studies on Hgt1p have faced several difficulties. The low levels of Hgt1p expression in yeast and toxicity of this protein when expressed in *E. coli* has hampered the crystal structure determination (PhD thesis, Kaur J, 2009) To identify the substrate binding residues in transporters, the possibility of using Substituted Cysteine Accessibility Method (SCAM), another powerful tool to study structure-function characterization was initially evaluated (Kaur *et al.* 2009). However this requires a functional cysteine free protein. Hgt1p contains twelve cysteine residues, including two that are conserved. A cysteine free Hgt1p was created and was found to be non-functional preventing the usage of the SCAM approach. There is no information about any post-translational modifications, such as glutathionylation or oligomer formation, a single disulphide bond however seems likely. A genetic suppressor approach, to isolate a functional protein from the non-functional one yielded molecules with the two conserved cysteines, C622 and C632 reverting back and all evidence seems to suggest that they are covalently linked with each other via disulphide bond (Kaur *et al.* 2009). Thus the major tool towards understanding Hgt1p has been the molecular genetic approach.

In the absence of any previous information on the important domains or residues in Hgt1p (or any other member of the OPT family), 22 charged and polar residues within the transmembrane domains of Hgt1p were targeted for mutational analysis to identify the structural features that govern the substrate specificity (Fig.1.3) (Kaur & Bachhawat 2009). Functional analysis followed by detailed kinetic studies revealed four transmembrane domains (TMD1, TMD4, TMD9 and TMD12) and the intracellular loops (ICL) in the region 537-568 as being essential for the activity by Hgt1p. The residues N124 (TMD1), Q222 (TMD4), Q526 (TMD9) and K562 (ICL) were found to be directly or indirectly participating in glutathione recognition and transport. Q222 and Q526 were found to be required for substrate recognition by Hgt1p while no role was assigned to K562. Q222 (TMD4) was found to be widely conserved in the OPT family whereas Q526 (TMD9) were present only in the OPT members known to function in glutathione uptake, suggesting that this residue might be required specifically for glutathione recognition. Based on this study a further investigation of TMD9 was carried out where all the residues corresponding to TMD9 were targeted (Thakur & Bachhawat 2010). This identified F523 residue to be important for glutathione recognition by Hgt1p. Subsequently with the eventual goal of targeting all the predicted TMDs of the Hgt1 protein, another study targeted the TMDs 1, 5, 7, 8, 11 for alanine scanning mutagenesis (Yadav 2014). However, the mutants were not analyzed in detail.

Hgt1p is a proton coupled glutathione symporter (Osawa *et al.* 2006). In addition to identify the binding sites for glutathione, it is also important to understand the proton coupling and transport to unravel the mechanism of active transport by this high affinity glutathione transporter. This has never been attempted for Hgt1p or any other member of the OPT family. However, the Major Facilitator Superfamily (MFS) of transporters, which constitutes the largest known family of secondary transporter proteins, have members that are proton coupled symporters. Although the Hgt1p is different from these MFS family members in terms of structure and function, they are mechanistically related in a sense of being proton coupled. The lactose permease (LacY) of *E. coli* belonging to the major facilitator superfamily (MFS) serves as a paradigm for the study of polytopic membrane proteins catalyzing substrate proton symport (Abramson *et al.* 2004; Kaback 2015). Therefore, I have briefly discussed

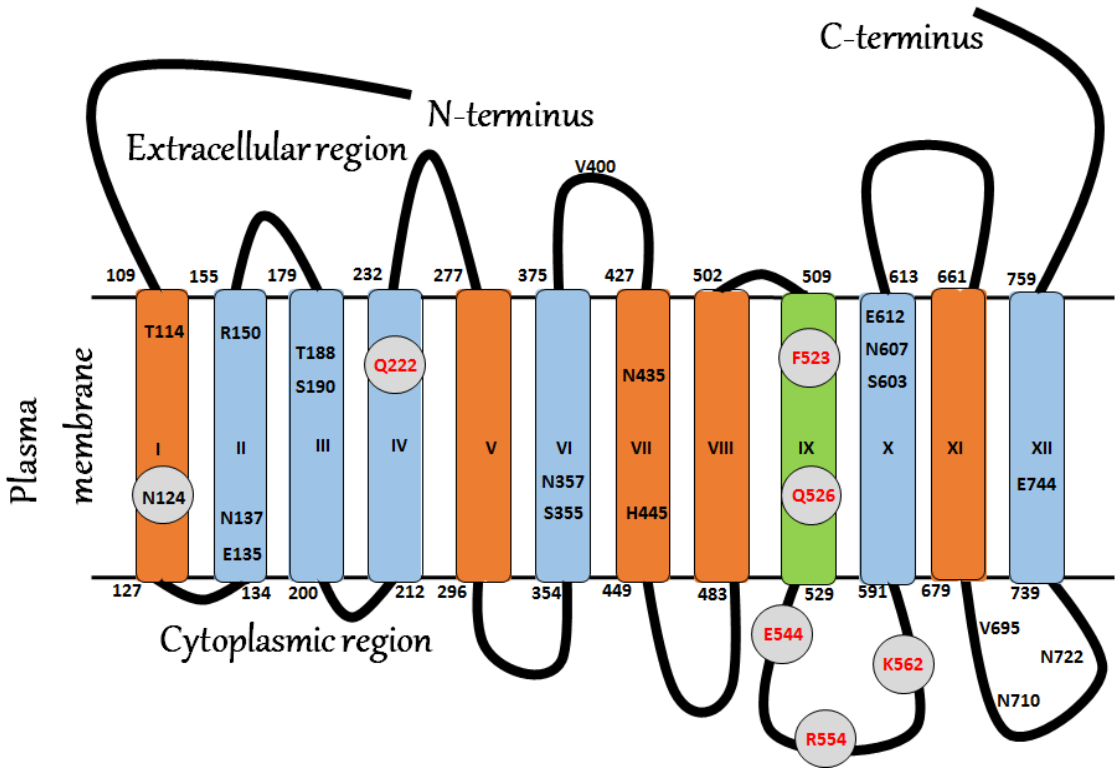

Fig 1.3. Pictorial presentation of putative Hgt1p topology showing TMDs and residues targeted for mutagenesis: The 12 predicted transmembrane domains are represented as rectangular bars and the numbers above and below the bars represent the beginning and end of the TMD. The identity and location of amino acid residues targeted for mutagenesis in the previous studies are shown as residue with number. The complete TMDs targeted for mutagenesis includes TMD9 (green bar), studied in detail, followed by TMD1, TMD5, TMD7, TMD8 and TMD11 (orange bars). The residues marked in circles were found to be critical for glutathione transport by Hgt1p.

the structure and mechanism of transport by lactose permease, LacY at the end of this chapter.

1.3.1.2. Yeast Oligopeptide Transporter 2 (*OPT2*):

Saccharomyces cerevisiae contains two other members of the OPT family. *OPT2* (YPR194C) which shares approximately 60% sequence similarity with Hgt1p and is a member of the PT clade. YGL114W is a remote homologue (30% sequence identity) of Hgt1p and belongs to the YSL clade. Despite a few studies on *OPT2*, the function of the transporter remains controversial. Even the localization of this protein remains controversial. Overexpression of Opt2 has not been able to complement Hgt1p, although it is capable of transporting a few peptides, suggesting either a different localization or different substrate specificity (PhD Thesis, Srikant C.V.). One study has suggested, the involvement of *OPT2* in detoxification of toxic chemicals that are typically detoxified by the vacuole. In addition *opt2Δ* mutants were found to have several small vesicles instead of large functional vacuole indicating its role in fusion of small vesicles to form the large vacuole (Aouida *et al.* 2009). More recently, *OPT2*, was shown to localize to peroxisomes and was suggested to transport GSSG out of peroxisomes thereby affecting peroxisomal, mitochondrial and cytosolic glutathione redox homeostasis (Elbaz-Alon *et al.* 2014). However yet another study has shown *OPT2* to localize to the plasma membrane and golgi and demonstrated that Opt2p mediates the exposure of phospholipids during cellular adaptation to altered lipid asymmetry. In addition Opt2p was found to be required for polarized cell growth and maintenance of normal vacuolar morphology (Yamauchi *et al.* 2015).

1.3.1.3. *Schizosaccharomyces pombe* and *Schizosaccharomyces japonicus* Glutathione Transporters:

The *S. pombe* ortholog of Hgt1p, *pgt1*$^{+}$ (*SpOPT1*), has been shown to encode for a high affinity glutathione transporter (Thakur *et al.* 2008). In initial attempts to characterize this hypothetical ORF, which bears significant similarity (53%) to the *S. cerevisiae* glutathione transporter (Hgt1p), Pgt1p failed to complement the *S. cerevisiae*, *hgt1Δ* mutants. Subsequent genetic and biochemical characterization of the *ORF* in its native host (*S. pombe*) revealed that it encodes for a plasma membrane localized, high affinity, glutathione transporter (*Km* = 63 µM) as significant inhibition in glutathione uptake was observed only with reduced glutathione and its conjugates,

GSSG and GS-NEM. Pgt1p was shown to be regulated by sulphur but unlike Hgt1p, Pgt1p overexpression did not show any glutathione dependent toxicity. Another independent study also showed *SpOPT1* as a plasma membrane glutathione transporter (Dworeck *et al.* 2009). A genetic investigation into the reason behind the failure of *Pgt1*$^{+}$ to complement in *S. cerevisiae hgt1Δ* strain, despite being so similar, suggested a block in protein expression due to defect in the RNA secondary structure in the heterologous system (Thakur & Bachhawat 2013).

The *S. japonicus* ortholog of Hgt1p, has also been shown to transport glutathione with high affinity and named as *Sj*-Hgt1p. Having a high sequence identity (51%) with Hgt1p, *Sj*-Hgt1 complemented growth of *met15Δhgt1Δ* of *S. cerevisiae* at low glutathione concentrations. Subsequent functional and biochemical characterization suggested *Sj-HGT1* to encode for a plasma membrane protein transporting glutathione with reasonably high affinity (*Km* = 204.1 µM) (Thakur & Bachhawat 2010). However substrate specificity analysis for this protein has not been carried out in detailed.

1.3.1.4. *Candida albicans* Glutathione Transporter:

The genome sequence of *Candida albicans*, reveals eight members of the OPT family out of which seven belong to the PT clade (*OPT1–OPT7*), whereas OPT8 belonged to the more remote YS clade (Reuß & Morschhäuser 2006). *CaOPT1*, the closest homologue (39% identity) of *HGT1* in *C. albicans* was not found to transport glutathione. Instead a remote homologue *CaOPT7* having 25% identity with Hgt1p, functioned as the glutathione transporter as suggested by [^{35}S] GSH uptake assays. This GSH uptake was significantly inhibited by nonlabelled GSH and GSSG. However this transporter showed broad substrate specificity as compared to other yeast glutathione transporters as the uptake was inhibited by tripeptides in addition to GSH and GSSG but not by dipeptides which was further confirmed by growth based assays. The *Km* of *OPT7* for glutathione was found to be 205 µM which reflects a reasonably high affinity glutathione transporter in *C. albicans*. However this transporter was not found to be essential for virulence of this pathogen (Desai *et al.* 2011).

In contrast to the above studies, *Candida glabrata* which is phylogenetically much closer to *Saccharomyces cerevisae*, than to *Candida albicans* was found to lack the

ability to utilize exogenously provided glutathione. Genome sequence analysis have revealed that a large number of *ORFs* including the homologs of members of the OPT family have been lost in *C. glabrata* in comparison with its close relative *S. cerevisiae.* Thus it fails to transport and utilize glutathione when provided from external sources (Yadav *et al.* 2011).

1.3.1.5. Other OPT Fungal Glutathione Transporters:

Glutathione transporters from other yeasts belonging to the PT clade of the OPT family have also been characterized. The orthologs of Hgt1p of *S. cerevisiae* in other closely related yeasts were investigated for their ability to function as glutathione transporters by complementation studies in *met15Δhgt1Δ* of *S. cerevisiae* or *S pombe cys1a*Δ*pgt1*Δ. The functional evaluation of these orthologs under strong constitutive promoter revealed that the orthologs in *Kluyveromyces lactis* (*Kl-HGT1*), *Pichia guilliermondii* (*Pg-HGT1*) and *Cryptococcus neoformans* (*Cn-HGT1*) were able to grow at low glutathione concentrations similar to Hgt1p (Thakur & Bachhawat 2010). A strong correlation exists between the ability of transporters to complement at low concentrations of glutathione and their affinity for the substrate (Kaur & Bachhawat 2009). Thus, complementation at low concentration of glutathione (15-30 μM) requires a transporter to have a high affinity for the substrate. The *Km* of glutathione for *Kl-HGT1* was found to be 64 μM, while that of *C. neoformans* was 82.5 μM, suggesting that they are indeed high affinity glutathione transporter. However the substrate specificities of these transporters were not studied in detail (Thakur & Bachhawat 2010).

1.3.1.6. Plant OPT Glutathione Transporters:

The identification of Hgt1p as a glutathione transporter suggested the possibility of some plant homologues to function as glutathione transporters. Using growth-based complementation studies followed by radioactive uptake assay in *HGT1* knockout *S. cerevisiae* strain, *AtOPT6* of *Arabidopsis thaliana, BjGT1* in *Brassica juncea* and *OsGT1* in *Oryza sativa* were described as low affinity glutathione transporters based on very weak complementation phenotypes (Bogs *et al.* 2003; Cagnac *et al.* 2004; Zhang *et al.* 2004). *AtOPT6* was also suggested to be a low affinity glutathione transporter by patch clamp experiments in *Xenopus oocytes*, where an inward current was observed in response to GSH but not GSSG. However, no complementation of

growth was observed in *hgt1Δ, S. cerevisiae* strain. Further kinetic analysis revealed a high *Km* of 566 µM for GSH, further confirming it as a low affinity glutathione transporter (Osawa *et al.* 2006).

Recently all the 9 AtOPTs were cloned and screened for the possibility of plant glutathione transporter using sulphur auxotroph mutant (*met15Δhgt1Δ*) of *S. cerevisiae* (Zhang *et al.* 2016). Only *AtOPT4* rescued the growth in the presence of GSH as the sole sulphur source similar to *HGT1*. However when growth curves were compared in yeast, Hgt1p reached saturation much earlier as compared to *AtOPT4*. Further using [^{35}S] GSH uptake, *AtOPT4* was shown to be low affinity GSH transporter following Michaelis–Menten kinetics with an apparent *Km* of 1.4 ± 0.3 mM and *Vmax* of 2.1 ± 0.3 nmol of GSH.mg protein $^{-1}$.min^{-1}. In addition AtOPT8 showed a weak growth phenotype but this observation was not consistent. Surprisingly AtOPT1,3, 5, 6 and 7 inhibited yeast growth in control galactose-inducing media but not in glucose-containing media, suggesting a limitation of functional analyses using a heterologous system which was also observed by another group doing similar study using *AtOPT3* (Mendoza-Cózatl *et al.* 2014). However when GSH levels were measured in different tissues of *atopt4*Δ or *atopt4*Δ *atopt2*Δ (*AtOPT2* is the closest homologue of *AtOPT4*) mutant plants, no significant decrease in GSH levels were observed in roots, stem and leaves. Only the siliques of both the mutants had lower GSH content suggesting the role of *AtOPT4* in GSH loading/unloading in siliques. Further no significant growth difference was observed in both the mutants suggesting the presence of additional low affinity or another high affinity GSH transporter compensating for the loss of *AtOPT4* (Zhang *et al.* 2016).

ZmGT1 expressed in roots, stems and leaves of maize (*Zea mays*), is also suggested to transport glutathione and glutathione conjugates based on complementation studies in *hgt1Δ* yeast strain and measurement of [^{14}C] GS-NEM (GSH conjugated to N-ethylmaleimide) transport. Under normal growth conditions *ZmGT1* was found to be weakly expressed however, upon exposure to the herbicide, gene expression was greatly enhanced suggesting that *ZmGT1* may be involved in the detoxification of xenobiotics in plants, and may contribute to the tolerance of maize against herbicides (Pang *et al.* 2010).

A somewhat unclear picture, thus exists with respect to glutathione transport by the plant OPT homologues in the light of conflicting results from different studies (Koh *et al.* 2002; Cagnac *et al.* 2004; Osawa *et al.* 2006; Mendoza-Cózatl *et al.* 2014). The use of different strain backgrounds, expression vectors as well as different evaluation parameters such as growth, radiolabelled uptake and competition assays, to measure transport activity in the different studies, which essentially are not equivalent in terms of interpretation of transport activity, might explain these discrepancies (Lubkowitz 2006; Osawa *et al.* 2006). Further, use of a heterologous system might not always readily lead to detection of transport (Osawa *et al.* 2006; Thakur *et al.* 2008).

1.3.2. Glutathione Transporters in the ABC Superfamily (Table 1.2):

1.3.2.1. The Multidrug Resistance Associated Protein (MRP) Family Involved in Low Affinity Glutathione Efflux:

The *MRP/CFTR* proteins belongs to the family C of the ABC superfamily (ABCC) and are long known to be involved in multidrug resistance. ATP binding and hydrolysis provides the driving force to pump the substrates out of the cell. In humans, this family comprises of nine MRP transporters (MRP1 to MRP9) and the gene defective in cystic fibrosis (CFTR). All these transporters are present on the plasma membrane and function as multi specific organic anion transporters. MRPs generally have two membrane spanning domains (MSDs) each comprising of six transmembrane helices. In addition some MRPs (MRP1, MRP2, MRP3, MRP6 and MRP7) have extra N-terminal MSD (termed as MSD0) comprising of 5 TM helices. Thus, MRPs with 17 TM α-helices are "long" MRPs, whereas MRPs with 12 TM α-helices (MRP4, MRP5, MRP8, MRP9 and CFTR) are referred as "short" MRPs (Cole & Deeley 2006).

The first indirect evidence for the role of mammalian MRP family in GSH transport came from the observation that increased expression of MRP1 (*ABCC1*) in cell lines led to increased efflux of glutathione (Zaman *et al.* 1995; Lautier *et al.* 1996). Further studies with Mrp1 knockout mice revealed that there was high correlation between the expression of MRP1 in tissues and glutathione levels, providing further indirect evidence for a link between glutathione efflux through MRP1 (Lorico *et al.* 1997; Rappa *et al.* 1999). Proteoliposomes enriched in MRP1 (Mao *et al.* 2000) and rat liver canalicular plasma membrane vesicles expressing

MRP2 (Rebbeor *et al.* 2002) were confirmed to be transporting glutathione. Subsequently, studies have established the role of MRP1, MRP2, MRP4, MRP5 and CFTR in low affinity, glutathione efflux in different tissues (Reviewed in Ballatori *et al.*, 2009). While MRP3 has been shown not to transport glutathione, the other MRPs (MRP6, MRP7, MRP8 and MRP9) have been recently identified and their role in glutathione uptake is yet to be explored. The mechanism of glutathione efflux through MRPs is still not completely understood and based upon results from different studies, four potential models have been proposed. First, GSH itself is a low-affinity substrate for MRP1. Second, GSH is co-transported along with other substrates of MRPs. Third, transport of some substrates by MRPs is stimulated or dependent on GSH without itself being translocated across the plasma membrane. Fourth, GSH transport is enhanced by certain drugs that are not themselves transported by MRPs (Ballatori *et al.* 2009).

MRP1: Among all the MRPs, MRP1 which is expressed in all tissues is the best characterized in terms of substrate specificity and structure-function relationships. The first and best characterized physiological substrate for MRP1 is the GSH-conjugate, cysteinyl LT4 ($Km \approx 100$nM). Other metabolites transported by MRP1 includes GSH conjugates of 4-hydroxynonenal, prostaglandins (PG)A_2 and 15-deoxy-$\Delta^{12,14}$-PGJ_2. Xenobiotic substrates include GSH conjugates of carcinogens such as 4-nitroquinoline, aflatoxin B_1. MRP1 also transports glutathione disulfide (GSSG) with a relative high affinity ($Km \approx 100$ μM) and MRP1-mediated GSSG efflux occurs during oxidative stress in endothelial cells and astrocytes. In contrast to GSSG, the affinity for GSH is relatively low ($Km \approx 5–10$ mM) (Cole & Deeley 2006).

To investigate the structural features of MRP1 protein required for transport, various techniques such as electron microscopy, NMR, infrared and mass spectrometry have been applied on purified MRPs to decipher the mechanism of transport, with some degree of success (reviewed in He et al., 2011). A truncated MRP1 mutant lacking the entire MSD0 region behaved like wild-type MRP1 in vesicles (Bakos *et al.* 1998). Several homology based model for second and third MSDs of MRP1 have been generated using bacterial ABC proteins as templates (Campbell *et al.* 2004; DeGorter *et al.* 2008; He *et al.* 2011) and have been used for different biochemical studies. Site-directed mutagenesis have identified a number of residues that are either critical for substrate specificity or influence the overall activity

Table 1.2 List of glutathione transporters of ABC superfamily

Transporter	Known substrates	Remarks
Mammals		
MRP1	GSSG *Km* = 100 µM GSH *Km* = 1-10 mM GS-conjugates	Expressed in all tissues
MRP2	GS-conjugates GSSG GSH	Expressed in apical membrane of epithelial cells
MRP3	GS-conjugates	Differential expression in different tissues
MRP4	GS-conjugates GSH ± other substrates GSH	Expressed in basolateral membrane
MRP5	GS-conjugates GSH ± other substrates GSH	Expressed ubiquitously
CFTR	Chloride GSSG GSH	Chloride channel allowing GSH efflux
ABCG2	Methotrexate GSH	Involved in maintanince of cellular redox homeostasis
Plants		
At-MRP1	GS-conjugates, *Km* in low mM Glutathionylated Herbicides Glutathionylated anthocyanins	Transport into plant vacuoles
At-MRP2	GS-conjugates, Km in low mM Glutathionylated Herbicides Glutathionylated anthocyanins	Transport into plant vacuoles
Yeast		
Yeast MRPs **Ycf1p** **Bpt1p**	GS-Cd GSSG GS-adenine pigment precursor GSH *Km* = 15mM (Ycf1p), 3mM (Bpt1p)	Transport into yeast vacuoles
Atm1p	GSSG *Km* = 109 GS-S-SG GS-S0-SG	Export from Mitochondria
Gxa1p	GSH	Involved in export of GSH

of MRP1. However only few residues have been identified that specifically affect transport of GSH or GSH conjugates, such as LTC4. These include His335 and Lys332 (TM6), which substantially reduce GSH transport and selectively eliminate LTC4 and arsenic triglutathione transport activity but do not affect the transport of other MRP1 substrates such as methotrexate and glucuronide conjugates. Alanine scanning of TM6 (320-337) further identified mutations of Lys319, Asp336 and Lys347 to severely affect MRP1 activity further suggesting critical role of TM6 in substrate binding and transport by MRP1 (Haimeur *et al.* 2002; Haimeur *et al.* 2004). Other important residues identified for LTC4 or GSH transport includes Arg433 (ICL4), Lys396 (TM7) Thr550, Trp553, Thr556, Pro557, Tyr568 (ICL5), Arg593, Phe594 (TM11), Arg1138 (TM15), Lys1141, Arg1142 (ICL7), Arg1197, Glu1204 (TM16) and Trp1246, Arg1249 (TM17). However these residues when mutated also affected non-GSH substrate transport (He *et al.* 2011).

MRP2: Unlike MRP1, MRP2 has limited distribution but the substrate specificity is similar to that of MRP1 *i.e.* high affinity for glucuronide conjugates, methotrexate and glutathione conjugates such as LTC4 (Paulusma *et al.* 1999). MRP2 probably have two similar but non-identical substrate binding sites, one site which is directly involved in substrate transport and second site that regulates the affinity for the substrate (Ryu *et al.* 2000; Zelcer *et al.* 2003). Selective site-directed mutagenesis have been carried out on MRP2 based on the important amino acid residues located in TM helices of other related ABC transporters such as MRP1 and MDR1 and identified TM6 (K324A, K325M), TM9 (K483A), TM11 (R586L), TM16 (R1210A) and TM17 (W1254, R1257A) to be important for GSH conjugates (LTC4 and 2,4-dinitrophenyl GSH) and methotrexate transport activity (Ryu *et al.* 2000).

MRP4 (*ABCC4*) and MRP5 (*ABCC5*): GSH and its conjugates have been suggested to be a substrate for both MRP4 and MRP5 (Wijnholds *et al.* 2000; Liqi & Theresa 2002). Overexpression of MRP4 in HepG2 cells and MRP5 in MDKCII cells is associated with a marked increase in GSH efflux with concurrent decrease in the intracellular GSH levels (Wijnholds *et al.* 2000; Liqi & Theresa 2002). In addition MRP4 has been shown to transport bimane-GS and fluorescent GSH conjugate (Bai *et al.* 2004). MRP4 also co-transports bile acid and salts with GSH (Rius *et al.* 2003; Rius *et al.* 2006). Unlike other MRPs, MRP4 and MRP5 also transport cyclic nucleotides cAMP and cGMP but GSH dependent transport is contradictory

(Jedlitschky *et al.* 2000; Chen *et al.* 2001; van Aubel *et al.* 2002; Wielinga *et al.* 2003). Targeted mutagenesis data based on MRP1 studies suggested that TM6 and TM12 may comprise important part of the substrate binding pocket. A structural homology model for MRP4 was generated using the crystal structure of bacterial ABC transporter Sav1866 from *S. aureus* and ATP-binding domain of human P-glycoprotein as templates suggesting Arg375 and Arg998 facing into the central aqueous pore of MRP4 and hence could be involved in substrate binding (El-Sheikh *et al.* 2008; Moon *et al.* 2015).

1.3.2.2. Yeast MRPs

Vacuolar Ycf1p (yeast cadmium factor-1) and the Bile Pigment Transporter-1 (Bpt1p):

The vacuolar membrane protein, Ycf1p and the bile pigment transporter-1 (Bpt1p) are homologues of multidrug resistance associated proteins (MRPs) and has been shown to be required for cadmium resistance in *S. cerevisiae* (Szczypka *et al.* 1994) which is achieved by the transport of glutathione conjugates (GS-X: for example GS-Cd and GS-adenine pigment precursor) into the vacuole (Li *et al.* 1996; Chaudhuri *et al.* 1997). Ycf1p and Bpt1p has also been shown to transport reduced GSH into the vacuole, although its affinity for GSH has been shown to be very low (for Ycf1 Km = 15 ± 4 mM and for Bpt1p Km = 3 mM) (Rebbeor *et al.* 1998b; Rebbeor *et al.* 2002; Sharma *et al.* 2002).

A few attempts of structure-function characterization on Ycf1p have been carried out (Wemmie & Moye-Rowley 1997; Falcón-Pérez *et al.* 1999; Falcón-Pérez *et al.* 2001). Investigators have targeted and carried out an extensive series of site directed mutagenesis within NBD1, NBD2, the R domain and intracellular loop 4, present between TMD 15 and 16. The choice of mutagenesis was based on conservation pattern between animal MRP1 and CFTR and mutants were assessed for cadmium resistance *in vivo* and vacuolar transport activity *in vitro* using radiolabelled LTC4 (a glutathione conjugate). Majority of the mutations were deleterious due to loss of function (G663V, G756D, D777N, L826S, G835R, G1306E, and G1311R) or loss of protein expression (I711S, L712D, F713D, and N1366K). However few mutants (L817S, L825T, Y855L, A910G, I840P and R1143C) showed differential effects on the ability of the yeast cells to grow on cadmium and LTC4 transport activity (Falcón-

Pérez *et al.* 1999). In addition, suppressor studies with mutations that inactivate Ycf1p function was also carried out. Gain-of-function suppressor analysis for mutant D777N in the Walker B motif of NBD1 which inactivates Ycf1p dependent transport function, yielded mutations in NBD1, NBD2, MSD1 and MSD2 suggesting a functional interaction of NBD1 with other domains of Ycf1p (Falcón-Pérez *et al.* 2001).

1.3.2.3. Plant MRPs:

A. thaliana genome has 15 members of the MRP family, while in rice 17 members have been detected (Wanke & Üner Kolukisaoglu 2010). Initial studies with some of the *A. thaliana* MRPs indicated that these are primarily localized to the vacuolar membrane and in contrast to animal cells, there is no report on the role of plant MRPs in glutathione efflux across the plasma membrane. Hydropathy plots of plant MRPs resemble the animal MRPs to a great extent suggesting a similar arrangement of the membrane spanning domains (Rea 1999; Klein *et al.* 2006). Although *AtMRP2* has been shown to act as low affinity glutathione transporter, the role of these MRPs in transport of reduced glutathione is less clear. Instead the plant MRPs have been shown to be involved in transport of glutathione conjugates (GSSG, glutathionylated anthocyanins, glutathionylated herbicides) and chlorophyll catabolites with *Km* values in low milli molar range into plant vacuoles. AtMRP1 has a lower affinity for GSSG as compared to AtMRP2 but both these transporters were found to have similar affinities for other conjugates (Foyer *et al.* 2001; Liu *et al.* 2001).

1.3.2.4. Mammalian ATP-binding Cassette Sub-Family G Member 2 (ABCG2):

ABCG2 belongs to the ABCG subfamily of the ABC transporters and has been shown to confer resistance to methotrexate (MTX). It is similar to MRPs in its ability to protect cells against chemical damage. Human ABCG2 is a half transporter consisting of six putative TM segments with N- and C-terminal facing the cytosol and was thought to exist and work as a homo-dodecamer with a minimum stable unit of homo-tetramer (Xu *et al.* 2004). Cys603 present in the interconnecting loop between transmembrane segments, TM5 and TM6 was identified to form the intermolecular disulphide bond and has been suggested to be involved in dimer formation (Henriksen *et al.* 2005).

ABCG2 was identified as a GSH efflux pump by treatment of different cell lines using 2-5-dihydroxychalcone, an effective stimulant promoting cellular glutathione efflux. This was subsequently confirmed using *S. cerevisiae* lacking the high affinity glutathione transporter (*hgt1Δ*). Yeast cells expressing human ABCG2 exhibited 2.5 fold more GSH in the extracellular medium. Overexpression or suppression of ABCG2 in human epithelial cells resulted in increased or decreased levels of extracellular GSH (Brechbuhl *et al.* 2010). Functional ABCG2 has a wide range of substrate specificity (Hardwick *et al.* 2007) and recently it has been suggested to transport enterolactone which is produced by the gut microbiota from plant lignans. However no statistically significant differences in the levels of enterolactone between *abcg2* knockout and wild-type mice in the plasma were noted (Miguel *et al.* 2014). This protein also has a number of polymorphisms that affect its substrate specificity, expression and alter drug metabolism (Tamura *et al.* 2006).

1.3.2.5. Yeast Glutathione Export ABC Protein 1, Gxa1:

An ATP-dependent permease Adp1p, was identified as a novel glutathione exporter in *S. cerevisiae* based on the homology of the protein sequence with known human ABCG2 and named as glutathione export ABC protein 1 (Gxa1p). Using low glutathione utilizing (LGU) *S. cerevisiae* strain, where genes responsible for decreasing extracellular GSH, γ-GT (involved in GSH degradation) and Hgt1p (involved in GSH uptake) were deleted, extracellular glutathione concentration was found to be 2.2 fold higher than that of the parental strain. When Gxa1p was overexpressed in LGU strain, the extracellular glutathione levels increased continuously in Gxa1 overexpressing cells depending on the cultivation time (Kiriyama *et al.* 2012). However these findings need to be substantiated using direct measurements of glutathione transport.

1.3.2.6. Eukaryotic ATP-Binding Cassette Transporter of the Mitochondria (ATM1):

Human ABCB7 and yeast Atm1p belongs to the ABC transporter family and are present on the inner mitochondrial membrane (Csere *et al.* 1998). A single missense mutation (E433K) in exon 10 of the ABCB7 gene has been shown to be the cause of X-linked sideroblastic anemia associated with cerebellar ataxia. (Shimada *et al.* 1998; Bekri *et al.* 2000). Initial studies suggested that iron-sulphur cluster (ISC) machinery

inside the mitochondria synthesizes an unknown, sulphur-containing molecule that is exported by Atm1p (Kispal *et al.* 1999). To identify the substrates and mechanism of transport, and to understand its role in iron metabolism, the three dimensional crystal structures of yeast Atm1p (Srinivasan *et al.* 2014) (Fig1.4) and its bacterial homologue (Lee *et al.* 2014) (discussed in the bacterial glutathione transporter section) were recently solved revealing a typical architecture, where the functional form is a dimer with two nucleotide-binding domains (NBDs) facing inwards (yeast ATM1 towards mitochondrial matrix) and hence are thought to function as exporter. The N-terminal forms the transmembrane domains and the C-terminal forms the NBDs. The NBDs couple the energy released from binding and hydrolysis of ATP to the translocation of substrate through the transmembrane domains. The TM5 and TM6 helices of each monomer form a domain swapped like structure with TM1-3 and TM6 helices of the other monomer resulting in a V-shaped molecule with large substrate binding cavity. The yeast Atm1p structure was obtained with a GSH molecule bound to a positively charged, hydrophilic cavity through interaction with conserved residues Arg280 and Arg284 (TM4), Asn343 (TM5), Asn390, Ser394, Arg397, and Asp398 (TM6). In the crystal structure, GSH molecule was bound without any ATP suggesting that substrate binding can occur in absence of ATP. In addition the two NBDs are placed close to each other by a scissor-like interaction of the two C-terminal α-helices stabilizing the protein. On the basis of two structures (with or without GSH), alternating access transport mechanism was proposed which consist of the following steps: a) substrate enters and binds to the hydrophilic cavity of the transporter in an inward-open facing orientation from the matrix side b) ATP binds to the NBDs c) ATP hydrolysis leading to the rearrangement of transmembrane helices, creating an exit pathway for substrate release (Srinivasan *et al.* 2014).

Although, the structure was obtained with a GSH molecule bound to the substrate binding sites, the true substrate specificity for this transporter is still unclear. The ATPase activity of Atm1p was shown to be stimulated by GSH, suggesting that this tripeptide may be directly involved in the transport process (Kuhnke *et al.* 2006). However, when various putative substrates were tested for their capacity to stimulate the ATPase activity of purified yeast Atm1p and *Arabidopsis* Atm3p, the ATPase activity was stimulated by GSSG and GS-S-SG but not by GSH, GSSH, lactoylglutathione, cysteine or Cys-Gly (Schaedler *et al.* 2014). Further transport

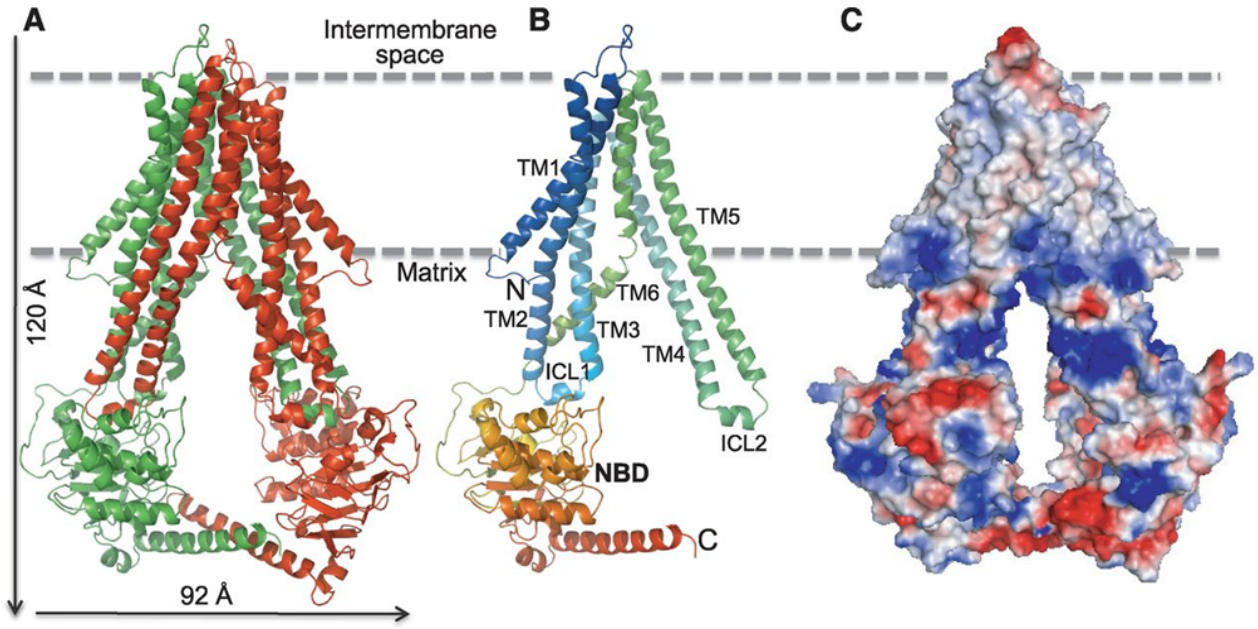

Fig 1.4.Crystal structure of the *S. cerevisiae* mitochondrial ABC transporter Atm1p. (**A**) Demonstration of the nucleotide-free Atm1p homodimer, with monomers colored in red and green with the NBDs facing towards the mitochondrial matrix. The dashed line represents the approximate positioning of the lipid bilayer. (**B**) The Atm1p monomer is depicted in rainbow colors showing the crossover of the TM4 and TM5 to the other monomer (not shown), resulting in the formation of a V-shaped molecule with a large cavity. The N and C termini, the NBDs, and the coupling helices ICL1 and ICL2 that form the transmission interface between the transmembrane helices and the NBDs are indicated. (**C**) Electrostatic surface potential representation of the Atm1p dimer (blue, positive; red, negative; and white, neutral). The substrate binding cavity is located near the hydrophilic surface of the membrane that is positively charged. This figure has been reproduced from Srinivasan et al., 2014, using publisher's permission.

experiments in *L. lactis* inside-out membrane vesicles using [^{35}S]-labeled GSH or GSSG confirmed that *ScATM1* or *AtATM3* show ATP dependent uptake of [^{35}S]GSSG with an apparent *Km* of 109 ± 6 µM and not for [^{35}S]GSH. Transportomics approach in combination with *in vitro* and genetic interaction studies suggested trisulphide (GS-S0-SG), as a physiological substrate for these proteins (Schaedler *et al.* 2014).

1.3.2.7. Bacterial ABC Glutathione Transporters (Table 1.3):

A typical bacterial ABC type importer consist of two transmembrane subunits forming the translocation channel of the permease, two nucleotide binding subunits for binding and hydrolysis of ATP and a solute binding protein (SBP) acting as receptor for substrate and delivering the cargo for transport process. SBPs are generally fused to the permease or lipid-anchored to the cell membrane and are the main determinants of substrate specificity of the related transporter. The Gram positive and Gram negative bacteria differ in the type of SBPs used to prime the transport. In contrast, the exporters lack these SBPs and are generally involved in drug and antibiotic resistance or in the biogenesis of extracellular polysaccharaides (Davidson *et al.* 2008; Vergauwen *et al.* 2013).

Importers:

The *YliABCD* operon encodes a multi-subunit protein and has been suggested to be involved in GSH uptake in *E. coli* (Suzuki *et al.* 2005). The disruption of *yliA* and *yliB* in an *E. coli* strain lacking a functional γ-glutamyl transpeptidase (*ggt*Δ) led to a significant decrease in GSH uptake as well as defective ability to utilize glutathione as a sole source of organic sulphur. These four genes *yliA, yliB, yliC,* and *yliD* are located downstream of *ybiK,* and are transcribed with *ybiK*. The proteins encoded by the genes *yliA, yliB, yliC* and *yliD* are multi-subunit proteins belonging to the periplasmic binding-protein-dependent ABC transporter family of the prokaryotes. *YliA* has the ATP-binding motif, *YliB* encodes for the type 5 periplasmic binding protein and *YliC* and *YliD* encode for the transmembrane domains of the transporter. The study established that this ABC transporter together with the periplasmic γ-glutamyltranspeptidase form an important pathway for the use of extracellular glutathione as a sole sulphur source in bacteria (Suzuki *et al.* 2005).

Table 1.3 List of bacterial glutathione transporters of ABC superfamily

Transporter	Structural subunits	Organism	Known substrates
Importer			
Encoded by *YliABCD* operon	*YliA* – ATP-binding subunit *YliB* – Periplasmic peptide-binding protein *YliC* &D –Transmembrane domains	*Escherichia coli*	GSH
Encoded by *OppBCDA* operon	*OppD* – ATP/GTP-binding subunit *OppA* – Periplasmic peptide-binding protein *OppB* &C –Transmembrane domains	*Mycobacterium bovis*	GSH
Encoded by *DppBCDF* operon + *GbpA*	*DppD & F* – ATP-binding subunit *DppB* &C –Transmembrane domains *GbpA* – Periplasmic peptide-binding protein	*Haemophilus influenzae*	GSSG *Kd* =12.9 µM GSH *Kd* =56.4 µM Heme *Kd* =655 µM
Encoded by *DppBCDF* operon + *GshT*	*GshT*– Periplasmic peptide-binding protein	*Streptococcus mutans*	GSH Kd = 0.47 µM S-methyl-GSH Kd = 2.3 µM GSSG Kd = 12.2 µM GSH-monoethylester Kd = 16.1 µM Homo-glutathione Kd = 20.7 µM
Exporter			
CydDC		*Escherichia coli*	GSH GS-conjugates Cysteine
Atm1p		*Novosphingobium aromaticivorans*	mM S-Ag GSH *Km*= 0.012 S-Hg GSH *Km* = 0.12 S-DNB GSH *Km*= 0.21 S-Hexyl GSH *Km*= 0.40 GSSG *Km*= 0.97 S-BimaneGSH *Km*=1.2 GSH *Km* = 15 γ-Glu-Cys *Km* = 10

Another membrane protein belonging to the periplasmic binding protein-dependent ABC transporter family is encoded by the operon *OppBCDA* and has been implicated in glutathione uptake in *Mycobacterium bovis* BCG. The gene *OppB* and *OppC* encodes for the inner membrane permease, *OppD* encodes for a protein with ATP/GTP-binding motifs and *OppA* encodes for the periplasmic peptide-binding protein. Deletion of O*ppD* showed reduced GSH uptake (Green *et al.* 2000).

In *H. influenza*, a periplasmic solute-binding protein *GbpA* (also known as *HbpA*), which binds oxidized and reduced glutathione with physiologically relevant affinities to prime the transport by dipeptide permease *DppBCDF*, belonging to ABC family. *GbpA* is a type 5 SBP, found exclusively in Gram negative *Pasteurellaceae*, and is thought to be derived from canonical *DppA* gene sequence by duplication. *GbpA* does not bind to glutathione derivatives with C-terminal modifications or bulky glutathione-S-conjugates. In HI1184-HI1187 operon, the genes *DppB* and *DppC* code for the membrane-spanning domains, and *DppD* and *DppF* encodes the nucleotide-binding domains. To understand how *GbpA*-family of proteins can serve as glutathione-binding platforms for priming their cognate dipeptide permeases, the crystal structre of *HbpA* from *Haemophilus parasuis* in complex with GSSG was solved (Vergauwen *et al.* 2010). GSSG (consisting of GS1 and GS2) was bound to a large solvent filled interface between the N- and C-terminal halves of the protein adopting a collapsed conformation. Substrate binding shifts the equilibrium toward a closed state by "Venus flytrap" mechanism. In this closed ligand-bound form, SBPs associate with their cognate membrane-embedded permease to deliver the cargo for transport. In the structure GS1 and GS2 occupied two well defined compartments in an asymmetric fashion making numerous interactions with N- and C-terminal domains of *HbpA*. γ-Glu-1 forms possible hydrogen bonds with Gly46, Arg379, Ser430 and Arg379, Cys-1 interacts with Tyr521 which forms the aromatic bed against the disulphide of GSSG whereas Gly-1 forms H-bond with Ala380, Ser381, Ser430. On the other hand γ-Glu-2 forms interactions with Phe504 and Gln516, Cys-2 forms H-bonds with two water molecules and Gly-2 interacts with Gly46, Arg379 and Arg33.

In case of Gram positive bacteria such as *Streptococcus mutans*, transporters substrate specificity is different from that of Gram negative bacteria (Thomas 1984; Sherrill & Fahey 1998). In addition no type 5 SBPs or apparent homologue is present

suggesting that *GbpA*/*DppBCD*F is not a valid candidate for transporting GSH. Instead type 3SBP, SMU_1942c also known as *GshT*, showed the characteristic binding affinities for GSH and GSSG in *S. mutans* (Vergauwen *et al.* 2013). However, as compared to *GbpA*, *GshTs* are small proteins and show differential substrate specificity and can bind GSH, GSSG and wide variety of GS-conjugates with different affinities. As compared to *GbpA* which favors GSSG over GSH, *GshT* showed highest affinity for GSH (*Kd* of 0.47 μM), followed by S-methyl-GSH (*Kd* of 2.3 μM), GSSG (*Kd* of 12.2 μM), GSH-monoethylester (*Kd* of 16.1 μM) and homoglutathione (*Kd* of 20.7 μM). This SBP share the transport machinery with that of cystine permiase *TycABC*. This sharing of SBPs is not common in bacteria. In order to provide structural framework for these observations, GshT crystal structure was determined with GSSG bound and was found to adopt a "*Venus fly trap*", closed conformation typically observed for ligand bound solute binding proteins. GS-1 was found to interact by a wide range of polar interactions contributed almost equally by two lobes of the GshT. In contrast GS-2 was found to have only three specific interactions with GshT. And the disulphide bond of GSSG was buried in the hydrophobic pocket made up of Val10, Val115 and Trp51 (Vergauwen *et al.* 2013).

Exporters:

Bacterial ATM1

Homologs of yeast Atm1p are widespread among bacteria except *E. coli*. The ortholog of Atm1p in *Cupriavidus metallidurans* CH34 (a model system for mesophilic bacteria that are resistant to high concentrations of transition metal cations), AtmAp shares 46% identity to the yeast protein and is shown to be involved in resistance to heavy metals including cobalt and nickel but not to iron (Mikolay & Nies 2009). To address the molecular mechanism and physiological roles of these transporter in metal homeostasis, crystal structure of *Novosphingobium aromaticivorans* (*Na*Atm1p) which shares ~45% sequence identity with yeast Atm1p and human ABCB7 was solved (Fig1.5) (Lee *et al.* 2014). Like yeast ATM1, NaATM1 forms a dimer, with each subunit containing six transmembrane (TM) domains fused to the nucleotide-binding domain. Interestingly the crystal structure was obtained in complex with oxidized glutathione (GSSG) suggesting glutathione or its conjugates as substrates for this transporter. Functional activity of *Na*Atm1p by

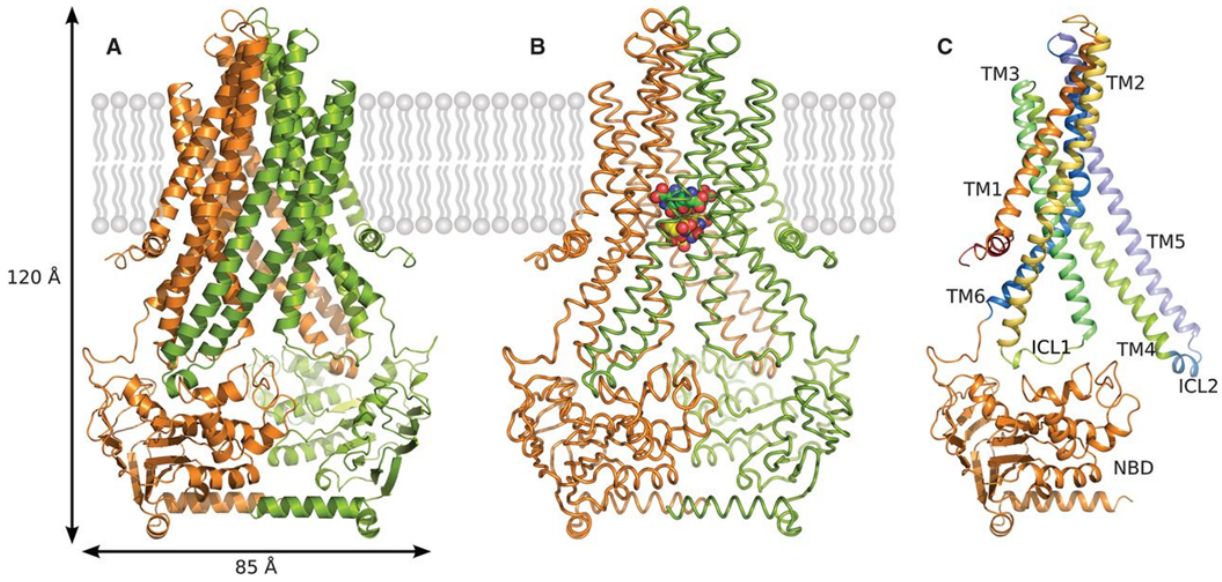

Fig. 1.5. Structural representations of *Na*Atm1p. (**A**) Ribbon diagram representing the dimeric structure of *Na*Atm1p, viewed normal to the molecular two-fold axis with the membrane-spanning domains and NBDs oriented toward the top and bottom, respectively. The approximate position of the membrane is designated by the gray bilayer, with the periplasm- and cytoplasm-facing surfaces toward the top and bottom, respectively. (**B**) Binding sites for GSSG illustrated in the same orientation as (A), with the ligand depicted as space-filling models; primary and secondary binding sites are represented by green and yellow carbons, respectively. (**C**) Representation of one *Na*Atm1p subunit emphasizing the secondary structure arrangement. This figure has been reproduced from Lee et al., 2014, using publisher's permission.

measuring the ability of ligands to stimulate the ATPase activity of *Na*Atm1p suggested that highest activity (*Kcat/Km*) was observed with metallated GSH complex (Ag-GSH and Hg-GSH), aromatic hydrocarbon–conjugated, and oxidized GSH derivatives suggesting that the heavy metal toxicity resistance by *Na*Atm1p is likely through export of metallated GSH complexes out of cell.

In the crystal structure, TM5 and TM6 and their dimeric equivalent TM11 and TM12 form the majority of the interactions with the GSSG molecule. Critical interactions are formed between the free $–NH_2$ and -COOH groups of GSSG and the protein and includes residues Tyr156 (TM3), Asn269, Gln272 (TM5), Asp316, Gly319 and Met320 (TM6). The residues on TM3 and TM6 that interact with GSSG are positioned near helical irregularities, and represents the regions that may undergo conformational changes during the transport cycle. In addition, the nonpolar interactions are primarily formed by the side chains of the broadly conserved residues Leu265 and Leu268 against the Gly moiety of GSSG, and by the more variable side chains of Met317 and Met320 interacting near the disulfide bond. In addition to this, a second, lower-occupancy binding site for GSSG toward cytoplasmic surface is also present although the actual physiological relevance of this site is not known. The binding site involves conserved Arg206 and Arg323, along with a variable Arg210. In addition, two additional Arg (Arg91 and Arg313) residues are positioned in the translocation pathway toward the periplasmic side that may be involved in the transient binding of ligands in the outward facing orientation.

E. coli CydDC, Cysteine/Glutathione Exporter:

An ABC dependent glutathione efflux pump, in *E. coli* has also been reported (Pittman *et al.* 2005). CydDC is a heterodimeric protein (consisting of two subunits CydC and CydD) and in contrast to NaATMp which have higher preference for glutathione conjugates, this protein mediates reduced glutathione and cysteine efflux in an ATP-dependent manner and is crucial for the maintaining the redox-homeostasis in the periplasm (Kaluzna & Bartosz 1997).

1.3.3. Glutathione Transporters in the Mammalian Solute Carrier family (Table 1.4)

1.3.3.1. Plasma membrane Organic Anion Transporter (Oat1, Oat3) and Sodium Dependent Dicarboxylate Carrier 2 (NaC2):

In mammals, although virtually all cells can synthesize GSH, the liver is the primary source of extracellular glutathione. Hepatocytes release one half of their glutathione in plasma and the other half into the bile. Thus, the GSH concentration within liver is in dynamic equilibrium between synthesis and efflux into bile and blood plasma. Biliary glutathione serve as means of hepatic detoxification and is degraded into its constituent amino acids and is returned to liver through entero-hepatic circulation for resynthesis whereas about 80% of the plasma GSH is taken by the kidneys through basolateral uptake (two-thirds) or glomerular filtration and is the major site for degradation and turnover. However, intact glutathione uptake by the putative transporters has been controversial (Lash 2009) .

Evidence of GSH transport across these membranes have been obtained from pharmacological and toxicological studies where GSH was found to be involved in nephroprotection during toxicant exposures (Reviewed by Lash, 2009). Studies with other tissues such as jejunal epithelial cells of rat small intestine, epithelial cells of rat lung and retinal pigment epithelial cells also showed GSH import suggesting that GSH uptake across the basolateral membrane is a basic property of the epithelial cells. Further isolated basolateral membrane vesicles and proximal tubular cells were tested for GSH transport in presence of inhibitors of sodium independent organic anion transporters (OATs) and sodium dependent dicarboxylate carrier 2 (NaC2). Three carrier protein Oat1p (SLC22A6), Oat3p (SLC22A8) and NaC2p (SLC13A3) showed inhibition of glutathione uptake in presence of their specific inhibitors providing indirect evidence for the involvement of specific transporters in GSH uptake. Oat1p and Oat3p are electroneutral exchangers having broad-substrate specificity mediating the uptake of organic anions in exchange for 2-oxoglutarate (2-OG). However, of these three, only Oat3p was reconstituted in liposomes and was shown to transport intact GSH in exchange of 2-oxoglutarate (2-OG) and p-aminohippurate (PAH) (Lash 2009) .

Table 1.4 List of glutathione transporters of other families

Transporter	Organism	Localization	Known substrates
Mammalian Solute Carrier family			
Oat1p (SLC22A6)	Mammals	Plasma membrane	Efflux: GSH, Drugs, Xenobiotics Influx: methotrexate, GSH, Acetylsalicylate, Urate
Oat1p3 (SLC22A8)	Mammals	Plasma membrane	Efflux: GSH, Drugs, Xenobiotics Influx: p-Aminohippurate (PAH),2-OG, GSH
NaC3 (SLC13A3)	Mammals	Plasma membrane	Citrate, Succinate, GSH, α-Ketoglutarate
DCC (SLC25A10)	Mammals	Mitochondrial inner membrane	GSH *Km* = 2.8 mM, Malonate, Glutamate
OGC (SLC25A11)	Mammals	Mitochondrial inner membrane	GSH, Glutamate, 2-Oxoglutatrate
MFS Superfamily			
Glutathione-proton exchanger proteins Gex1p Gex2p	*S. cerevisiae*	Plasma membrane Vacuolar membrane	GSH efflux
Plastid CLT1-3	*A. thaliana*	Plastids	GSH efflux from chloroplast to cytoplasm

However increasing lines of evidence seems to suggest that an uptake transporter for freely available GSH in the extracellular medium is absent in mammalian cells (Ballatori *et al.* 2009). As the catabolism of GSH is a rapid phenomenon, where GSH is cleaved by ectoenzyme, γ-glutamyltranspeptidase (γ-GT) into Glu and Cys-Gly followed by uptake (either Cys-Gly and Glu or Cys-Gly further acted upon by ecto-dipeptidases to release Cys, Gly) of the constituent inside the cell and re-synthesis of glutathione (Frey *et al.* 2007). The possibility thus exist that, in mammalian cells uptake of GSH moiety does not occur and only the constituent moieties are taken up followed by re-synthesis. Once GSH is exported out of the cell it is rapidly degraded. The half-life of GSH in blood plasma ranges from few seconds to minutes (Meister & Tate 1976; Meister & Anderson 1983). This leads to low extracellular GSH levels (≈ 10μM) in circulation which is about three fold less in magnitude as compared to intracellular concentrations. Thus for GSH uptake by a transporter at such low concentrations the transporter needs to have a very high affinity for GSH and would have to overcome the large outwardly directed glutathione electrochemical gradient in order to facilitate uptake. None of the putative GSH transporter identified for uptake exhibit the necessary kinetic properties for intact glutathione uptake under physiological conditions (Ballatori *et al.* 2009).

The OATP family of transporters has been suggested to function primarily in efflux of organic solutes from the cell (Hagenbuch & Meier 2003). Rat OATPs has been shown to also carry out the transport of glutathione conjugates, leukotriene C4 (LTC-4) and S-(2, 4-dinitrophenyl)-glutathione (DNP-SG) in *Xenopus laevis* oocytes injected with Oatp1 complementary RNA (cRNA) (Li *et al.*, 1998). This suggests that rat OATP1 and OATP2 might function as GSH/organic solute exchanger, coupling glutathione efflux to uptake of organic solutes. However, no role of human homologues of OATP in glutathione efflux or energizing uptake of organic solutes has been investigated (König *et al.* 2000; Nozawa *et al.* 2004; Mahagita *et al.* 2007).

1.3.3.2. Mitochondrial Dicarboxylate Carriers (DCC) and 2-Oxoglutarate Carriers (OGC):

In case of mitochondria, two members of anion carriers, dicarboxylate carriers (DCC) and 2-oxoglutarate carriers (OGC) present in the inner mitochondrial membrane have been shown to transport glutathione in the epithelial cells from rat

kidney cortex (Lash 2005, 2006). Considering that glutathione exists as an anion at physiological pH conditions, it was anticipated that one (or more) of the 8 anion carrier proteins in the inner mitochondrial membrane might be involved in glutathione translocation into the matrix. By assessing the effect of substrate and specific inhibitors of these known anion carriers on glutathione uptake in isolated mitochondria, it was established that DCC which mediates the electroneutral exchange of dicarboxylates for inorganic phosphate and OGC which can exchange 2-oxoglutarate for other dicarboxylates, respectively constitute the low affinity, high capacity glutathione uptake in the mitochondria of kidney (Chen & Lash 1998). Direct evidence for a role in glutathione uptake by these carriers was obtained by reconstitution of these partially purified mitochondrial carriers proteins into proteoliposomes (Chen *et al.* 2000). Subsequent study on glutathione uptake into liver mitochondria revealed that DCC and OGC together accounted for only 45-50% of the total glutathione uptake against 70-80% contribution in kidney mitochondria (Zhong *et al.* 2008). This study suggests tissue specific difference in the role of these carriers in glutathione uptake into mitochondria and also raise the possibility of existence of some yet "unknown" glutathione transporters.

However, very recently the role of these transporters in GSH uptake in mitochondria was disputed (Booty *et al.* 2015). Human DIC and OGC were overexpressed in *Lactococcus lactis* and isolated membrane vesicles were fused with liposomes that were loaded with substrates to measure exchange with radiolabelled substrates. Both DIC and OGC transported their canonical substrates and were inhibited by known substrate inhibitors but this transport was not inhibited by GSH or glutathione disulphide. Further, no detectable [^{35}S] GSH transport was observed suggesting that these carriers do not transport GSH. Hence, the effects seen in the previous studies of overexpression of OGC and DIC within cells are likely to be secondary consequences of metabolite redistribution between mitochondria and the cytosol (Booty *et al.* 2015). However, in response to this study, Lash, 2015 argued that the authors used *Lactococcus lactis* system for overexpression and characterization of human DIC and OGC, which is an established experimental system to examine yeast carriers but not the mammalian carrier proteins. In addition, although the impact of secondary effects cannot be excluded but to conclude that only such secondary effects and not the transport is responsible for increased GSH concentrations in the mitochondria by overexpression of these transporters is not logical (Lash 2015).

1.3.4. Glutathione Transporters in the Major Facilitator Superfamily (Table 1.4):

1.3.4.1. Yeast Glutathione Exchanger Protein, Gex1p:

Recently Gex1p and its paralog Gex2p, localized in vacuolar and plasma membrane of yeast has been shown as a glutathione/proton antiporter (Dhaoui *et al.* 2011). These proteins belong to the major facilitator superfamily (MFS) of transporters and display similarities to the *ARN* (Aft1-regulon) family of siderophore transporters although a *gex1Δgex2Δ* strain displayed no defect in siderophore uptake. The *gex1Δgex2Δ* strain grows poorly in medium containing heavy toxic metal cadmium. In addition, Gex1p overexpressing strain had low cadmium content as compare to the control strain suggesting the role of Gex1p in cadmium export from the plasma membrane. Presence of Gex1 at the vacuolar membrane may thus mediate cadmium import into the vacuolar lumen for cadmium detoxification. In addition cells overproducing Gex1p were found to have low intracellular glutathione content with increased acidification, whereas the deletion mutant accumulated intracellular glutathione suggesting Gex1p as a proton/ glutathione antiporter. At the vacuolar membrane, H^+ is suggested to be exported into the cytosol and glutathione imported through the vacuolar membrane. This export facilitates cadmium detoxification when cells are grown in the presence of this metal. However the role of these proteins in glutathione efflux needs to be substantiated with direct measurements of glutathione transport.

GEX1 expression was induced under conditions of iron depletion and after H_2O_2 treatment. Gex1p was found to localize mostly at the vacuolar membrane and to a lesser extent, at the plasma membrane. The production and location of Gex1p probably depend on the presence of both substrates. Early in the exponential growth phase, Gex1p is present mostly at the plasma membrane and mediates cytosol acidification and the extrusion of glutathione. The low pH of the cytosol induces acidification of the yeast vacuole, probably inducing the targeting of Gex1p to the vacuolar membrane, where it can import glutathione and export H^+ out of the vacuolar lumen (Dhaoui *et al.* 2011).

1.3.4.2. Plant Plastid CLT1-3:

The malarial parasite Chloroquine Resistance Transporter (PfCRT) homologue of *Arabidopsis thaliana* belonging to MFS family has recently been demonstrated to transport glutathione. Plastid and cytosolic glutathione thiol pools are closely integrated and this integration requires a family of three plastid thiol transporters

(CLT1-3) and a homologue of the *Plasmodium falciparum* chloroquine-resistance transporter, PfCRT. *Arabidopsis* mutants lacking these transporters are heavy metal-sensitive, GSH-deficient, and hypersensitive to *Phytophthora* infection confirming a direct requirement for GSH homeostasis in defense responses. Compartment-specific measurements of the glutathione redox potential using redox-sensitive GFP showed that knockout of the entire transporter family resulted in a more oxidized glutathione redox potential in the cytosol, but not in the plastids, indicating the GSH-deficient phenotype is restricted to the cytosolic compartment. Expression of these transporters in *Xenopus* oocytes confirmed that these proteins can mediate glutathione uptake (Maughan *et al.* 2010).

1.4. Mechanism of Proton-Coupling in the MFS Proton Symporters:

In this section, I discuss the current understanding of proton binding and transport by the proton coupled symporters belonging to the major facilitator superfamily (MFS) as these are mechanistically related to Hgt1p, in a sense of being proton coupled. LacY, lactose-proton symporter, has been discussed in detail as this protein have been rigorously examined for almost half a century using different approaches and serve as a paradigm for the study of other proton coupled transporters.

The MFS superfamily proteins are ubiquitously present in all kingdoms of life (Pao *et al.* 1998; Reddy *et al.* 2012). These transporters function in a variety of important physiological process and have been the subject of numerous structure-function studies. They typically contain 12 transmembrane (TM) helices, although some members have 14 TM helices (Kaback 2005). The substrate transport require alternate exposure of the binding sites to either side of the membrane whereas the translocation of protons involves protonation and deprotonation of certain residues including Asp/Glu/His (most frequently) or Arg/Lys/Tyr (less frequently) (Yan 2013).

This “alternative access” model of transport was hypothesized several years ago for membrane transporters and is now widely accepted (Jardetzky 1966; Tanford 1982). However for this “alternating access” model several mechanisms have been proposed that includes the rocker-switch mechanism, gated-pore mechanism, elevator mechanism and toppling mechanism of transport (Slotboom 2014). Multiple snapshots of several non-MFS transporters have been captured during the transport cycle supporting this model of transport (Oldham *et al.* 2008; Rees *et al.* 2009; Morth

et al. 2011; Palmgren & Nissen 2011; Shi 2013). In contrast, for a long time no MFS transporter crystal structure was available in more than one conformation. Visualization of the alternate access model of transport by MFS family of proteins was therefore largely derived from biochemical and biophysical studies. Since these transporters undergo cycles of conformational change to achieve the alternating access of substrate across the membrane, obtaining structures of multiple conformations of a given protein was required to better understand its transport mechanism. Recently however structures for more than one conformational state of the LacY, XylE (D-xylose:proton symporter), NarU (nitrate:nitrite antiporter) and the MelB (melibiose:cation symporter) have been obtained resulting in a more mechanistic understanding of this superfamily of transporters (Quistgaard *et al.* 2013; Yan *et al.* 2013; Kumar *et al.* 2014; Wisedchaisri *et al.* 2014; Yan 2015).

1.4.1. The Lac Permease of *E. coli*, a Paradigm for the Study of Proton Coupled Symporters:

The lactose permease (LacY) of *E coli* belongs to the major facilitator superfamily (MFS) and has been at the forefront for the study of polytopic membrane proteins catalyzing substrate proton symport (Abramson *et al.* 2004; Kaback 2015). LacY is a 12 transmembrane domain, galactoside/H^+ symporter, comprising of 417 amino acid residues. All these residues were individually mutated in Cys-less LacY and studied by SCAM which identified only six irreplaceable residues for active transport. Efflux, exchange and counterflow experiments on purified proteins in absence of proton gradient are critical for the identification of proton binding residues and to delineate the kinetic scheme of the transport cycle. In these experiments, before measuring transport, membrane vesicles or the proteoliposomes were concentrated and equilibrated with radioactive lactose at a given pH and then rapidly diluted into buffer of the same pH in the absence (efflux) or presence of cold lacotose (exchange). In counterflow experiments the concentrated solution of cold lactose at high concentrations are equilibrated passively followed by rapid dilution of the vesicles in buffer containing radioactive lactose (Kaback *et al.* 2001). Based on these studies Glu126 (TMD4) and Arg144 (TMD5) was found to be crucial for substrate binding, whereas, Glu269 (TMD8) was suggested to be involved in both substrate binding and

proton translocation. In addition Arg302 (TMD9), His322 and Glu325 (TMD10) was found to be important for H^+ translocation (Kaback 2005).

The initial 3D X-ray crystal structures of LacY (conformationally restricted mutant, C154G and WT LacY) consisted of 12 TMDs that are organized into two pseudosymmetrical six helix bundles that surround a large interior hydrophilic cavity opening towards the cytoplasmic side (Abramson *et al.* 2003; Guan & Kaback 2006; Mirza *et al.* 2006; Guan & Kaback 2007). LacY contains a single galactoside binding pocket. The sugar binding site and the residues probably involved in H^+ translocation that were identified from earlier studies were present approximately in middle of the helix bundle and distributed at the apex of the hydrophilic cavity. The side chains important for substrate recognition are predominantly present in the N-terminal helix bundle whereas the side chains that are involved in proton binding and translocation are mainly in the C-terminal helix bundle (Smirnova *et al.* 2009). The periplasmic side of LacY is tightly packed, and the sugar binding site is not accessible from that side of the molecule (Smirnova *et al.* 2009). These structural studies in combination with other biochemical and spectroscopic studies suggested that an "alternating access" model functional through a "rocker-switch" like mechanism, where the two pseudo-symmetrical six helix bundle rotate against each other around the middle of LacY, exposing the substrate binding site alternatively to either side of the membrane (Kaback 2015).

The affinity (*Kd*) of WT LacY for galactosides varies with pH (Smirnova *et al.* 2008; Smirnova *et al.* 2009; Smirnova *et al.* 2011). In addition, no change in the ambient pH was observed during sugar binding to purified LacY protein in detergent suggesting that LacY is protonated over the physiological pH range. Hence, a symmetrical ordered kinetic mechanism of transport in which the protonation precedes the sugar binding on one side of the membrane followed by sugar and proton dissociation on the other side. Hence, the mechanism of sugar transport by LacY consist of the following steps (Fig 1.6) (Kaback 2015):

a) In the ground state, LacY is protonated (possibly at Glu325)

b) In this conformation, ligand binds at the interface between TMD4 (Glu126) and TMD5 (Arg144 and Cys148) at the outer surface of the membrane with relatively high affinity.

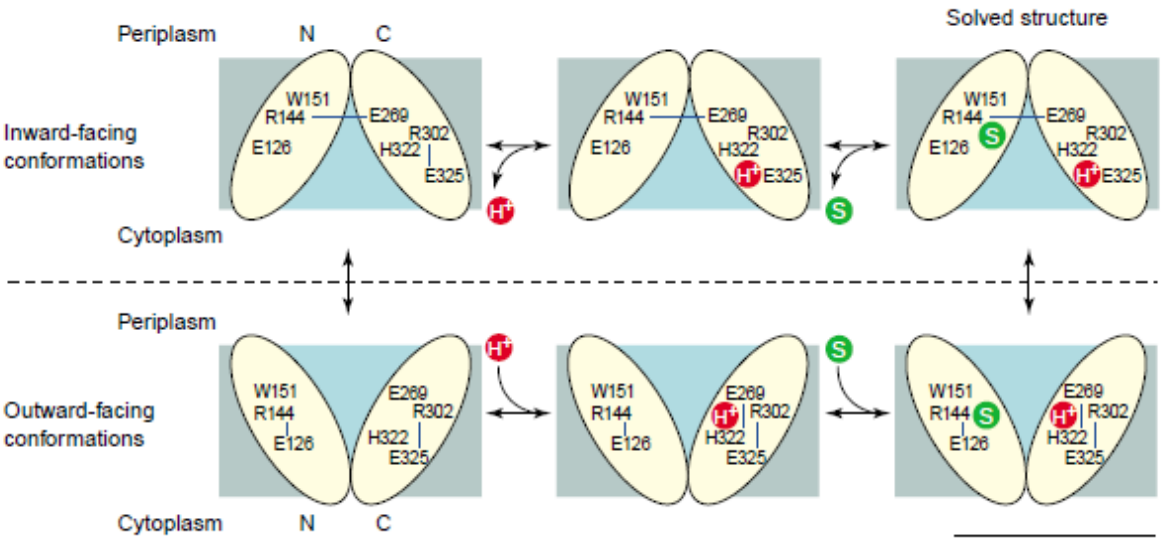

Figure 1.6: Proposed mechanism of transport by LacY: The N- and C-terminal domains are represented as yellow ovals and the water-filled cavity is represented as a light blue area. The critical residues are labeled, and hydrogen bonds are shown as blue lines. H^+ and the substrate (S) are shown as red and green circles, respectively. This figure has been reproduced from DeFelice, 2004, using publisher's permission.

c) This substrate binding induces a conformational change in the protein and reorientation of the sugar binding site to the inner surface with a decrease in affinity.

d) Sugar dissociates, releasing the energy of binding.

e) A conformational change allows Arg302 to deprotonate Glu325.

f) After releasing the proton, transition take place from inside facing empty transporter toward the outward-facing conformation to re-initiate the cycle.

1.4.2. Other MFS Proton-Coupled Symporters:

The other proton coupled MFS symporters and the residues involved in proton transport includes:

A) In Fucose/H^+ symporter (**FucP**) of *E. coli*, Asp46 (TMD1) and Glu135 (TMD4) are the primary conserved residues along the transport path that are capable of protonation and deprotonation. Using *in vivo* uptake and *in vitro* counterflow experiments, Asp46 was found to be irreplaceable for proton coupling but was not involved in the substrate binding whereas Glu135 was found to be involved in substrate binding and not proton coupling (Dang *et al.* 2010).

B) In the proton dependent oligopeptide transporter (POT) subfamily, which includes **PepT$_{St}$** of *Streptococcus thermophiles*, contains a conserved ExxERFxYY (TM1) motif that was predicted to be involved in both substrate binding and proton translocation. Based on proton driven and peptide driven counterflow assays in liposome reconstituted with mutants of this motif identified, Glu22, Glu25, Arg26, and Tyr30 to be involved in proton translocation, and Tyr29 important for the peptide specificity. In addition the Lys126 (TMD4) was also found to be essential for proton dependent substrate transport (Solcan *et al.* 2012; Doki *et al.* 2013).

C) In the peptide transporter (**PepT$_{So}$**) from *Shewanella oneidensis*, *in vivo* peptide uptake assay based on other characterized proton coupled symporters (LacY of *E. coli* and human peptide transporters, PepT1 and PepT2) identified a partially conserved His61 and Asp316 to be essential for proton binding and the opening of the extracellular gate (Newstead *et al.* 2011).

1.5. OBJECTIVES OF THE PRESENT STUDY.

As discussed in the general introduction, glutathione is critical for cell growth in almost all eukaryotes and plays numerous role in cellular metabolism under normal and stress conditions. Glutathione transporters play a very important role in glutathione homeostasis and thus understanding these transporters is very important. Although, the structures of some of the eukaryotic glutathione transporters have been solved, they have been shown to bind and transport glutathione conjugates with higher affinity as compared to reduced glutathione (GSH). In contrast Hgt1p (Opt1p) of *Saccharomyces cerevisiae* was reported as a high-affinity transporter of reduced glutathione. Although significant inhibition in radioactive glutathione uptake was observed with glutathione-conjugates, a detailed kinetic study with glutathione-conjugates has not been undertaken with Hgt1p, and we felt such a study was needed.

Hgt1p is currently predicted to have 12 transmembrane domains (TMDs) although some prediction tools have suggested 13 or 14 TMDs. As a comprehensive TMD scanning was planned, it prompted us to also revisit the topology determination.

To identify the residues important for glutathione binding and transport by Hgt1p, a few structure-function studies have been carried out but not all TMDs were investigated in detail. Transport mediated by Hgt1p is also proton-dependent and the identification of residues involved in proton transport is thus a first step to be able to understand the mechanism of transport by Hgt1p. However no effort has been made towards this goal. Therefore, in the current thesis, I have attempted to consolidate and extend earlier studies of Hgt1p to comprehensively map the residues that are important for substrate and proton transport by Hgt1p.

With this background, the objectives of the current thesis have been framed as follows:

1. Determination of the substrate specificity of Hgt1p towards different glutathione-conjugates and glutathione analogs.

2. Alanine scanning mutagenesis of TMD2, TMD3, TMD4, TMD6, TMD10, TMD12 and TMD13 of Hgt1p and further evaluation of all the 269 TMD mutants for their role in glutathione transport.

3. Identification of residues involved in proton binding and transport by Hgt1p.

CHAPTER 2:

Materials and Methods

SECTION A: MATERIALS

2.1. CHEMICALS AND REAGENTS

Chemicals used in this study were of analytical grade and procured from commercial sources. Growth medium components, fine chemicals and reagents were obtained from Sigma Aldrich USA, Difco USA, Merck India, USB Corporation USA and HiMedia India. Oligonucleotides were obtained from Sigma India and Integrated DNA Technologies, India. Vent DNA polymerase, Phusion® DNA polymerase, restriction enzymes and DNA-modifying enzymes, their buffers, dNTPs and protein molecular weight markers were purchased from New England Bio Labs, USA. DNA molecular weight markers were procured from Biocheme, India. Glutathione, S-methylglutathione, S-hexylglutathione, S-decylglutathione, S-lactoylglutathione, glutathione sulphonate, oxidized glutathione, met- enkephalin and γ-Glu-Cys were obtained from Sigma, USA. Peptides (β-Asp-Cys-Gly, γ-Glu-Ser-Gly, γ-Glu-Cys-Ala, γ-Glu-Cys-β-Ala, γ-Glu-Cys-Ala-$CONH_2$ and γ-Glu-Cys-$CONH_2$) were custom synthesized to >95% purity with peptide mass verified were obtained from Pepmic, China. Membrane filters and glass fiber filters were purchased from Advanced Microdevices, India. Plasmid mini-prep and gel-extraction kits were obtained from Thermo Scientific, USA or Qiagen, USA. Acid washed glass beads (425 to 600 µm) were procured from Sigma, USA. Hybridization nitrocellulose membrane (filter type 0.45µm) and Luminata^{TM} forte Western HRP substrate were purchased from Millipore. HA-tagged mouse monoclonal antibody and horse anti-mouse HRP-linked antibody were procured from Cell Signalling Technology, USA. Zymolyase enzyme was obtained from Seikagaku, Japan and lyticase was procured from Sigma, USA. Alexa Fluor® 488-conjugated goat anti-mouse antibody was obtained from Molecular Probes, USA. Vectashield Antifade Mounting Medium was purchased from Vector laboratories, USA. [^{35}S] Glutathione, 100µCi (3.7MBq) was obtained from Perkin Elmer, USA.

2.2. OLIGONUCLEOTIDES

The list of various oligonucleotide primers used in this study is listed in **Table 2.1.**

2.3. STRAINS AND PLASMIDS

The *E. coli* strain and the list of various yeast strains used in the study are given in **Table 2.2**. The list of various plasmids used in this study is given in **Table 2.3.**

Table 2.1

List of Oligonucleotides and their sequences in this study

Oligomer	Sequence (5' to 3')
TMD2	
L134A FOR	CCCTGAGATATCCATCGGCAGAGATCAACTTCCTTG
L134A REV	CAAGGAAGTTGATCTCTGCCGATGGATATCTCAGGG
I136A FOR	GATATCCATCGCTAGAGGCCAACTTCCTTGTTGCACAAG
I136A REV	CTTGTGCAACAAGGAAGTTGGCCTCTAGCGATGGATATC
F138A FOR	CCATCGCTAGAGATCAACGCCCTTGTTGCACAAGTTGTTTGC
F138A REV	GCAAACAACTTGTGCAACAAGGGCGTTGATCTCTAGCGATGG
L139A FOR	CGCTAGAGATCAACTTCGCTGTTGCACAAGTTGTTTGCTACCC
L139A REV	GCAAACAACTTGTGCAACAGCGAAGTTGATCTCTAGCGATGG
V140A FOR	GCTAGAGATCAACTTCCTTGCTGCACAAGTTGTTTGCTACCC
V140A REV	GGTAGCAAACAACTTGTGCAGCAAGGAAGTTGATCTCTAGCG
A141G FOR	GAGATCAACTTCCTTGTTGGACAAGTTGTTTGCTACCC
A141G REV	GGGTAGCAAACAACTTGTCCAACAAGGAAGTTGATCTC
Q142A FOR	CTTCCTTGTTGCAGCAGTTGTTTGCTACCCAATTGG
Q142A REV	GTAGCAAACAACTGCTGCAACAAGGAAGTTGATCTCTAGCG
V143A FOR	CTTCCTTGTTGCACAAGCTGTTTGCTACCCAATTGGTAGG
V143A REV	CCAATTGGGTAGCAAACAGCTTGTGCAACAAGGAAGTTGATC
V144A FOR	CCTTGTTGCACAAGTTGCTTGCTACCCAATTGGTAGG
V144A REV	CCTACCAATTGGGTAGCAAGCAACTTGTGCAACAAGGAAG
C145A FOR	GTTGCACAAGTTGTTGCCTACCCAATTGGTAGGATACTGG
C145A REV	CCTACCAATTGGGTAGGCAACAACTTGTGCAACAAGGAAG
Y146A FOR	GCACAAGTTGTTTGCGCCCCAATTGGTAGGATACTGGC
Y146A REV	CCAGTATCCTACCAATTGGGGCGCAAACAACTTGTGCAAC
P147A FOR	GCACAAGTTGTTTGCTACGCAATTGGTAGGATACTGGC
P147A REV	GCCAGTATCCTACCAATTGCGTAGCAAACAACTTGTGC
I148A FOR	GTTGTTTGCTACCCAGCTGGTAGGATACTGGCTCTCTTGCC
I148A REV	GAGCCAGTATCCTACCAGCTGGGTAGCAAACAACTTGTGC
G149A FOR	GTTGTTTGCTACCCAATTGCTAGGATACTGGCTCTCTTGCCC
G149A REV	GAGAGCCAGTATCCTAGCAATTGGGTAGCAAACAACTTGTGC
I 151A FOR	GCTACCCAATTGCTAGGGCACTGGCTCTCTTGCCCGACTGG
I151A REV	CGGGCAAGAGAGCCAGTGCCCTAGCAATTGGGTAGCAAAC
L152A FOR	CCCAATTGGTAGGATAGCGGCTCTCTTGCCCGACTGGAAG

L152A REV	CCAGTCGGGCAAGAGAGCCGCTATCCTACCAATTGGGTAGC
A153G FOR	CCAATTGGTAGGATACTGGGTCTCTTGCCCGACTGGAAGTG
A153G REV	CCAGTCGGGCAAGAGACCCAGTATCCTACCAATTGGGTAGC
L154A FOR	GGTAGGATACTGGCTGCCTTGCCCGACTGGAAGTGTTC
L154A REV	CACTTCCAGTCGGGCAAGGCAGCCAGTATCCTACCAATTGGG
L155A FOR	GGTAGGATACTGGCTCTCGCGCCCGACTGGAAGTGTTC
L155A REV	GAACACTTCCAGTCGGGCGCGAGAGCCAGTATCCTACC
TMD3	
A179G FOR	ACCAAAAAGGAACACGGCGTGGTCACAATTGCCGTGGC
A179G REV	CGGCAATTGTGACCACGCCGTGTTCCTTTTTGGTAAATG
V180A FOR	CCAAAAAGGAACACGCCGCGGTCACAATTGCCGTGGCGC
V180A REV	CCACGGCAATTGTGACCGCGGCGTGTTCCTTTTTGG
V181A FOR	AAGGAACACGCCGTGGCCACAATTGCCGTGGCGCTTAC
V181A REV	GCGCCACGGCAATTGTGGCCACGGCGTGTTCCTTTTTGG
T182A FOR	AAGGAACACGCCGTGGTCGCAATTGCCGTGGCGCTTAC
T182A REV	AGTAAGCGCCACGGCAATTGCGACCACGGCGTGTTCC
I183A FOR	GGAACACGCCGTGGTCACAGCTGCCGTGGCGCTTACTTCC
I183A REV	GGAAGTAAGCGCCACGGCAGCTGTGACCACGGCGTGTTCC
A184G FOR	CACGCCGTGGTCACAATTGGCGTGGCGCTTACTTCCTCTAC
A184G REV	GAGGAAGTAAGCGCCACGCCAATTGTGACCACGGCGTG
V185A FOR	CCGTGGTCACAATTGCCGCGGCGCTTACTTCCTCTACTGC
V185A REV	GTAGAGGAAGTAAGCGCCGCGGCAATTGTGACCACGGCG
A186G FOR	GTGGTCACAATTGCCGTGGGGCTTACTTCCTCTACTGC
A186G REV	GCAGTAGAGGAAGTAAGCCCCACGGCAATTGTGACCACGG
L187A FOR	GTCACAATTGCCGTGGCGGCTACTTCCTCTACTGCATACGC
L187A REV	CGTATGCAGTAGAGGAAGTAGCCGCCACGGCAATTGTG
S189A FOR	ATTGCCGTGGCGCTTACTGCCTCTACTGCATACGCTATG
S189A REV	CATAGCGTATGCAGTAGAGGCAGTAAGCGCCACGGCAATTG
T191A FOR	CGCTTACTTCCTCTGCTGCATACGCTATGTACATTTTG
T191A REV	ATGTACATAGCGTATGCAGCAGAGGAAGTAAGCGCCAC
A192G FOR	GCGCTTACTTCCTCTACTGGATACGCTATGTACATTTTGAAC
A192G REV	CAAAATGTACATAGCGTATCCAGTAGAGGAAGTAAGCGCC
Y193A FOR	GCTTACTTCCTCTACTGCAGCCGCTATGTACATTTTGAACGC
Y193A REV	CGTTCAAAATGTACATAGCGGCTGCAGTAGAGGAAGTAAGCG
A194G FOR	CTTCCTCTACTGCATACGGTATGTACATTTTGAACGCC

A194G REV	CGTTCAAAATGTACATACCGTATGCAGTAGAGGAAGTAAGC
M195A FOR	CCTCTACTGCATACGCTGCGTACATTTTGAACGCCCAG
M195A REV	CTGGGCGTTCAAAATGTACGCAGCGTATGCAGTAGAGG
Y196A FOR	CTACTGCATACGCTATGGCCATTTTGAACGCCCAGGGAAG
Y196A REV	CTGGGCGTTCAAAATGGCCATAGCGTATGCAGTAGAGG
I197A FOR	CTGCATACGCTATGTACGCTTTGAACGCCCAGGGAAGC
I197A REV	CCCTGGGCGTTCAAAGCGTACATAGCGTATGCAGTAG
L198A FOR	GCATACGCTATGTACATTGCGAACGCCCAGGGAAGCTTTTAC
L198A REV	GCTTCCCTGGGCGTTCGCAATGTACATAGCGTATGCAG
N199A FOR	TACGCTATGTACATTTTGGCCGCCCAGGGAAGCTTTTACAAC
N199A REV	GTAAAAGCTTCCCTGGGCGGCCAAAATGTACATAGCGTATG
A200G FOR	GCTATGTACATTTTGAACGGCCAGGGAAGCTTTTACAACATG
A200G REV	GTAAAAGCTTCCCTGGCCGTTCAAAATGTACATAGCGTATG
TMD4	
G212A FOR	CATGAAACTTAATGTCGCATATCAGTTCTTGTTGGTTTGG
G212A REV	CAACAAGAACTGATATGCGACATTAAGTTTCATGTTG
Y213A FOR	CATGAAACTTAATGTCGGAGCTCAGTTCTTGTTGGTTTG
Y213A REV	CCAAACCAACAAGAACTGAGCTCCGACATTAAGTTTCATG
Q214A FOR	CTTAATGTCGGATATGCGTTCTTGTTGGTTTGGACATC
Q214A REV	CCAAACCAACAAGAACGCATATCCGACATTAAGTTTCATG
F215A FOR	CTTAATGTCGGATATCAGGCCTTGTTGGTTTGGACATCTC
F215A REV	GTCCAAACCAACAAGGCCTGATATCCGACATTAAGTTTC
L216A FOR	GTCGGATATCAGTTCGCGTTGGTTTGGACATCTCAAATG
L216A REV	GAGATGTCCAAACCAACGCGAACTGATATCCGACATTAAG
L217A FOR	GGATATCAGTTCTTGGCGGTTTGGACATCTCAAATGATTGG
L217A REV	CATTTGAGATGTCCAAACCGCCAAGAACTGATATCCGAC
V218A FOR	GATATCAGTTCTTGTTGGCTTGGACATCTCAAATGATTGGTTATGG
V218A REV	CATTTGAGATGTCCAAGCCAACAAGAACTGATATCCGACATTAAG
W219A FOR	CAGTTCTTGTTGGTTGCGACATCTCAAATGATTGGTTATGG
W219A REV	CCAATCATTTGAGATGTCGCAACCAACAAGAACTGATATCC
T220A FOR	GTTCTTGTTGGTTTGGGCATCTCAAATGATTGGTTATGG
T220A REV	CCAATCATTTGAGATGCCCAAACCAACAAGAACTG
S221A FOR	CTTGTTGGTTTGGACAGCTCAAATGATTGGTTATGG
S221A REV	CCAATCATTTGAGCTGTCCAAACCAACAAGAACTG
M223A FOR	GTTTGGACATCTCAAGCGATTGGTTATGGTGCTGCAGG

M223A REV	CAGCACCATAACCAATCGCTTGAGATGTCCAAACCAAC
I224A FOR	GTTTGGACATCTCAAATGGCTGGTTATGGTGCTGCAGGTC
I224A REV	GCAGCACCATAACCAGCCATTTGAGATGTCCAAACCAACAAG
G225A FOR	GGACATCTCAAATGATTGCTTATGGTGCTGCAGGTCTTACC
G225A REV	GACCTGCAGCACCATAAGCAATCATTTGAGATGTCCAAACC
Y226A FOR	CATCTCAAATGATTGGTGCTGGTGCTGCAGGTCTTACCAG
Y226A REV	AAGACCTGCAGCACCAGCACCAATCATTTGAGATGTCCAAACC
G227A FOR	CTCAAATGATTGGTTATGCTGCTGCAGGTCTTACCAGAAGATG
G227A REV	CTGGTAAGACCTGCAGCAGCATAACCAATCATTTGAGATGTCC
A228G FOR	TCAAATGATTGGTTATGGTGGTGCAGGTCTTACCAGAAGATGG
A228G REV	CTGGTAAGACCTGCACCACCATAACCAATCATTTGAGATGTCC
A229G FOR	GATTGGTTATGGTGCTGGAGGTCTTACCAGAAGATGGGTCG
A229G REV	CCATCTTCTGGTAAGACCTCCAGCACCATAACCAATC
G230A FOR	GGTTATGGTGCTGCAGCTCTTACCAGAAGATGGGTCGTC
G230A REV	CCATCTTCTGGTAAGAGCTGCAGCACCATAACCAATC
L231A FOR	GTTATGGTGCTGCAGGTGCTACCAGAAGATGGGTCGTC
L231A REV	CCCATCTTCTGGTAGCACCTGCAGCACCATAACCAATC
T232A FOR	ATGGTGCTGCAGGTCTTGCCAGAAGATGGGTCGTCAAC
T232A REV	GACGACCCATCTTCTGGCAAGACCTGCAGCACCATAACC
TMD 6	
V354A FOR	CGCCACACCATTCTACGCCTCCGCCAACACCTATGCATC
V354A REV	GCATAGGTGTTGGCGGAGGCGTAGAATGGTGTGGC
A356G FOR	CACCATTCTACGTCTCCGGCAACACCTATGCATCAGTG
A356G REV	CTGATGCATAGGTGTTGCCGGAGACGTAGAATGGTGTG
T358A FOR:	TTCTACGTCTCCGCCAACGCCTATGCATCAGTGTTGATATTC
T358A REV:	ATATCAACACTGATGCATAGGCGTTGGCGGAGACGTAG
Y359A FOR	CGTCTCCGCCAACACCGCTGCATCAGTGTTGATATTC
Y359A REV	GAATATCAACACTGATGCAGCGGTGTTGGCGGAGAC
A360G FOR	CTCCGCCAACACCTATGGATCAGTGTTGATATTCTTC
A360G REV	GAATATCAACACTGATCCATAGGTGTTGGCGGAGAC
S361A FOR	CCGCCAACACCTATGCAGCAGTGTTGATATTCTTCGTC
S361A REV	GACGAAGAATATCAACACTGCTGCATAGGTGTTGGCGG
V362A FOR	CCAACACCTATGCATCAGCGTTGATATTCTTCGTCATAG
V362A REV	GACGAAGAATATCAACGCTGATGCATAGGTGTTGG
L363A FOR	CACCTATGCATCAGTGGCGATATTCTTCGTCATAGTG

L363A REV	CTATGACGAAGAATATCGCCACTGATGCATAGGTGTTG
I364A FOR	CTATGCATCAGTGTTGGCATTCTTCGTCATAGTGCTG
I364A REV	GCACTATGACGAAGAATGCCAACACTGATGCATAGGTG
F365A FOR	GCATCAGTGTTGATAGCCTTCGTCATAGTGCTGCC
F365A REV	CAGCACTATGACGAAGGCTATCAACACTGATGCATAG
F366A FOR	CATCAGTGTTGATATTCGCCGTCATAGTGCTGCCATGTC
F366A REV	CATGGCAGCACTATGACGGCGAATATCAACACTGATGCATAG
V367A FOR	GTGTTGATATTCTTCGCCATAGTGCTGCCATGTC
V367A REV	GACATGGCAGCACTATGGCGAAGAATATCAACACTGATG
I368A FOR	GTGTTGATATTCTTCGTCGCAGTGCTGCCATGTCTTTATTTTAC
I368A REV	TAAAGACATGGCAGCACTGCGACGAAGAATATCAACAC
V369A FOR	GATATTCTTCGTCATAGCGCTGCCATGTCTTTATTTTAC
V369A REV	GTAAAATAAAGACATGGCAGCGCTATGACGAAGAATATCAAC
L370A FOR	GATATTCTTCGTCATAGTGGCGCCATGTCTTTATTTTACGAATAC
L370A REV	GTAAAATAAAGACATGGCGCCACTATGACGAAGAATATC
P371A FOR	CTTCGTCATAGTGCTGGCATGTCTTTATTTTACGAATACC
P371A REV	CGTAAAATAAAGACATGCCAGCACTATGACGAAGAATATCAAC
C372A FOR	CGTCATAGTGCTGCCAGCTCTTTATTTTACGAATACC
C372A REV	GGTATTCGTAAAATAAAGAGCTGGCAGCACTATGACG
L373A FOR	CATAGTGCTGCCATGTGCTTATTTTACGAATACCTGG
L373A REV	CAGGTATTCGTAAAATAAGCACATGGCAGCACTATGAC
Y374A FOR	CATAGTGCTGCCATGTCTTGCTTTTACGAATACCTGGTATGCC
Y374A REV	CATACCAGGTATTCGTAAAAGCAAGACATGGCAGCACTATGAC
TMD 10	
L591A FOR:	GAAGGTTTCCCCTCGTGCGATCTTTGCCGTTCAAATC
L591A REV	GATTTGAACGGCAAAGATCGCACGAGGGGAAACCTTCATG
I592A FOR	GGTTTCCCCTCGTTTGGCCTTTGCCGTTCAAATCTATG
I592A REV	GATTTGAACGGCAAAGGCCAAACGAGGGGAAACCTTC
F593A FOR	GTTTCCCCTCGTTTGATCGCTGCCGTTCAAATCTATGCCAC
F593A REV	GCATAGATTTGAACGGCAGCGATCAAACGAGGGGAAACC
A594G FOR	CCCCTCGTTTGATCTTTGGCGTTCAAATCTATGCCACTATC
A594G REV	GTGGCATAGATTTGAACGCCAAAGATCAAACGAGGGGAAAC
V595A FOR	CTCGTTTGATCTTTGCCGCTCAAATCTATGCCACTATC
V595A REV	GATAGTGGCATAGATTTGAGCGGCAAAGATCAAACGAGGGG
Q596A FOR	GCCTGATATGATAGTGGCATAGATTGCAACGGCAAAG

Q596A REV	GCCGTTGCAATCTATGCCACTATCATATCAGGCATGGTTAACG
I597A FOR	GATCTTTGCCGTTCAAGCCTATGCCACTATCATATCAG
I59A REV	GATATGATAGTGGCATAGGCTTGAACGGCAAAGATCAAAC
Y598A FOR	CTTTGCCGTTCAAATCGCTGCCACTATCATATCAGGC
Y598A REV	CCTGATATGATAGTGGCAGCGATTTGAACGGCAAAGATC
A599G FOR	TTTGCCGTTCAAATCTATGGCACTATCATATCAGGCATGG
A599G REV	CATGCCTGATATGATAGTGCCATAGATTTGAACGGCAAAG
T600A FOR	GCCGTTCAAATCTATGCCGCTATCATATCAGGCATGGTTAAC
T600A REV	CCATGCCTGATATGATAGCGGCATAGATTTGAACGGCAAAG
I601A FOR	TCAAATCTATGCCACTGCCATATCAGGCATGGTTAAC
I601A REV	GTTAACCATGCCTGATATGGCAGTGGCATAGATTTGAACGG
I602A FOR	CAAATCTATGCCACTATCGCATCAGGCATGGTTAACGTTG
I602A REV	CGTTAACCATGCCTGATGCGATAGTGGCATAGATTTG
G604A FOR	ATGCCACTATCATATCAGCCATGGTTAACGTTGGTGTCC
G604A REV	CACCAACGTTAACCATGGCTGATATGATAGTGGCATAG
M605A FOR	CCACTATCATATCAGGCGCGGTTAACGTTGGTGTCCAG
M605A REV	GGACACCAACGTTAACCGCGCCTGATATGATAGTGGC
V606A FOR	CTATCATATCAGGCATGGCTAACGTTGGTGTCCAGGAATG
V606A REV	TCCTGGACACCAACGTTAGCCATGCCTGATATGATAG
V608A FOR	CATATCAGGCATGGTTAACGCTGGTGTCCAGGAATGGATG
V608A REV	TCCATTCCTGGACACCAGCGTTAACCATGCCTGATATG
G609A FOR	CAGGCATGGTTAACGTTGCTGTCCAGGAATGGATGATGC
G609A REV	ATCATCCATTCCTGGACAGCAACGTTAACCATGCCTGAT
V610A FOR	CATGGTTAACGTTGGTGCCCAGGAATGGATGATGCAT
V610A REV	GCATCATCCATTCCTGGGCACCAACGTTAACCATGCC
W613A FOR	CGTTGGTGTCCAGGAAGCGATGATGCATAATATCGATG
W613A REV	CGATATTATGCATCATCGCTTCCTGGACACCAACGTTAA
P 704A FOR	CACAGGCCCAGGTAATATTGCACCAAGCACACCTTATAAC
P 704A REV	GTTATAAGGTGTGCTTGGTGCAATATTACCTGGGCCTGTG
P 705A FOR	CAGGCCCAGGTAATATTCCAGCAAGCACACCTTATAACTAC
P 705A REV	GTAGTTATAAGGTGTGCTTGCTGGAATATTACCTGGGCCTG
TMD12	
T707A FOR	GGTAATATTCCACCAAGCGCACCTTATAACTACTC
T707A REV	ATGAGTAGTTATAAGGTGCGCTTGGTGGAATATTACC
Y709A FOR	CCACCAAGCACACCTGCTAACTACTCATTATTTTTTGC

Y709A REV	AATAATGAGTAGTTAGCAGGTGTGCTTGGTGGAATATTACC
Y711A FOR	CCAAGCACACCTTATAACGCCTCATTATTTTTTGCAATGTC
Y711AREV	GCAAAAAATAATGAGGCGTTATAAGGTGTGCTTGG
S712A FOR	CACACCTTATAACTACGCATTATTTTTTGCAATGTC
S712A REV	GACATTGCAAAAAATAATGCGTAGTTATAAGGTGTGC
L713A FOR	CCTTATAACTACTCAGCATTTTTTGCAATGTCATTCTGC
L713A REV	GAATGACATTGCAAAAAATGCTGAGTAGTTATAAGGTGTGC
F714A FOR	CCTTATAACTACTCATTAGCTTTTGCAATGTCATTCTGCC
F714A REV	GCAGAATGACATTGCAAAAGCTAATGAGTAGTTATAAGG
F715A FOR	AACTACTCATTATTTGCTGCAATGTCATTCTGCCTAAAC
F715A REV	GCAGAATGACATTGCAGCAAATAATGAGTAGTTATAAGG
A716G FOR	CTACTCATTATTTTTTGGAATGTCATTCTGCCTAAACTTG
A716G REV	GTTTAGGCAGAATGACATTCCAAAAAATAATGAGTAG
M717A FOR	CTCATTATTTTTTGCAGCGTCATTCTGCCTAAACTTG
M717A REV	CAAGTTTAGGCAGAATGACGCTGCAAAAAATAATGAGTAGT
S718A FOR	CATTATTTTTTGCAATGGCATTCTGCCTAAACTTGATAAG
S718A REV	CAAGTTTAGGCAGAATGCCATTGCAAAAAATAATGAG
F719A FOR	TTTTTTGCAATGTCAGCCTGCCTAAACTTGATAAGAAAAAG
F719A REV	CTTATCAAGTTTAGGCAGGCTGACATTGCAAAAAATAATG
C720A FOR	TTTGCAATGTCATTCGCCCTAAACTTGATAAGAAAAAG
C720A REV	CTTATCAAGTTTAGGGCGAATGACATTGCAAAAAATAATG
L721A FOR	GCAATGTCATTCTGCGCAAACTTGATAAGAAAAAGATGG
L721A REV	CCATCTTTTTCTTATCAAGTTTGCGCAGAATGACATTGC
L723A FOR	GTCATTCTGCCTAAACGCGATAAGAAAAAGATGGAGAGC
L723A REV	CCATCTTTTTCTTATCGCGTTTAGGCAGAATGACATTGC
I724A FOR	CTGCCTAAACTTGGCAAGAAAAAGATGGAGAGCTTGG
I724A REV	GCTCTCCATCTTTTTCTTGCCAAGTTTAGGCAGAATGAC
TMD13	
M739A FOR	TAAGTACAATTTCGTCGCGGGGGCCGGTGTTGAAGCA
M739A REV	CTTCAACACCGGCCCCCGCGACGAAATTGTACTTATTG
G740A FOR	AGTACAATTTCGTCATGGCGGCCGGTGTTGAAGCAGGTG
G740A REV	CCTGCTTCAACACCGGCCGCCATGACGAAATTGTACTTA
A741G FOR	CAATTTCGTCATGGGGGGCGGTGTTGAAGCAGGTGTG
A741G REV	CACCTGCTTCAACACCGCCCCCCATGACGAAATTGTAC
G742A FOR	TTTCGTCATGGGGGCCGCTGTTGAAGCAGGTGTGGCA

G742A REV	CCACACCTGCTTCAACAGCGGCCCCCATGACGAAATTG
V743A FOR	CGTCATGGGGGCCGGTGCTGAAGCAGGTGTGGCAATC
V743A REV	TTGCCACACCTGCTTCAGCACCGGCCCCCATGACGAA
A745G FOR	GGGGGCCGGTGTTGAAGGAGGTGTGGCAATCTCCGTC
A745G REV	CGGAGATTGCCACACCTCCTTCAACACCGGCCCCCATG
G746A FOR	GGCCGGTGTTGAAGCAGCTGTGGCAATCTCCGTCGTC
G746A REV	CGACGGAGATTGCCACAGCTGCTTCAACACCGGCCCC
V747A FOR	CGGTGTTGAAGCAGGTGCGGCAATCTCCGTCGTCATC
V747A REV	TGACGACGGAGATTGCCGCACCTGCTTCAACACCGGC
A748G FOR	TGTTGAAGCAGGTGTGGGAATCTCCGTCGTCATCATC
A748G REV	TGATGACGACGGAGATTCCCACACCTGCTTCAACACC
I749A FOR	TGAAGCAGGTGTGGCAGCCTCCGTCGTCATCATCTTC
I749A REV	AGATGATGACGACGGAGGCTGCCACACCTGCTTCAAC
S750A FOR	GCAGGTGTGGCAATCGCCGTCGTCATCATCTTCTTGTG
S750A REV	CAAGAAGATGATGACGACGGCGATTGCCACACCTGCTTC
V751A FOR	AGGTGTGGCAATCTCCGCCGTCATCATCTTCTTGTGTG
V751A REV	CACAAGAAGATGATGACGGCGGAGATTGCCACACCTGC
V752A FOR	GTGTGGCAATCTCCGTCGCCATCATCTTCTTGTGTGTAC
V752A REV	ACACACAAGAAGATGATGGCGACGGAGATTGCCACACC
I753A FOR	GGCAATCTCCGTCGTCGCCATCTTCTTGTGTGTACAG
I753A REV	GTACACACAAGAAGATGGCGACGACGGAGATTGCCAC
I754A FOR	CAATCTCCGTCGTCATCGCCTTCTTGTGTGTACAGTAC
I754A REV	ACTGTACACACAAGAAGGCGATGACGACGGAGATTGC
F755A FOR	CTCCGTCGTCATCATCGCCTTGTGTGTACAGTACCCAG
F755A REV	GGTACTGTACACACAAGGCGATGATGACGACGGAGATTG
L756A FOR	CGTCGTCATCATCTTCGCGTGTGTACAGTACCCAGGTG
L756A REV	CTGGGTACTGTACACACGCGAAGATGATGACGACGGAG
C757A FOR	CGTCATCATCTTCTTGGCTGTACAGTACCCAGGTGG
C757A REV	CCACCTGGGTACTGTACAGCCAAGAAGATGATGACGACGG
V758A FOR	CATCATCTTCTTGTGTGCACAGTACCCAGGTGGTAAG
V758A REV	TACCACCTGGGTACTGTGCACACAAGAAGATGATGACG
Other primers used in the study	
D78A FOR	CTCGTTTGGAAGGGCGCCCCTACATACTTGCCCAATTC
D78A REV	GGGCAAGTATGTAGGGGCGCCCTTCCAAACGAGACCTTC

E89A FOR	CCAATTCTCCATATCCTGCAGTGAGATCGGCGGTGTCCATC
E89A REV	CACCGCCGATCTCACTGCAGGATATGGAGAATTGGGCAAG
D98A FOR	GCGGTGTCCATCGAGGCTGACCCCACCATCCGCCTCAAC
D98A REV	GGCGGATGGTGGGGTCAGCCTCGATGGACACCGCCGATC
D99A FOR	GGTGTCCATCGAGGATGCCCCCACCATCCGCCTCAACC
D99A REV	GAGGCGGATGGTGGGGGCATCCTCGATGGACACCGCC
D157A FOR	CTGGCTCTCTTGCCCGCCTGGAAGTGTTCTAAAGTGCC
D157A REV	CTTTAGAACACTTCCAGGCGGGCAAGAGAGCCAGTATCC
E177A FOR	CCATTTACCAAAAAGGCACACGCCGTGGTCACAATTGC
E177A REV	GTGACCACGGCGTGTGCCTTTTTGGTAAATGGGCC
D335A FOR	CGTTGCCAATTACATTTGCCTACACCCAGGTTTCCCAAGC
D335A REV	GGGAAACCTGGGTGTAGGCAAATGTAATTGGCAACGCACC
D393A FOR	TCAGGTTCTACTTATGCCAACACTCAAAACAAATAC
D393A REV	GTATTTGTTTTGAGTGTTGGCATAAGTAGAACCTGAAATGAC
D408A FOR	CAAAGATTCTTAACGAGGCTTATTCCATTAATCTTGAG
D408A REV	CTCAAGATTAATGGAATAAGCCTCGTTAAGAATCTTTGTTAC
D453A FOR	CTTATACCACGGTAAAGCTATTGTCGCCAAGTTTAAAGAC
D453A REV	CTTTAAACTTGGCGACAATAGCTTTACCGTGGTATAAGATGC
T466A FOR	CGTAAAAATGGTGGCGCTGACATTCACATGAGAATCTAC
T466A REV	GATTCTCATGTGAATGTCAGCGCCACCATTTTTACGGTC
D467A FOR	CGTAAAAATGGTGGCACTGCCATTCACATGAGAATCTACTCC
D467A REV	GTAGATTCTCATGTGAATGGCAGTGCCACCATTTTTACGGTC
D479A FOR	CCAAGAACTATAAGGCTTGTCCCGATTGGTGGTATTTAC
D479A REV	CCACCAATCGGGACAAGCCTTATAGTTCTTGGAGTAG
D482A FOR	CTATAAGGATTGTCCCGCTTGGTGGTATTTACTTTTGC
D482A REV	CAAAAGTAAATACCACCAAGCGGGACAATCCTTATAGTTC
D504A FOR	GCAGTGTGCTGTTTCGCTACTAAGTTCCCAGCTTGGGC
D504A REV	GCTGGGAACTTAGTAGCGAAACAGCACACTGCTAC
E530A FOR	CCGCAAGGTATCTTGGCAGCAATGACTAACCAACACG
E530A REV	GTGTTGGTTAGTCATTGCTGCCAAGATACCTTGCGGGATG
D578A FOR	GCTTGAATTTGAGTAGAGCTTTGAAATTAGCCATGTACATG
D578A REV	GTACATGGCTAATTTCAAAGCTCTACTCAAATTCAAGCC
D778A FOR	GGAAAAGAACGTATGCTAATGATTATAAAAAATTTTATACC
D778A REV	AATTTTTTATAATCATTAGCATACGTTCTTTTCCAAACG
E135 KHRDQ FOR	TGAGATATCCATCGCTAVAM ATCAACTTCCTTGTTGCAC

E135 KHRDQ REV	GCAACAAGGAAGTTGATKTB TAGCGATGGATATCTCAG
E135W FOR	GATATCCATCGCTATGGATCAACTTCCTTGTTGCACAAG
E135W REV	CAACAAGGAAGTTGATCCATAGCGATGGATATCTCAGGG
E135G FOR	GATATCCATCGCTAGGGATCAACTTCCTTGTTGCACAAG
E135G REV	CAACAAGGAAGTTGATCCCTAGCGATGGATATCTCAGGG
E135 ST FOR	CTGAGATATCCATCGCTAWCGATCAACTTCCTTGTTGCAC
E135 ST REV	TGCAACAAGGAAGTTGATCGWTAGCGATGGATATCTCAG
D157 NAQHE FOR	ACTGGCTCTCTTGCCCVMWTGGAAGTGTTCTAAAGTGCCATT
D157 NAQHE REV	CACTTTAGAACACTTCCAWKB GGGCAAGAGAGCCAGTATC
N710 ERHKQ REV	CCACCAAGCACACCTTATVRSTACTCATTATTTTTTGCAATG
N710 ERHKQ REV	GCAAAAAATAATGAGTASYBATAAGGTGTGCTTGGTGG
p416TEF FOR	TTGATATTTAAGTTAATAAACGG
HGT1 1400 FOR	CATTCACATGAGAATCTACTCCAAGA
HGT1 1400 REV	AGTAGATTCTCATGTGAATGTCAGT
HGT1 1400 FOR	TAGAGATCAACTTCCTTGTTGCACA
HGT1 1950 REV	GATACTTTGGCAAAGACCAGATAAT
Hgt1BamH1 FOR	ACACACGGATCCATGAGTACCATTTATAGGGAGAG
Hgt1 Ecor1 REV	ACACACGAATTCTTACCACCATTTATCATAACCAA
PGT1 FOR	ATGCCGGATCCATGACAGCTCGCAATTCTGCTAG
PGT1 REV	ATGCGCCCGGGTTACCAATTGGTGTAACCAAAG
Pgt1S182KQHN FOR	CGTTATCCGGCTTTGMAWATCAGTTTCATTGTCGCTC
Pgt1S182KQHN REV	GAGCGACAATGAAACTGATWTKCAAAGCCGGATAACG

Table 2.2

List of bacteria and yeast strains used in the study

Strain	Genotype	Source
Escherichia coli strains		
ABE 460 (DH5α)	*F⁻ gyrA96*(Nal) *recA1 relA1 endA1 thi-1 hsdR17* (rk^- mk^+) *glnV44 deoR*Δ *(lacZYA-argF) U169* [ϕ80dΔ *(lacZ) M15*]	Lab stock
ABE 962 (XL1-Blue)	*F'::Tn10* (tet^r) *proA⁺B⁺ lacI^q* Δ*(lacZ) M15 /recA1 endA1 gyrA96* (Nal^r) *thi-1 hsdR17* (rk^-mk^-) *glnV44 relA1lac*	Lab stock
***Saccharomyces cerevisiae* strain**		
ABC 817	*MATa his3Δ1 leu2Δ0 met15Δ0 ura3Δ0 hgt1Δ::LEU2*	Lab stock
ABC 5061	*Saccharomyces cerevisiae MATa his3Δ1 leu2Δ0 met15Δ0 ura3Δ0, PMA1*-FLAG tagged at the C-terminus in the genome	Dr. K. Ganesan (IMTECH, Chandigarh)

Table 2.3

List of Plasmids used in the study

Plasmid name	Clone no.	Description
p416TEF	ABE 443	The CEN-vector bearing *URA3* marker and TEF promoter-MCS-terminator for yeast expression and Ampr marker for selection in *E. coli (Mumberg et al. 1995)*
pRS313TEF	ABE 3569	pRS313 vector digested with Sac1-Apa1 and ligated with Sac1-Apa1 digested fragment (1941bp) of p416TEF vector.
p416TEF M1-His-HGT1m- HA	ABE 1912	The plasmid contains the *HGT1* gene in p416M1-TEF (ABE 1888) at *Bam*HI/*Eco*RI sites. *Msc*I *(Bal*I)and *Xba*I sites introduced at position 1366 and 1584 in *HGT1*, in pTEF-His-HGT1-HA plasmid (ABE 1897) (Kaur & Bachhawat 2009a). All mutants were created in this backbone.
pHLuorin in PVT100U plasmid	ABE4134	pHLuorin expressed under ADH promoter and have Ura3 selection marker (Maresova *et al.* 2010).

TMD 1		
pT109A	ABE 3074	p416-TEF-His-HGT1-HA with T109A mutation
pW110A	ABE 3665	p416-TEF-His-HGT1-HA with W110Amutation
pF111A	ABE 3666	p416-TEF-His-HGT1-HA with F111A mutation
pL112A	ABE 3667	p416-TEF-His-HGT1-HA with L112A mutation
pT113A	ABE 3504	p416-TEF-His-HGT1-HA with T113A mutation
pT114A	ABE 2242	p416-TEF-His-HGT1-HA with T114A mutation (Kaur et al.,2009)
pV115A	ABE 4005	p416-TEF-His-HGT1-HA with V115A mutation
pF116A	ABE 4006	p416-TEF-His-HGT1-HA with F116A mutation
pV117A	ABE 3668	p416-TEF-His-HGT1-HA with V117A mutation
pV118A	ABE 3669	p416-TEF-His-HGT1-HA with V118A mutation
pV119A	ABE 3670	p416-TEF-His-HGT1-HA with V119A mutation
pF120A	ABE 3671	p416-TEF-His-HGT1-HA with F120A mutation
pA121G	ABE 3672	p416-TEF-His-HGT1-HA with A121G mutation
pG122A	ABE 3673	p416-TEF-His-HGT1-HA with G122A mutation
pV123A	ABE 3674	p416-TEF-His-HGT1-HA with V123A mutation
pN214A	ABE 2248	p416-TEF-His-HGT1-HA with N214A mutation(Kaur et al.,2009)
pQ125A	ABE 3505	p416-TEF-His-HGT1-HA with Q125A mutation
pV126A	ABE 3675	p416-TEF-His-HGT1-HA with V126A mutation
pF127A	ABE 4008	p416-TEF-His-HGT1-HA with F127A mutation
TMD2		
pL134A	ABE 3777	p416-TEF-His-HGT1-HA with L134A mutation
pE135A	ABE 2249	p416-TEF-His-HGT1-HA with E135A mutation(Kaur et al.,2009)
pI136A	ABE 3778	p416-TEF-His-HGT1-HA with I136A mutation
pN137A	ABE 2260	p416-TEF-His-HGT1-HA with N137A mutation(Kaur et al.,2009)
pF138A	ABE 3779	p416-TEF-His-HGT1-HA with F138A mutation
pL139A	ABE 3780	p416-TEF-His-HGT1-HA with L139A mutation
pV140A	ABE 3781	p416-TEF-His-HGT1-HA with V140A mutation
pA141G	ABE 3782	p416-TEF-His-HGT1-HA with A141G mutation
pQ142A	ABE 3202	p416-TEF-His-HGT1-HA with Q142A mutation
pV143A	ABE 3783	p416-TEF-His-HGT1-HA with V143A mutation

pV144A	ABE 3784	p416-TEF-His-HGT1-HA with V144A mutation
pY146A	ABE3785	p416-TEF-His-HGT1-HA with Y146A mutation
pP147A	ABE 2851	p416-TEF-His-HGT1-HA with P147A mutation
pI148A	ABE 3786	p416-TEF-His-HGT1-HA with I148A mutation
pG149A	ABE 3787	p416-TEF-His-HGT1-HA with G149A mutation
pR150A	ABE 1911	p416-TEF-His-HGT1-HA with R150A mutation(Kaur et al.,2009)
pI151A	ABE 3788	p416-TEF-His-HGT1-HA with I151A mutation
pL152A	ABE 3789	p416-TEF-His-HGT1-HA with L152A mutation
pA153G	ABE 3790	p416-TEF-His-HGT1-HA with A153G mutation
pL154A	ABE 3791	p416-TEF-His-HGT1-HA with L154A mutation
pL155A	ABE 3792	p416-TEF-His-HGT1-HA with L155A mutation
TMD3		
pA179G	ABE 3850	p416-TEF-His-HGT1-HA with A179G mutation
pV180A	ABE 3851	p416-TEF-His-HGT1-HA with V180A mutation
pV181A	ABE 4057	p416-TEF-His-HGT1-HA with V181A mutation
pT182A	ABE 3659	p416-TEF-His-HGT1-HA with T182A mutation
pI183A	ABE 3852	p416-TEF-His-HGT1-HA with I183A mutation
pA184G	ABE 3853	p416-TEF-His-HGT1-HA with A184G mutation
pV185A	ABE 3854	p416-TEF-His-HGT1-HA with V185A mutation
pA186G	ABE 3855	p416-TEF-His-HGT1-HA with A186G mutation
pL187A	ABE 3856	p416-TEF-His-HGT1-HA with L187A mutation
pT188A	ABE 2039	p416-TEF-His-HGT1-HA with T188A mutation
pS189A	ABE 3660	p416-TEF-His-HGT1-HA with S189A mutation
pS190A	ABE 2373	p416-TEF-His-HGT1-HA with S190A mutation
pA192G	ABE 3857	p416-TEF-His-HGT1-HA with A192G mutation
pY193A	ABE 3858	p416-TEF-His-HGT1-HA with Y193A mutation
pA194G	ABE 3859	p416-TEF-His-HGT1-HA with A194G mutation
pM195A	ABE 3860	p416-TEF-His-HGT1-HA with M195A mutation
pI197A	ABE 3861	p416-TEF-His-HGT1-HA with I197A mutation
pL198A	ABE 3862	p416-TEF-His-HGT1-HA with L198A mutation
pN199A	ABE 3664	p416-TEF-His-HGT1-HA with N199A mutation
pA200G	ABE 3863	p416-TEF-His-HGT1-HA with A200G mutation
TMD4		
pG212A	ABE 3192	p416-TEF-His-HGT1-HA with G212A mutation

pY213A	ABE 3193	p416-TEF-His-HGT1-HA with Y213A mutation
pQ214A	ABE 3082	p416-TEF-His-HGT1-HA with Q214A mutation
pF215A	ABE 3194	p416-TEF-His-HGT1-HA with F215A mutation
pL216A	ABE 3195	p416-TEF-His-HGT1-HA with L216A mutation
pL217A	ABE3196	p416-TEF-His-HGT1-HA with L217A mutation
pV218A	ABE 3198	p416-TEF-His-HGT1-HA with V218A mutation
pW219A	ABE 3197	p416-TEF-His-HGT1-HA with W219A mutation
pT220A	ABE 3199	p416-TEF-His-HGT1-HA with T220A mutation
pS221A	ABE 3347	p416-TEF-His-HGT1-HA with S221A mutation
pQ222A	ABE 2041	p416-TEF-His-HGT1-HA with Q222A mutation(Kaur et al.,2009)
pM223A	ABE 3508	p416-TEF-His-HGT1-HA with M223A mutation
pI224A	ABE 3448	p416-TEF-His-HGT1-HA with I224A mutation
pG225A	ABE 3449	p416-TEF-His-HGT1-HA with G225A mutation
pY226A	ABE 3450	p416-TEF-His-HGT1-HA with Y226A mutation
pG227A	ABE 3451	p416-TEF-His-HGT1-HA with G227A mutation
pA228G	ABE 3452	p416-TEF-His-HGT1-HA with A228G mutation
pA229G	ABE 3453	p416-TEF-His-HGT1-HA with A229G mutation
pG230A	ABE 3454	p416-TEF-His-HGT1-HA with G230A mutation
pL231A	ABE 3509	p416-TEF-His-HGT1-HA with L231 mutation
pT232A	ABE 3510	p416-TEF-His-HGT1-HA with T232A mutation
TMD5		
pF277A	ABE 3711	p416-TEF-His-HGT1-HA with F277A mutation
pF278A	ABE 3712	p416-TEF-His-HGT1-HA with F278A mutation
pL279A	ABE 3713	p416-TEF-His-HGT1-HA with L279A mutation
pI280A	ABE 3714	p416-TEF-His-HGT1-HA with I280A mutation
pV281A	ABE 3715	p416-TEF-His-HGT1-HA with V281A mutation
pL282A	ABE 3716	p416-TEF-His-HGT1-HA with L282A mutation
pI283A	ABE 3717	p416-TEF-His-HGT1-HA with I283A mutation
pG284A	ABE 3718	p416-TEF-His-HGT1-HA with G284A mutation
pS285A	ABE 3075	p416-TEF-His-HGT1-HA with S285A mutation
pF286A	ABE 3955	p416-TEF-His-HGT1-HA with F286A mutation
pI287A	ABE 3956	p416-TEF-His-HGT1-HA with I287A mutation
pW288A	ABE 3719	p416-TEF-His-HGT1-HA with W288A mutation
pY289A	ABE 3720	p416-TEF-His-HGT1-HA with Y289A mutation

pW290A	ABE 3721	p416-TEF-His-HGT1-HA with W290A mutation
pV291A	ABE 3722	p416-TEF-His-HGT1-HA with V291A mutation
pP292A	ABE 2852	p416-TEF-His-HGT1-HA with P292A mutation
pG293A	ABE 3723	p416-TEF-His-HGT1-HA with G293A mutation
pF294A	ABE 3724	p416-TEF-His-HGT1-HA with F294A mutation
pL295A	ABE 3725	p416-TEF-His-HGT1-HA with L295A mutation
pF296A	ABE 3726	p416-TEF-His-HGT1-HA with F296A mutation
TMD6		
pV354A	ABE 4054	p416-TEF-His-HGT1-HA with V354A mutation
pS355A	ABE 2241	p416-TEF-His-HGT1-HA with S355A mutation(Kaur et al.,2009)
pA356G	ABE 4056	p416-TEF-His-HGT1-HA with A356G mutation
pN357A	ABE 2234	p416-TEF-His-HGT1-HA with N357A mutation(Kaur et al.,2009)
pT358A	ABE 3661	p416-TEF-His-HGT1-HA with T358A mutation
pY359A	ABE 4055	p416-TEF-His-HGT1-HA with Y359A mutation
pA360G	ABE 3881	p416-TEF-His-HGT1-HA with A360G mutation
pV362A	ABE 3882	p416-TEF-His-HGT1-HA with V362A mutation
pL363A	ABE 3883	p416-TEF-His-HGT1-HA with L363A mutation
pI364A	ABE 3884	p416-TEF-His-HGT1-HA with I364A mutation
pF365A	ABE 4058	p416-TEF-His-HGT1-HA with F365A mutation
pF366A	ABE 3885	p416-TEF-His-HGT1-HA with F366A mutation
pV367A	ABE 3886	p416-TEF-His-HGT1-HA with V367A mutation
pI368A	ABE 4059	p416-TEF-His-HGT1-HA with I368A mutation
pI369A		p416-TEF-His-HGT1-HA with I369A mutation
pL370A	ABE 3887	p416-TEF-His-HGT1-HA with L370A mutation
pP371A	ABE 2853	p416-TEF-His-HGT1-HA with P371A mutation
pC372A	ABE 4011	p416-TEF-His-HGT1-HA with C372A mutation
pL373A	ABE 3888	p416-TEF-His-HGT1-HA with L373A mutation
pY374A	ABE 3889	p416-TEF-His-HGT1-HA with Y374A mutation
TMD7		
pS427A	ABE 3662	p416-TEF-His-HGT1-HA with S427A mutation
pY428A	ABE 3840	p416-TEF-His-HGT1-HA with Y428A mutation
pL429A	ABE 3953	p416-TEF-His-HGT1-HA with L429A mutation
pL430A	ABE 3924	p416-TEF-His-HGT1-HA with L430A mutation

pS431A	ABE 3866	p416-TEF-His-HGT1-HA with S431A mutation
pY432A	ABE 3841	p416-TEF-His-HGT1-HA with Y432A mutation
pA433G	ABE 3842	p416-TEF-His-HGT1-HA with A433G mutation
pL434A	ABE 3843	p416-TEF-His-HGT1-HA with L434A mutation
pN435A	ABE 2005	p416-TEF-His-HGT1-HA with N435A mutation(Kaur et al.,2009)
pV436A	ABE 3867	p416-TEF-His-HGT1-HA with V436A mutation
pA437G	ABE 3954	p416-TEF-His-HGT1-HA with A437G mutation
pA438G	ABE 3868	p416-TEF-His-HGT1-HA with A438G mutation
pV439A	ABE 3844	p416-TEF-His-HGT1-HA with V439A mutation
pI440A	ABE 3845	p416-TEF-His-HGT1-HA with I440A mutation
pA441G	ABE 3846	p416-TEF-His-HGT1-HA with A441G mutation
pV442A	ABE 4009	p416-TEF-His-HGT1-HA with V442A mutation
pF443A	ABE 4010	p416-TEF-His-HGT1-HA with F443A mutation
pV444A	ABE 3515	p416-TEF-His-HGT1-HA with V444A mutation
pH445A	ABE 2235	p416-TEF-His-HGT1-HA with H445A mutation(Kaur et al.,2009)
pC446A	ABE 4060	p416-TEF-His-HGT1-HA with C446A mutation
pI447A	ABE 4012	p416-TEF-His-HGT1-HA with I447A mutation
pL448A	ABE 3847	p416-TEF-His-HGT1-HA with L448A mutation
pY449A	ABE 3848	p416-TEF-His-HGT1-HA with Y449A mutation
TMD8		
pW483A	ABE 3925	p416-TEF-His-HGT1-HA with W483A mutation
pW484A	ABE 3849	p416-TEF-His-HGT1-HA with W484A mutation
pY485A	ABE 4013	p416-TEF-His-HGT1-HA with Y485A mutation
pL486A	ABE 3926	p416-TEF-His-HGT1-HA with L486A mutation
pL487A	ABE 3927	p416-TEF-His-HGT1-HA with L487A mutation
pL488A	ABE 3928	p416-TEF-His-HGT1-HA with L488A mutation
pQ489A	ABE 3203	p416-TEF-His-HGT1-HA with Q489A mutation
pI490A	ABE 3929	p416-TEF-His-HGT1-HA with I490A mutation
pV491A	ABE 3930	p416-TEF-His-HGT1-HA with V491 mutation
pM492A	ABE 3931	p416-TEF-His-HGT1-HA with M492A mutation
pI493A	ABE 3932	p416-TEF-His-HGT1-HA with I493A mutation
pG494A	ABE 3933	p416-TEF-His-HGT1-HA with G494A mutation
pL495A	ABE 4014	p416-TEF-His-HGT1-HA with L495A mutation

pG496A	ABE 4015	p416-TEF-His-HGT1-HA with G496A mutation
pF497A	ABE 3934	p416-TEF-His-HGT1-HA with F497 mutation
pV498A	ABE 3935	p416-TEF-His-HGT1-HA with V498A mutation
pA499G	ABE 4016	p416-TEF-His-HGT1-HA with A499G mutation
pV500A	ABE 3936	p416-TEF-His-HGT1-HA with V500A mutation
pC501A	ABE 4061	p416-TEF-His-HGT1-HA with C501A mutation
TMD10		
pL591A	ABE 3823	p416-TEF-His-HGT1-HA with L591A mutation
pI592A	ABE 3824	p416-TEF-His-HGT1-HA with I592A mutation
pF593A	ABE 3825	p416-TEF-His-HGT1-HA with F593A mutation
pA594G	ABE 3826	p416-TEF-His-HGT1-HA with A594G mutation
pV595A	ABE 3827	p416-TEF-His-HGT1-HA with V595A mutation
pQ596A	ABE 3076	p416-TEF-His-HGT1-HA with Q596A mutation
pI597A	ABE 3828	p416-TEF-His-HGT1-HA with I597A mutation
pY598A	ABE 3829	p416-TEF-His-HGT1-HA with Y598A mutation
pA599G	ABE 3830	p416-TEF-His-HGT1-HA with A599G mutation
pT600A	ABE 3922	p416-TEF-His-HGT1-HA with T600A mutation
pI601A	ABE 3831	p416-TEF-His-HGT1-HA with I601A mutation
pI602A	ABE 3832	p416-TEF-His-HGT1-HA with I602A mutation
pS603A	ABE 2320	p416-TEF-His-HGT1-HA with S603A mutation(Kaur et al.,2009)
pG604A	ABE 3833	p416-TEF-His-HGT1-HA with G604A mutation
pM605A	ABE 3834	p416-TEF-His-HGT1-HA with M605A mutation
pV606A	ABE 3835	p416-TEF-His-HGT1-HA with V606A mutation
pN607A	ABE 2019	p416-TEF-His-HGT1-HA with N607A mutation(Kaur et al.,2009)
pV608A	ABE 3836	p416-TEF-His-HGT1-HA with V608A mutation
pG609A	ABE 3837	p416-TEF-His-HGT1-HA with G609A mutation
pV610A	ABE 3838	p416-TEF-His-HGT1-HA with V610A mutation
pQ611A	ABE3077	p416-TEF-His-HGT1-HA with Q611A mutation
pE612A	ABE 2374	p416-TEF-His-HGT1-HA with E612A mutation(Kaur et al.,2009)
pW613A	ABE 3839	p416-TEF-His-HGT1-HA with W613A mutation
TMD11		
pL661A	ABE 3937	p416-TEF-His-HGT1-HA with L661A mutation

pM662A	ABE 3938	p416-TEF-His-HGT1-HA with M662A mutation
pW663A	ABE 3939	p416-TEF-His-HGT1-HA with W663A mutation
pF664A	ABE 3940	p416-TEF-His-HGT1-HA with F664A mutation
pF665A	ABE 3941	p416-TEF-His-HGT1-HA with F665A mutation
pL666A	ABE 3950	p416-TEF-His-HGT1-HA with L666A mutation
pI667A	ABE 3951	p416-TEF-His-HGT1-HA with I667A mutation
pG668A	ABE 4017	p416-TEF-His-HGT1-HA with G668A mutation
pL669A	ABE 3942	p416-TEF-His-HGT1-HA with L669A mutation
pL670A	ABE 3943	p416-TEF-His-HGT1-HA with L670A mutation
pF671A	ABE 3944	p416-TEF-His-HGT1-HA with F671A mutation
pP672A	ABE 2854	p416-TEF-His-HGT1-HA with P672A mutation
pL673A	ABE 3945	p416-TEF-His-HGT1-HA with L673A mutation
pA674G	ABE 3946	p416-TEF-His-HGT1-HA with A674G mutation
pV675A	ABE 3947	p416-TEF-His-HGT1-HA with V675A mutation
pY676A	ABE 3948	p416-TEF-His-HGT1-HA with Y676A mutation
pA677G	ABE 3952	p416-TEF-His-HGT1-HA with A677G mutation
pV678A	ABE 3949	p416-TEF-His-HGT1-HA with V678A mutation
pQ679A	ABE 3078	p416-TEF-His-HGT1-HA with Q679A mutation
TMD12		
pT707A	ABE 4507	p416-TEF-His-HGT1-HA with T707A mutation
pP708A	ABE 2857	p416-TEF-His-HGT1-HA with P708A mutation
pY709A	ABE 4508	p416-TEF-His-HGT1-HA with Y709A mutation
pN710A	ABE 1937	p416-TEF-His-HGT1-HA with N710A mutation
pY711A	ABE 4509	p416-TEF-His-HGT1-HA with Y711A mutation
pS712A	ABE 4510	p416-TEF-His-HGT1-HA with S712A mutation
pL713A	ABE 4511	p416-TEF-His-HGT1-HA with L713A mutation
pF714A	ABE 4512	p416-TEF-His-HGT1-HA with F714A mutation
pF715A	ABE 4513	p416-TEF-His-HGT1-HA with F715A mutation
pA716G	ABE 4514	p416-TEF-His-HGT1-HA with A716G mutation
pM717A	ABE 4515	p416-TEF-His-HGT1-HA with M717A mutation
pS718A	ABE 4516	p416-TEF-His-HGT1-HA with S718A mutation
pF719A	ABE 4517	p416-TEF-His-HGT1-HA with F719A mutation
pL721A	ABE 4518	p416-TEF-His-HGT1-HA with L721A mutation
pL723A	ABE 4519	p416-TEF-His-HGT1-HA with L723A mutation
pI724A	ABE 4520	p416-TEF-His-HGT1-HA with I724A mutation

TMD13		
pM739A	ABE 3957	p416-TEF-His-HGT1-HA with M739A mutation
pG740A	ABE 3869	p416-TEF-His-HGT1-HA with G740A mutation
pA741G	ABE 3958	p416-TEF-His-HGT1-HA with A741G mutation
pG742A	ABE 3870	p416-TEF-His-HGT1-HA with G742A mutation
pV743A	ABE 3871	p416-TEF-His-HGT1-HA with V743A mutation
pE744A	ABE 1910	p416-TEF-His-HGT1-HA with E744A mutation(Kaur et al.,2009)
pA745G	ABE 3872	p416-TEF-His-HGT1-HA with A745G mutation
pG746A	ABE 3873	p416-TEF-His-HGT1-HA with G746A mutation
pV747A	ABE 3959	p416-TEF-His-HGT1-HA with V747A mutation
pA748G	ABE 3874	p416-TEF-His-HGT1-HA with A748G mutation
pI749A	ABE 3875	p416-TEF-His-HGT1-HA with I749A mutation
pS750A	ABE 3079	p416-TEF-His-HGT1-HA with S750A mutation
pV751A	ABE 3960	p416-TEF-His-HGT1-HA with V751A mutation
pV752A	ABE 3876	p416-TEF-His-HGT1-HA with V752A mutation
pI753A	ABE 3877	p416-TEF-His-HGT1-HA with I753A mutation
pI754A	ABE 3961	p416-TEF-His-HGT1-HA with I754A mutation
pF755A	ABE 3878	p416-TEF-His-HGT1-HA with F755A mutation
pL756A	ABE 3879	p416-TEF-His-HGT1-HA with L756A mutation
pC757A	ABE 4062	p416-TEF-His-HGT1-HA with C757A mutation
pV758A	ABE 3880	p416-TEF-His-HGT1-HA with V758A mutation
pQ759A	ABE 3083	p416-TEF-His-HGT1-HA with Q759A mutation
Other plasmids used in this study		
pHXE135KD157N	ABE 3228	p416-TEF-HGT1-Hydroxyamine mutagenized E135K, D157N mutation
pE135K	ABE 3271	p416-TEF-HGT1 containing E135K mutation
pE135H	ABE 3272	p416-TEF-HGT1 containing E135H mutation
pE135Q	ABE 3273	p416-TEF-HGT1 containing E135Q mutation
pE135N	ABE 3274	p416-TEF-HGT1 containing E135N mutation
pE135D	ABE 3275	p416-TEF-HGT1 containing E135D mutation
pE135G	ABE 3506	p416-TEF-HGT1 containing E135G mutation
pE135W	ABE 3507	p416-TEF-HGT1 containing E135W mutation
pD157E	ABE 3276	p416-TEF-HGT1 containing D157E mutation

pD157N	ABE 3278	p416-TEF-HGT1 containing D157N mutation
pN710E	ABE 4696	p416-TEF-HGT1 containing N710E mutation
pN710S	ABE 4697	p416-TEF-HGT1 containing N710S mutation
pN710G	ABE 4698	p416-TEF-HGT1 containing N710G mutation
pE135A N710A	ABE 4722	p416-TEF-HGT1 containing E135A N710A mutation
pE177A	ABE 4723	p416-TEF-HGT1 containing E177A mutation
pD335A	ABE 4724	p416-TEF-HGT1 containing D335A mutation
pD453A	ABE 4725	p416-TEF-HGT1 containing D453A mutation
pD467A	ABE 4726	p416-TEF-HGT1 containing D467A mutation
pD479A	ABE 4727	p416-TEF-HGT1 containing D479A mutation
pD482A	ABE 4728	p416-TEF-HGT1 containing D482A mutation
pD504A	ABE 4729	p416-TEF-HGT1 containing D504A mutation
pD578A	ABE 4730	p416-TEF-HGT1 containing D578A mutation
pD778A	ABE 4731	p416-TEF-HGT1 containing D778A mutation
pD393A	ABE 4894	p416-TEF-HGT1 containing D393A mutation
pD408A	ABE 4895	p416-TEF-HGT1 containing D408A mutation
pE530A	ABE 4896	p416-TEF-HGT1 containing E530A mutation
pH178A	ABE 5074	p416-TEF-HGT1 containing H178A mutation
pH258A	ABE 5075	p416-TEF-HGT1 containing H258A mutation
p313TEF HGT1	ABE 4897	pRS313-TEF-HGT1
p313TEF-E135A	ABE 4898	pRS313-TEF-HGT1 containing E135A mutation
p313TEF-E135Q	ABE 4899	pRS313-TEF-HGT1 containing E135Q mutation
p313TEF-N710A	ABE 4900	pRS313-TEF-HGT1 containing N710A mutation
p313TEF-E135N N710E	ABE 4901	pRS313-TEF-HGT1 containing E135N N710E mutation
p313TEF-D157N	ABE 4904	pRS313-TEF-HGT1 containing D157N mutation
p313TEF-D578A	ABE 4905	pRS313-TEF-HGT1 containing D578A mutation
p313TEF-K562A	ABE 4906	pRS313-TEF-HGT1 containing K562A mutation
p313TEF-E744T	ABE 4907	pRS313-TEF-HGT1 containing E744T mutation
p313TEF-N710S	ABE 4908	pRS313-TEF-HGT1 containing N710S mutation
p313TEF-R150A	ABE 4909	pRS313-TEF-HGT1 containing R150A mutation
p313TEF-E177A	ABE 4910	pRS313-TEF-HGT1 containing E177A mutation
p313TEF-Y226A	ABE 4911	pRS313-TEF-HGT1 containing Y226A mutation
p313TEF-Y374A	ABE 4912	pRS313-TEF-HGT1 containing Y374A mutation
p313TEF-D335A	ABE 4913	pRS313-TEF-HGT1 containing D335A mutation

p313TEF-H445A	ABE 4914	pRS313-TEF-HGT1 containing H445A mutation
p313TEF-E530A	ABE 4915	pRS313-TEF-HGT1 containing E530A mutation
p313TEF-R554A	ABE 4916	pRS313-TEF-HGT1 containing R554A mutation
p313TEF-E554A	ABE 4917	pRS313-TEF-HGT1 containing E554A mutation
p313TEF-D482A	ABE 4918	pRS313-TEF-HGT1 containing D482A mutation
p313TEF-F523A	ABE 4919	pRS313-TEF-HGT1 containing F523A mutation
p313TEF-E612A	ABE 4920	pRS313-TEF-HGT1 containing E612A mutation
p313TEF-E744A	ABE 4921	pRS313-TEF-HGT1 containing E744A mutation

2.4 MEDIA

Growth media for bacteria and yeast were prepared using deionized water (Elix 4, Millipore) and were sterilized by autoclaving at 15 lb/inch^2 pressures at 121 °C for 15 minutes. Agar if required was added, at a final concentration of 2.2%. Additional amino acid and nutrients were prepared as sterile stock using filter sterilization and added as per requirements. Ampicillin if required was added at a final concentration of 100 μg/ml.

2.4.1. LB (Luria–Bertani) Medium	Yeast extract	5 g/l
	Tryptone	10 g/l
	NaCl	10 g/l
	pH of the above medium was adjusted to 7.0 with 1N NaOH	
2.4.2. YPD (Yeast extract-Peptone-Dextrose) Medium	Yeast extract	10 g/l
	Peptone	20 g/l
	Dextrose	20 g/l
2.4.3. SD (Synthetic Defined) Medium	YNB (Yeast Nitrogen Base) (without amino acids and ammonium sulphate)	1.7 g/l
	$(NH_4)_2 SO_4$	5 g/l
	Dextrose	20 g/l
	Amino acids (as required)	50 mg/l
	(pH was adjusted to 5.5 – 8.0 using 5N NaOH before preparing the plates)	

2.4.4. EMM	Potassium hydrogen phosphate pathalate	3.0 g/l
(Edinburgh minimal Medium)	Disodium hydrogen phathalate	2.2 g/l
	Sodium glutamate	5.0 g/l
	Glucose	20.0g/l
	Salt Stock 50X	20.0ml/l
	Vitamin stock (1000X)	1.0ml/l
	Mineral stock (10000X)	0.1ml/l
	Amino acids	50mg/l
Salt Stock (50X)	$MgCl_2.6H_2O$	53.3g
	$CaCl_2.2H_2O$	0.735g
	KCl	50g
	Na_2SO_4	2g
Vitamin stock (1000X)	Nicotinic acid	10g
	Myo-Inositol	10g
	Pantothenic acid	1g
	Biotin	10g
Mineral stock (10000X)	H_3BO_3	5g
	$MnSO_4$	4g
	$ZnSO_4.7H_2O$	4g
	$FeCl_3.6H_20$	2g
	$MoO_4.2H_20$	1.6g
	KI	1g
	$CuSO_4.5H_2O$	0.4g
	Citric acid	10g

2.5. BUFFERS AND STOCK SOLUTIONS

All buffers and stock solutions were prepared using deionized water (Elix4, Millipore) unless otherwise mentioned. As recommended they were sterilized either by autoclaving at 15 lb/inch2 pressures at 121ºC for 15 minutes, or by using membrane filters of pore size 0.2- 0.45 µm.

2.5.1. Ampicillin Stock Solution (100 mg/ml)

The required amount of ampicillin (sodium salt) was dissolved in the required volume of deionized water, and it was filter-sterilized using 0.2 µm filter membrane. Aliquots were made and was stored at -20°C**.**

2.5.2. GSH Stock Solution (100 mM)

The required amount of reduced GSH was dissolved in 10 ml of deionized water and was filter-sterilized using 0.2 µm filter membrane. It was stored at -20°C in aliquots.

2.5.3. Methionine Stock Solution (100 mM)

The required amount of methionine was dissolved in 10 ml of deionized water and was filter-sterilized using 0.2 µm filter membrane. It was stored at 4°C in tight 25 ml Schott bottle.

2.5.4. 50% Glycerol

Used for preparing –80°C stocks of *E. coli* harboring desired plasmids.

2.5.5. 25% Glycerol

Used for preparing –80°C stocks of yeast strains.

2.5.6. Alkaline Lysis Buffers for plasmid DNA preparation from *E. coli*

a) Solution-I **(Resuspension Solution)**	50 mM Glucose 25 mM Tris-HCl (pH 8.0) 10 mM EDTA (pH 8.0) Autoclaved and stored at 4ºC.
b) Solution-II **(Lysis Solution)**	0.2 N NaOH (freshly diluted from a 10N stock) 1% SDS (freshly diluted from a 10% stock) Freshly prepared and stored at RT
c) Solution-III **(Neutralization Solution)**	5 M Potassium acetate 60 ml Glacial acetic acid 11.5 ml Deionized water 28.5 ml

	It was stored at 4ºC.
d) TE Buffer (Tris-EDTA) (pH 8.0)	10 mM Tris-HCl (pH 8.0). 1 mM EDTA (pH 8.0).
e) TE-RNAse (stock prepared at 10 mg/ml	Working stock 20µg/ml in TE Buffer, pH 8.0.

2.5.7. Agarose Gel Electrophoresis Reagents

a) 1× TAE (Tris-acetate-EDTA) Buffer (per 1000 ml) (prepared from 50× TAE stock)	40 mM Tris-acetate. 1mM EDTA (pH 8.0). Autoclaved and stored at room temperature.
b) Orange-G dye (Gel loading dye, 6X)	0.25% Orange-G in 30% glycerol.
c) 0.8 - 1.2 % Agarose gel in 1× TAE	Final working concentration used at 0.5 µg/ml.
d) Ethidium Bromide (10 mg/ml) Stock	

2.5.8. Solutions for preparation of chemical-competent *E. coli* cells (Sambrook 1989b)

a) SOB	Bactotryptone 20 g Bacto yeast extract 5 g NaCl 0.5 g Above mentioned components were dissolved in 950 ml of water. 10 ml of 250 mM KCl was added and pH was adjusted to 7 with 5N NaOH, volume was made up to 995 ml and autoclaved. Just before use, 5 ml of filter sterilized 2 M $MgCl_2$ was added.
b) SOC	SOB + 20 mM Glucose
c) 1 mM $CaCl_2$	
d) 10% glycerol	

2.5.9. Yeast Transformation Solutions (*S. cerevisiae*) (Ito *et al.* 1983a)

a) 0.1 M Lithium acetate in TE (pH 7.5) Autoclave and store at RT.

b) 50% PEG-3350 in 0.1 M Lithium acetate in TE (pH 7.5). Autoclave and store at RT.

2.5.10. STES Lysis mixture (for plasmid / genomic DNA isolation from yeast)

10 mM Tris-HCl (pH 8.0)

1 mM EDTA (pH 8.0)

100 mM NaCl

1% SDS

2% Triton X-100

2.5.11. Solution for Hydroxlyamine mutagenesis (Rose & Fink 1987)

NaOH 90 mg

Hydroxylamine HCl 350 mg

Dissolved in 5 ml cold water and pH adjusted to 6.5. The solution was made fresh just before use.

2.5.12. Transport assay reagents (Bourbouloux *et al.* 2000; Kaur *et al.* 2009)

a) MES buffer (pH 5.5)	20 mM MES/KOH pH 5.5 0.5 mM $CaCl_2$ 2.5 M $MgCl_2$
a) Resuspension buffer	2% glucose in MES buffer (pH 5.5)
b) Sigma-Fluor, high performance LSC cocktail, Sigma. (Cat#: S4023-4L)	

2.5.13. Yeast Breaking Buffer (pH 7.5) (Aggarwal & Mondal 2006)

a) Yeast whole cell extract preparation.	50 mM Tris-HCl (pH 7.5) 1% Sodium deoxycholate 1% Triton X-100 0.1% SDS 5 mM EDTA 0.05% Phenylmethylsulfonyl fluoride (PMSF) Protease inhibitor cocktail (Complete Mini, EDTA free, and Roche Cat #: 11836170001). One table was

	dissolved 10 ml of the buffer, immediately before use and used for lysis of approximately 12× 50 O.D. of cells. 10 mM Tris-HCl, pH 7.5
b) Sorbitol buffer	300 mM Sorbitol 100 mM NaCl 5 mM $MgCl_2$ 10 mM EDTA 0.05% Phenylmethylsulfonyl fluoride (PMSF)

2.5.14. SDS-PAGE Solutions and Reagents (Sambrook 1989a)

a) 30% Acrylamide Mix	29.2% (w/v) Acrylamide 0.8% (w/v) N, N' methylenebisacrylamide Filtered before use.
b) Resolving (Lower) Gel Tris Buffer (Stock-4X) 1.5 M Tris-HCl (pH 8.8)	18.18 g Tris pH adjusted to 8.8 with 6N HCl and volume made up to 100 ml. (0.4% SDS can be added to the buffer).
c) Stacking (Upper) Gel Tris Buffer (Stock) 0.5 M Tris-HCl (pH 6.8)	6.06 g Tris pH adjusted to 6.8 with HCl and volume made up to 100 ml. (0.4% SDS can be added to the buffer).
d) 0.4% SDS	
e) TEMED	
f) 10% APS (Ammonium persulphate)	
g) Tris-Glycine Gel Running Buffer (Laemmli Buffer) (pH 8.3)	25 mM Tris base 250 mM Glycine (electrophoresis grade) 0.1% SDS
h) 5× Sample Buffer/Gel Loading Buffer (pH 6.8)	0.15 M Tris-HCl (pH 6.8) 5% SDS

	25% Glycerol 12.5% β-mercaptoethanol 0.006% Bromophenol blue
i) Gel Staining Solution	40% Methanol 10% Glacial Acetic acid 0.1% Coomassie Brilliant Blue (R250)
j) Gel Destaining Solution	40% Methanol 10% Glacial Acetic acid

Composition of SDS-PAGE Resolving (Lower) Gel (9%) (For 10 ml)

a) Distilled water	4.35 ml
b) Resolving (Lower) Gel Tris Buffer (Stock) (4×) 1.5 M Tris-HCl (pH 8.8) with 0.4% SDS	2.5 ml
c) 30% Acrylamide Mix	3.35 ml
d) 10% APS (Ammonium persulphate)	0.05 ml
e) TEMED (N, N, N', N'-Tetramethylethylenediamine)	0.01 ml

Composition of SDS-PAGE Stacking (Upper) Gel (4%) (For 10 ml)

a) Distilled water	6.1 ml
b) Stacking (Upper) Gel Tris Buffer (Stock) 0.5 M Tris-HCl (pH 6.8) with 0.4% SDS	2.5 ml
c) 30% Acrylamide Mix	1.3 ml
d) 10% APS (Ammonium persulphate)	0.05 ml
e) TEMED (N, N, N, N-Tetramethylethylenediamine)	0.01 ml

2.5.15. Immunoblotting (Western Blotting) Reagents (Sambrook 1989a)

a) Transfer Buffer (pH 9.2)	48 mM Tris base 39 mM Glycine 0.037% SDS 20% Methanol
b) Stripping Buffer	62.5 mM Tris-HCl, pH 6.7 100 mM β-mercaptoethanol 2% SDS

c) Tris-Buffered Saline (TBS)	150 mM NaCl 20 mM Tris-HCl (pH 7.5) (Made as 10× stock and kept at 4°C)
d) Washing Buffer **TBS-Tween 20 (TBST) Buffer**	0.1% Tween 20 in TBS (pH7.5)
e) Blocking Agent	5% Skim milk in TBST.
f) Ponceau S Staining Solution	0.5% Ponceau S 1% Glacial Acetic acid

2.5.16. Immunofluorescence Reagents

a) Potassium phosphate buffer (100 mM, pH 6.5)	
b) Polylysine stock (1% w/v in sterile water) (10×)	Dilute five times in 1× PBS just before use. (For coating the cover slips, 15 µl of the working stock of polylysine is dropped on each cover slip and a stack is prepared. Kept in a moist chamber at 4°C overnight. Coated coverslips were washed in sterile water and dried before use).
c) Fixative buffer	4% Paraformaldehyde prepared in 100 mM Potassium phosphate buffer (pH 6.5). 4.0 g of Paraformaldehyde was dissolved in 50 ml of sterile water and kept on magnetic stirrer with heating around 60°C. To this 50 ml of 200 mM phosphate buffer (pH 6.5) is added. pH adjusted to around 6.5 with NaOH and allowed to dissolve. Kept in aliquots at -20°C.
d) Sorbitol Buffer	1.2 M Sorbitol in 0.1 M phosphate buffer
e) 50 mg/ml Zymolase	50 mg/ml stock prepared in 50% glycerol or in Sorbitol buffer and kept at -20°C (up to 6 months).
f) 50 mg/ml Lyticase	50 mg/ml stock prepared in 50% Sorbitol

	buffer and kept at -20°C.
g) Phosphate-Buffer Saline (PBS)	40 mM K_2HPO_4 10 mM KH_2PO_4 pH 7.4 150 mM NaCl. Prepared as 10X stock pH of stock comes around 6.7.
h) Permeabilization buffer	0.4% Triton X-100 in PBS
i) Blocking/ antibody dilution buffer	1% BSA (w/v) in PBS

SECTION B: METHODS

2.6 Growth and maintenance of bacteria and yeast strains

The *Escherichia coli* strains DH5α was routinely used as a cloning host and grown in LB medium at 37°C. *E. coli* transformants were selected and maintained on LB medium supplemented with ampicillin.

The *S. cerevisiae* strains were regularly maintained on YPD medium and grown at 30°C. The yeast transformants were selected and maintained on SD medium with supplements as per the requirement.

2.7.Recombinant DNA methodology (restriction digestion, ligation, transformation of *E. coli* PCR amplification, etc.)

All the molecular techniques used in the study for manipulation of DNA, protein, bacteria and yeast were according to standard protocols (Sambrook 1989a; Guthrie & Fink 1991) or as per manufacturer's protocol, unless specifically mentioned.

2.8. Construction of Site-directed mutants of *HGT1*

HGT1, having hexahistidine epitope at the N-terminus and HA tag at the C-terminus was cloned downstream of the TEF promoter at BamH1 and EcoR1 site of p416TEF vector resulting in plasmid p416TEF-His-HGT1-HA. This construct was further used as a template for creation of different site-directed mutants of *HGT1* by splice overlap extension strategy. The PCR products generated with these oligonucleotides were sub-cloned back into the empty TEF vector background using appropriate restriction sites. The desired nucleotides changes were confirmed by sequencing. The different mutagenic oligonucleotides primers used for generation of these mutants are given in Table 2.1.

2.9. *In vitro* Random Mutagenesis using Hydroxylamine Solution

The protocol for *in vitro* mutagenesis was adopted from Rose and Fink, (1987). 10 μg plasmid DNA was dissolved in 0.5 ml of Hydroxylamine solution (90 mg NaOH, 350 mg hydroxylamine HCl in 5 ml water, pH around 6.5. freshly made up before use). This mixture was incubated at 37°C for 20 hrs and the DNA was purified using Qiagen column. The pool of mutagenized plasmid was directly transformed into the appropriate yeast strain.

2.10. Transformation of yeast

The transformation of *S. cerevisiae* strains were carried out by lithium acetate method (Ito *et al.* 1983b). *S. cerevisiae* cultures were grown in YPD at 30°C with shaking for overnight and then reinoculated in fresh YPD to an initial OD_{600} of 0.1, cells were allowed to grow at 30°C for 4-5 hours with shaking. Cells were harvested at 6000 rpm for 5 min, washed twice with sterile water followed by subsequent wash with 0.1 M lithium acetate solution (prepared in TE, pH 7.5) and were finally resuspended in the same solution. Cells were incubated at 30°C for 30 min with shaking. The cells were pelleted, suspended in 0.1 M lithium acetate solution to a cell density of 1×10^9 cells/ml and divided into 100μl aliquots. Approximately 50 μg (5 μl of 10 mg/ml stock solution) of heat denatured, salmon sperm single strand carrier DNA, followed by 0.3 μg- 0.7μg of plasmid/DNA fragment were added to each aliquot and whole cell suspension was incubated at 30°C for 30 min. After the incubation, 300 μl of 50% PEG 3350 (prepared in 0.1 M lithium acetate, pH 7.5) was added to each tube, mixed well and again kept at 30°C for 45 min. The cell suspensions were subjected to heat shock at 42°C for 10 min. and the cells were allowed to cool at room temperature. The cells were pelleted down at 8000 rpm for 5 min. The cell pellet was washed and resuspended in sterile water and appropriate volume of cell suspension was plated on selection plates.

2.11. Isolation of plasmid from yeast

Selected yeast transformants were inoculated in 3 ml of selection medium and the cultures were incubated at 30°C with shaking for 18-20 hrs. After the incubation, the cells were harvested at 8,500 rpm for 5 min at room temperature and the pellets were resuspended in plasmid mini prep resuspension solution. Equal amounts of sterile, acid-washed glass beads were added and the cell

suspensions were vortexed vigorously for 1 min ×5 at room temperature. The lysis ssolution was added, mixed properly by inverting followed by neutralization solution. The lysates were spun down at 12,000 rpm for 5 min at RT and the supernatant was loaded in plasmid mini prep columns and eluted in 30 µl elution buffer. 10 µl of this DNA was transformed in *E. coli* and transformants were selected on LB plates (containing ampicillin). The *E. coli* transformants were then grown to isolate plasmids and verified by re-transformation into yeast.

2.12. Isolation of genomic DNA from yeast

Genomic DNA from *S. cerevisiae* strains was isolated as described by (Kaiser *et al.* 1994) using the glass bead lysis method and the STES lysis buffer, described in section 2.5.10.

2.13. Growth assay by dilution spotting

For growth assay, *S. cerevisiae* strains carrying the plasmid were grown overnight in SD minimal medium without uracil and reinoculated in fresh medium to an OD_{600} of 0.1 and grown for 6 hours. The cells in the exponential phase were harvested, washed twice and resuspended in sterile water to an OD_{600} of 0.2. These were serially diluted to 1:10, 1:100 and 1:1000. 10 µl of these cell resuspension were spotted on minimal medium plates containing different concentrations of glutathione or methionine as sole sulphur source. The plates were incubated at 30ºC for 2-3 days and photographs were taken.

For evaluation of the functional activity of Hgt1p mutants using plate based dual-complementation-toxicity assay was used. *S. cerevisiae* ABC 817 was transformed with a single-copy centromeric empty vector or vector expressing wild-type or different mutants of HGT1 expressed downstream of the TEF promoter. Transformants were selected and grown in minimal media without uracil and containing methionine as a sulphur source along with other supplements. After overnight growth in this media, cultures were reinoculated in fresh media and allowed to grow until they reached the OD_{600} of 0.6-0.8. An equal volume of cells were harvested, washed with water, and resuspended in sterile water at an OD_{600} of 0.2. These were serially diluted to 1:10, 1:100, and 1:1000 in 1 ml and 10 µl of these cell resuspensions were spotted on minimal medium containing methionine (200 µM) or different concentrations of glutathione (15, 30, 50, 100 and 200 µM) as sole source of organic sulphur.

HGT1 under the strong TEF promoter is able to confer the ability to grow on low (15 µM) concentrations of glutathione. However growth at higher concentrations (>50 µM) leads to excessive uptake of glutathione causing toxicity. Using this growth phenotype *i.e.* complementation of the *hgt1*Δ defect at low GSH concentrations, and toxicity at higher GSH concentrations, we have been able to grade the mutants. The plates were incubated at 30 °C for 2–3 days and photographs were taken. For pH based plate assay, SD media plates of different pH was used for evaluation of growth phenotype.

2.14. Transport assay

The *Saccharomyces cerevisiae* ABC 817 strain transformed with wild-type or HGT1 mutants plasmid constructs under TEF promoter was grown in minimal media containing methionine and other supplements, without uracil for 12-14 hours. These cultures were reinoculated in the fresh media and allowed to grow until they reached OD_{600} of 0.6-0.8. Cells were harvested, washed with ice cold water followed by ice cold MES-buffer (20mM MES/KOH, 0.5mM CaCl2, 0.25mM MgCl2, pH 5.0, 5.5, 6.0 or 6.5) or HEPES-buffer (20mM HEPES, 0.5mM CaCl2, 0.25mM MgCl2, pH 7.0, 7.5, 8.0 or 8.5) and cells were finally resuspended into respective buffer containing 2% glucose (resuspension buffer). 200 µl of cells at OD_{600} of 3.75 ml^{-1} were aliquoted and kept on ice. After a 5 min incubation of cells at 30 °C, glutathione uptake was initiated by addition of 200 µl of assay medium containing radiolabelled glutathione ([^{35}S]-GSH, specific activity 768 Ci $mmol^{-1}$). The uptake was stopped by diluting the medium with 20-fold volume of ice-cold water and cells were collected on the glass fiber filter using vacuum filtration. The harvested cells were washed with the same volume of ice-cold water twice and the filters were immersed in 3 mL of scintillation fluid (Sigma-Fluor Universal LSC cocktail) and radioactivity was measured using a liquid scintillation counter (Perkin Elmer) (Thakur *et al.* 2008).

For saturation kinetics (*Km* and *Vmax* determination), the initial rate of glutathione uptake was measured at a range (12.5 µM to 400 µM) of glutathione concentrations with specific activity being kept constant at each concentration (10^{-3} Ci $mmol^{-1}$). To determine the *Ki*, GSH uptake kinetics were performed in the presence of different fixed inhibitor concentrations (0, 50, 100, 200, 400 µM). Estimates of *Km* (app) and *Vmax* were obtained by nonlinear regression analysis of V vs. [S] for each inhibitor concentration followed by Michaelis-

Menten fit using GraphPad Prism 5.0. Further in a plot of *Km* (app)/*Vmax* versus inhibitor concentration [I] (µM), intercept of line on x-axis represents *–Ki*. The initial rate of glutathione uptake in cells containing test plasmids was determined after subtracting corresponding values from cells containing empty vector. For the measurements of total protein, the 100 µl of the above cell suspension (used for the transport assay) was boiled with 15% NaOH for 10 min, followed by neutralization of total cell lysate by addition of HCl; 100 µl of this crude cell lysate was incubated with 0.1% Triton X-100 for 10 min at RT and total protein was estimated by using the Bradford reagent using bovine serum albumin as a standard.

2.15. Yeast whole cell extract preparation

Total crude cell extract were prepared as described previously with certain modifications (Aggarwal & Mondal 2006). Briefly, overnight cultures of transformants grown in minimal media containing methionine and other supplements without uracil, were reinoculated at OD_{600} of 0.1 in 50 ml of fresh medium and grown to exponential phase (OD_{600} of ~0.6 to 0.8). Cells were harvested by centrifugation and resuspended in yeast breaking buffer for whole cell extract preparation containing protease inhibitors. Acid-washed glass beads were added to the cell suspension and cells were lysed by vigorous vortexing. The resulting homogenate was centrifuged for 10 min at 13,000 rpm and the supernatant fraction was collected.

2.16. Protein estimation

Protein estimation of the samples was done by Bradford Assay (Bradford 1976) using Bradford reagent as per the manufacturer's instructions. The protein samples were diluted 10 times and 2.5µl of the diluted sample was used for protein estimation, using BSA as standard. Protein estimations were done in triplicates.

2.17. Protein electrophoresis and western blotting

The western blot analysis was done using a modified protocol of the standard western blot (Kaur & Bachhawat 2009b). Equal amount of protein samples (20 µg) were resolved by 9% SDS–polyacrylamide gel electrophoresis and electroblotted onto Hybond ECL nitrocellulose membrane in a mini transblot apparatus (Bio-Rad) at 120V for 1 hour using Tris-glycine transfer buffer. Immediately after the transfer, the membrane was incubated at 55°C for 15 min

in the stripping buffer. After blocking the membrane for 1 hour at room temperature in 5% skim milk in TBST buffer, it was probed with mouse monoclonal anti-HA primary antibody at a dilution of 1:2000 in the TBST buffer for 4 hours at room temperature. After 4×10 minutes washing of the blot with TBST, the membrane blot was incubated for 1 hour in horse anti-mouse (horseradish peroxidase-conjugated) antibody at a dilution of 1:2500 in the TBST buffer. The signal was detected with an ECL plus Western detection kit as per the manufacturer's instruction.

Densitometry analysis of the unsaturated band signals was performed using the Scion Image software to quantify the protein expression levels in different mutants. The resulting signal intensity was normalized with respect to the band surface area (in square pixels) and expressed in arbitrary units. The relative protein expression levels in the mutant Hgt1p were represented as percentage expression relative to wild-type Hgt1p.

2.18. Cellular localization of the mutants by confocal microscopy

To check localization of Hgt1p and its different mutants, indirect immunofluorescence was performed using a modified published protocol (Kaur & Bachhawat 2009a). Briefly yeast cells having plasma membrane H^+-ATPase (Serrano *et al.* 1986) FLAG tagged at C-terminus in the genome was transformed with WT or mutants plasmid construct under TEF promoter. Single colony was picked and grown in minimal media containing methionine and other supplements without uracil overnight. These cultures were reinoculated in fresh media and harvested at OD_{600} of 0.5-0.7. Cells were fixed using 4% paraformaldehyde followed by spheroplasting using lyticase enzyme. Spheroplasts were washed in sorbitol buffer and was adhered on the polylysine coated coverslips. The spheroplasts were permeabilized by treatment of 0.4% Triton X-100 in PBS (pH 7.4) followed by blocking with 1% BSA in PBS (blocking buffer). Overnight incubation with mouse anti-HA and rabbit anti-Flag primary antibodies (1:1000 dilution) at 4°C followed by washing and treatment with secondary antibodies (goat anti-mouse IgG-Alexa 488 and mouse anti-rabbit IgG Alexa 647, 1:500 dilution) for 4 hours at RT. Coverslips were washed with blocking buffer and inverted onto a slide using vectashield antifade mounting medium. Images were obtained with an inverted LSM780 laser scanning confocal microscope (Carl Zeiss) with a Plan-Apochromat X63, oil

immersion objective with numerical aperture 1.4 at RT. The 488-nm argon ion laser and 633-nm of He-Ne ion laser line was directed over an MBS 488/561/633 beam splitter, and fluorescence was detected. Images obtained were processed using ImageJ software.

To confirm the predicted topology, we used HGT1 construct having hexahistidine epitope at the N-terminus and HA-tag at the C-terminus. The localization of N- and C-terminus was verified by indirect immunofluorescence using peptide directed antibodies against these epitopes in permeabilized spheroplasts by treatment of 0.4% Triton X-100 or non-permeabilized spheroplasts. Signal detection in non permeabilized cells will suggest the extracellular localization of the tag which will also be detected in permeabilized cells. However if the tag is intracellular, signal will not be detected in non-permeabilized cells but will be detected in permeabilized cells only suggesting its intracellular localization.

2.19. Sequence analysis

The *HGT1* protein sequences was retrieved from the *Saccharomyces* genome database (SGD). The Hgt1p sequence was used as query sequence in BLAST search of protein database from Entrez at NCBI website, (http://www.ncbi.nlm.nih.gov/) to retrieve a list of homologues of Hgt1p. The multiple sequence alignment of the protein sequences was generated using MUSCLE programme (Edgar 2004).

2.20. Modelling the transmembrane segments of Hgt1p

The transmembrane helices were identified using TM prediction programs, such as OCTOPUS (Viklund & Elofsson 2008), HMMTOP (Tusnady & Simon 2001), and MEMSAT-SVM (Nugent & Jones 2009), and yielded a consensus of 13 TM helices. Hgt1p belongs to the OPT family of transmembrane proteins and there are no structures available for any member of this family of proteins. We therefore attempted to model the structure initially with *ab initio* modelling using Rosetta. Fragments were generated using the Robetta server (Kim *et al.* 2004), and the assembled membrane structure was modelled using Rosetta *ab initio* membrane protocol, which also utilizes the lipophobicity profile for modelling the helices (Yarov-Yarovoy *et al.* 2006; Barth *et al.* 2007). However, more number of helices and the longer inter-helical loops made it difficult to use the *ab initio* protocol alone. The helices thus obtained in *ab initio* structure were then

further restrained using Cα-Cα restraints calculated from the known crystal structures of proteins, containing 12-13 TM helices and belonging to the MFS family (PDBs: 1PV7, 3O7Q, 1PW4, 2XUT). The most probable structure was selected with helical orientation with defined pore formation for substrate transport and the probable pore lining helices (also predicted by MEMSAT-SVM) were matched with the experimental mutagenesis data.

2.21. Cytosolic acidification Measurement

The yeast ABC 817 strain expressing pHluorin were transformed with WT or HGT1 mutant plasmid constructs under TEF promoter and was grown overnight in minimal media containing methionine. The cultures were then reinoculated in a fresh media and further allowed to grow until they reached OD_{600} of 0.6-0.8. Cells were harvested, washed and finally resuspended (3.5 OD_{600}/ml) into resuspension buffer (20mM MES/KOH, 0.5mM CaCl2, 0.25mM MgCl2, 2% glucose, pH 5.5). After a 10 min incubation at 30°C, cell resuspension was transferred to cuvettes and fluorescence intensity was monitored for 30 min using FluoroMax 4 spectrofluorometer (Horiba Jobin Yvon Inc.) at 508 nm with excitation at 405 nm and 485 nm every 30 sec at 30 °C with constant stirring (1mM GSH was added after 3 min). Background signals (cells without pHluorin) were subtracted and the ratio of ex 405/ ex485 was calculated and plotted vs. time using GraphPad Prism 5 software.

CHAPTER 3:

Determination of Substrate Specificity of Hgt1p toward Reduced Glutathione and Different Glutathione Conjugates

INTRODUCTION

Hgt1p, a member of the oligopeptide transporter family has been described as a high-affinity glutathione transporter since disruption of this gene in yeast led to a complete loss of glutathione uptake ability and the kinetic analysis demonstrated it having a *Km* of 54 µM for reduced glutathione. However this glutathione transport was also inhibited by oxidized glutathione (GSSG), and some specific glutathione-conjugates (Bourbouloux et al., 2000). Simultaneously this ORF *YJL212c* was also described as an oligopeptide transporter, *ScOPT1* by Hauser and co-workers since it could transport the endogenous opioids leucine enkephalin (Tyr-Gly-Gly-Phe-Leu) and methionine enkephalin (Tyr-Gly-Gly-Phe-Met) (Hauser et al., 2000). The radiolabelled leucine enkephalin kinetics exhibited a *Km* of 310 µM. The substrate specificity of Hgt1p/ ScOpt1p was further investigated by Osawa and co-workers using two-electrode voltage clamp experiments in *Xenopus laevis* oocytes. They compared the oligopeptide and glutathione transport ability of Hgt1p and demonstrated that Hgt1p produced inward currents in the oocytes in response to GSH, GSSG, glutathione derivatives phytochelatin (PC) and tetrapeptide GGFL, but not by KLGL suggesting that Hgt1p retains a level of substrate specificity among oligopeptides. Further kinetic analysis revealed that the Hgt1p/ScOpt1p mainly functions as a transporter of GSH or GSH-derived compounds (Osawa et al., 2006) (Discussed in general introduction 1.3.1.1)

In contrast to Hgt1p, other reported eukaryotic glutathione transporters that includes the mammalian plasma membrane ABC transporter, multidrug resistance-associated protein (MRP1) (orthologous to the yeast vacuolar YCF1) which exports glutathione out of the cytosol with low affinity (in the millimolar range) while transporting glutathione-conjugates with far higher affinity (in the micromolar range), and thus are better referred to as glutathione-conjugate pumps (Cole and Deeley, 2006; Li et al., 1996). The other well-characterized transporter is the mitochondrial ABC transporter, ATM1 in yeast (orthologous to plant ATM3 and vertebrate ABCB7) whose crystal structure was recently solved in complex with glutathione (Srinivasan et al., 2014). However, these proteins (Atm1p and Atm3p) preferentially transport GSSG rather than GSH out of the mitochondrial matrix. Further *in vitro* and genetic interaction studies provide evidence for the export of glutathione trisulphides (GS-S0-SG) as a physiological substrate for these transporters suggesting that despite a crystal structure with glutathione bound to it, these are also glutathione-conjugate

transporters (Schaedler et al., 2014). Thus, except Hgt1p, all reported eukaryotic GSH transporters had been shown to transport GSH-conjugates rather than reduced glutathione with higher affinity.

In this chapter, we have revisited the substrate specificity of Hgt1p since transport of reduced glutathione was significantly inhibited by oxidized glutathione and glutathione conjugates suggesting that these are likely substrates as well (Bourbouloux et al., 2000). However, the relative kinetics was never rigorously compared. Investigations carried out in this chapter have addressed that lacuna. To further investigate the importance of each residue of the glutathione tripeptide (γ-Glu-Cys-Gly), we carried out the comparative inhibition studies using custom synthesized analogs of glutathione and could demonstrate the critical requirement for the γ-glutamyl and cysteine residues for recognition by Hgt1p.

3.1. Hgt1p transporter has a distinct preference for reduced glutathione when compared to other naturally occurring conjugates:

As discussed above except Hgt1p, all reported eukaryotic GSH transporters have been shown to preferentially transport GSH-conjugates rather than reduced glutathione with higher affinity. We therefore, sought to investigate the substrate specificity of Hgt1p in greater detail. We initially carried out comparative inhibition studies where we measured the [^{35}S] GSH uptake in the presence of 10-fold excess of potential competing ligands such as GSH, S-methyl-GSH, S-hexyl-GSH, S-decyl-GSH, S-lactoyl-GSH, glutathione sulphonate and GSSG (Fig 3.1a). The addition of a ten-fold excess of cold GSH decreases the amount of radioactive GSH transported into the cells (Fig 3.1b). We observed about 85% inhibition in the glutathione uptake by Hgt1p as expected upon addition of a 10-fold excess of cold GSH. Interestingly amongst the different ligands used, significant inhibition was observed with S-decyl-GSH (87%), S-hexyl-GSH (86%) and S-methyl-GSH (83%). Slightly lower levels of inhibition were observed with S-lactoyl-GSH (76%) and GSSG (72%) as compared to GSH suggesting that both GSH as well as glutathione-S-conjugates to be substrates for Hgt1p. However very little inhibition was observed in the case of glutathione sulphonate (<5%) suggesting that although Hgt1p can transport a wide variety of GSH conjugates, it still retains a level of substrate specificity.

A more rigorous comparison of affinities of these possible ligands becomes possible with the determination of kinetic parameters. The apparent *Km* of WT Hgt1p for glutathione was estimated to be 27.8 ± 1.2 µM and the *Vmax* was found to be 54.0

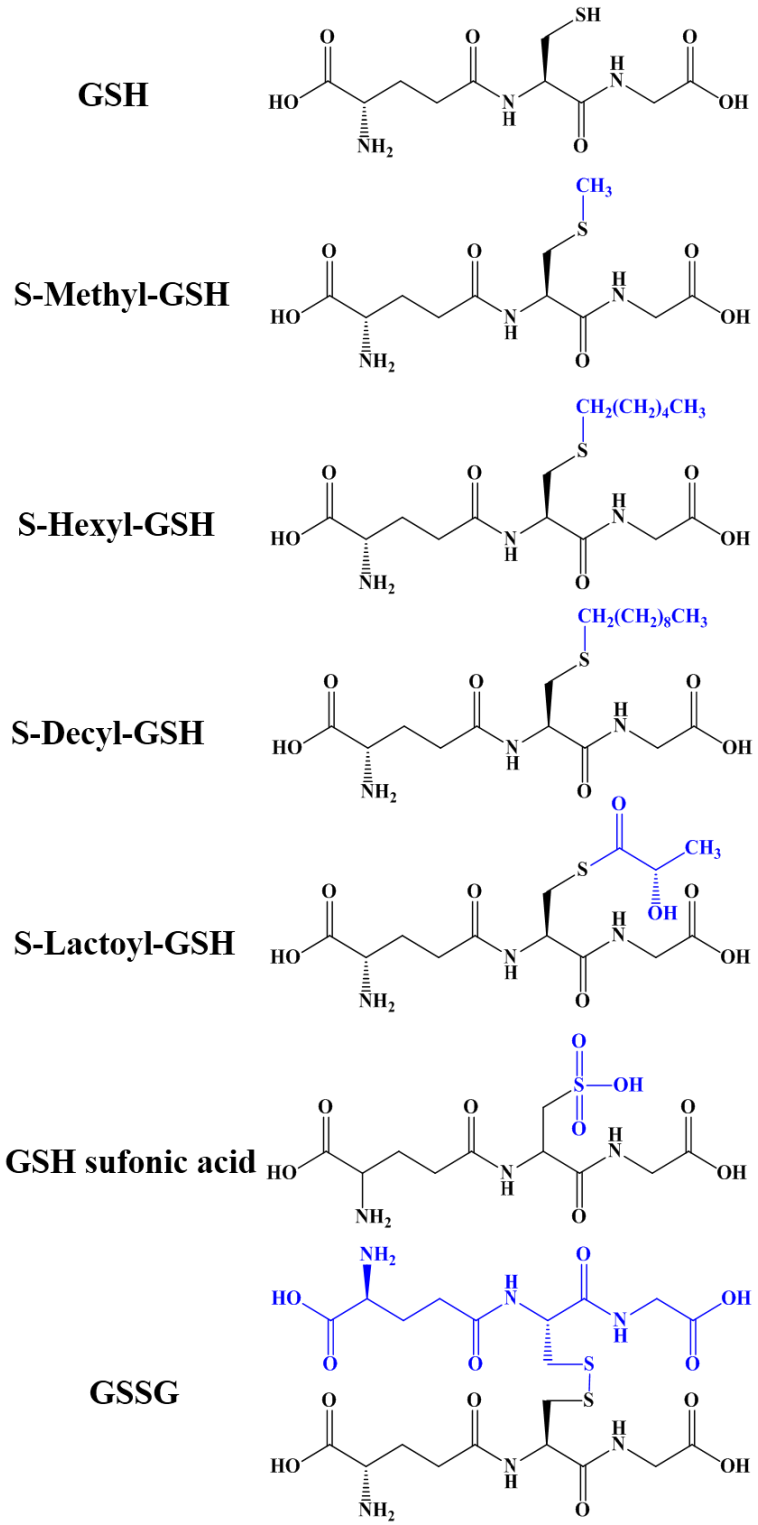

Figure 3.1a: Chemical structures of GSH and its conjugates examined in this study.

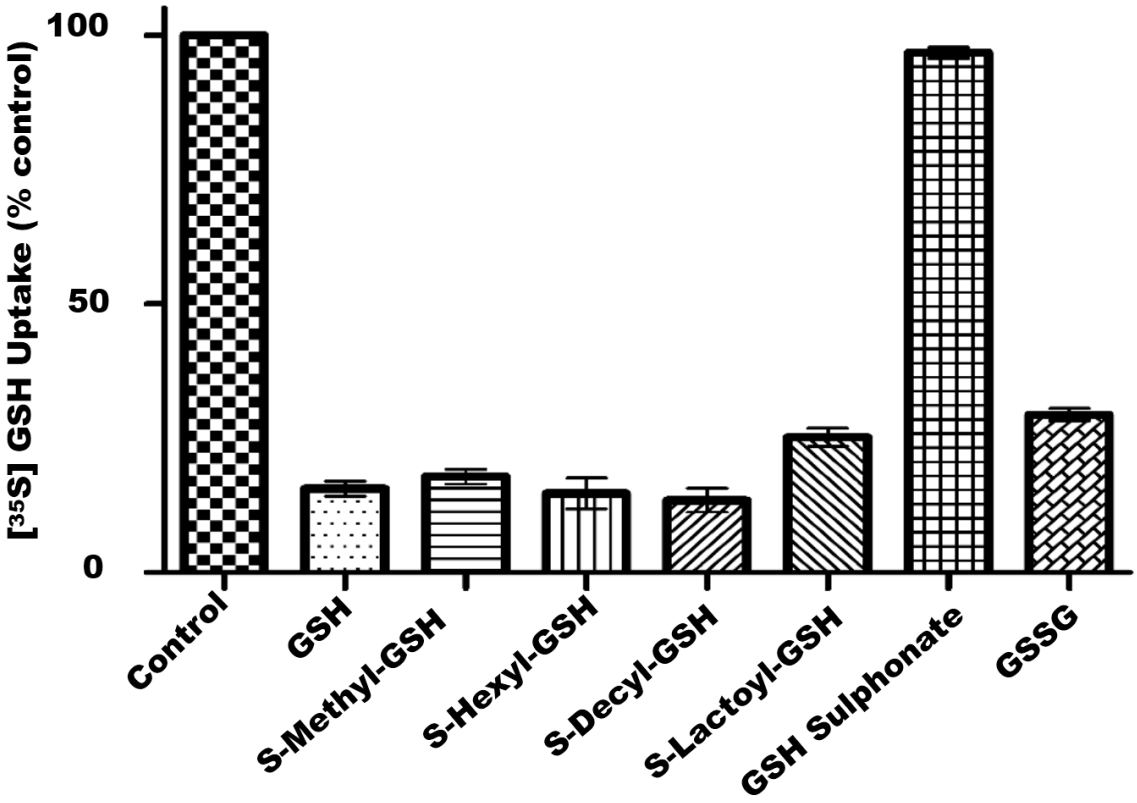

Figure 3.1b: Inhibition of glutathione uptake by different glutathione conjugates: The initial rate of [^{35}S]GSH uptake was measured in ABC 817 transformed with TEF-HGT1 at 30°C in the absence (control) or presence of 500 μM of GSH or glutathione conjugates (S-methyl-GSH, S-hexyl-GSH, S-decyl-GSH, S-lactoyl-GSH, glutathione sulphonate and GSSG). The cells were harvested at 1 and 3 min intervals and results were plotted as % control. Data are representative of two different experiments and shown as mean ± S.D. (n = 4).

± 0.8 nmol of glutathione.mg of protein^{-1}.min^{-1}. Although the *Vmax* value was close to that of previously reported value (57.8 ± 5.5 nmol of glutathione.mg of protein^{-1}.min^{-1}), the *Km* value in the present study was found to be lower than that of the previously reported *Km* (≈ 50 µM) (Kaur and Bachhawat, 2009). Since *Km* values are highly dependent on pH values, one possible explanation for the difference in the *Km* may be due to the small difference in the pH adjustment of the transport buffer under two different lab conditions. Alternatively this could be due to the different source of radioactivity used in the two studies (from Perkin Elmer, USA in the current study as opposed BARC, Mumbai, India in the previous studies). The *Km* determination of the other compounds however, was not possible owing to the lack of availability of these radio-labelled conjugates. We, therefore, sought to determine the *Ki* of a few selected inhibitors showing significant inhibition (S-methyl-GSH, S-hexyl-GSH, S-lactoyl-GSH and GSSG) for detailed kinetic analysis. The *Ki* was determined as a measure of substrate affinity by measuring substrate-velocity curves in the presence of several fixed inhibitor concentrations (0, 25, 50, 100, 200 and 400 µM). Our results indicated that all these ligands were competitive inhibitors as the *Vmax* remained constant but the effective *Km* increased with increasing inhibitor concentrations (Fig. 3.1c A-E). The *Ki* of GSH was also determined for comparison and was found to be 24.2 ± 6.5 µM. The *Ki* for GSSG (92.5 ± 9.8 µM) was significantly higher than GSH suggesting a significantly lower affinity of Hgt1p for GSSG as compared to GSH. The *Ki* for S-hexyl-GSH (34.2 ± 8.0 µM) was found to be close to that of reduced glutathione followed by S-lactoyl-GSH (51.2 ± 3.3 µM) and S-methyl-GSH (65.4 ± 4.2 µM) (Fig. 3.1c F). These results suggest that Hgt1p preferentially binds GSH but also binds to a broad range of GSH derivatives with variable affinity, but preferring those with a hydrophobic group linked to the sulfhydryl group of glutathione. However, competition by the substrates do not necessarily indicate that they are transported.

3.2. GSSG and S-lactoyl glutathione can be utilized as sulphur source:

From the above studies, Hgt1p was shown to recognize and transport glutathione, but it can also bind to oxidized glutathione (GSSG), S-lactoyl-GSH, S-methyl-GSH, S-hexyl-GSH and S-decyl-GSH with significant affinity. The competition assays are performed on a shorter time scale, while the growth assay is based upon prolonged incubation period. The latter might be more sensitive in identifying minute differences in the transport properties. For example, in the inhibition assay, γ-Glu-Cys did not inhibit glutathione uptake significantly

(Bourbouloux *et al.*, 2000) but in the plate-based growth assay, HGT1 overexpressing strain was able to use γ-Glu-Cys as a sulphur source at higher concentrations when incubated for a longer period of time. Therefore, in addition to radiolabelled competition experiments, we examined the behavior of Hgt1p in relation to different substrates by a growth based assay. The assay exploited an organic sulphur auxotroph (ABC817, *met15*Δ*hgt1*Δ) that was also deleted for the glutathione transporter. This strain was transformed with p416TEF HGT1 to see how the different ligands could support growth.

The conjugates S-methyl-GSH, S-hexyl-GSH and S-decyl-GSH in spite of showing very good inhibition and being potentially good substrates for Hgt1p, did not support growth at any of the tested concentrations (Fig. 3.2a). A possible explanation is that *S. cerevisiae* is either not equipped to catalyze the cleavage of the thioether linkage in glutathione conjugates or these substrates can bind the transporter with high affinity but are not transported inside and hence cannot be used as a source of sulphur. Only S-lactoyl-GSH and GSSG in addition to GSH showed growth phenotype starting from low conc. (15 µM) and showed toxicity at higher concentrations (>100 µM) due to excess accumulation (Fig.3.2b). However, as compared to glutathione improved growth phenotype was observed at same concentrations of GSSG and S-lactoyl glutathione. In contrast met-enkephalin which was suggested to be low affinity substrate for Hgt1p (Hauser *et al*. 2000), showed growth only at higher concentrations.

3.3. Inhibition studies with glutathione analogs reveals the involvement of all three amino acids of glutathione in the recognition by Hgt1p:

Previous studies have shown that the γ-glutamyl group of glutathione is critical for recognition by the glutathione transporters since the normal tri-peptide Glu-Cys-Gly is not transported by Hgt1p (Thakur et al., 2008). To further investigate the importance of each residue of the glutathione tripeptide (γ-Glu-Cys-Gly), we custom synthesized analogs of glutathione. Each analog had one of the three amino acid residues replaced by an amino acid most similar in properties (Fig. 3.3a). In the first peptide, the glutamate residue was replaced with aspartate residue (to yield β-Asp-Cys-Gly) which contains the side chain carboxyl group of aspartic acid involved in the peptide bond formation, similar to the γ-glutamyl group. When we examined β-Asp-Cys-Gly for the ability to inhibit [^{35}S]-glutathione transport, we could not find any inhibition suggesting that this analog was not recognized by the transporter (Fig.

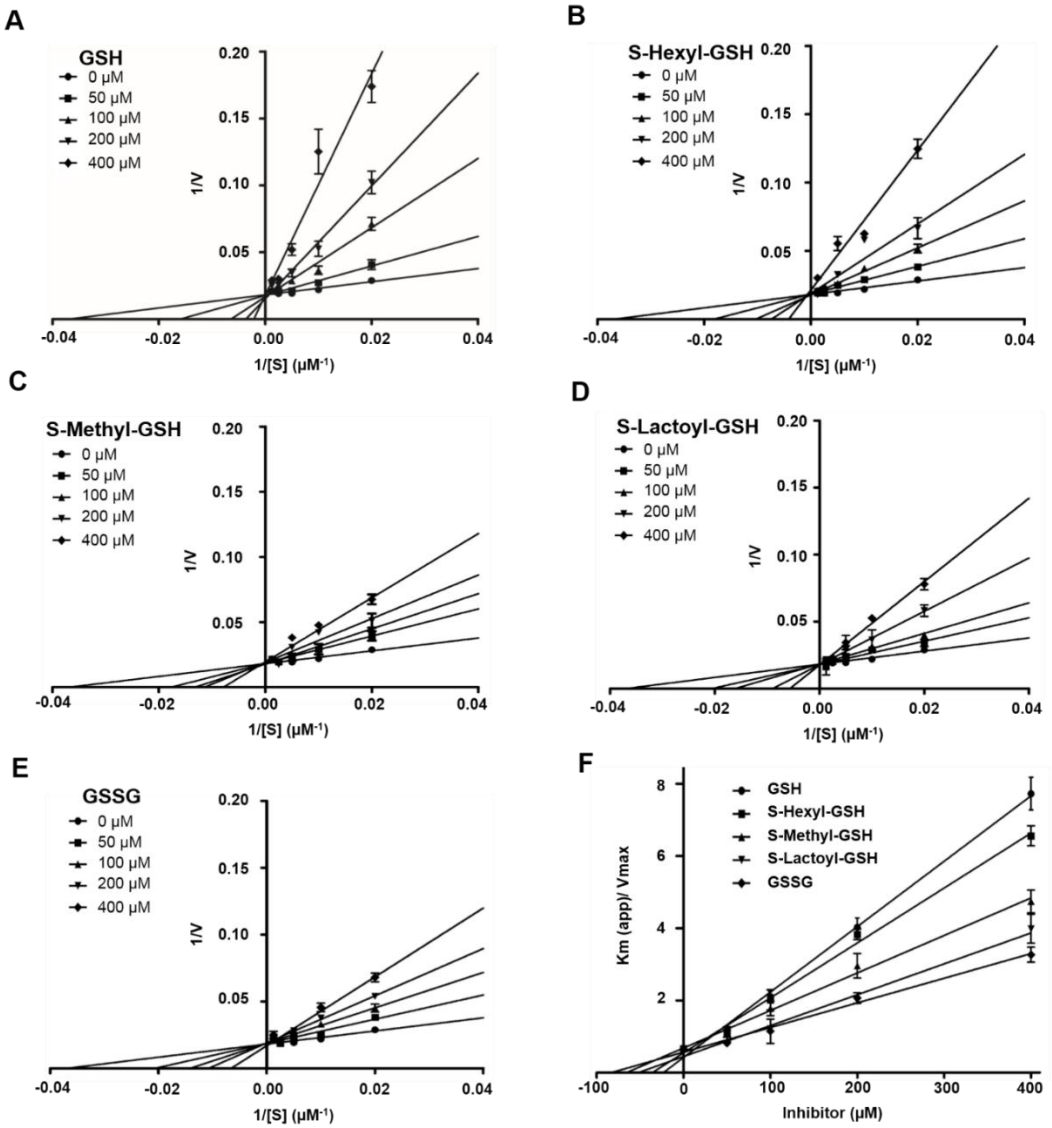

Figure 3.1c: Determination of *Ki* of GSH and its conjugates: Lineweaver-Burk double-reciprocal plots depicting the competitive inhibition of [^{35}S] GSH uptake by **(A)** GSH **(B)** S-Hexyl-GSH **(C)** S-Methyl-GSH **(D)** S-Lactoyl-GSH and **(E)** GSSG. Uptake kinetics were performed in the presence of different fixed inhibitor concentrations (0, 50, 100, 200, 400 µM). Data are representative of two different experiments and shown as mean ± SD (n = 4) **(F)** Plot of *Km*(app)/*Vmax* versus inhibitor concentration [I] (µM) to determine *Ki*. Estimates of *Km*(app) and *Vmax* were obtained by nonlinear regression analysis of V vs. [S] followed by Michaelis-Menten fit using GraphPad Prism 5.0 software for all the above mentioned possible inhibitors. Data are mean ± S.D. for n = 4. Solid line are linear regression analysis of data and intercept of line on x-axis represents –*Ki*.

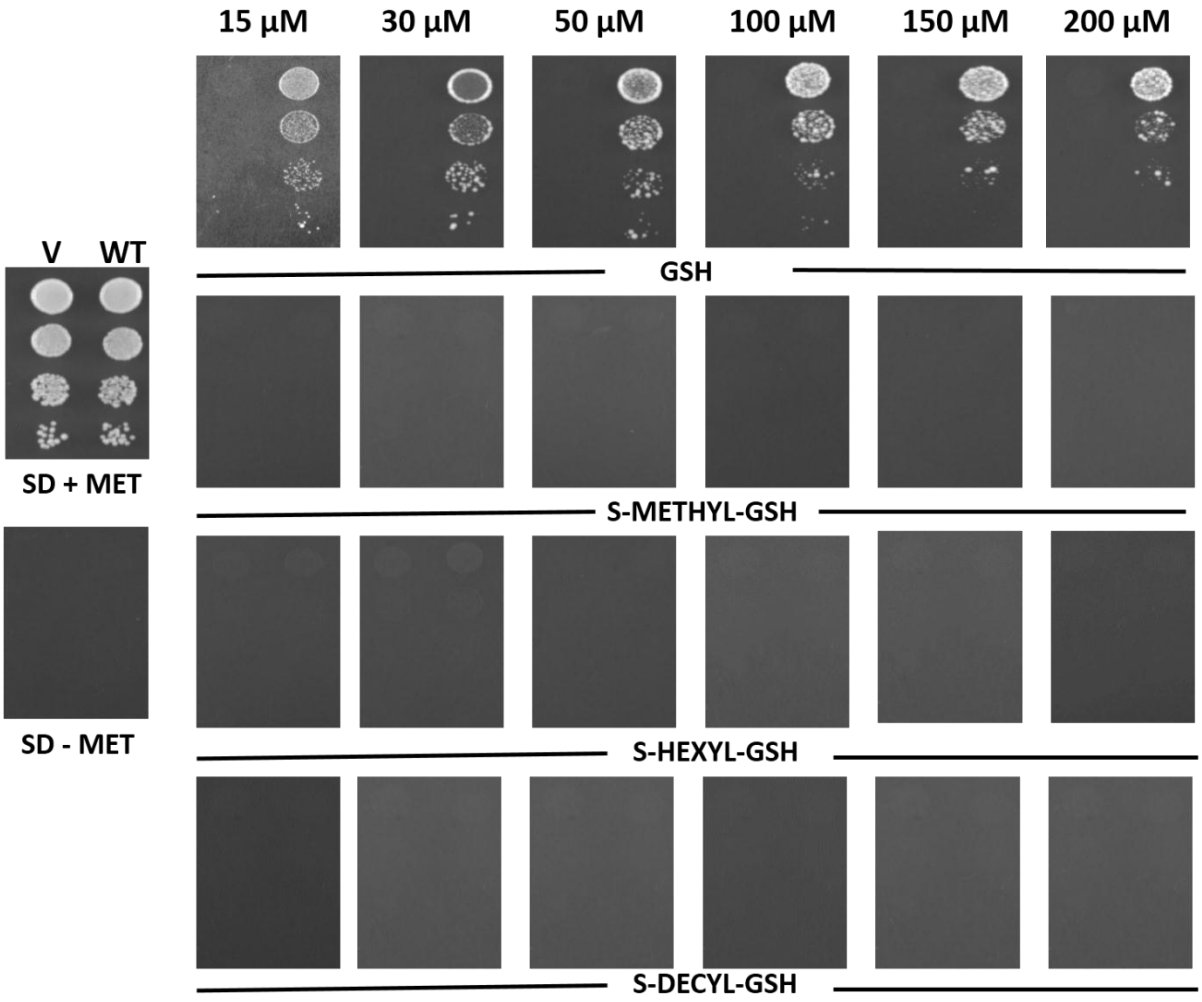

Figure 3.2 a: Functional analysis of WT and severely affected mutants on GSH and different GSH-conjugates: Growth of ABC 817 transformed with empty or wild type (WT) HGT1 under TEF promoter on minimal media containing no methionine (SD-MET), 200 µM methionine (SD+MET) or 15, 30, 50, 100, 200 µM of GSH, S-Methyl-GSH, S-Hexyl-GSH, S-Decyl-GSH. Experiment were repeated with three independent transformations.

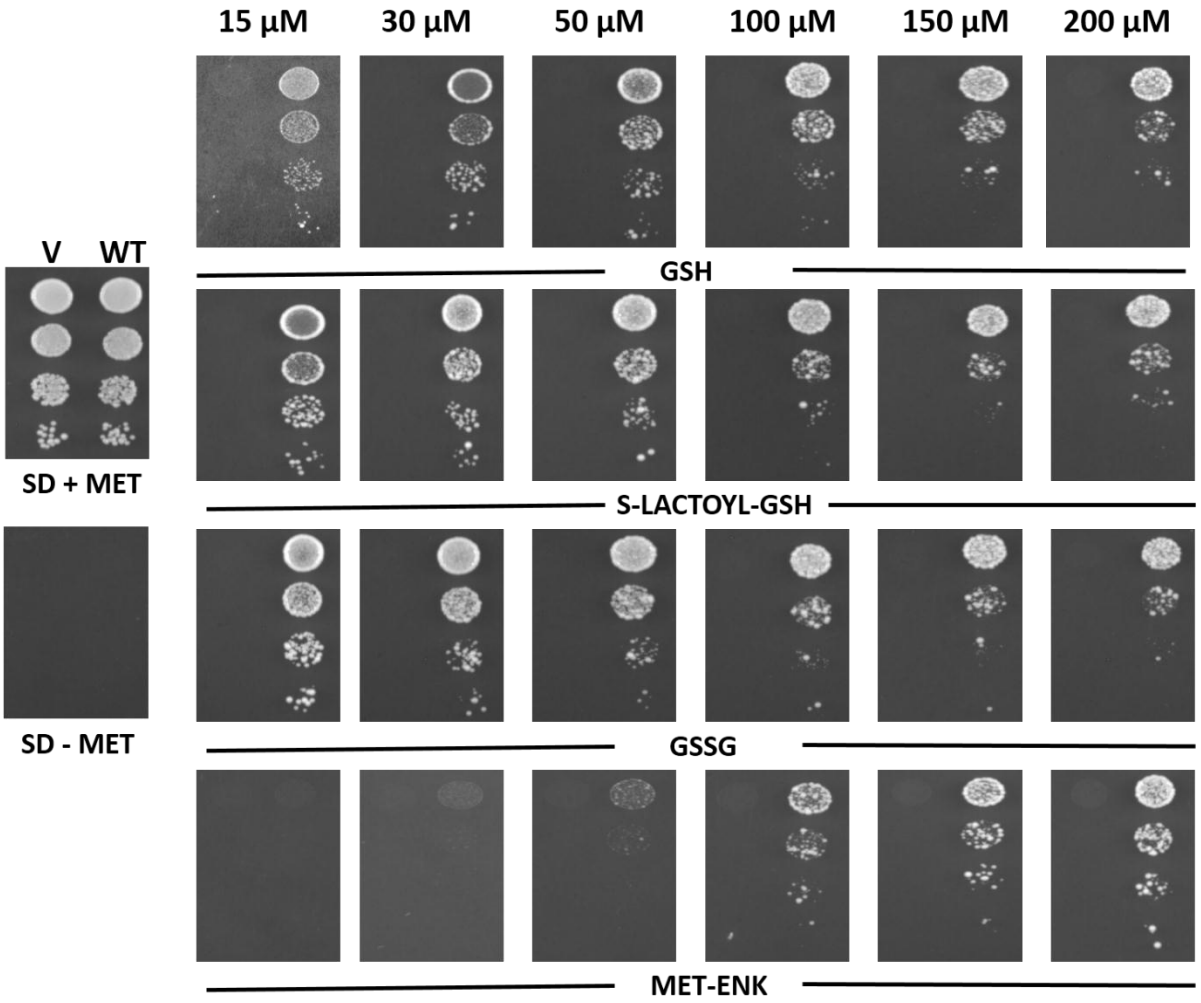

Figure 3.2 b: Functional analysis of WT and severely affected mutants on GSH and different GSH-conjugates: Growth of ABC 817 transformed with empty or wild type (WT) HGT1 under TEF promoter on minimal media containing no methionine (SD-MET), 200 µM methionine (SD+MET) or 15, 30, 50, 100, 200 µM of GSH, S-Lactoyl-GSH, GSSG or Met-Enkephalin. Experiment were repeated with three independent transformations.

γ-Glu-Cys-Gly

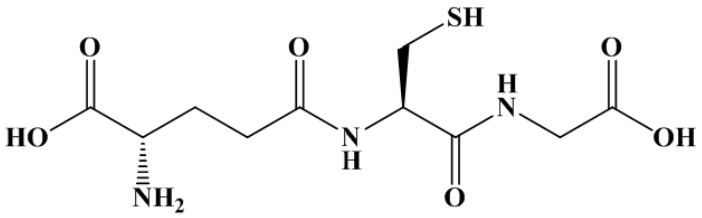

β-Asp-Cys-Gly

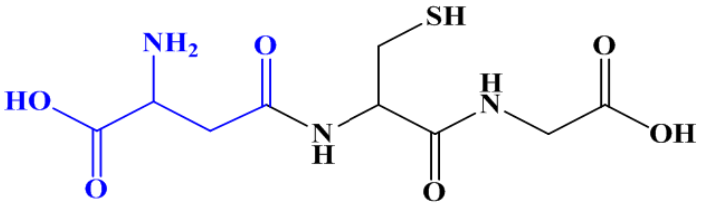

γ-Glu-Ser-Gly

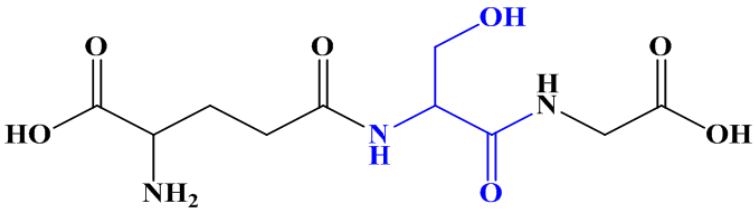

γ-Glu-Cys-Ala

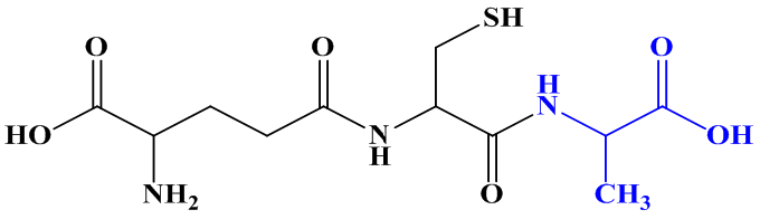

γ-Glu-Cys-β-Ala

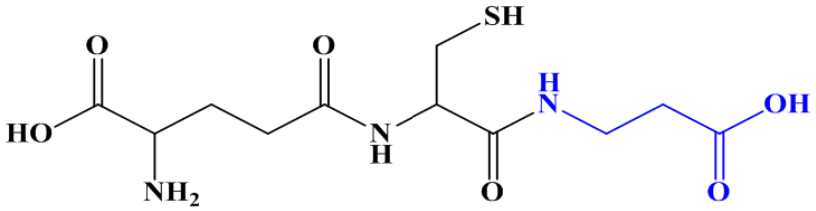

γ-Glu-Cys-Gly-amide

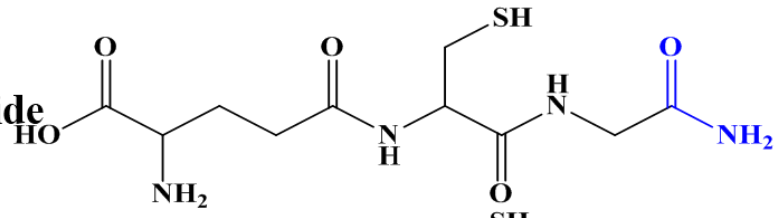

γ-Glu-Cys

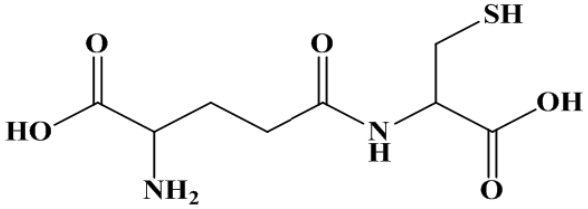

γ-Glu-Cys-amide

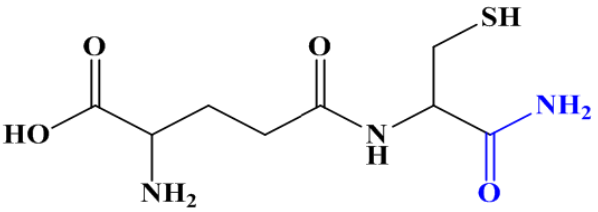

Figure 3.3 a: Chemical structures of GSH analogs modified at γ-Glu, Cys or Gly position examined in this study.

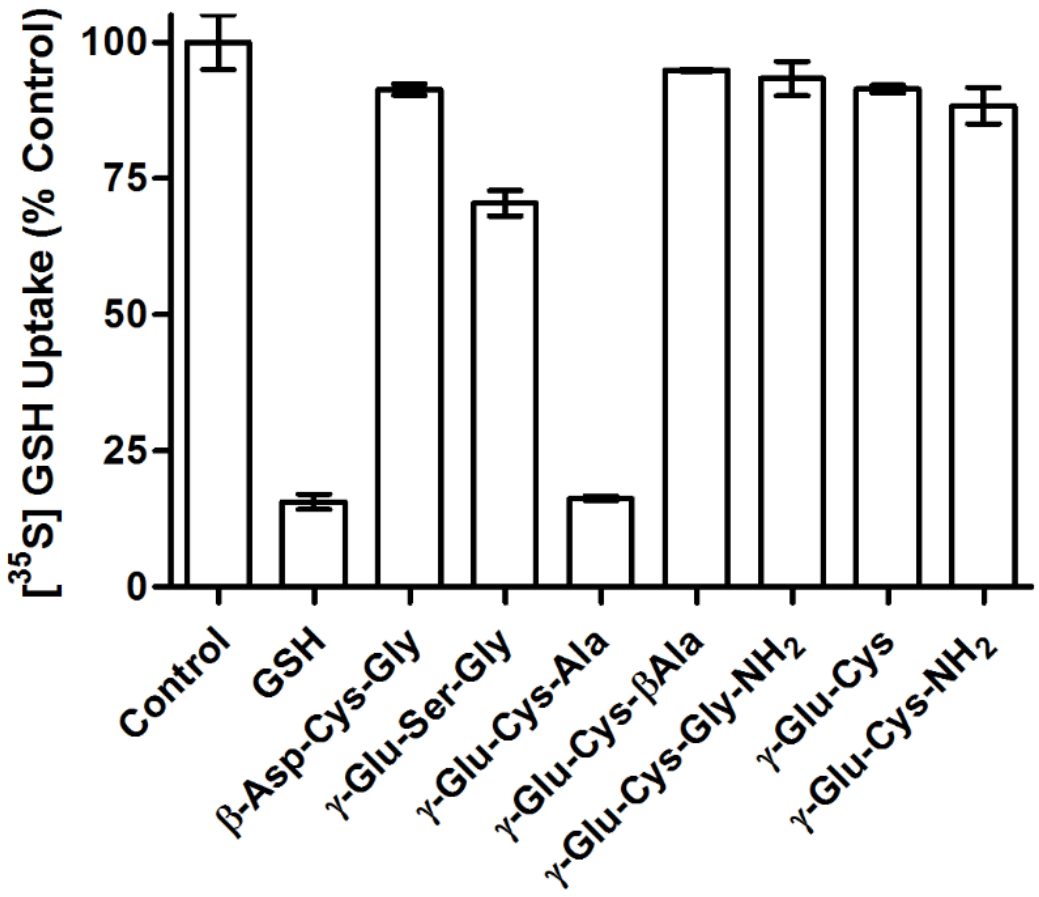

Figure 3.3 b: Effect of GSH analogs containing γ-Glu, Cys or Gly substitutions on [^{35}S]GSH uptake by Hgt1p: [^{35}S]GSH uptake was measured in ABC 817 overexpressing Hgt1p in the absence (control) or presence of GSH or custom synthesized analogues of glutathione (β-Asp-Cys-Gly, γ-Glu-Ser-Gly, γ-Glu-Cys-Ala, γ-Glu-Cys-β-Ala, γ-Glu-Cys-Ala-$CONH_2$, γ-Glu-Cys or γ-Glu-Cys-$CONH_2$) at 500 µM concentration and results were plotted as % control and columns represent means of two different experiments (± S.D, n = 4)

3.3b). We also custom synthesized the analog, γ-Glu-Ser-Gly, where the cysteine of glutathione was replaced with serine to enable one to assess the importance of cysteine in the recognition by Hgt1p. The analog γ-Glu-Ser-Gly did not significantly compete with glutathione since very low levels of inhibition in transport was observed. This indicated that γ-Glu-Ser-Gly was not a substrate for Hgt1p, and thus the cysteine residue was very critical for recognition by Hgt1p. In the third set of experiments we replaced the terminal glycine residue of γ-Glu-Cys-Gly with alanine, to yield γ-Glu-Cys-Ala. This analog competed well with glutathione and caused significant inhibition. This seemed to suggest that the third position was not as critical for recognition since replacement at the third Gly residue could still be recognized by Hgt1p. To further assess the importance of this position, we examined γ-Glu-Cys-β-Ala (homoglutathione) as a substrate, and also the dipeptide, γ-Glu-Cys lacking an amino acid at the third position. However, neither γ-Glu-Cys-β-Ala nor γ-Glu-Cys could be recognized by Hgt1p. This indicated that despite the greater flexibility at the third position, a third amino acid at this position was essential, and not all amino acids were tolerated. To further dissect the role of the C-terminal carboxylate group we further custom synthesized γ-Glu-Cys-Gly$CONH_2$ and γ-Glu-Cys$CONH_2$ where an amide group replaced the C-terminal carboxylate. Surprisingly with γ-Glu-Cys-Gly-$CONH_2$ we could not find significant inhibition suggesting that this analog was not recognized by the transporter and a free C-terminal carboxylate is indispensable for recognition by Hgt1p. In addition, γ-Glu-Cys-$CONH_2$ also showed no inhibition and thus like γ-Glu-Cys was not recognized by this transporter.

3.4. Discussion:

The work described in this chapter provides new insights into the substrate specificity of Hgt1p. All the previously reported eukaryotic glutathione transporters have been shown to preferentially bind and transport glutathione-conjugates with several fold higher affinity than reduced glutathione. It was therefore important to evaluate the relative preference of Hgt1p towards glutathione versus glutathione conjugates more quantitatively. We observed that reduced glutathione was a preferred substrate over oxidized glutathione, another naturally occurring metabolite. Thus Hgt1p appears to be principally a glutathione transporter unlike the other reported eukaryotic glutathione-conjugate transporters, but even so it is able to transport many glutathione conjugates with reasonable affinities.

Further examination of the substrates showing very good inhibition and being potentially good substrates for Hgt1p using growth based assay suggested that conjugates having thioether linkage did not support growth at any of the tested concentrations. The reason for these differences is uncertain and may be due to the absence of enzymes capable of cleaving the thioether linkage in these glutathione conjugates, or these substrates can interact with the transporter with high affinity but are not transported. A further examination is required to understand this process. For S-lactoyl-GSH and GSSG a better growth phenotype was observed at similar low concentrations of these substrates as compared to GSH, but the reason for the better growth is not clear.

We also examined the importance of each amino acid of the tripeptide glutathione, governing recognition and transport by Hgt1p using custom synthesized analogs and could demonstrate the critical requirement for the γ-glutamyl and cysteine residues for recognition by Hgt1p. The importance of γ-Glu and Cys residues has also been suggested to be essential for the interaction of glutathione to MRP1 (a low-affinity eukaryotic glutathione transporter) and GST isoenzymes (Adang et al., 1990; Leslie et al., 2003). The β-aspartyl group would be very similar to the γ-glutamyl group except in terms of the volume they occupy. It suggests that the molecular volume of the γ-Glu side chain and the γ-glutamyl bond with Cys as critical for effective interaction with the substrate binding pocket in both these proteins. Substitution of Ser at the Cys position also showed similar transport properties in Hgt1p and MRP1. However, a greater flexibility at the third position was observed in Hgt1p as compared to MRP1, although a third amino acid at this position was essential and not all amino acids were tolerated. In conclusion, these findings should greatly facilitate the understanding of the nature of the substrate binding pocket of Hgt1p.

CHAPTER 4:

Alanine Scanning Mutagenesis of TMD2, TMD3, TMD4, TMD6, TMD10, TMD12 and TMD13 of Hgt1p and Evaluation of All the 269 TMD Mutants for their Role in Glutathione Transport

INTRODUCTION

In the previous chapter we demonstrated that Hgt1p, a member of the poorly characterized oligopeptide transporter (OPT) family, appears to be principally a glutathione transporter unlike the other reported eukaryotic glutathione-conjugate transporters, but even so, it is able to transport many glutathione conjugates with reasonable affinities. However, the majority of the OPT members have still unknown substrate specificity despite the discovery of this family, more than a decade ago. The ability to assign functions to the members of the OPT family has been hampered by the very limited information yet available on mechanistic or structural aspects of its members. Hence the structural features that confer the distinct substrate specificity among the individual members need to be elucidated.

Hgt1p represents the most extensively studied OPT members in terms of structure-function relationship. We have been interested in understanding how Hgt1p transports reduced glutathione with high affinity. However, the toxicity of this protein when expressed in *E.coli*, and the low level of protein expression in yeast, has limited our options, and we have thus tried to investigate this protein primarily through genetic approaches. Previous mutagenic studies of charged residues had targeted 19 amino acids across the different predicted TMDs, while a subsequent study targeted TMD9 for alanine-scanning mutagenesis revealing the importance of a few residues in the transport process (Kaur and Bachhawat, 2009; Thakur and Bachhawat, 2010). However, despite these insights, the studies were limited in their scope as they only addressed the role of a few amino acid residues in the predicted TMDs or of a particular TMD, TMD9.

In the present study we have embarked on a detailed and more thorough investigation by targeting all the remaining predicted TMDs of the Hgt1 protein, to comprehensively map the residues that are important for substrate binding and translocation. Hgt1p is a 799 amino acid protein predicted to have 12 transmembrane domains (TMDs). Although the accepted topology of HGT1 is a 12 TMD spanning protein, predictions have variously indicated between 12-14 TMDs (Wiles et al., 2006). Hence a reasonably reliable topology model is a pre-requisite for targeting the residues in the TMDs before initiating this study. To resolve this issue, we re-evaluated the topology and our studies described here indicated that Hgt1p is best considered as a 13 TMD protein. These predicted TMDs comprised of 269 amino acid residues out of which 39 were targeted in earlier studies. Among these, TMD1,

TMD5, TMD7, TMD8, and TMD11 were also subjected to alanine scanning mutagenesis although the detailed functional analysis was not carried out (Yadav S, MS thesis, 2014). Hence I have subjected the remaining predicted TMDs (TMD2, TMD3, TMD4, TMD6, TMD10, TMD12, and TMD13) to alanine scanning mutagenesis.

The detailed functional analysis of all the 269 mutants of 13 TMDs followed by kinetic analysis of the severely defective mutants that are expressed and localized properly on the membrane revealed that the residues V185, G225, Y226, Y374, P292 and L429 in addition to the previously identified Q222, F523 and Q526 are probably involved in substrate binding. Substitution of these residues to alanine resulted in a significant decrease in the affinity of the transporter for glutathione. An *ab initio* based computational approach was further used to derive a structural model for Hgt1p, and this model building was also facilitated by the detailed comprehensive map of residues likely to form the substrate channel. Thus, this study has provided insights into the role of every residue in all the predicted TMDs in substrate transport by this high affinity glutathione transporter.

4.1 Topological re-evaluation of Hgt1p:

As the approach being taken in this study was to carry out a comprehensive mutational analysis of all the amino acids in all the predicted TMDs, it was important to establish the number of TMDs in this protein. Previous studies have been based on a 12 transmembrane domain topology (Kaur and Bachhawat, 2009; Thakur and Bachhawat, 2010; Wiles et al., 2006). However, Hgt1p was originally predicted to have 12-14 transmembrane domains. As two of the predicted domains corresponding to the regions 536-568 and 704-724 were proline rich motifs -EXIXGYX2PG[R/K] PXAX4KX2G and PPX [N/T]P, these were not considered as TMDs. Motifs consisting of proline residues in proximity to glycine residue theoretically disfavors the region to form a helix (Wiles et al., 2006). Hence these were predicted to form loops in the predicted topology model. However, as this was done almost a decade ago, and an accurate topology prediction was critical for this study. The topology prediction was reinvestigated more rigorously, using multiple different topology prediction software (PHDhtm (Rost et al., 1996), HMMTOP 2.0 (Tusnady and Simon, 2001), TOPPRED 2.0 (von Heijne, 1992), TMHMM (Krogh et al., 2001; Sonnhammer et al., 1998), MEMSAT3 (Jones, 2007), TMSEG (Yachdav et al., 2014), SCAMPI (Bernsel et al., 2008), PRODIV (Viklund and Elofsson, 2004), OCTOPUS

(Viklund and Elofsson, 2008), TOPCONS (Tsirigos et al., 2015), SABLE (Adamczak et al., 2004, 2005), PolyPhobius (Kall et al., 2005) and MEMSAT-SVM (Nugent and Jones, 2009)) for the two controversial TMDs (Table 4.1). These software's were selected based on several reports that used these theoretical prediction softwares for the successful prediction of the topology of various membrane transporters and we focused on the two controversial TMDs that were not included in the previous studies.

Our analysis suggests that the region 707-724 is a TMD as predicted by the majority of the prediction softwares with the proline-rich motif outside the helix. Region 537-568 was considered as a TMD by only 60% of the softwares with proline-rich motif inside the TMD. The lack of significant consensus along with the proline-rich nature of this domain led us to exclude it from among the TMDs consistent with the earlier analysis of this region. Hence the final topological model that emerges includes 13 TMDs with the N-terminus outside and C-terminus inside. The new predicted TMD appears after the 11^{th} TMD; thus the nomenclature of the first 11 TMDs remains unchanged with previous studies.

To experimentally validate this topology we used the HGT1 construct having hexahistidine epitope at the N-terminus and HA-tag at the C-terminus. The localization of N- and C-terminus was verified by indirect immunofluorescence using peptide directed antibodies against these epitopes in permeabilized and non-permeabilized spheroplasts. Spheroplasts were prepared as described in materials and methods section 2.18. If the tag is accessible to antibodies without permeabilization, it will suggest an extracellular localization. The His-tag was detected in both permeabilized and non-permeabilized spheroplasts suggesting an extracellular localization. However, the HA-tag was not detected in non-permeabilized spheroplasts but was detected in permeabilized spheroplasts confirming an intracellular localization (Fig 4.1). This demonstrates that the N and C termini are oriented at opposite sides of the membrane as predicted by computational methods, hence strengthening the currently predicted topology model.

4.2 Alanine scanning mutagenesis of the TMDs of Hgt1p:

The 13 transmembrane domains of Hgt1p are comprised of 269 amino acid residues in the TMDs. Some of these residues (including a complete TMD9) have been targeted in previous studies that left a total of 230 amino acid (205 non-alanine, 25 alanine) residues to be studied. We subjected 205 of these non-alanine residues to alanine mutagenesis while the 25 alanine residues were mutated to glycine. Of these

230 amino acid residues, 94 alanine mutants (TMD1, 5, 7, 8, and 11) were made by Mr. Shambhu Yadav and the list of primers and strains have been documented in his BS-MS final year thesis titled "A mutational study of transmembrane domains of yeast glutathione transporter, Hgt1p of *Saccharomyces cerevisiae*" (Yadav S., MS thesis, 2014). However, they were not functionally analyzed and thus the analysis was included as part of this thesis. In addition, proline residues in or near TMDs are shown to be directly or indirectly involved in substrate binding (Ni et al., 2011). We therefore also mutated two proline residues (P704A and P705A) present just outside TMD12. Each mutant was first evaluated by the plate based "Dual complementation-cum-toxicity" assay (as discussed in materials and methods section, 2.13) designed for evaluation of functional activity of the mutants. The reliability of this plate based assay has been established previously by biochemical assays using [^{35}S]-GSH uptake (Kaur and Bachhawat, 2009; Kaur et al., 2009; Thakur and Bachhawat, 2010). Based on this assay, mutants were grouped into four different classes: (a) Complementation defective or severely affected mutants *i.e.* no growth at 15µM GSH and growth at higher GSH concentrations with no signs of toxicity. (b) Moderately defective mutants complement at 15µM GSH but shows no toxicity at higher GSH levels. (c) Mildly defective mutants grow at low GSH concentration and shows mild toxicity at higher GSH levels. (d) Mutants showing no effect and grow similar to wild type TEF-HGT1 *i.e.* showing growth at low GSH concentrations and severe toxicity at higher concentrations.

Based on the plate based assay of all 269 mutants, 26 mutants were severely defective (Fig. 4.2) out of which 6 have been shown to be complementation defective in earlier studies (Kaur and Bachhawat, 2009; Thakur and Bachhawat, 2010), 77 moderately defective, 89 minor defective and 77 with no defect. These are listed TMD-wise below and in Table 4.2.

TMD1 (T109–F127) contains 19 amino acid residues. 18 of them were individually converted to alanine (T114A and N124A studied earlier) while A121 converted to glycine. Based on the plate based assay (Fig 4.2a) W110A, T114A and N124A were found to be severely defective. L112A, T114A, F120A, F126A and F127A moderately defective, F116A, V117A, V118A, V119A, A121G and G122A mild defective while remaining mutants showed no defect.

TMD2 (L134-L155) has 22 amino acid residues. 20 amino acid residues were mutated to alanine (E135A, N137A, and R150A studied earlier) and two residues

Table 4.1. Re-evaluation of topology model of Hgt1p, as a platform for structure-function analysis: Hgt1p primary sequence reanalysed using 13 different algorithms (PHDhtm, HMMTOP 2.0, TOPPRED 2.0, TMHMM, MEMSAT3, TMSEG, SCAMPI, PRODIV, OCTOPUS, TOPCONS, SABLE, PolyPhobius and MEMSAT-SVM) using default parameters to identify the possible TMDs. 12 TMDs (referred to as TMD1, 2, 3, 4, 5, 6, 7, 8, 9, 10, 11 and 13 in this chapter) were common to all with slight variation in the boundaries. Only two regions, H536-V568 and P704-I724 were controversial as TMDs that were omitted in previous studies are compared here.

Topology Prediction algorithms	H536-V568	P704-I724
PHDhtm	536-553	707-724
HMMTOP 2.0	549-568	705-724
TOPPRED 2.0	-----	704-724
TMHMM	-----	707-724
MEMSAT3	546-568	706-724
TMSEG	555-573	693-718
SCAMPI	-----	709-729
PRODIV	553-573	701-721
OCTOPUS	-----	-----
TOPCONS	-----	-----
SABLE	556-568	710-733
PolyPhobius	556-570	709-725

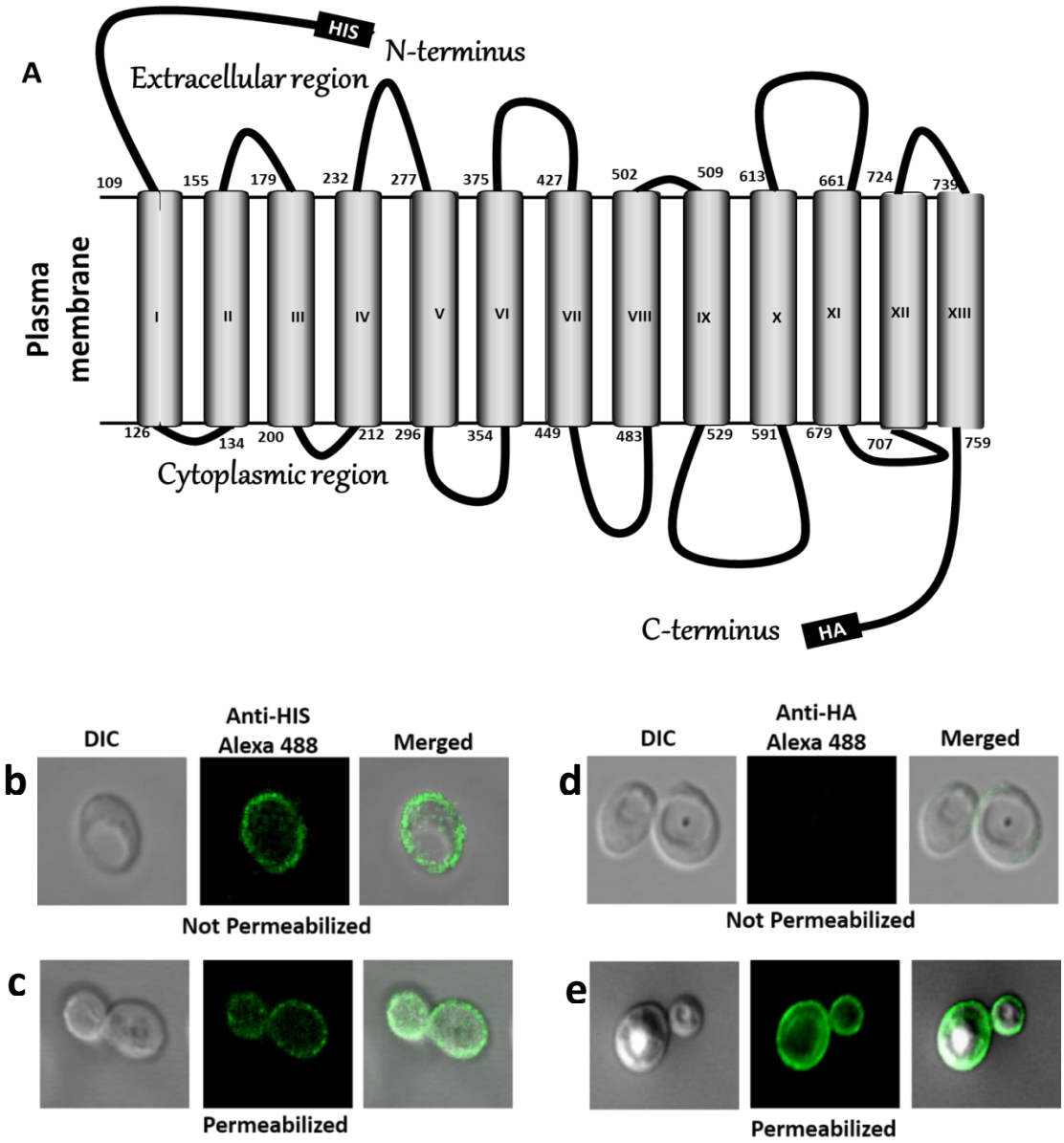

FIGURE 4.1: Hgt1p topology: a) Pictorial presentation of Hgt1p predicted topology based upon consensus generated using different topology prediction softwares (Table 4.1). HGT1 was tagged with hexa-His epitope at the N-terminus and HA tag at the C-terminus. The localization of N- and C-terminus was verified by indirect immunofluorescence using peptide directed antibodies as described in chapter 2 (section 2.18". Experiment was repeated twice (n=4) using independent transformations and DIC and fluorescence images have been shown. The His-tag was detected in both b) permeabilized and c) non-permeabilized spheroplasts suggesting extracellular localization. However the HA-tag was not detected in d) non-permeabilized spheroplasts but was detected in e) permeabilized spheroplasts confirming its intracellular localization.

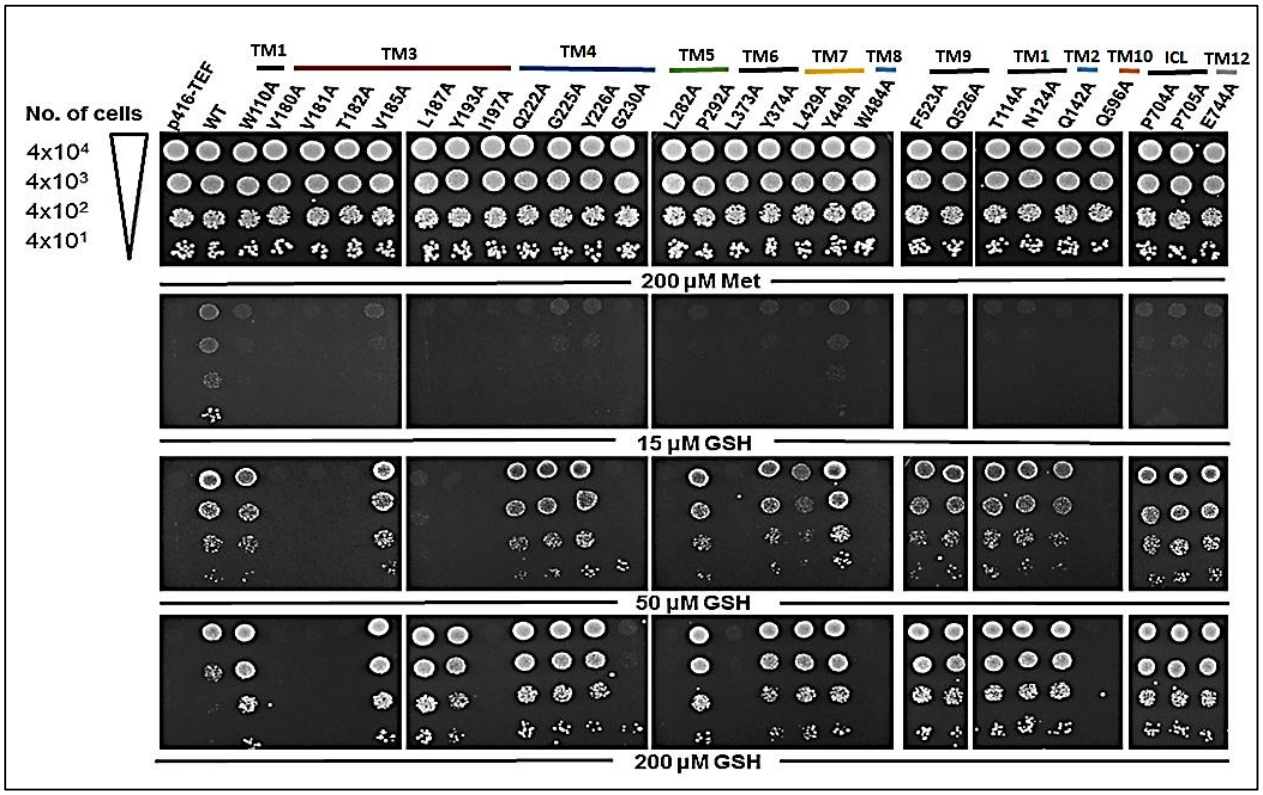

FIGURE 4.2: Functional characterization of severely defective alanine mutants of Hgt1p: Empty vector (p416-TEF), Wild type (WT) and the different severely defective alanine mutants of Hgt1p under TEF promoter were transformed in ABC 817. Transformants were subjected to plate based "Dual complementation-cum-toxicity" assay (as described in chapter 2, section 2.13) by serial dilution spotting on minimal media containing different concentrations (15, 50, 200 µM) of glutathione or 200µM methionine (control). The photographs were taken after 2-3 days of incubation at 30°C. Experiment was repeated with three independent transformations.

Table 4.2. Grouping of the mutants of Hgt1p based on their effect on the functional activity of the transporter using dual complementation-cum-toxicity assay: Functional activity of the mutants were analysed using sensitive plate based dual complementation-cum-toxicity assay and mutants were categorized into four groups depending on their ability to complement ABC 817 (*met15Δhgt1Δ*) at low (15 µM) glutathione concentration and cause toxicity to the cells at higher (> 50 µM) glutathione concentrations.

TMD	Severe defect	Moderate defect	Minor defect	No defect
TMD1 (T109 - F127)	W110A,T114A*, N124A*	L112A, F120A, F126A, F127A	F116A, V117A, V118A, V119A, A121G ,G122A	T109A, F111A, T113A, V115A, V123A, Q125A
TMD2 (L134-L155)	Q142A	L134A, E135A*, N137A*, L139A, V140A, Y146A, P147A	I136A, F138A, V143A , C145A	A141A, V144A, I148A, G149A, R150A*, I151A, L152A, A153G, L154A , L155A
TMD3 (A179-A200)	V180A, V181A T182A, V185A, L187A,Y193A, I197A	A179G, I183A, A186G, M195A, Y196A, L198A, N199A, A200G	A184G, S189A, S190A, T191A , A192G	T188A ,A194G
TMD4 (G212-T232)	Q222A*, G225A, Y226A, G230A	S221A, I224A, G227A,A228G, A229G	Q214A, F215A, L216A, W219A, T220A , T232A	G212A, Y213A, L217A, V218A, M223A, L231A
TMD5 (F277-F296)	L282A, P292A	Y289A, W290A	S285A, I287A	F277A, F278A, L279A, I280A, V281A, I283A, G284A, F286A ,W288A, V291A, G293A, F294A, L295A, F296A
TMD6 (V354-Y374)	L373A ,Y374A	N357A*, T358A, Y359A, V362A, F365A, F366A, L370A, P371A	L363A, I364A, I368A, C372A	V354A, S355A*, A356G, A360G, S361A, V367A, I369A
TMD7 (S427-Y449)	L429A, Y449A	A438G, V439A, H445A*, I447A, L448A	L430A, S431A, Y432A, A433G, L434A, N435A*, F436A, A437G, I440A, A441G, V442A, F443A, V444A, C446A	S427A, Y428A
TMD8 (W483-C502)	W484A	L488A	W483A, Y485A, L486A, L487A, Q489A, I490A, V491A, N492A, I493A, G494A, L495A, G496A, F497A, V498A, A499G, V500A, C501A, C502A	
TMD9 (A509 –L529)	F523A*, Q526A*	A515G*, I524A*, P525A*, L529A*	W510A*,F512A*,I516A*, I518A*, I528A*	A509G*, A511G*,V513A*, I514A*, L517A*, S519A*, L520A*, V521A*, N522A*, G527A*
TMD10 (L591-W613)	Q596A	L591A, I592A, F593A, V595A, I597A, Y598A, S603A*, V608A	A594G, A599G, I601A, I602A, V606A	T600A, G604A, N607A*, G609A, V610A, Q611A, E612A*, W613A.
TMD11 (L661-Q679)		L666A, I667A, L669A, L670A, F671A,P672A, L673A, A674G	G668A, V675A, Y676A, A677G, V678A, Q679A	L661A, M662A, W663A F664A, F665A
TMD12 (T707 –I724)		T707A, P708A,Y709A, F715A, S718A, F719A, C720A, L721A,N722A, L723A , I724A	N710A, Y711A, S712A, L713A, F714A,A716G, M717A	
TMD13 (M739-Q759)	E744A*	V743A,G746A,V747A, A748G, F755A, L756A	G740A, A741G, G742A, I749A, S750A, V758A, Q759A	M739A, A745G, V751A, V752A, I753A, I574A, C757A

* Mutants from earlier studies(Kaur and Bachhawat, 2009; Thakur and Bachhawat, 2010)

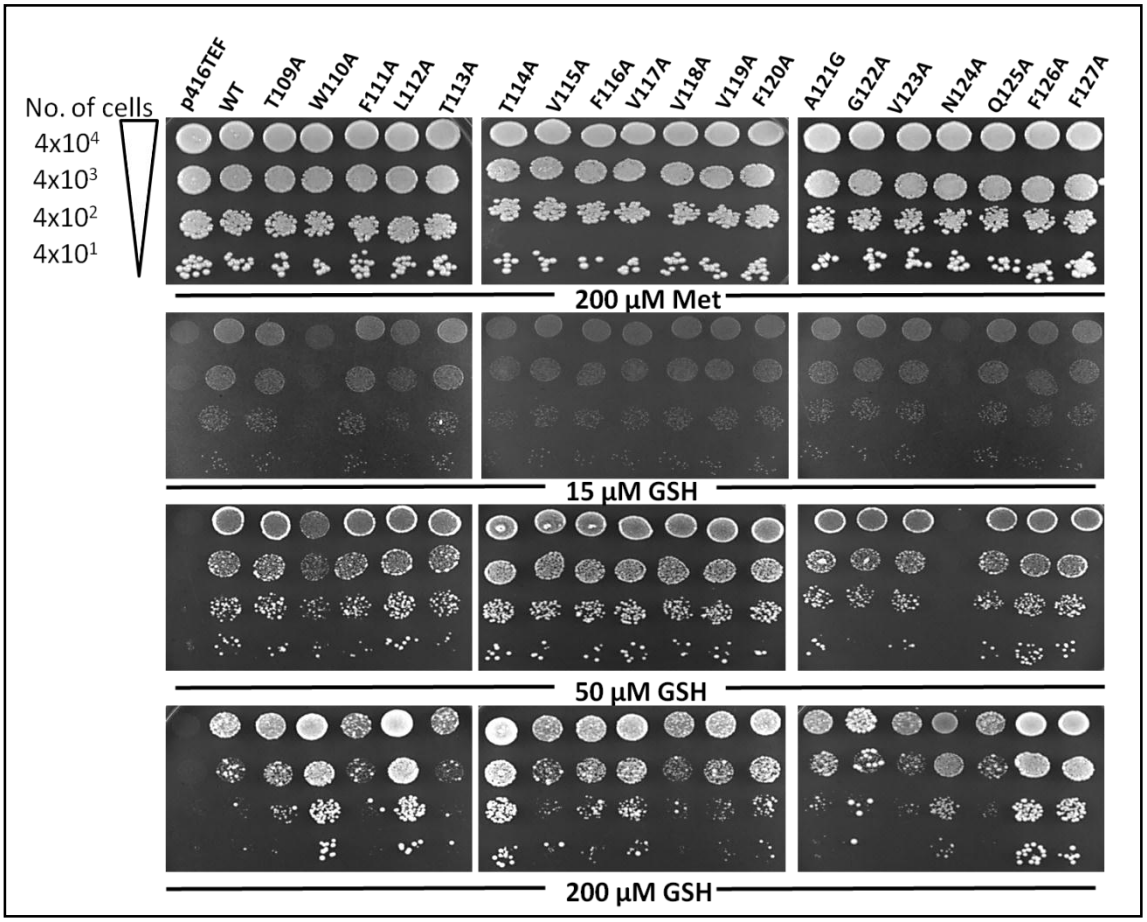

FIGURE 4.2a: Functional characterization of putative TMD1 alanine mutants of Hgt1p: Empty vector (p416-TEF), Wild type (WT) Hgt1p and the different TMD1 mutants of Hgt1p under TEF promoter were transformed in ABC 817. Transformants were serially diluted and spotted on minimal media plates containing different concentrations (15, 50, 200 µM) of glutathione or 200µM methionine (control).The photographs were taken after 2-3 days of incubation at 30 ˚C.

A141 and A153 were mutated to glycine. Out of these Q142A was found to be severely defective (Fig 4.2b). L134A, E135A, N137A, L139A, V140A, Y146A, and P147A were moderately defective, I136A, F138A, V143A, and C145A were mildly defective, and the remaining showed no defect.

TMD3 (A179-A200) contain 22 amino acid residues. 16 amino acid residues were mutated to alanine, and six alanine residues were mutated to glycine. TMD3 has seven severely defective mutants (Fig 4.2c). V180A, V181A, and T182A did not grow at any of the glutathione concentrations tested but other severely defective mutants V185A, L187A, Y193A, and I197A started growing only at high glutathione concentrations (>50 µM GSH). Moderately defective mutants include A179G, I183A, A186G, M195A, Y196A, L198A, N199A, and A200G.The mutants showing a minor defect were A184G, S189A, S190A, T191A, and A192G. Only two mutants T188A and A194G had no defect and were similar to WT protein.

TMD4 (G212-T232) has 21 amino acid residues. 19 amino acid residues were mutated to alanine (Q222A studied earlier) and two alanine residues were mutated to glycine. Q222A, G225A, Y226A, and G230A showed a severe defect in glutathione transport (Fig 4.2d). S221A, I224A, G227A, A228G, and A229G showed a moderate defect whereas Q214A, F215A, L216A, W219A, T220A, and T232A were mildly defective. The remaining mutants showed no defect and were similar to WT.

TMD5 (F277-F296) is composed of 20 amino acid residues and was not targeted by previous studies as they only have one polar (S285) residue. All the residues were mutated to alanine, and we found that two were severely defective (L282A, P292A), two moderately defective (Y289A, W290A) and two mildly defective (S285A, I287A) (Fig 4.2e).The remaining 14 residues did not have any defect in glutathione transport.

TMD6 (V354-Y374) has 21 amino acid residues. 19 were mutated to alanine (S355A and N357A studied earlier), and two alanine were mutated to glycine. Mutants L373A and Y374A were severely defective on low concentrations of glutathione (Fig 4.2f). Moderately defective mutants include N357A, T358A, Y359A, V362A, F365A, F366A, L370A, P371A, mildly defective mutants were L363A, I364A, I368A and C372A and the remaining mutants showed no defect.

TMD7 (S427-Y449) consist of 23 amino acid residues out of which 19 were mutated to alanine (N435A and H445A studied earlier), and the four alanine residues were mutated to glycine. Severely defective mutants included L429A, H445A, and

Y449A. An earlier study showed H445A as moderately defective, but when the same construct was used for the present study, it showed a severe defect on plates. Four mutants were moderately defective A438G, V439A, I447A and L448A (Fig 4.2g). A majority of the mutants exerted mild defect including L430A, S431A, Y432A, A433G, L434A, N435A, F436A, A437G, I440A, A441G, V442A, F443A, V444A, and C446A with only two mutants with no significant defect, S427A, and Y428A.

TMD8 (W483-C502) has a total of 20 amino acid residues including two cysteines. 19 residues were mutated to alanine and one alanine residue was mutated to glycine. Only W484A had a severe effect on Hgt1p function, and a single mutant L488A led to moderate defect (Fig 4.2h). Whereas the rest of them had a mild effect on functionality W483A, Y485A, L486A, L487A, Q489A, I490A, V491A, N492A, I493A, G494A, L495A, G496A, F497A, V498A, A499G, V500A, C501A, and C502A.

TMD9 (A509 – L529) has been investigated earlier(Thakur and Bachhawat, 2010). To summarize the results, out of 21 residues F523A and Q526A were found to be severely defective, A515G, I524A, P525A, L529A Moderate defective, W510A, F512A, I516A, I518A, I528A minor defective and the remaining had no effect on functionality. These were reconfirmed in the present study.

TMD10 (L591-W613) has a total of 22 amino acid residues out of which 20 were mutated to alanine (S603A, N607, and E612 studied earlier) and 2 alanine residues were mutated to glycine. Q596A did not grow at any of the glutathione concentrations (Fig 4.2i). Moderately defective mutants included L591A, I592A, F593A, V595A, I597A, Y598A, S603A, and V608A. Mildly defective mutants were A594G, A599G, I601A, I602A and V606A and the remaining mutants showed no defect.

TMD11 (L661-Q679). Similar to TMD5, TMD 11 have only one polar residue (Q679) and was not targeted in earlier studies. It has a total of 19 amino acid residues. 17 were mutated to alanine and 2 alanine mutated to glycine. Not a single mutant showed a severe defect (Fig 4.2j). Moderately defective mutants included L666A, I667A, L669A, L670A, F671A, P672A, L673A, and A674G. Mild defective was G668A, V675A, Y676A, A677G, V678A, and Q679A and remaining mutants had no defect.

TMD12 (T707–I724) is the smallest TMD of Hgt1p consisting of only 18 amino acid residues. Seven were mutated to alanine (N710 and N722 studied earlier) and one alanine residue was mutated to glycine. No severely defective mutants were observed

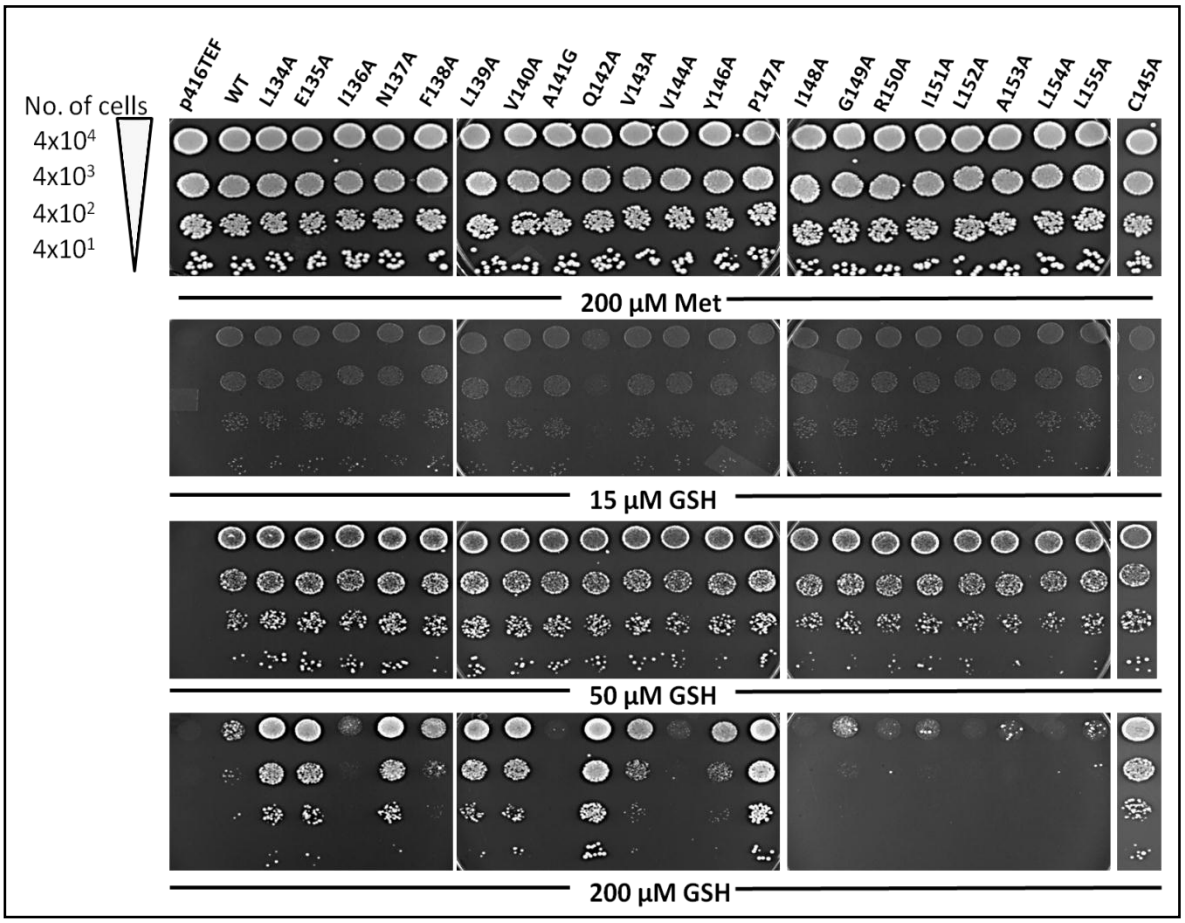

FIGURE 4.2b: Functional characterization of putative TMD2 alanine mutants of Hgt1p: Empty vector (p416-TEF), Wild type (WT) Hgt1p and the different TMD2 mutants of Hgt1p under TEF promoter were transformed in ABC 817. Transformants were serially diluted and spotted on minimal media plates containing different concentrations (15, 50, 200 µM) of glutathione or 200µM methionine (control).The photographs were taken after 2-3 days of incubation at 30 ˚C.

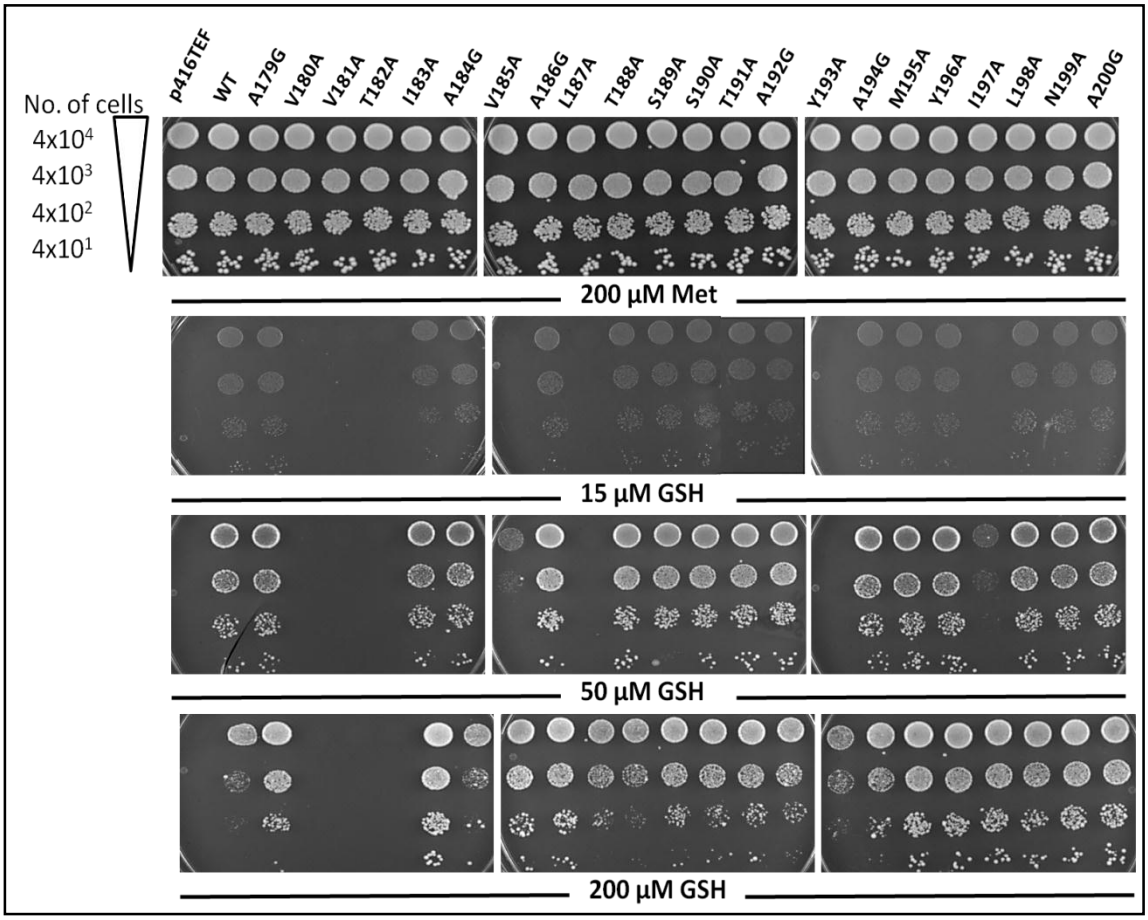

FIGURE 4.2c: Functional characterization of putative TMD3 alanine mutants of Hgt1p: Empty vector (p416-TEF), Wild type (WT) Hgt1p and the different TMD3 mutants of Hgt1p under TEF promoter were transformed in ABC 817. Transformants were serially diluted and spotted on minimal media plates containing different concentrations (15, 50, 200 µM) of glutathione or 200µM methionine (control).The photographs were taken after 2-3 days of incubation at 30 ˚C.

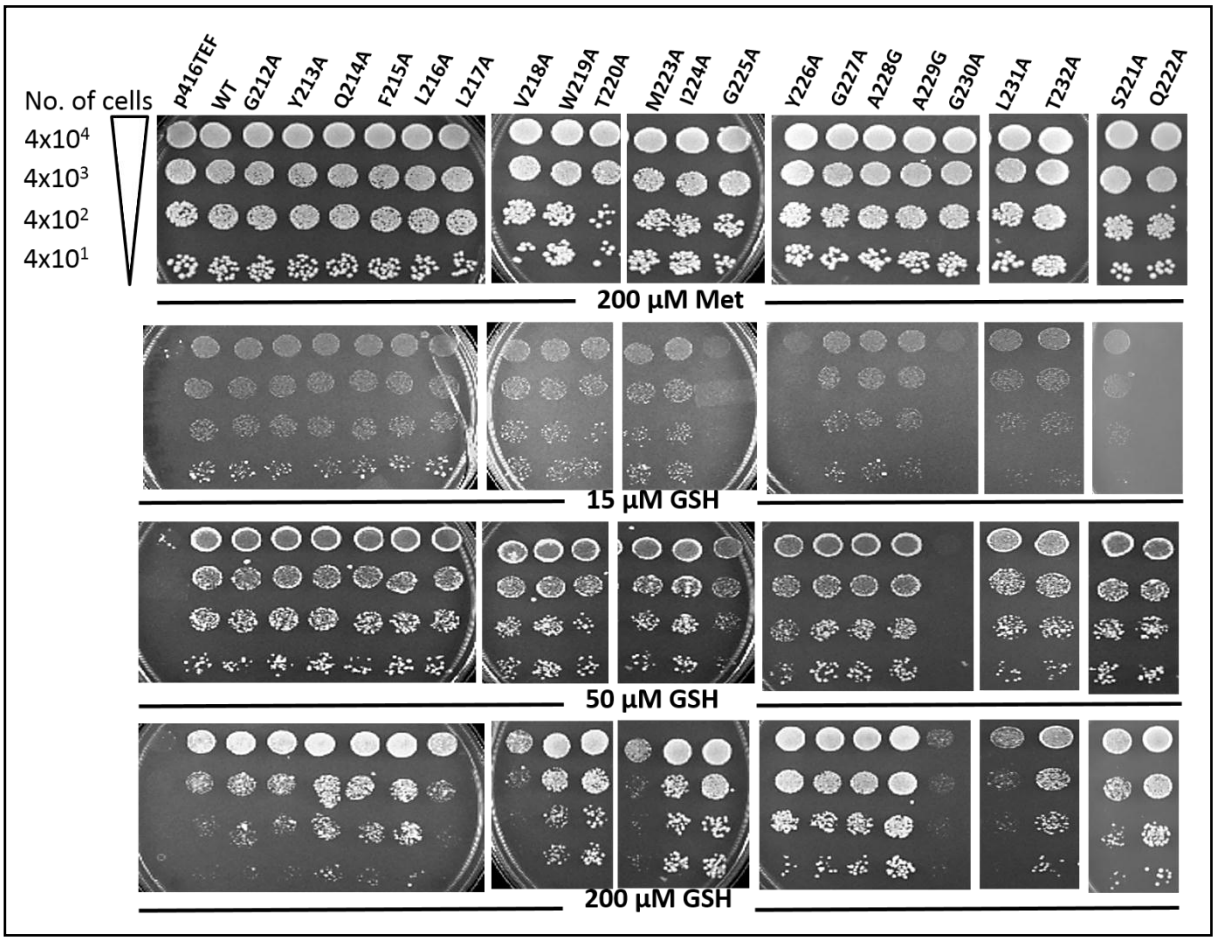

FIGURE 4.2d: Functional characterization of putative TMD4 alanine mutants of Hgt1p: Empty vector (p416-TEF), Wild type (WT) Hgt1p and the different TMD4 mutants of Hgt1p under TEF promoter were transformed in ABC 817. Transformants were serially diluted and spotted on minimal media plates containing different concentrations (15, 50, 200 µM) of glutathione or 200µM methionine (control).The photographs were taken after 2-3 days of incubation at 30 ˚C.

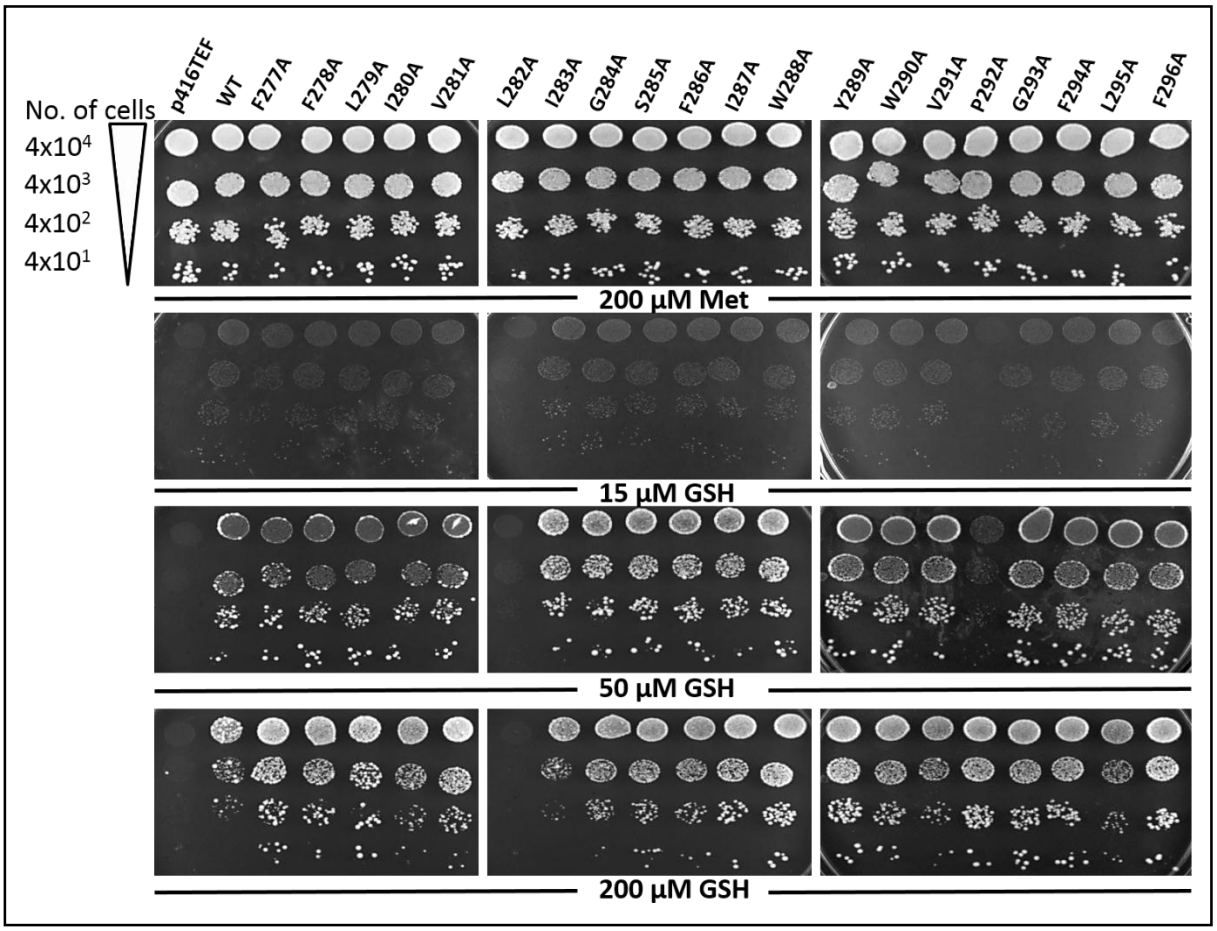

FIGURE 4.2e: Functional characterization of putative TMD5 alanine mutants of Hgt1p: Empty vector (p416-TEF), Wild type (WT) Hgt1p and the different TMD5 mutants of Hgt1p under TEF promoter were transformed in ABC 817. Transformants were serially diluted and spotted on minimal media plates containing different concentrations (15, 50, 200 µM) of glutathione or 200µM methionine (control).The photographs were taken after 2-3 days of incubation at 30 ˚C.

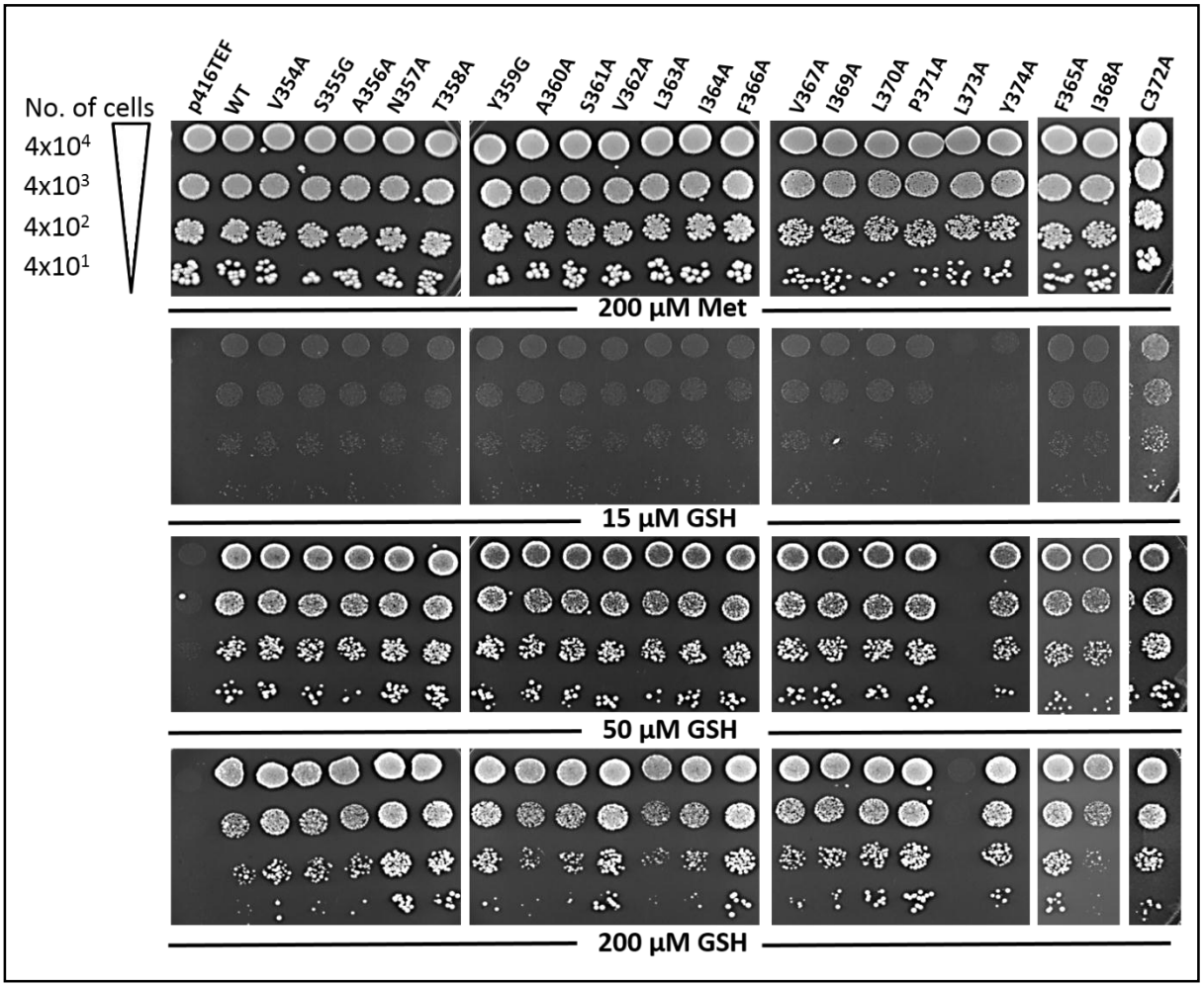

FIGURE 4.2f: Functional characterization of putative TMD6 alanine mutants of Hgt1p: Empty vector (p416-TEF), Wild type (WT) Hgt1p and the different TMD6 mutants of Hgt1p under TEF promoter were transformed in ABC 817. Transformants were serially diluted and spotted on minimal media plates containing different concentrations (15, 50, 200 µM) of glutathione or 200µM methionine (control).The photographs were taken after 2-3 days of incubation at 30 ˚C.

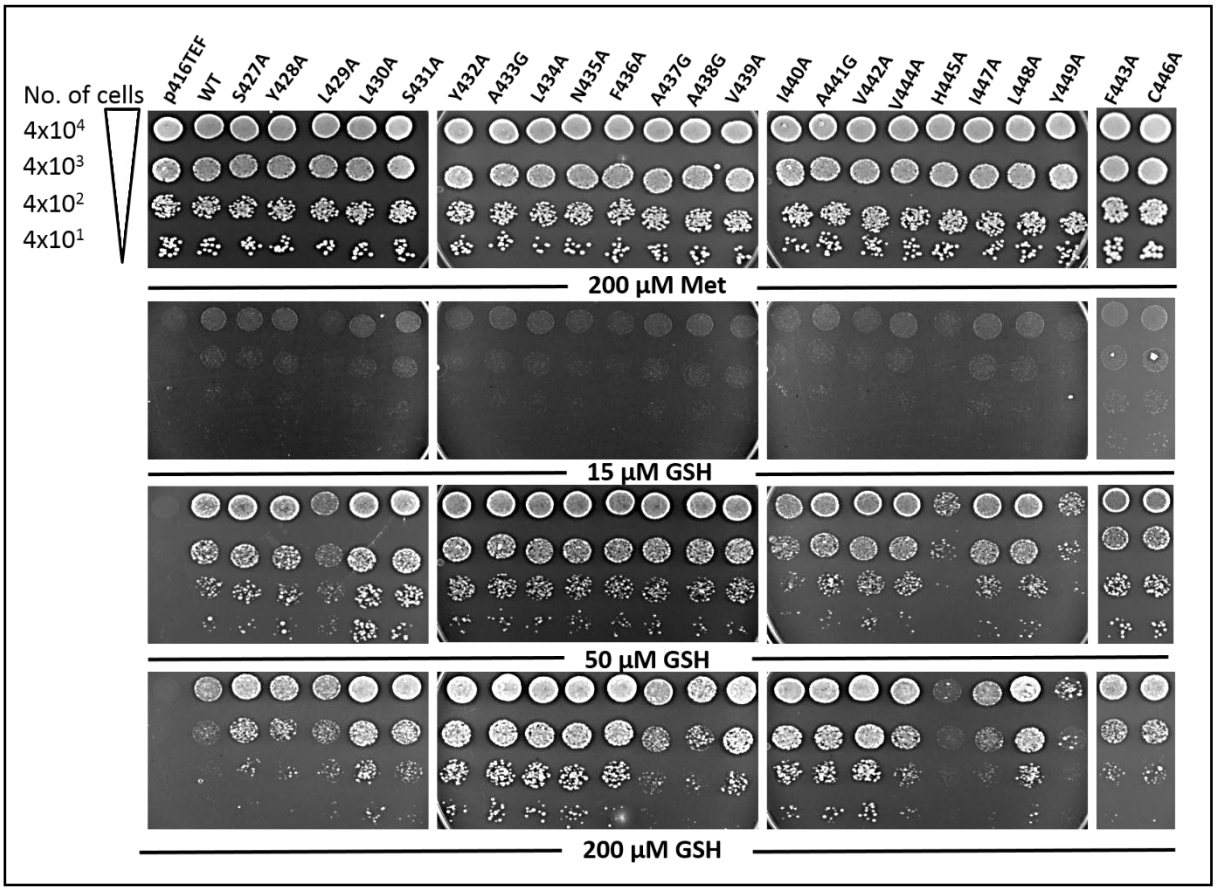

FIGURE 4.2g: Functional characterization of putative TMD7 alanine mutants of Hgt1p: Empty vector (p416-TEF), Wild type (WT) Hgt1p and the different TMD7 mutants of Hgt1p under TEF promoter were transformed in ABC 817. Transformants were serially diluted and spotted on minimal media plates containing different concentrations (15, 50, 200 µM) of glutathione or 200µM methionine (control).The photographs were taken after 2-3 days of incubation at 30 ˚C.

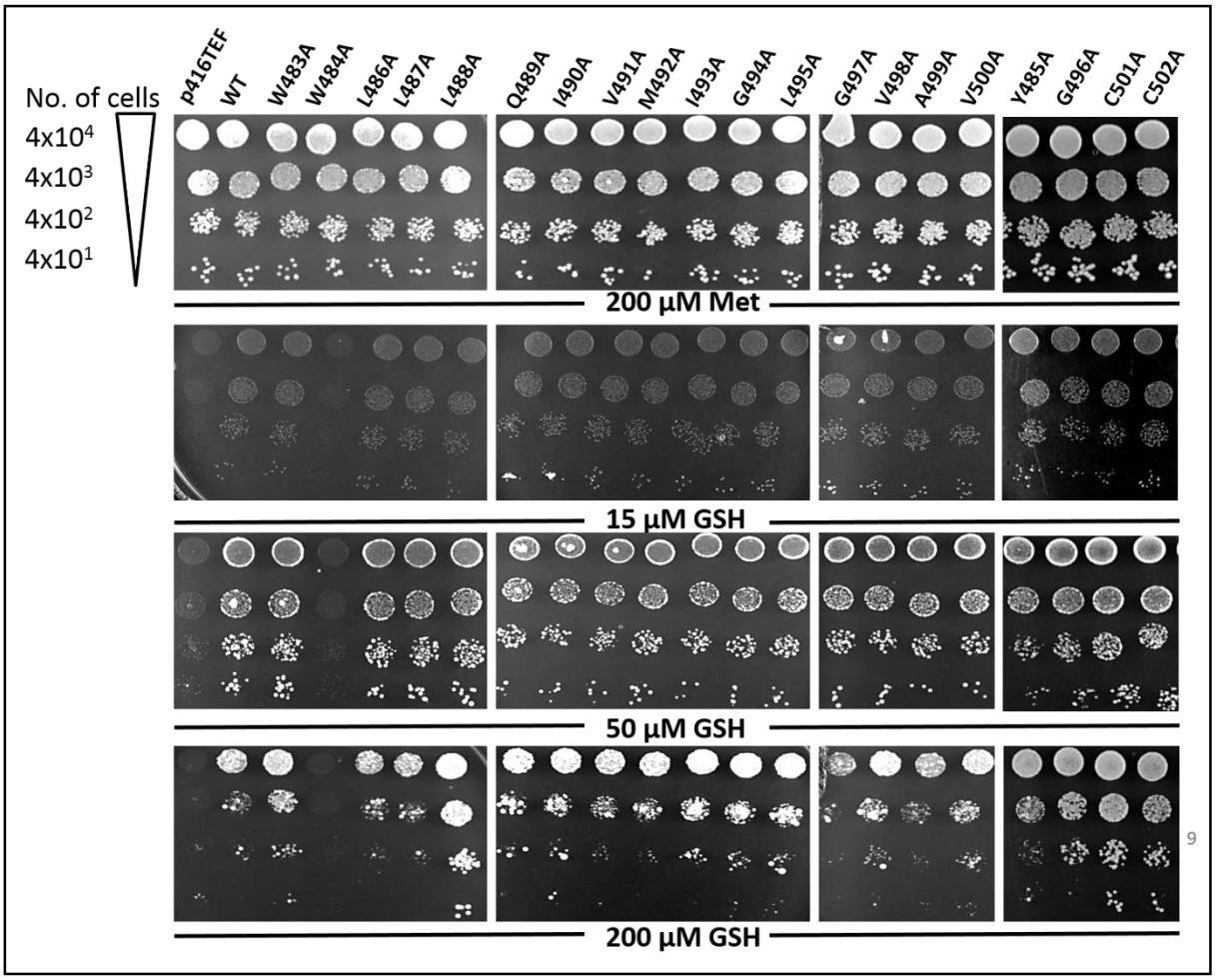

FIGURE 4.2h: Functional characterization of putative TMD8 alanine mutants of Hgt1p: Empty vector (p416-TEF), Wild type (WT) Hgt1p and the different TMD8 mutants of Hgt1p under TEF promoter were transformed in ABC 817. Transformants were serially diluted and spotted on minimal media plates containing different concentrations (15, 50, 200 µM) of glutathione or 200µM methionine (control).The photographs were taken after 2-3 days of incubation at 30 ˚C.

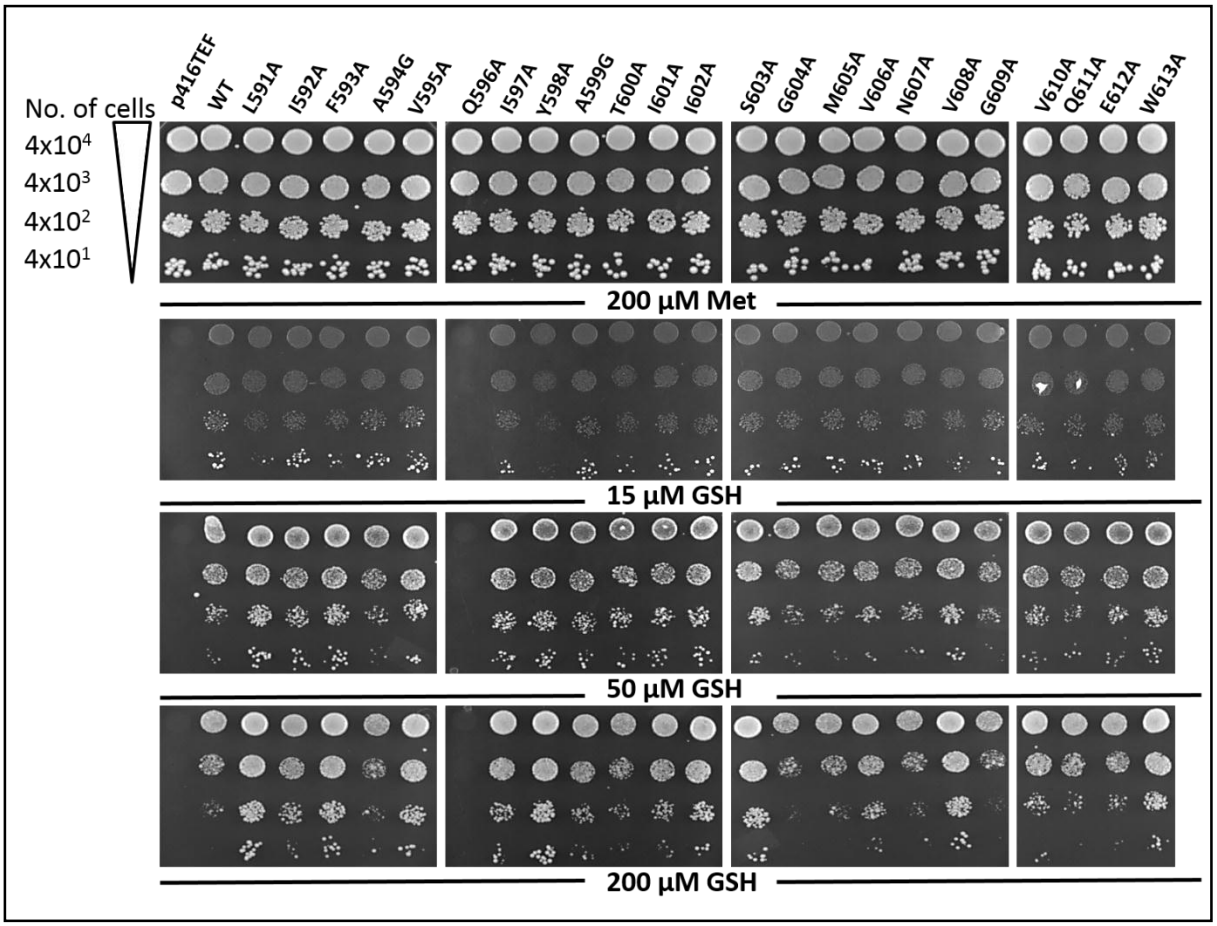

FIGURE 4.2i: Functional characterization of putative TMD10 alanine mutants of Hgt1p: Empty vector (p416-TEF), Wild type (WT) Hgt1p and the different TMD10 mutants of Hgt1p under TEF promoter were transformed in ABC 817. Transformants were serially diluted and spotted on minimal media plates containing different concentrations (15, 50, 200 µM) of glutathione or 200µM methionine (control).The photographs were taken after 2-3 days of incubation at 30 ˚C.

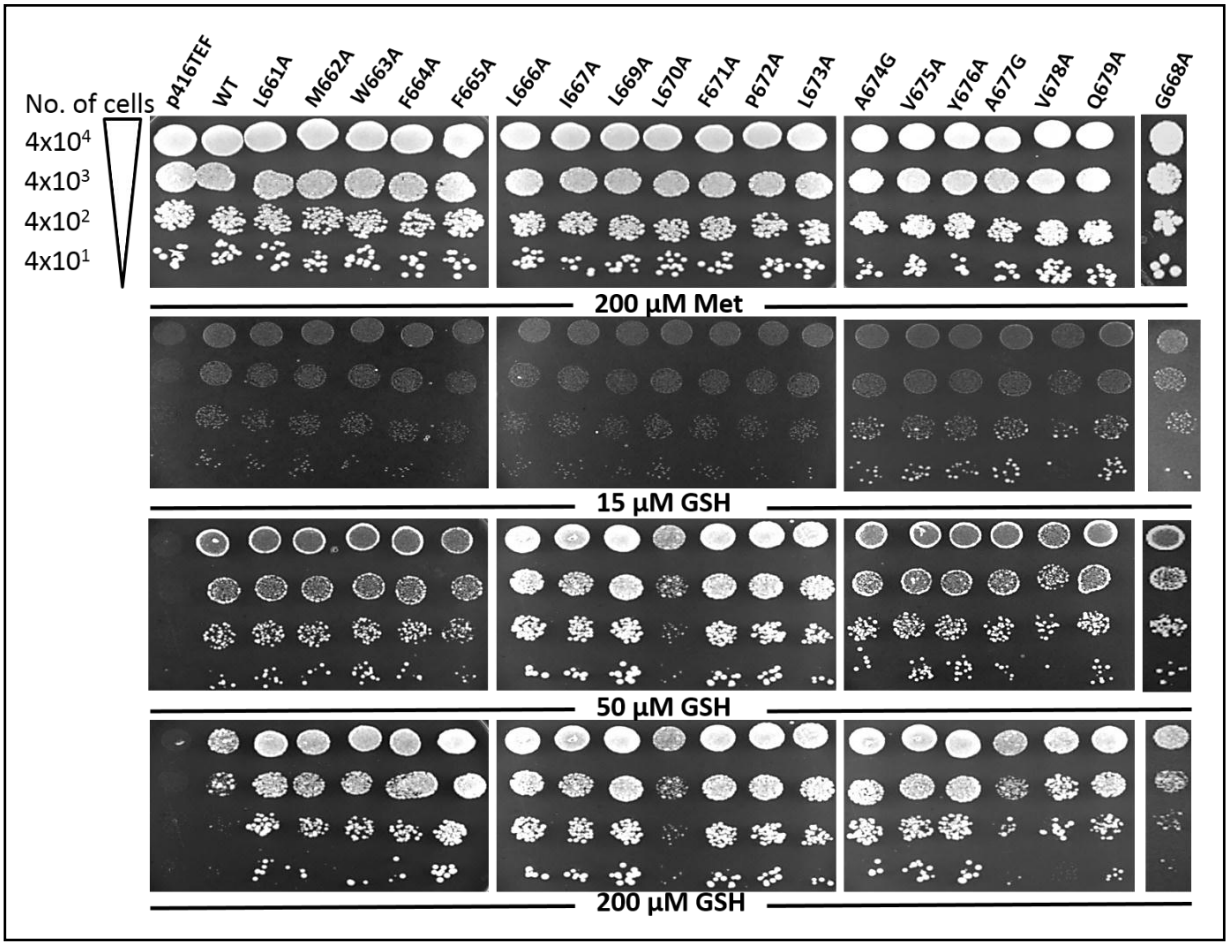

FIGURE 4.2j: Functional characterization of putative TMD11 alanine mutants of Hgt1p: Empty vector (p416-TEF), Wild type (WT) Hgt1p and the different TMD11 mutants of Hgt1p under TEF promoter were transformed in ABC 817. Transformants were serially diluted and spotted on minimal media plates containing different concentrations (15, 50, 200 µM) of glutathione or 200µM methionine (control).The photographs were taken after 2-3 days of incubation at 30 ˚C.

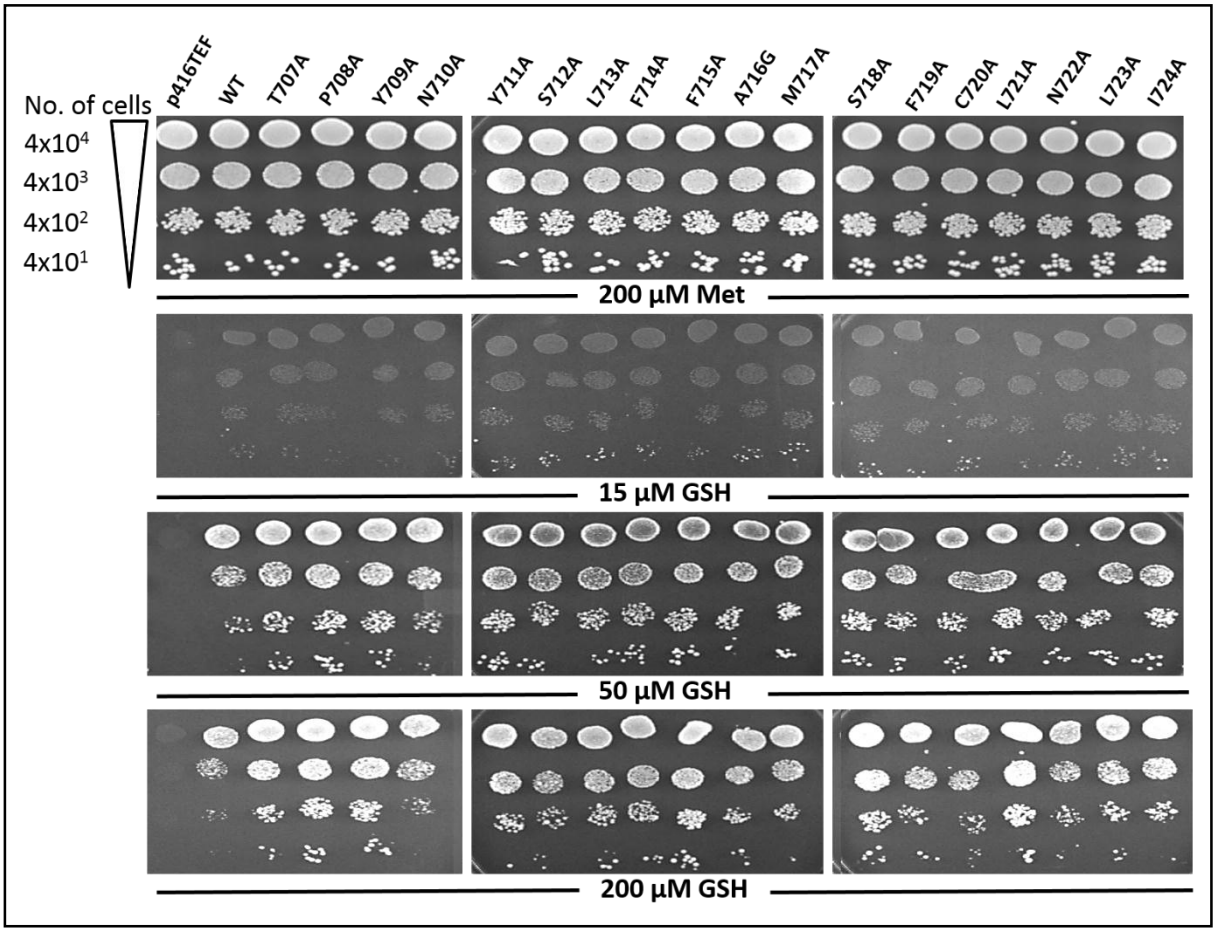

FIGURE 4.2 k: Functional characterization of putative TMD12 alanine mutants of Hgt1p: Empty vector (p416-TEF), Wild type (WT) Hgt1p and the different TMD12 mutants of Hgt1p under TEF promoter were transformed in ABC 817. Transformants were serially diluted and spotted on minimal media plates containing different concentrations (15, 50, 200 µM) of glutathione or 200µM methionine (control).The photographs were taken after 2-3 days of incubation at 30 ˚C.

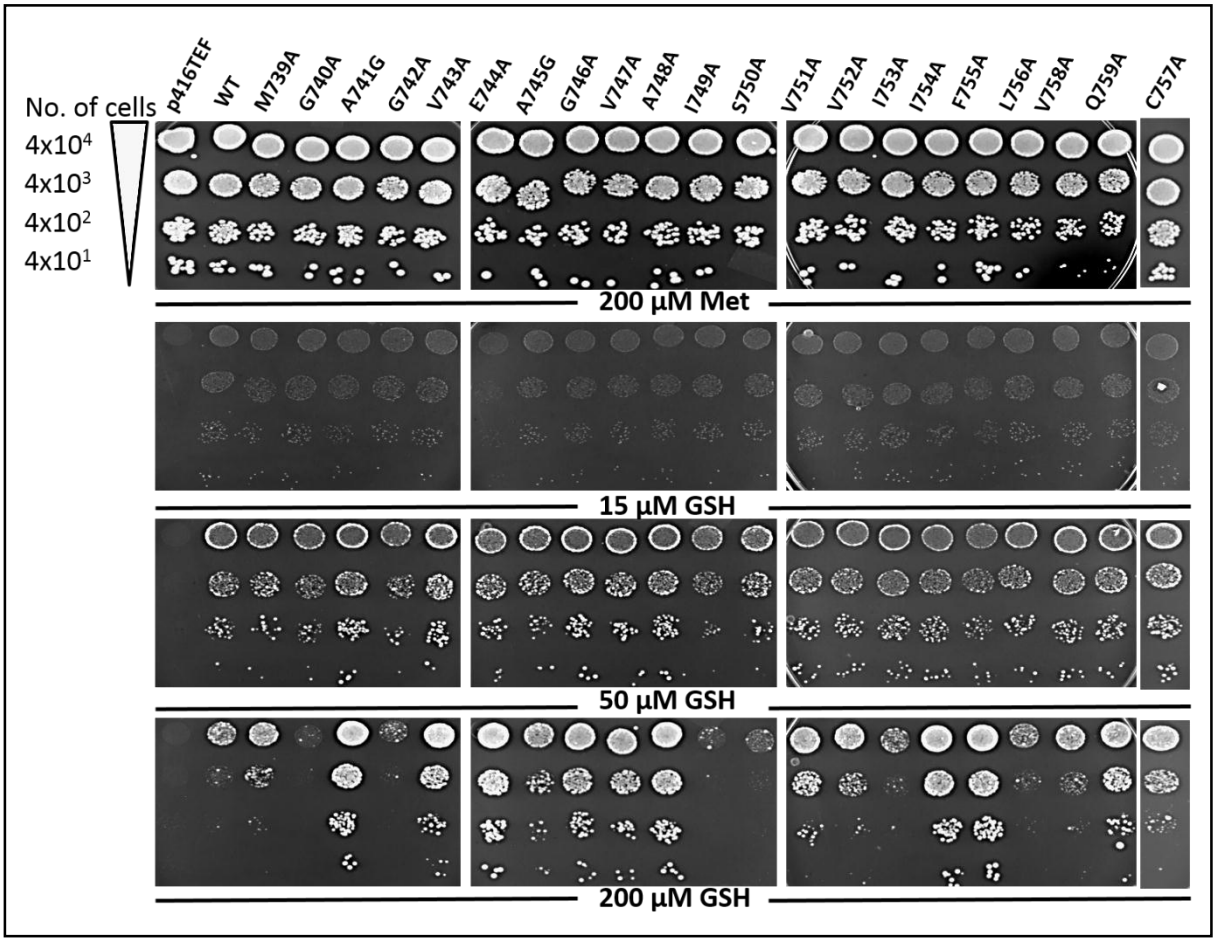

FIGURE 4.2l: Functional characterization of putative TMD13 alanine mutants of Hgt1p: Empty vector (p416-TEF), Wild type (WT) Hgt1p and the different TMD13 mutants of Hgt1p under TEF promoter were transformed in ABC 817. Transformants were serially diluted and spotted on minimal media plates containing different concentrations (15, 50, 200 µM) of glutathione or 200µM methionine (control).The photographs were taken after 2-3 days of incubation at 30 ˚C.

(Fig 4.2k). The moderately defective mutants were T707A, P708A, Y709A, F715A, S718A, F719A, C720A, L721A, N722A, L723A, and I724A. Mildly defective mutants included N710A, Y711A, S712A, L713A, F714A, A716G, and M717A. Proline residues in or near TMDs are shown to be directly or indirectly involved in substrate binding. We, therefore, mutated two proline residues (P704A and P705A) present just outside this TMD and both the mutants interestingly showed a severe defect.

TMD13 (M739-Q759) is composed of 21 amino acid residues. 19 were mutated to alanine (E744 studied previously), and two alanine residues were mutated to glycine. E744A showed a severe defect (Fig 4.2l). Moderately defective mutants included V743A, G746A, V747A, A748G, F755A, and L756A. Mildly defective were G740A, A741G, G742A, I749A, S750A, V758A, and Q759A and remaining mutants had no defect.

Besides the two proline mutants (P704A and P705A) were also severely defective in glutathione uptake. The 22 severely defective mutants that were not analyzed earlier were pursued further.

4.3 Evaluation of protein expression levels and cell surface localization of severely defective mutants:

The decrease in activity of mutants of Hgt1p based on growth assay can be attributed either to decreased protein expression levels, a defect in localization to cell surface or loss of the activity of the protein itself. Steady state protein expression levels were measured by immunoblotting. Crude protein extracts were prepared from the *S. cerevisiae* ABC 817 strain transformed with the plasmids bearing the severely defective mutants of Hgt1p, and equal amounts were resolved using SDS-PAGE and electroblotted onto the nitrocellulose membrane and probed with anti-HA monoclonal antibody. An 85 kDa band corresponding to the wild-type Hgt1p was observed for all the mutants. The 22 complementation defective mutants showed variation in protein expression levels. Densitometry analysis of unsaturated band signals (Fig. 4.3a) revealed that V180A, V181A, T182A, L282A and W484 showed significantly low levels (10-20%) of protein expression as compared to WT suggesting their crucial role in protein folding and stability as being the basis for their loss in functional activity. These were not pursued further. For the other 17 mutants, protein expression levels ranged between 50-100% relative to wild-type protein level and were further analyzed for possible defects in trafficking.

Hgt1p is a plasma membrane localized transporter and any mutation that affecting its trafficking to the cell surface would also result in the loss of functional activity in a whole-cell based functional assay. Hence it was important to examine the subcellular localization of severely defective mutants expressed under the TEF promoter. Analysis of cell surface localization of these 17 mutants was carried out by indirect immunofluorescence and compared with PMA1-Flag tag localization. PMA1 encodes for the plasma membrane H^+-ATPase and serves as a marker for plasma membrane localization. A very bright fluorescence was observed at the cellular periphery for wild type Hgt1p as well as for majority of the mutants (Q142A, V185A, L187A, Y193A, I197A, G225A, Y226A, P292A, L373A, Y374A, L429A, P704A, and P705A) (Fig. 4.3b) co-localizing with the PMA1-Flag tagged marker protein suggesting that these mutants are properly localized on the plasma membrane. However, for four mutants W110A, G230A, Y449A, and Q596A the signal was primarily intracellular with poor cell surface localization as compared to PMA1 suggesting that these mutant proteins are not correctly localized on the plasma membrane and hence are defective in trafficking. These mutants were not studied further.

4.4 Comparative uptake and substrate saturation kinetics of severely affected mutants:

The 13 severely defective mutants that were not significantly defective in protein expression levels or in their localization to the cell surface were further analyzed by measuring the biochemical uptake of glutathione. These mutants were Q142A, V185A, L187A, Y193A, I197A, G225A, Y226A, P292A, L373A, Y374A, L429A, P704A, and P705A. We compared [^{35}S]-GSH uptake in these mutants and found that transport activity was indeed significantly lower (<15%) than wild type in all the mutants. Only Q142A showed greater transport above 30% suggesting that it belongs to the moderately defective category (Table 4.3). To obtain a better understanding of the possible role of these residues in glutathione transport, we carried out the kinetic analysis of these mutants by measuring the initial rates of [S^{35}] GSH uptake over a range of glutathione concentrations.

The apparent *Km* of wild-type Hgt1p for glutathione was estimated to be 27.8 ± 1.2 µM and the *Vmax* was found to be 54.0 ± 0.81 nmol of glutathione.mg of protein^{-1}.min^{-1}. Although the *Vmax* was in close agreement with the previously reported value (57.8 ± 5.5 nmol of glutathione.mg of protein^{-1}.min^{-1}), the *Km* value in the present

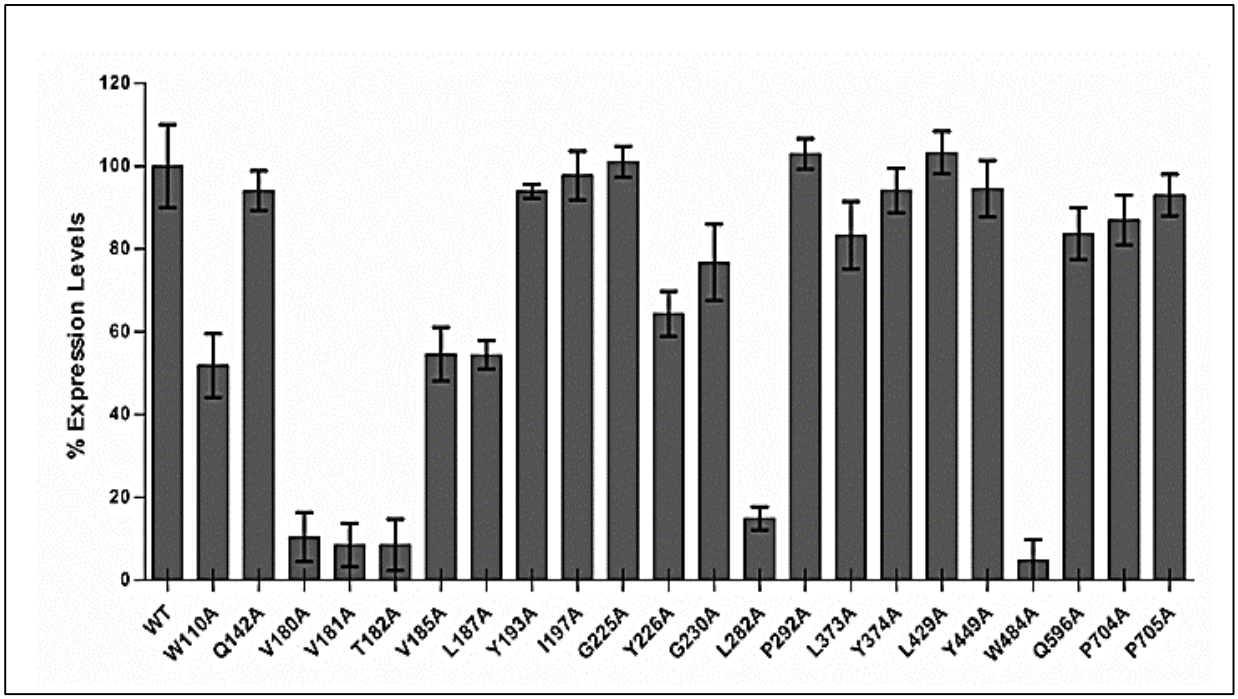

FIGURE 4.3a: Quantification of the total protein expression levels of the severely defective alanine mutants of Hgt1p: 20μg protein of crude extract prepared from ABC 817 strain transformed with plasmids overexpressing WT or the alanine mutants of Hgt1p was resolved using 10% SDS-PAGE and electroblotted on nitrocellulose membrane. The blot was incubated in stripping buffer (100mM β-mercaptoethanol, 2% SDS, 62.5mM Tris-HCl, pH 6.7) at 55°C for 15 min followed by two washes with TBST at RT. The blots were probed with mouse anti-HA antibody as the primary antibody and goat anti-mouse HRP conjugated IgG as secondary antibody. The signal was detected using Luminata^{TM} forte Western HRP substrate. The total protein expression was then quantified by densitometry analysis of protein bands. The data is expressed as the percentage protein expression compared to wild type (WT) expression level and are the mean ± S.D. of three independent experiments.

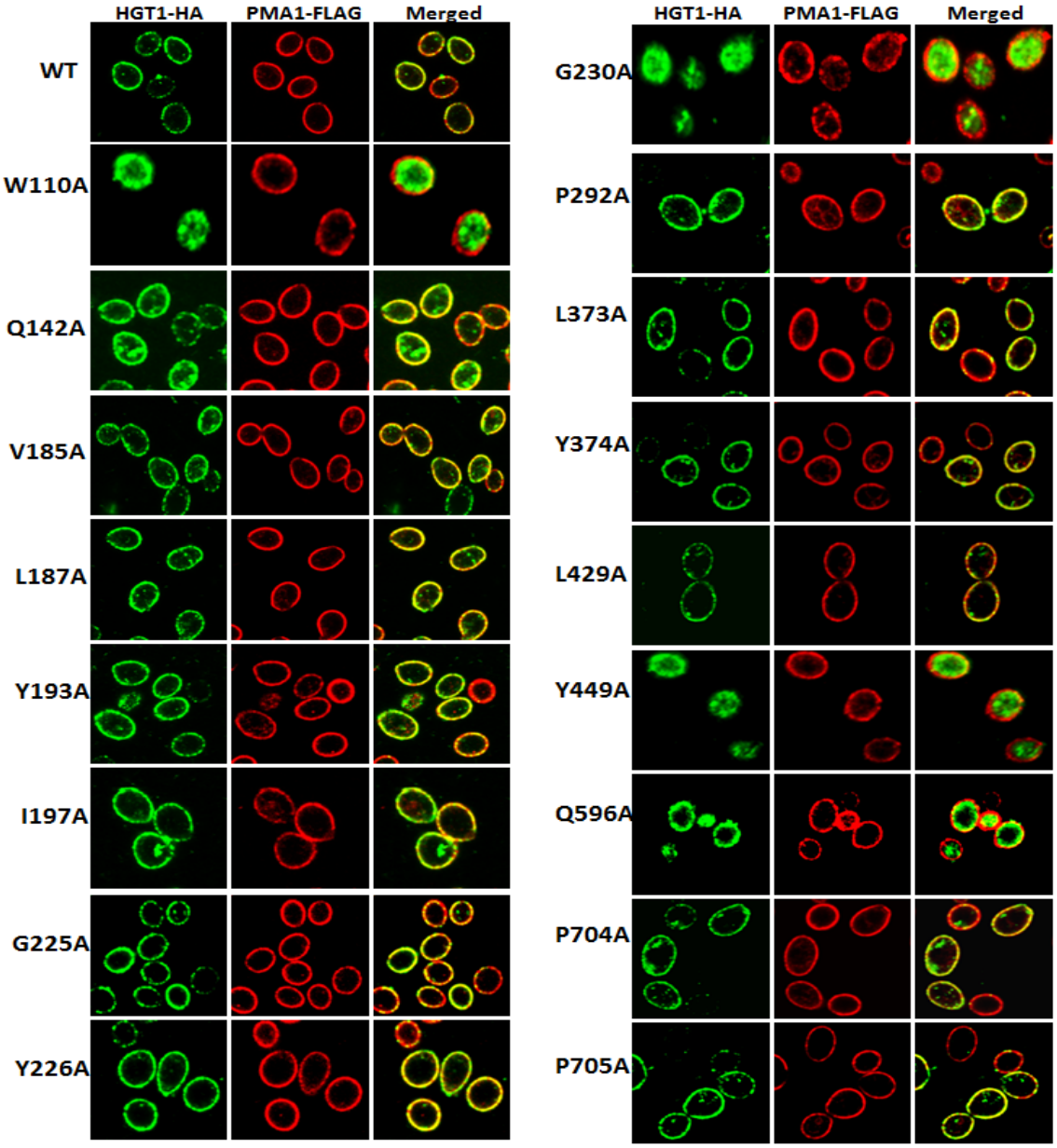

FIGURE 4.3b: Cell surface localization of severely defective alanine mutants of Hgt1p. BY4741 with PMA1 tagged with FLAG sequence at the C-terminus in the genome was transformed with plasmids bearing wild type (WT) or different alanine mutants of Hgt1p having a HA-tag at the C-terminus. The transformants were fixed, permeabilized and labelled by indirect immunofluorescence and visualized using confocal microscopy, as described in chapter2, section 2.18. Experiment was repeated twice (n=4) using independent transformations and only fluorescence images have been shown.

Table 4.3: Uptake activity and kinetic characterization of the mutant showing severe loss in activity: a) For quantification of functional activity of the mutants, initial uptake results are shown as % uptake as compared to the rate of glutathione uptake measured for the wild type Hgt1p (51.4 ± 3.2 nmol min^{-1}mg.$protein^{-1}$). Data were obtained from three independent experiments done in duplicates and are represented as percentage activity relative to wild-type Hgt1p and expressed as the mean ± S.E. **b)** The average *Km* (µM) and *V*max (nmol of glutathione.mg of $protein^{-1}.min^{-1}$) values were determined by nonlinear regression analysis of *V versus* [S] graphs showing saturation kinetics using GraphPad Prism Version 5.01 software. N.M., not measurable. **c)** *Vmax* was adjusted to the protein expression levels.

Mutants (TMD)	(a) **% Uptake activity**	**% Protein Expression**	(b) **Kinetic Parameters**		(c)**Corrected**	**Corrected**
			Km	***Vmax***	***Vmax***	***Vmax / Km***
WT- Hgt1p	100	100	27.8 ± 1.2	54.0 ± 0.8	54.0	1.94
SEVERE EFFECT (Complementation Defective)						
Q142A (TMD2)	30.1 ± 4.5	94	32.5 ± 6.4	51.7 ± 2.4	55.0	1.71
V185A (TMD3)	4.9 ± 1.3	55	87.9 ± 13.8	1.6 ± 0.1	2.9	0.03
Q222A (TMD4)	4.0 ± 0.8	91	115.9 ± 22.5	9.4 ± 1.6	12.5	0.10
G225A (TMD4)	5.8 ± 2.1	101	87.7 ± 5.5	12.3 ± 1.9	12.1	0.13
Y226A (TMD4)	3.1 ± 0.1	64	252.6 ± 36.1	16.0 ± 3.0	25.0	0.09
P292A (TMD5)	5.2 ± 2.7	102	183.2 ± 44.5	54.0 ± 0.8	52.9	0.28
Y374A (TMD6)	20.3 ± 3.7	94	55.0 ± 5.2	12.9 ± 1.2	13.7	0.24
L429A (TMD7)	4.0 ± 0.9	101	112 ± 22.4	3.5 ± 0.0	3.4	0.03
Q526A (TMD9)	6.5 ± 0.5	62	292.6 ± 48.6	24.0 ± 7.7	38.7	0.13
P704A	13.8 ± 1.2	87	34.8 ± 20.0	3.0 ± 1.5	3.4	0.09
P705A	13.6 ± 1.7	93	37.4 ± 12.5	6.1 ± 1.0	6.5	0.17
L187A (TMD3)	1.3 ± 0.4	54	N.M.		N.M	N.M
Y193A (TMD3)	1.3 ± 0.2	93	N.M		N.M	N.M
I197A (TMD3)	0.9 ± 0.3	97	N.M		N.M	N.M
L373A (TMD6)	0.9 ± 0.2	83	N.M		N.M	N.M

study was lower than the previously reported *Km* (≈ 50 µM) (Kaur and Bachhawat, 2009) as has been discussed in the previous chapter. Following the kinetic re-evaluation of the wild type Hgt1p, we carried out a detailed kinetic characterization of each of the severely defective mutants (Q142A, V185A, L187A, Y193A, I197A, G225A, Y226A, P292A, L373A, Y374A, L429, P704A, and P705A) that were not affected in either the expression or trafficking to determine the *Km*, corrected *Vmax* (i.e. adjusted to the protein expression levels) and transport efficiencies (*Vmax*/*Km*) (summarized in Table 4.3). This kinetic characterization of the new mutants revealed interesting insights into the role of these residues in the functional activity of the transporter. Y226A showed the highest increase (≈ ten-fold compared to WT) in *Km* (252.6 ± 36.1 µM) with about three-fold reduction in *Vmax* (16.0 ± 3.0 nmol of glutathione.mg of protein^{-1}.min^{-1}). P292A exhibited about a seven-fold increase in *Km* for glutathione without affecting the *Vmax*. Similarly, a nearly four-fold increase in the *Km* value was observed for L429A which also exhibited a significant loss in corrected *Vmax* value. Further V185A, G225A showed a nearly three-fold increase in *Km* with V185A also showing a significant reduction in *Vmax*. This significant decrease in the glutathione affinity of V185A, G225A, Y226A, P292A and L429A suggest that these residues play a critical role in interacting with the substrate. Kinetic analysis of Y374A revealed that although this mutant showed a drastic loss in transport efficiency, it displayed about a two-fold increase in *Km* values, placing it as a residue also possibly involved in substrate binding and translocation.

In contrast, the kinetic analysis of P704A and P705A revealed a drastic loss in the catalytic activity without affecting the *Km*. The *Vmax* values for P704A and P705A mutants were 3.4 ± 1.5 and 6.5 ± 1.0 nmol of glutathione.mg of protein^{-1}.min^{-1} respectively, showing a nearly sixteen and eight-fold decrease in transport efficiency of the mutants. The significant decreased *V*max values obtained for the mutants V185A, L429A, P704A and P705A which could not be attributed to the decreased protein levels or mislocalization of the mutant proteins, suggest that these residues might play some important role in the conformation changes in Hgt1p during translocation of the substrate.

The mutants L187A, Y193A, I197A, and L373A which expressed well and localized correctly to the plasma membrane showed very little uptake. The initial rate of glutathione uptake was less than 2% of the wild-type, thus making it difficult to obtain reliable kinetic parameters. Nevertheless, these mutants clearly have a role in

glutathione transport and are also strong candidates for being involved in substrate binding, although the precise role has not been determined.

4.5 Y226A and Y374A mutants are specifically defective in glutathione transport, but not oxidized glutathione and S-lactoyl glutathione:

While Hgt1p was shown to recognize and transport glutathione, it also binds to oxidized glutathione (GSSG), S-lactoyl-GSH, S-methyl-GSH, S-hexyl-GSH and S-decyl-GSH with significant affinity. We, therefore, sought to examine how the different severely defective mutants were affected in the utilization of different glutathione conjugates to be used as a sulphur source by the organic sulphur auxotroph of *S. cerevisiae* (ABC 817, *met15*Δ*hgt1*Δ). The conjugates S-methyl-GSH, S-hexyl-GSH, and S-decyl-GSH in spite of showing very good inhibition and being potentially good substrates for Hgt1p, did not support growth at any of the tested concentrations (Fig. 4.4a also Fig. 3.2a of Chapter3). A possible explanation is that *S. cerevisiae* is not equipped to catalyze the cleavage of the thioether linkage in glutathione conjugates. Only S-lactoyl-GSH and GSSG in addition to GSH showed growth on glutathione. Thus the two substrates GSSG and S-lactoyl-GSH were examined for growth using different mutants. We observed that the majority of mutants which were defective in utilizing reduced glutathione at low concentrations (15µM), were almost identically defective in utilizing both GSSG and S-lactoyl-GSH. Only Y226A and Y374A showed a consistently different growth on these 2 substrates (Fig. 4.4b). Q142A mutant which was initially isolated as severely defective also showed growth at low concentration on both substrates (but from later growth experiments seemed more appropriately a moderately-defective mutant, rather than severely-defective, as also confirmed by the transport data). However, Y226A which was severely detective on GSH showed significant growth on GSSG. Similarly, Y374A mutant which was severely defective on GSH did not show any significant defect on both S-lactoyl glutathione and GSSG plates. A possible explanation for growth on low GSSG is that at identical molar concentration GSSG will provide twice as much sulphur as compared to GSH. To confirm this, mutants (Q142A, V185A, G225A, Y226A, Y374A, and F523A) were spotted on lower (7.5 µM) GSSG concentration. We observed that V185A, G225A, and F523A (negative control) are indeed defective in utilizing GSSG as compared to WT, but Y226A and Y374A showed growth (Fig 4.4c). This suggests that Y226 and Y374 are specifically required by Hgt1p in binding to reduced GSH, but not to GSSG or SLG.

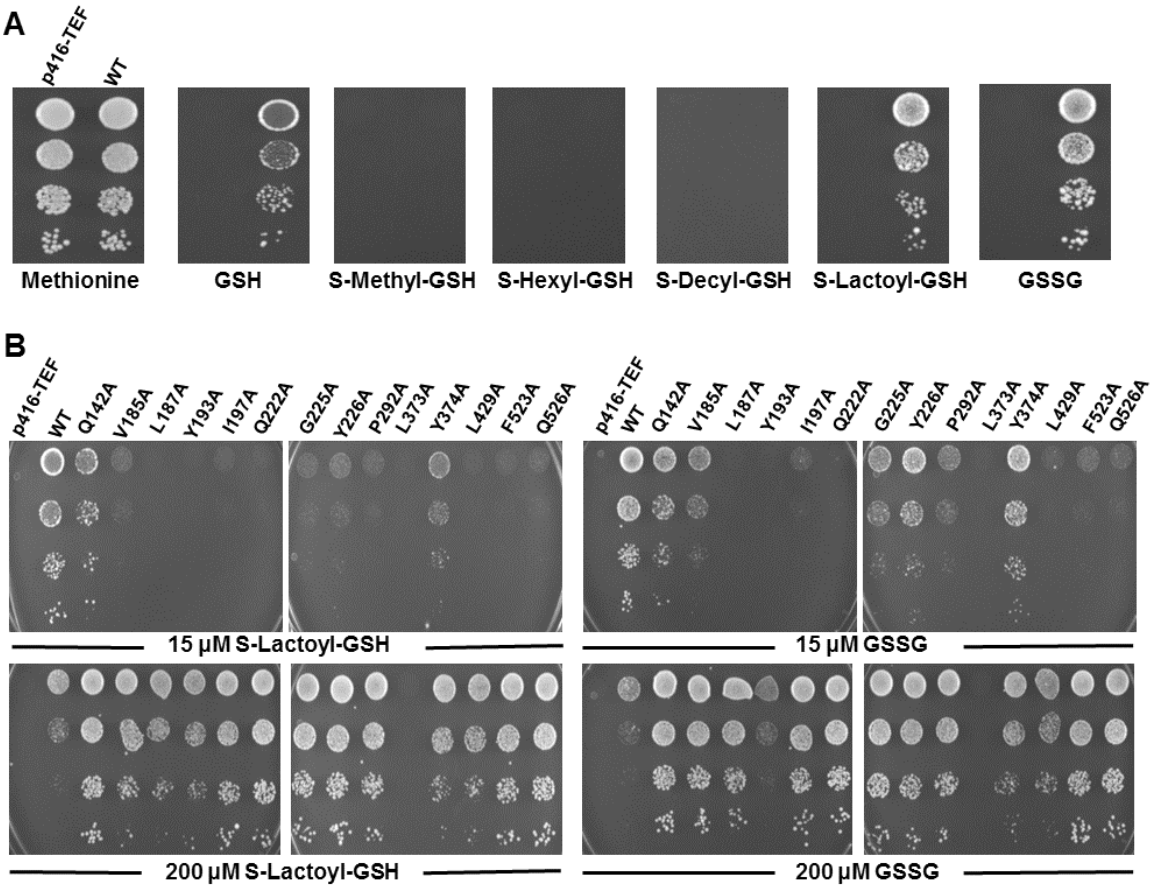

FIGURE 4.4: Functional analysis of WT and severely affected mutants on GSH and different GSH-conjugates: **(a)** Growth of ABC 817 transformed with empty or wild type (WT) HGT1 under TEF promoter on minimal media containing 200 µM methionine or 30 µM of GSH, S-Methyl-GSH, S-Hexyl-GSH, S-Decyl-GSH, S-Lactoyl-GSH and GSSG. **(b)** WT and mutants showing severe defect in transport were subjected to plate based "Dual complementation-cum-toxicity" assay by serial dilution spotting on minimal media containing different concentrations of S-Lactoyl-GSH and oxidized glutathione (GSSG). The photographs were taken after 2-3 days of incubation at 30°C. Experiments were repeated thrice each time using independent transformations.

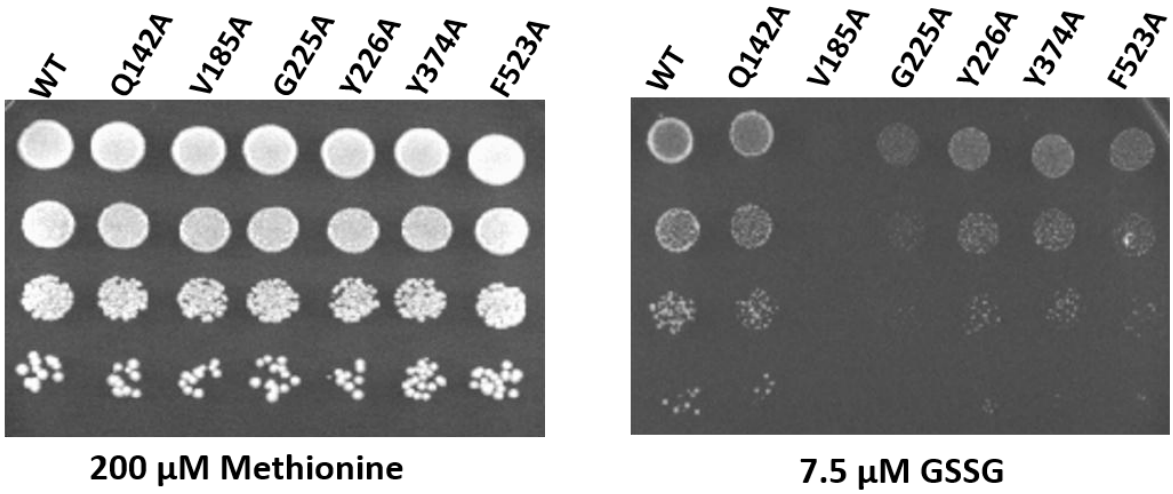

FIGURE 4.4c: Functional analysis of V185A, G225A, Y226A and Y374A on 7.5 µM GSSG: ABC 817 was transformed with plasmids bearing the empty vector (p416-TEF), wild type (WT), Q142A, V185A, G225A, Y226A, Y374A and F523A mutations in Hgt1p and used for plate-based dual complementation-cum-toxicity assay by dilution spotting on minimal media containing 200 µM methionine (control) and 7.5 µM GSSG.

4.6 Multiple sequence alignment of Hgt1p with other PT members of the OPT family:

Oligopeptide transporter (OPT) family is divided into two clades which are remotely related to each other. a) Peptide Transporter (PT) clade, mediating uptake of oligopeptides, glutathione and metal chelates and b) Yellow Stripe (YS) clade that mediate uptake of metals and secondary amino acid derivative (Lubkowitz, 2011). Within the PT clade, Hgt1p (of *S. cerevisiae)* and a few closely related organisms in which orthologues of Hgt1p are present form a cluster (Sc cluster) and have been shown to transport glutathione (Fig. 1.2, Chapter1) (Thakur and Bachhawat, 2010). These organisms include *S. cerevisiae, S. pombe, K. lactis, P. pastoris, P. guilliermondii* and *S. japonicus.* Another closely related cluster (Cn cluster) of organisms that include *Cryptococcus neoformans* were also shown to contain functional orthologues of Hgt1p that could transport glutathione (Thakur and Bachhawat, 2010). In contrast, the cluster (Caopt1 cluster) of organisms that included *Candida albicans* OPT1 were demonstrated not to be glutathione transporters, since this protein failed to transport glutathione to any significant extent(Thakur and Bachhawat, 2010) (Desai et al., 2011).

Multiple sequence alignment of these PT members (Fig. 4.5) revealed that Y193, G225, Y226, and P292, were conserved across both the glutathione transporter family as well as the larger family of oligopeptide transporters that included non-glutathione transporters such as CaOPT1. We have included Y226 in this group as in both *C. neoformans* and *C. albicans* the corresponding residue was Phe. Considering it was present in *C. neoformans* orthologue that encodes a glutathione transporter, it is likely that Tyr/Phe would both be acceptable residues for glutathione transport. The previously identified N124 and Q222 was also highly conserved among both the glutathione and non-glutathione transporters in the peptide transporter clade.

In contrast V185, L187, I197, L373, and Y374 were conserved only in the cluster of transporters known to be GSH transporters that included both the Sc cluster and the Cn cluster. This suggests their possible role in specifically binding and transporting glutathione similar to the previously identified residues, F523 and Q526 which are conserved only in the *S. cerevisiae* cluster of glutathione transporters. However, in the *C. neoformans* protein, acceptable amino acids F523I and Q526E were found, as has been demonstrated earlier, but the non-glutathione transporters contained residues that were not acceptable at these positions (Thakur and Bachhawat, 2010). The L429

residue was less well conserved. Even within the *S. cerevisiae* cluster, many of the orthologues had Ser in place of Leu. *C. neoformans* protein have Ser at this position. In the non-glutathione transporter, CaOPT1, the corresponding residue was Ala.

4.7 Modelling of Hgt1p to gain more insight into structural aspect:

The 3-D structure of Hgt1p or any member of the OPT family is not known, and the unique OPT transmembrane fold makes it difficult to find homologous structures in the protein databank for comparative modeling. An *ab initio* based computational approach was further developed using Rosetta *ab initio* membrane protocol (Barth et al., 2007; Yarov-Yarovoy et al., 2006) to derive the structural model of Hgt1p (discussed in Chapter 2, section 2.20). Combining this *ab initio* protocol with structural restraints from known 12-13 TMD helical proteins, we selected one probable conformation for the transmembrane core of the protein with pore-lining helices TMD3, TMD4, TMD5, TMD6, TMD7, TMD9, and TMD13 (Fig.4.6a). Interestingly TMD3, TMD4, TMD7, and TMD13 is also predicted as pore-lining helices by a "Support Vector Machine" classifier methodology prediction software. Although there is no supporting mutagenesis data for TMD13, the modeled structure also show its probability of involvement in lining the pore. In this model, the predicted positions of TMD helices are shown, but for clarity, the structures of the hydrophilic loops connecting TM helices are not displayed. As can be seen from the figure 4.6b, side chains of the residues critical for substrate transport (from mutagenesis data) point towards the transmembrane pore. Also, noteworthy is the probable location of critical residues Q222 and Y226 on TMD4 and residues F523 and Q526 on TMD9 helix. Their presence in the proximal region of either side of pore suggests their importance in substrate translocation as well. P292 forms a kink in TMD5, and usually, such prolines within transmembrane core play a role in packing and hinge dynamics of helices.

4.8 Discussion

We have been able to map the residues in the transmembrane segments for their involvement in glutathione binding and translocation through alanine scanning mutagenesis. All the of 269 amino acid residues comprising 13 predicted TMDs were included in the current mutagenic study. After eliminating mutants defective in either protein sorting or expression, the TMDs and the residues that were identified were TMD1 (N124), TMD3 (V185, L187, Y193, I197), TMD4 (Q222, G225, Y226), TMD5 (P292), TMD6 (L373, Y374), TMD7 (L429), and TMD9 (F523, Q526).

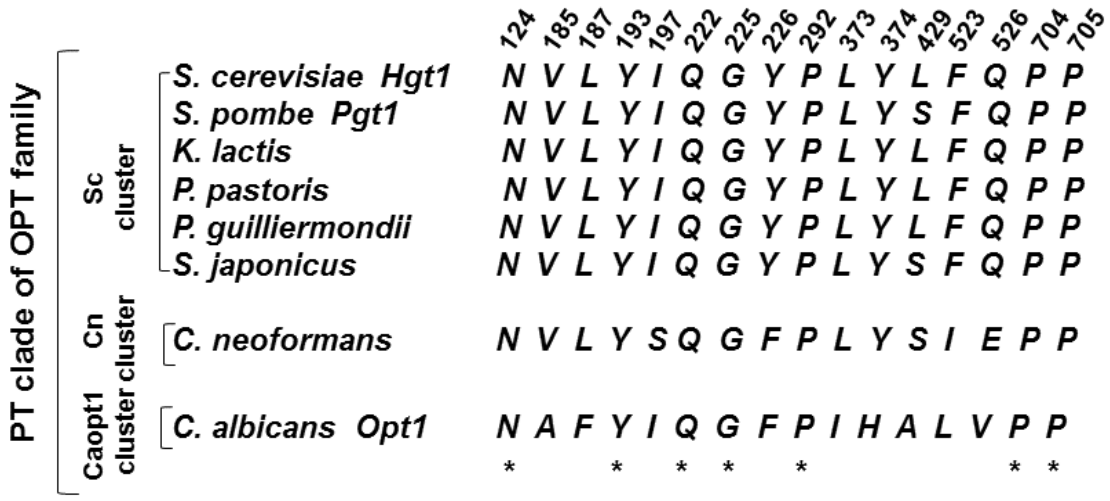

FIGURE 4.5: Multiple sequence alignment for the protein sequences of Hgt1p with known PT members of the OPT family: Multiple sequence alignment of Hgt1p with known glutathione transporters including *S. pombe* Pgt1, *K. lactis* (GenBank® accession number XP 453962.1), *P. pastoris* (GenBank® accession number XP 002493413.1), *P. guilliermondii* (GenBank® accession number XP 001486861.1), *S. japonicas* (GenBank® accession number XP 002172910.1), *C. neoformans* (GenBank® accession number XP 772672.1) and non-glutathione transporter *C. albicans* Opt1 (GenBank® accession number XP 718267.1) all belonging to PT clade of the OPT family. Sequences were retrieved from Entrez at the NCBI website and aligned using the MUSCLE program using default parameters. The sequence alignment has been edited to show only severely defective residues where aligned number indicates the amino acid position in the Hgt1 protein sequence.

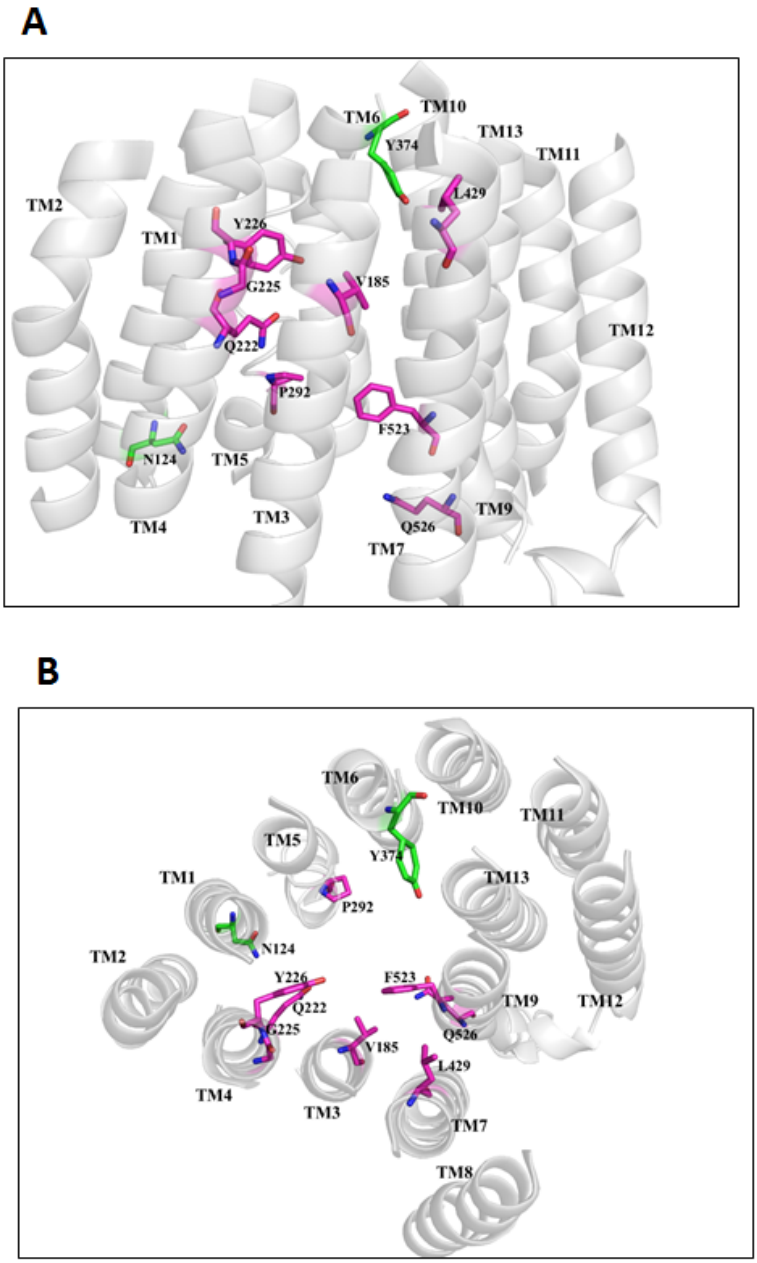

FIGURE 4.6: Structural models of Hgt1p based on ab initio modelling: TMD helices are numbered 1-13 and specific amino acid side chains are highlighted and labelled. Residues whose mutation effects substrate binding are coloured magenta while residues whose mutation cripples substrate translocation are highlighted in green. For clarity, the loop regions have been omitted. **(a)** Viewed parallel to the membrane **(b)** Periplasmic view. Structures in this figure were generated using PyMol

Considering the drastic effect of these mutants on the kinetic parameters, their conservation pattern in known glutathione transporters of the OPT family, and their positioning in the amphipathic face of the helices, it appears likely that these transmembrane domains line the translocation channel of the transporter. These TMDs are then supported by other peripheral TMDs (TMD2, TMD8, TMD10, TMD11, TMD12, and TMD13) whose alanine scanning mutagenesis did not show any significant defect in any of the residues.

The studies described here have also yielded an *ab initio* model of the transmembrane helical arrangements of Hgt1p which predicted TMD3, TMD4, TMD5, TMD6, TMD7, TMD9 and TMD13 to be the pore-lining helices. The mutational analysis predicted TMD1, TMD3, TMD4, TMD5, TMD6, TMD7 and TMD9 to form the translocation channel, facilitating the *ab initio* model of Hgt1p. Mapping of the critical residues involved in the substrate binding on the *ab initio* model revealed that V185, Q222, G225, Y226, P292, L429, F523, and Q526 were all present on the TMDs predicted to form the translocation channel and, more importantly, faced the permeation pathway. The latter observation was a strong validation of the model. In addition, mutations that cripple the translocation activity (N124 and Y374) also cluster around the central pore. The fact that both the experimental and computational approaches led to similar tertiary topology prediction further provides confidence that the model offers a reasonable representation of helix packing for Hgt1p.

Proline residues in or near the TMDs of polytopic membrane proteins are involved in substrate binding (Vilsen et al., 1989), conformational (Williams and Deber, 1991) or structural changes (Cordes et al., 2002) involved in the transport process. We therefore also analyzed the proline residues in TMDs including P704 and P705 present on the cusp of TMD 12 of Hgt1p. Functional and kinetic analyses suggested P704 and P705 to be involved in substrate translocation. However, when mapped on the *ab initio* model, it appeared to be distant from the translocation channel suggesting that it may serve structural roles in the transport process where it may indirectly cause a shift in overall helix packing. The other proline found to be important was P292 that was present facing the translocation channel creating a Pro-kink. This proline residue is likely to either directly affect substrate binding or it modifies the architecture of the Hgt1p substrate translocation pathway by changing the geometry of the TMD5.

This study has also been able to identify two residues Y226 and Y374 of Hgt1p that is specifically required for reduced glutathione uptake, but not for other substrates such as GSSG or SLG that are also transported by Hgt1p. Examination of the model reveals that Y226 and Y374 are present near the end of TMD4 and TMD6 at the periplasmic face on the *ab inito* model of Hgt1p, but the exact reasons for this interesting specificity may be understood only with the availability of the Hgt1p structure in complex with glutathione.

In conclusion, this study provides the first in-depth knowledge of substrate specificity with insights into the role of every residue in all the predicted TMDs in substrate transport by this high affinity glutathione transporter, Hgt1p. This study should form an excellent platform for not only understanding how glutathione transporters are able to transport glutathione but should also assist in studies and manipulation of other transporters of the OPT superfamily that carry out the transport of a variety of important substrates in plants and fungi.

CHAPTER 5:

Identification of Residues Involved in Proton Binding and Transport by Hgt1p

INTRODUCTION

In both fungi and plants primary energization of the plasma membrane is generally achieved through the action of plasma membrane proton pumps which generates an electrical and proton gradient across these membranes (negative and high pH within the cell). This electrochemical proton gradient acts as the driving force for the uptake and efflux of many metabolites and ions across the plasma membrane. Hence the majority of co-transporters in these organisms are proton-coupled (Sze *et al.* 1999). Transport mediated by the *Saccharomyces cerevisiae*, high-affinity glutathione transporter Hgt1p is also suggested to use the inwardly directed proton electrochemical gradient to drive the uphill transport of glutathione against a concentration gradient. This transport was also shown to be electrogenic i.e. protons are co-transported with substrates in stoichiometries that lead to a net positive charge per transport cycle irrespective of the negative/neutral charge of the substrate. However, at low external pH (i.e. high proton concentrations), Hgt1p dependent proton leak was observed in the absence of glutathione suggesting a loose coupling of the substrate with protons (Osawa *et al.* 2006).

Identification of residues involved in proton transport is central to the understanding of the mechanism of active transport by Hgt1p and remains to be elucidated. In this regard, structural and biochemical studies of several proton-coupled transporter belonging to MFS superfamily have been instrumental in providing clues for determining how protons may bind and get transported. The best example is lactose permease (lactose/ H^+ symporter, LacY), where Glu269 and His322 are important for substrate/proton coupling, Glu325 is important for proton release and Arg302 may facilitate deprotonation of Glu325 (Kaback *et al.* 2001; Andersson *et al.* 2012). Among other transporters, crystal structure analysis in combination with different biochemical, biophysical and molecular genetic approaches have identified residues involved in proton translocation (discussed in chapter 1, section 1.4). Thus different residues are involved in the proton translocation and these different residues play different role in the proton relay

In this chapter with the goal of identifying the residues involved in proton binding and transport by Hgt1p, we carried out an exhaustive analysis to screen for mutants showing pH independent growth on a pH based plate assay. Evaluation of all alanine

mutants of the 13 predicted TMDs in combination with *in vitro* random mutagenesis identified E135A and N710A to be important for pH-dependent transport. Biochemical characterization of these mutants also showed increased uptake at higher pH as compared to the WT Hgt1p but the transport was not completely pH independent. We, therefore, extended the search and targeted selective amino acid residues reported to be involved in binding and translocation of protons in other proton-coupled transporters. We targeted these based on their conservation pattern and their location in the predicted topology model and identified additional residues to be important for proton-dependent substrate transport by Hgt1p.

5.1. Isolation of Hgt1p mutants showing pH independent growth phenotype on glutathione:

A pH profiling of the Hgt1p transporter revealed that transport is optimal at pH 5.5 and falls drastically with increasing pH (Fig 5.1A). We have used this property (of low or no transport at high pH) as an initial strategy towards identifying the residues involved in proton binding and transport in Hgt1p. In this strategy, mutants that allowed growth at higher pH were identified. The logical basis for isolating such mutants has been that those residues which upon mutation can lead to growth at high pH, would be likely to play a role in proton binding/proton transport. To determine at what pH the screen should be performed, we evaluated TEF-HGT1 transformants at different pH (5.5-8.0) and different glutathione concentrations (15-200µM) (Fig.5.1B) (only growth at 15 µM GSH pH 5.5, pH 7.0 and pH 8.0 is shown). We observed that at pH 8.0, the cells were not able to grow at 15-30 µM GSH conc. although they were able to survive at higher GSH concentrations (>50 µM). These results are consistent with the [^{35}S] GSH uptake assay, where the WT Hgt1p shows almost negligible amount of transport at pH 8.0. Using the lack of growth at 15 µM GSH at pH 8.0 we embarked on an effort to identify mutants able to grow at pH 8.0 on glutathione.

As the proton binding residues are expected to lie within or in the periphery of the TMDs (Yerushalmi & Schuldiner 2000), we first focussed on the TMD residues. Hgt1p is predicted to have 13 TMDs comprising 269 amino acid residues. As described in the previous chapter, these 269 mutants were subjected to alanine scanning mutagenesis that identified residues defective in GSH transport. This collection of 269 alanine mutants were subjected to an evaluation of growth at 15-200

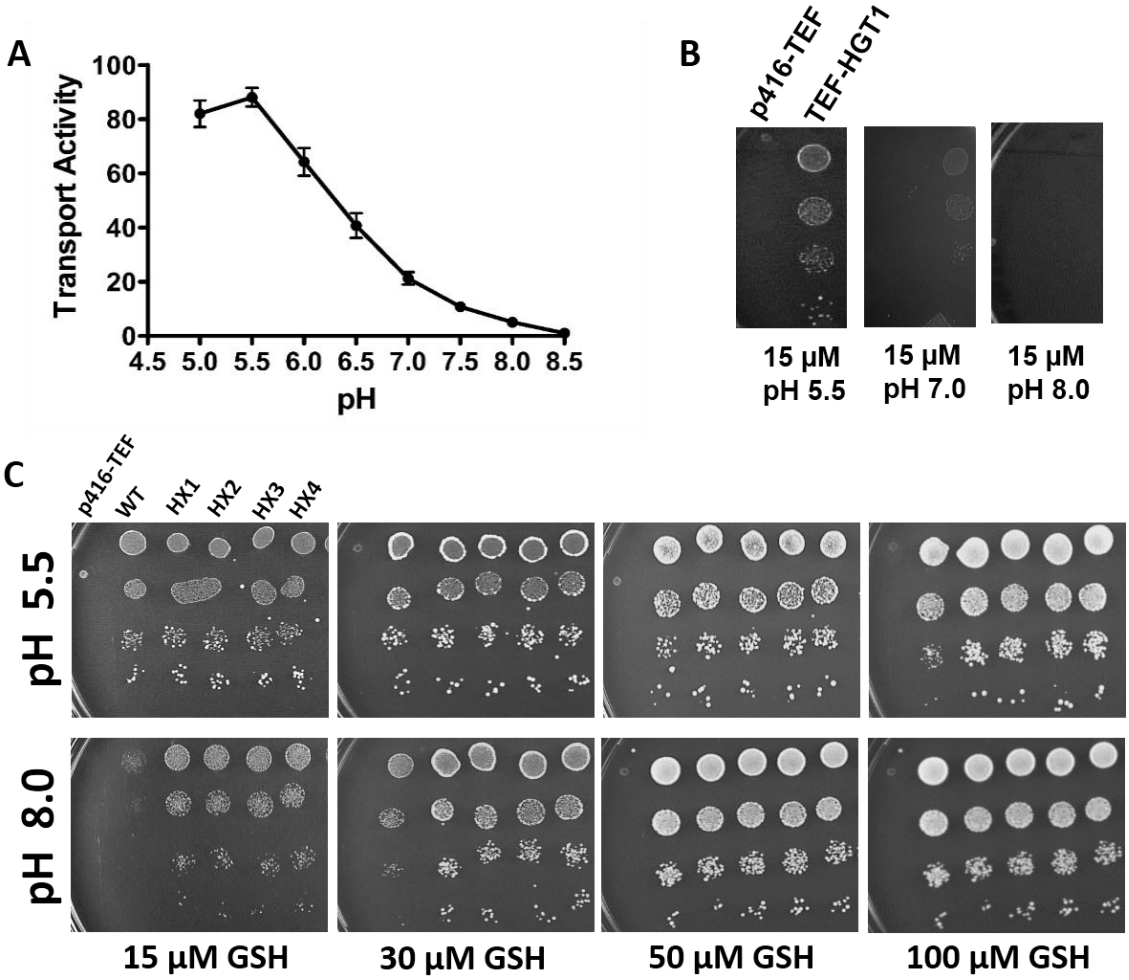

FIGURE 5.1A: pH dependence of [^{35}S] GSH uptake by Hgt1p: Initial rate of glutathione uptake was measured at different pH in ABC 817 (*met15*Δ*hgt1*Δ) strain, transformed with TEF-HGT1. The different pH were maintained using 20 mM MES/KOH (pH 5.0, 5.5 and 6.0) and 20 mM HEPES/KOH (pH 6.5, 7.0, 7.5, 8.0 and 8.5). In each case buffer contained 0.5 mM CaCl2, 0.25 mM MgCl2 and 2% glucose. **B) Functional analysis of Hgt1p on different pH plates:** Growth of ABC 817 transformed with empty vector or WT-HGT1 under TEF promoter on minimal media of different pH containing 15µM GSH. **C) Functional characterization of randomly mutagenized HGT1 showing pH independent growth phenotype:** ABC 817 yeast strain was transformed with empty vector, TEF-HGT1 or *in vitro* randomly mutagenized TEF-HGT1 plasmid (HX1-4, selected from mutagenesis screen showing pH independent growth phenotype on 15 µM GSH conc.). Transformants were subjected to pH based plate assay where dilution spotting on minimal media containing 200 µM methionine or different concentrations of glutathione at pH 5.5 and pH 8.0. The photographs were taken after 2-3 days of incubation at 30°C. All the above experiments were repeated with three independent transformations.

μM GSH at pH 5.5 and pH 8.0 (data no shown). This allowed us to identify two mutant residues, E135A (TMD2) and N710A (TMD12) that showed a better growth at pH 8.0 as compared to WT.

Although a screen of the 269 TMD mutant residues yielded 2 candidate residues, the search was restricted to the predicted TMDs (and also limited to Ala mutations). To enlarge the scope of the screen beyond the TMDs, we carried out a random mutational search to identify any other residues that might also lead to a pH independent growth phenotype. We performed *in vitro* hydroxylamine based random mutagenesis of the TEF- HGT1 plasmid and after transformation of the mutated plasmid in ABC 817 strain, we selected for mutants that were capable of growing on 15 μM GSH at pH 8.0 (Fig 5.1C). In the initial mutant search, only one mutant (HX1) was obtained. The plasmid was sequenced, and the *HGT1* gene was found to contain two mutations, E135K/D157N. The mutations were separated out, and it was found that only E135K was growing at pH 8.0, whereas D157N mutant failed to survive, suggesting that the E135K alone was responsible for the pH-dependent transport by Hgt1p. As the mutant hunt had revealed one mutant and did not appear to be saturated, we repeated the mutant isolation. Three independent mutants (HX2-4) were additionally identified. Interestingly all these 3 new mutants carried the E135K mutation. Thus the random mutagenesis screen did not reveal any new residues.

5.2. Analysis of pH-independence of E135 and N710 mutants:

At pH 5.5 the WT, TEF-HGT1 complements growth at low GSH concentrations and shows toxicity at higher glutathione concentrations (≥50 μM), due to excess accumulation of glutathione (also discussed in chapter4). However, at pH 8.0, WT-HGT1 do not grow at low GSH levels and starts growing at ≥50 μM GSH. To further elucidate the role of E135 and N710 residues, these residues were mutated to amino acids having different properties and transformed in ABC 817 yeast strain. Growth of the mutants were compared with WT-HGT1 at pH 5.5 and pH 8.0 followed by comparative [^{35}S] GSH uptake.

We first evaluated the behaviour of E135 mutants. Mutation of Glu to a similarly charged Asp (E135D), retains the carboxylate group at this position (Fig 5.2A). This mutant was found to behave like WT at pH 5.5 and pH 8.0. Substitution to Trp (E135W), led to a moderate defect in transport at pH 5.5 *i.e.* growth at low GSH

concentrations and no toxicity at higher GSH levels. However a complete loss of activity was observed for this mutant at pH 8.0 for all tested concentrations (15-200 µM GSH) suggesting that a large hydrophobic side chain was not tolerated for pH independent growth. In contrast, the mutants E135K, E135Q, E135N, E135S, E135A, E135G and E135H retained significant growth at low GSH concentrations at pH 8.0 but they showed a moderate defect at pH 5.5. These mutants were further analysed by biochemical uptake of [^{35}S] glutathione at the two different pH (Fig 5.2B). At pH 5.5, E135D mutant showed uptake comparable to WT. However, all the other mutants showed a reduced transport with E135W mutant showing the lowest transport activity. E135Q and E135N retained more than 50% activity, whereas E135A, E135K, E135H, E135G, E135S, E135W showed transport ranging from 30-50 % as compared to WT protein. However, at pH 8.0, WT-HGT1, E135D and E135W showed a drastic reduction in uptake. While a reduction was also seen the other mutants as well but with respect to WT (5 nanomoles/mg/min) they showed higher transport (10-13 nanomoles/mg/min) with E135Q and E135N showing the highest transport rate. Thus, in addition to the original E135, only E135D showed a lack of growth at 15 µM GSH, pH 8.0 suggesting the importance of an acidic residue at this position.

In the case of N710 residue, having a polar uncharged side chain when replaced with a charged residue, N710R and N710K led to a failure to grow at any GSH conc. at pH 8.0 (Fig 5.2C), and also very negligible uptake at pH5.5 suggesting that these charged residues were not tolerated well. Only N710S along with N710A showed an ability to grow at pH8.0. These results were also reflected in the radioactive glutathione uptake (Fig 5.2D). At pH 5.5, N710A and N710G showed similar uptake as compared to WT whereas N710E, N710K, N710H, N710R showed lesser uptake. However at pH 8.0, only N710S showed a better uptake suggesting that mutation to Ser was leading to pH independent uptake by Hgt1p.

Since E135 and N710 mutants demonstrated a similar ability to grow at pH 8.0, we attempted to determine if the two residues were interacting with each other or not. We created a double mutant, E135A N710A. However, this double mutant did not show an increase in the phenotype suggesting that the residues were probably functioning in the same pathway, or else were interacting (Fig 5.2E). To examine the latter possibility we carried out a residue swap where the E135 was changed to N and the N710 was changed to E. Though the double mutant was functional at pH 5.5, the

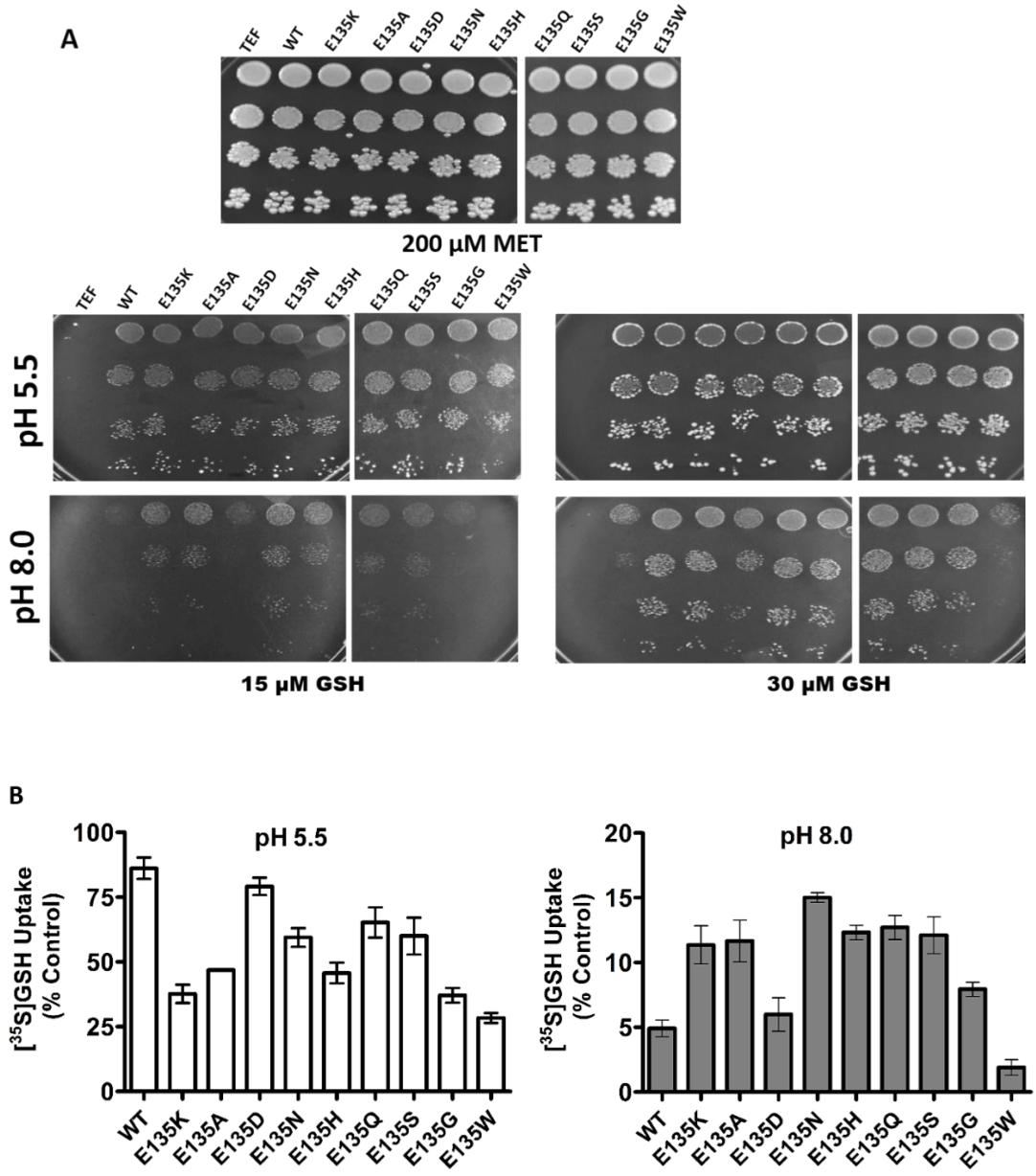

FIGURE 5.2A: Analysis of pH dependence of E135 mutants: ABC 817 yeast strain was transformed with empty vector, TEF-HGT1 or different E135 mutants. Transformants were subjected to pH based plate dilution spotting on minimal media containing 200 µM methionine, 15 or 30 µM GSH concentrations at pH 5.5 and pH 8.0. The photographs were taken after 2-3 days of incubation at 30°C. **B)** For quantification of the functional activity of the mutants, the initial rate of [^{35}S] GSH uptake was measured at pH 5.5 and pH 8.0. The results were normalized to the rate of uptake measured for the WT Hgt1p and represented as mean ± SD. The experiments were repeated with three independent transformations.

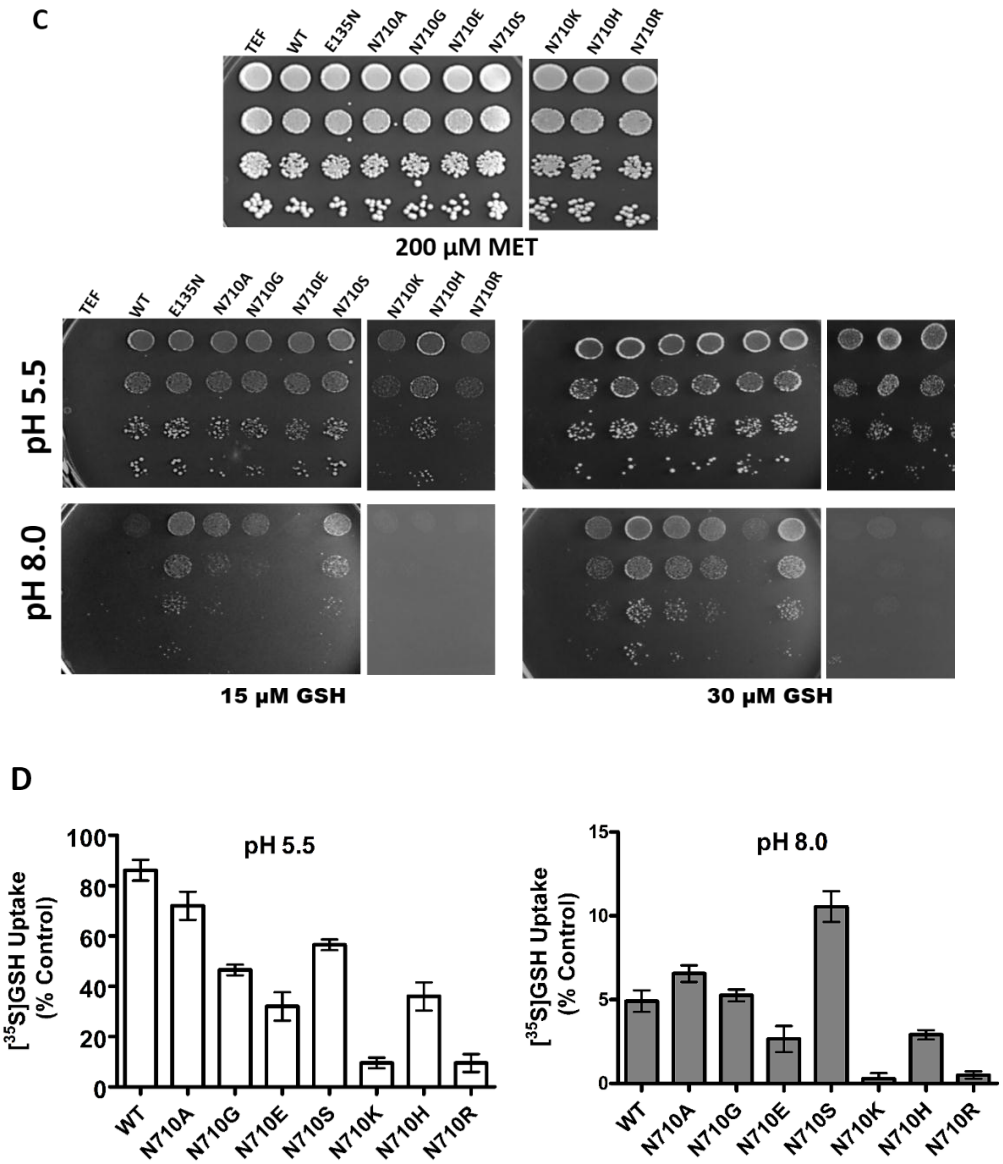

FIGURE 5.2C: Analysis of pH dependence of N710 mutants: ABC 817 yeast strain was transformed with empty vector, TEF-HGT1 or different N710 mutants. Transformants were subjected to pH based plate dilution spotting on minimal media containing 200 µM methionine, 15 or 30 µM GSH concentrations at pH 5.5 and pH 8.0. The photographs were taken after 2-3 days of incubation at 30°C. **D)** For quantification of the functional activity of the mutants, the initial rate of [^{35}S] GSH uptake was measured at pH 5.5 and pH 8.0. The results were normalized to the rate of uptake measured for the WT Hgt1p and represented as mean ± SD. The experiments were repeated with three independent transformations.

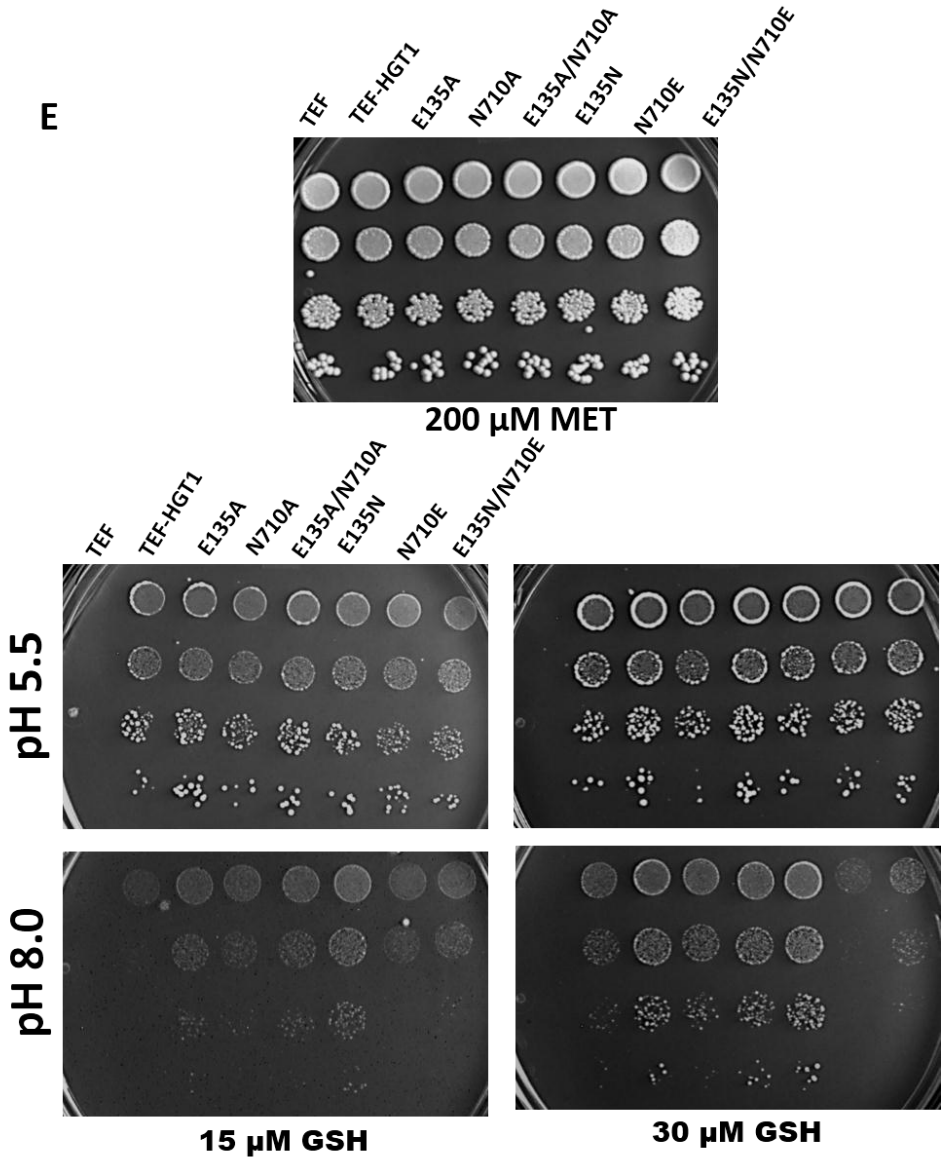

FIGURE 5.2E: Analysis of pH dependence of E135A/N710A and E135N/N710E double mutants: ABC 817 yeast strain was transformed with empty vector, TEF-HGT1 or different single and double mutants. Transformants were subjected to pH based, plate dilution spotting on minimal media containing 200 µM methionine, 15 or 30 µM GSH concentrations at pH 5.5 and pH 8.0. The photographs were taken after 2-3 days of incubation at 30°C. The experiments were repeated with three independent transformations.

swapped mutant did not show growth at pH 8.0 suggesting a possible interaction between the two residues. However the single N710E also showed no growth phenotype at higher pH contradicting the interaction between the two residues.

5.3. Kinetic characterization of E135 and N710 mutants at pH 5.5 and pH 8.0:

To further analyse these mutants, uptake kinetics for [^{35}S] GSH was determined at pH 5.5 and pH 8.0 over a range of concentrations (12.5-800 μM) in cells transformed with empty vector, or vector expressing WT-HGT1, E135 (E135A and E135N) or N710 (N710A and N710S) mutants (Fig. 5.3A). All the mutants showed protein expression levels similar to WT and mutant proteins were localized properly on the membrane.

At pH 5.5 the apparent *Km* of WT-HGT1 for GSH was estimated to be 27.8 ± 1.2 μM and the *Vmax* was found to be 57.0 ± 0.8 nmol of glutathione.mg of protein^{-1}.min^{-1} (Table 5.1). The *Km* values for E135A (28.4 ± 2.3 μM) and E135N (28.7 ± 1.9 μM) were found to be similar to WT-HGT1 suggesting that the mutation did not affect substrate binding. However, the *Vmax* for E135A (40.0 ± 3.8 nmol of glutathione.mg of protein^{-1}.min^{-1}) and E135N (45.5 ± 2.1 nmol of glutathione.mg of protein^{-1}.min^{-1}) decreased in both the mutants suggesting that the moderate defect as seen in plate-based assay is due to a slight defect in carrier translocation step. At pH 8.0, *Vmax* for WT was found to be 9.0 ± 3.3 nmol of glutathione.mg of protein^{-1}.min^{-1} suggesting six-fold decrease in translocation rate as compared to pH 5.5. However, for E135A and E135N, at pH 8.0, *Vmax* only decreased by three folds (Table 5.1). Hence, as the pH was increased from 5.5 to 8.0, there was a decrease in the translocation rate for both the WT and E135 mutants. However, the decrease was less than that observed for WT-Hgt1p suggesting that the E135 mutants are not completely independent of pH, but retain some pH sensitivity.

On the other hand, both N710A and N710S showed an increase in substrate affinity (*Km* = 24.6 ± 3.6 and 22.5 ± 3.8 μM) at pH 5.5 and only a slight defect in *Vmax* (47.7 ± 5.1 and 43.8 ± 4.9 nmol of glutathione.mg of protein^{-1}.min^{-1}) (Table 5.1). Whereas at pH 8.0, N710A mutant was found to have similar *Vmax* as compared to WT Hgt1p but with a lower *Km* (227.2 ± 67.8 μM). However, in the case of N710S mutant, *Km* further decreased to 154.8 ± 49.3 μM and *Vmax* increased to 15.4 ± 1.1

nmol of glutathione.mg of protein^{-1}.min^{-1} suggesting a better translocation rate as compared to WT.

5.4. Glutathione transport by E135N and N710S mutant does not lead to defect in cytosolic acidification:

Hgt1p is a proton-dependent symporter where GSH transport by Hgt1p will result in acidification of the cytosol. A proton independent transport, on the other hand, will not change the intracellular pH. Since E135N and N710S showed a loss in pH sensitivity of the transporter, it is possible that they may be directly or indirectly affecting proton-dependent glutathione uptake by Hgt1p. To check the possibility of the mutants for involvement in proton-dependent transport, we used yeast cells expressing ratiometric pHluorin in the cytosol (Maresova *et al.* 2010; Chan *et al.* 2012). The dual excitation wavelength of 405 and 485 nm represents an opposite pH-dependent fluorescence response despite both emitting at 508 nm. As the pH decreases, the fluorescence intensity decreases at 405 nm excitation and increases at 485 nm. Therefore a reduction in the excitation ratio of 405/485 nm represents acidification of the cytosol. We transformed yeast cells expressing pHluorin with empty vector and vectors overexpressing WT Hgt1p or the mutants (E135N and N710S) independently and measured the change in the fluorescence ratio in response to GSH transport for 27 min (Fig 5.4). For yeast cells having an empty vector, there was a negligible change in the fluorescence ratio (≈ 0.1) on glutathione addition suggesting no change in pH inside the cell. For WT Hgt1p there was a drastic decrease in the ratio from 1.78 to 1.22 after 12 min of GSH addition to the cells suggesting rapid acidification of the cytosol in response to GSH transport after which the ratio starts recovering. However, the mutants E135N and N710S showing pH independent growth showed a similar decrease in the ratio upon GSH addition suggesting acidification of the cytosol in response to GSH transport. Hence these mutants show proton-dependent GSH transport.

5.5. Evaluation of conserved charged residues for their role in proton translocation.

Although the mutants E135N and N710S led to pH independent growth, they were not defective in cellular acidification during glutathione transport. This suggests that they are not defective in proton uptake. We, therefore, decided to embark on an

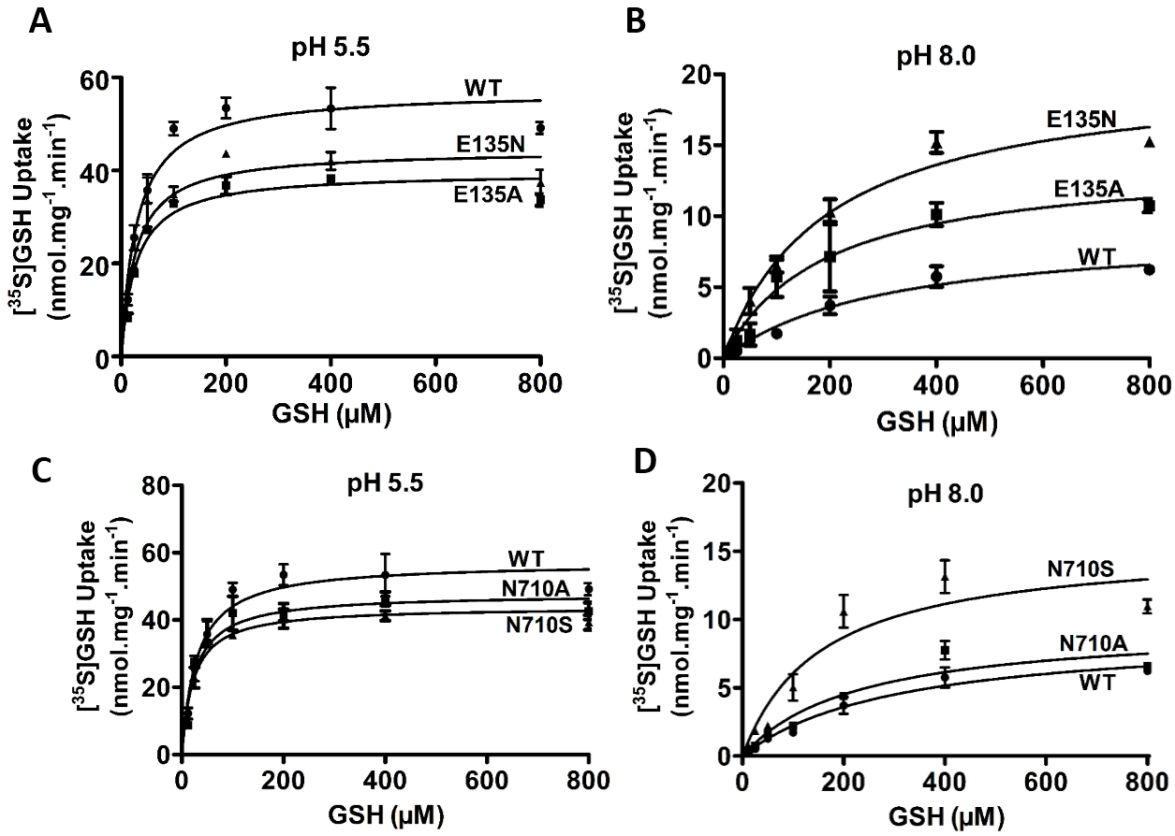

FIGURE 5.3A: Kinetic analysis of [^{35}S] GSH uptake for WT-HGT1 and mutants at pH 5.5 and pH 8.0: The initial rate of [^{35}S] glutathione uptake were measured in ABC 817 transformed with empty vector, TEF-HGT1 or different mutants (E135, E135N, N710A and N710S) under TEF promoter at glutathione concentrations ranging from 12.5 to 800 µM at 1 min and 3 min time intervals. After subtracting the initial rates of glutathione uptake in WT-HGT1 and mutants from empty vector, Michaelis-Menten curve was drawn using GraphPad Prism 5.0 software. The data shown are the mean of values ± SD of the initial rate of uptake at each glutathione concentration, obtained in three different experiments.

Table 5.1: Kinetic characterization WT-HGT1 and E135A, E135N, N710A and N710S mutants at pH 5.5 and pH 8.0. *Km* (µM) and *Vmax* (nmol of glutathione. mg of protein^{-1} .min^{-1}):

	pH 5.5		pH 8.0	
Mutants	***Km***	***Vmax***	***Km* (µM)**	***Vmax***
WT	27.8 ± 1.2	57.0 ± 0.8	305.6 ± 60.1	9.0 ± 3.3
E135A	28.4 ± 2.3	40.0 ± 3.8	189.6 ± 54.3	13.9 ± 2.5
E135N	28.7 ± 1.9	45.5 ± 2.1	194.8 ± 38.7	20.4 ± 3.4
N710A	24.6 ± 3.6	47.7 ± 5.1	227.4 ± 67.8	9.6 ± 3.4
N710S	22.5 ± 3.8	43.8 ± 4.9	154.8 ± 49.3	15.4 ± 1.1

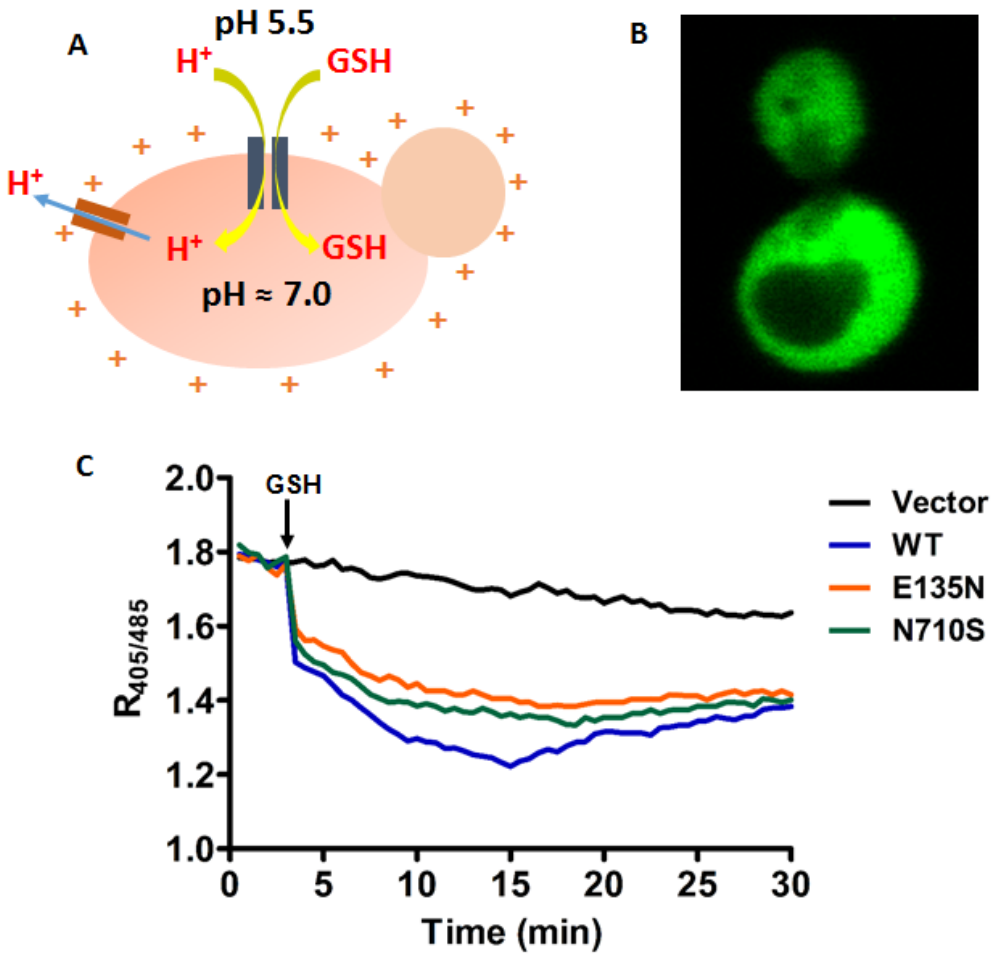

FIGURE 5.4A) Diagrammatic representation of proton coupled transport by Hgt1p in a yeast cell: Yeast cell is shown in pink color and Hgt1p is represented as blue bars. Plasma membrane proton efflux pump are represented as brown bar. **B) Fluorescence image of ABC 817 strain expressing phluorin in the cytosol. C) Cytosolic acidification measurement using pHluorin:** The yeast ABC 817 strain expressing pHluorin were transformed with empty vector, WT or HGT1 mutant (E135N or N710S) plasmid. Cells were harvested, washed and finally resuspended (3.5 OD_{600}/ml) into resuspension buffer. After a 10 min incubation at 30 °C, cell resuspension was transferred to cuvettes and fluorescence intensity was monitored for 30 min using FluoroMax 4 spectrofluorometer (Horiba Jobin Yvon Inc.) at 508 nm with excitation at 405 nm and 485 nm every 30 sec at 30 °C with constant stirring (1mM GSH was added after 3 min). Background signals (cells without pHluorin) were subtracted and the ratio of ex 405/ ex485 was calculated and plotted vs. time (min) using GraphPad Prism 5 software. The experiment was repeated thrice and the figure represents best of the data.

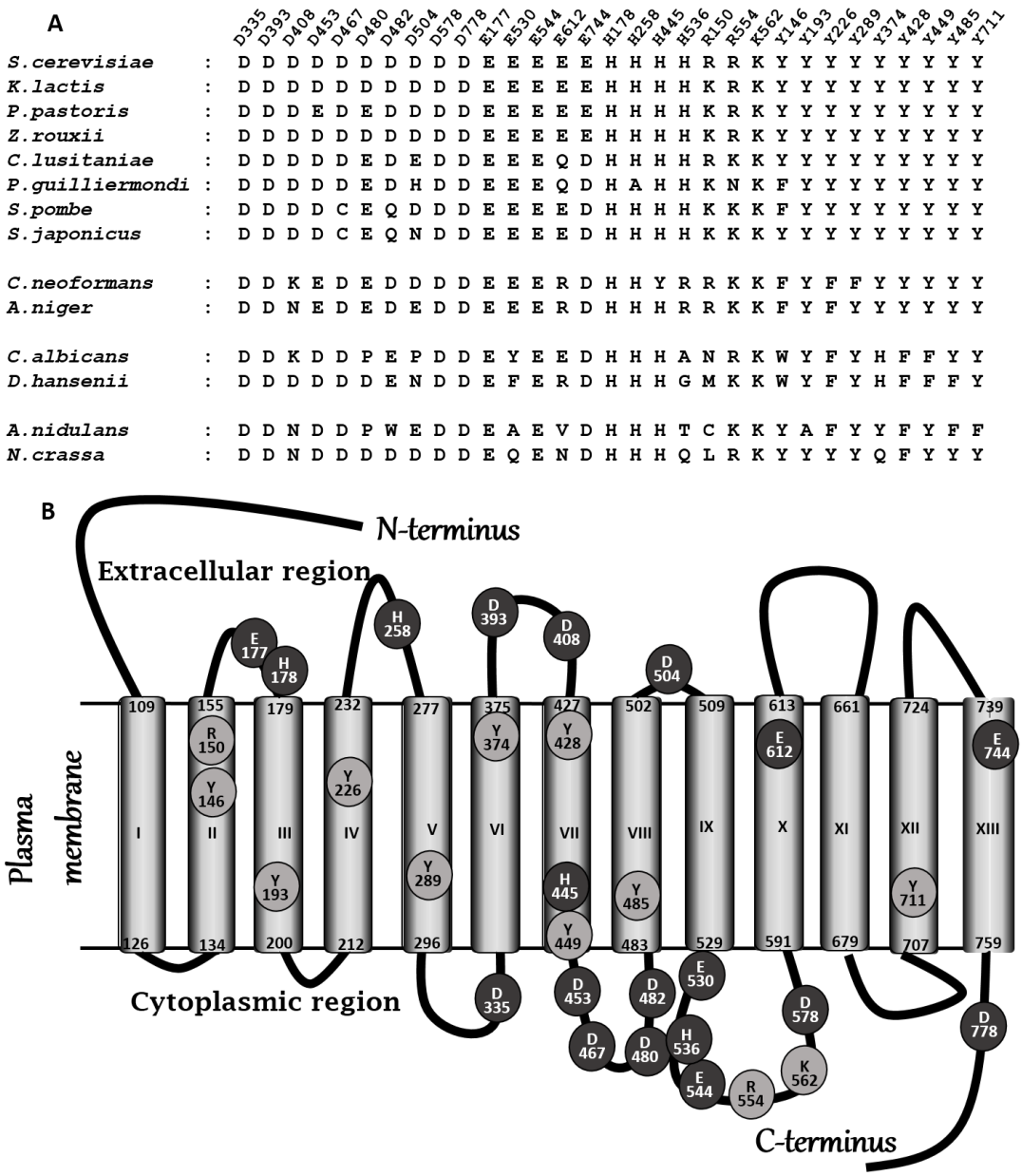

FIGURE 5.5A: Multiple sequence alignment of the protein sequence of Hgt1p with known PT members of the OPT family: Multiple sequence alignment of Hgt1p with known glutathione transporters of the PT clade of the OPT family. Sequences were retrieved from *Entrez* at NCBI website and aligned using MUSCLE program using default parameters. The sequence alignment has been edited to show only strictly or partially conserved Asp (D), Glu (E), His (H) that are present in the predicted TMDs or loops of Hgt1p (dark grey circles in Fig. 5B) and. Arg (R), Lys (K) and Tyr (Y) present in the predicted TMDs (light grey circles in Fig. 5B) **B) Pictorial presentation of putative topology showing TMDs and the residues targeted for mutagenesis.** The 13 predicted TMDs are represented as rectangular bars and the identity and location of amino acid residues targeted for mutagenesis are shown as residue with number in circles.

additional screening approach where, in this case, we would target the conserved charged residues (Glu, Asp, His, Lys and Arg) and evaluate them for growth and proton uptake. Owing to the large number of such residues in Hgt1p (which is a large protein of 799 amino acid residues), and the difficulty in subjecting all to mutational analysis, the search was limited by two criteria's. For Asp/Glu/His both strictly/ partially conserved residues and residues that changed to other protonable residues across species in the PT clade of the OPT family and are present in the predicted TMDs or interconnecting loops (ICLs) were included (Fig 5.5A). In addition the less favored conserved/ partially conserved Arg/Lys/Tyr present in the predicted TMDs were included. This represents a total of 31 residues to be explored for their involvement in proton binding, or transport, as shown in 2D, predicted topology model of Hgt1p (Fig 5.5B)

Among 31 residues selected, 17 TMD residues were already mutated to alanine and studied for effect on glutathione transport in the previous chapter (chapter 4), but the probability of their involvement in proton transport was never explored. The remaining 14 were therefore mutated to alanine, and all the 31 residues were functionally evaluated using "Duel complementation-cum toxicity" assay as described in section 2.13, chapter 2. Based on this assay majority of the mutants (D335A, D408A, D467A, D504A, D578A, E177A, E530A, E544A, E744A, R554A, K562A, Y193A, Y226A, Y289A Y374A, Y449A and Y485A) were found to be severely defective in glutathione transport (Fig 5.5C). Of these severely defective, Y289A and Y485A did no show a constant phenotype. Further to confirm the functionality of the mutants, we measured the initial rate of [^{35}S] GSH uptake in *met15Δ hgt1Δ* yeast strain transformed with WT or different alanine mutants of Hgt1p and found that the genetic plate based assay was clearly reflected in the uptake assay (Fig 5.5D). The initial rate of [^{35}S] GSH uptake ranged from 0.1–18% as compared to WT in severely defective mutants, 22-40 % in moderately defective mutants and 50–75 % in minor defective mutants.

Since a defect in proton translocation will severely impede glutathione transport by Hgt1p, only severely and moderately defective mutants showing less than 40% transport comprising of 19 mutants were studied further.

5.6. Analysis of protein expression levels and cell surface trafficking of mutants:

The decreased transport activity of the HGT1 mutants as observed in the plate-based growth assay or comparative uptake assay can be due to either decreased protein expression levels, a defect in trafficking to the plasma membrane or due to loss of the activity of the protein. As shown in the previous chapter, expression and localization studies of mutants Y193A, Y226A, Y374A, H445A, Y449A, E544A, R554A, K562A, and E744A suggested that except Y449A, K562A, and E744A all other mutants are properly expressed and localized to the plasma membrane. Hence these mutants were not evaluated for expression and localization studies.

Steady state protein expression analysis of remaining 10 mutants revealed that the majority of Hgt1p mutants (D335A, D482A, D578A, D778A, E177A, E530A and H258A) expressed protein ranging from 70-100 % as compared to WT. Thus suggesting that the mutation did not perturb the expression and stability of the protein (Fig 5.6A). In contrast, mutants D408A, D467A, and D504A showed a significant fall (15–40 %) in protein expression levels accounting for low transport levels in these mutants. The seven mutants expressing significant levels of protein were further analyzed for a defect in trafficking and localization if any by indirect immunofluorescence. A very bright fluorescence signal at the cellular periphery was observed for all the mutants similar to WT Hgt1p suggesting that these mutants are correctly localized on the plasma membrane (Fig 5.6B)

5.7. Cytosolic acidification monitoring by pHluorin based assay:

In the case of mutants D408A, D482A, E530A, E544A, D578A, D778A, H258A and Y226A there was a significant change in the ratio although less than WT upon GSH addition suggesting co-transport of the protons with substrate (Fig 5.7). Interestingly for mutants D335A, H445A, and R554A almost no acidification of cytosol was observed similar to vector alone whereas Y374A showed a slight decrease in the ratio suggesting very weak acidification in response to GSH transport as compared to mutants showing similar levels of [^{35}S] GSH transport. Hence these mutants can be involved in substrate/proton coupling and were studied further. In contrast the mutants E177A, and Y193A which expressed well and localized properly on the plasma membrane also showed no acidification of the cytosol as the initial rate of [^{35}S] GSH uptake ranged between 1-3% as compared to WT transport.

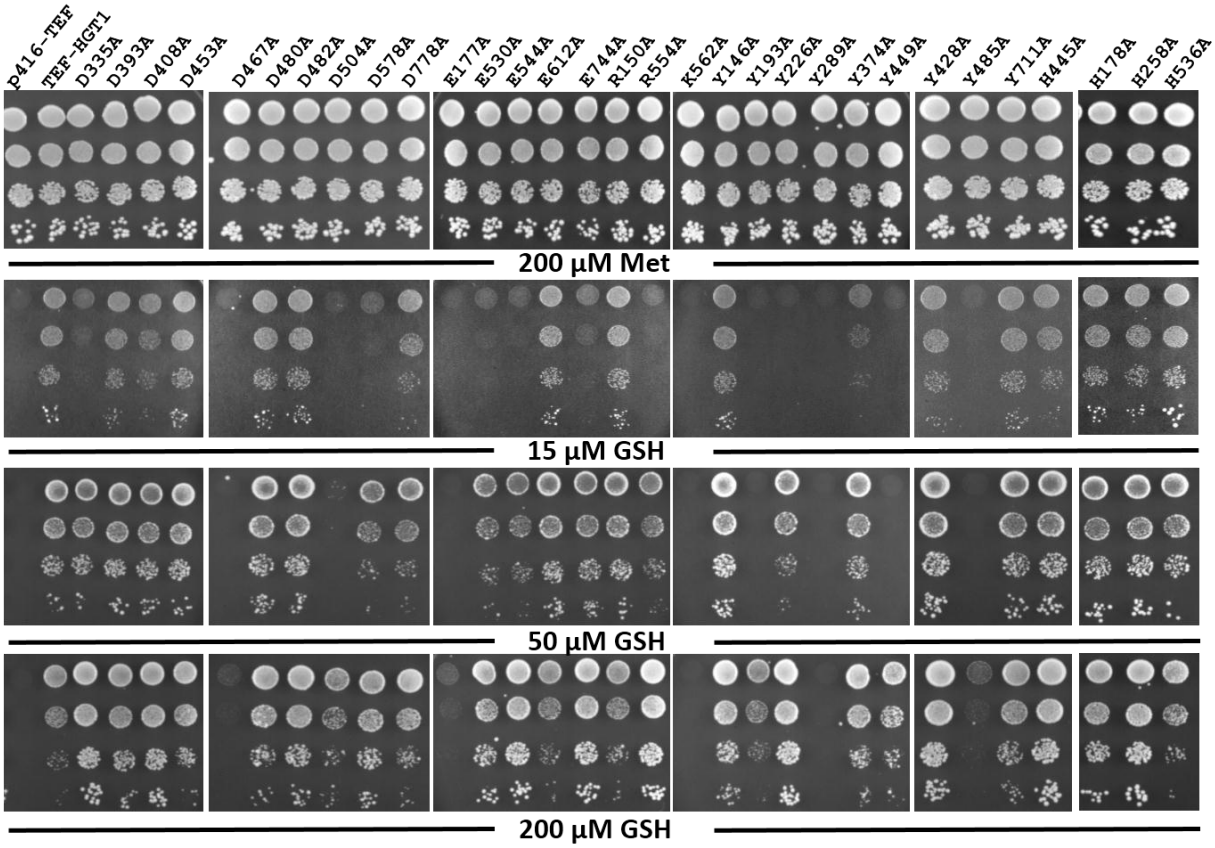

FIGURE 5.5C: Functional characterization of mutants based on plate based assay: Empty vector, WT and the different alanine mutants of Hgt1p under TEF promoter were transformed in ABC 817. Transformants were subjected to plate based "Dual complementation-cum-toxicity" assay (as described in chapter 2 section 2.13) by serial dilution spotting on minimal media containing different concentrations (15, 50, 200 µM) of GSH or 200 µM methionine (control). The photographs were taken after 2-3 days of incubation at 30°C. The experiments were repeated with three independent transformations.

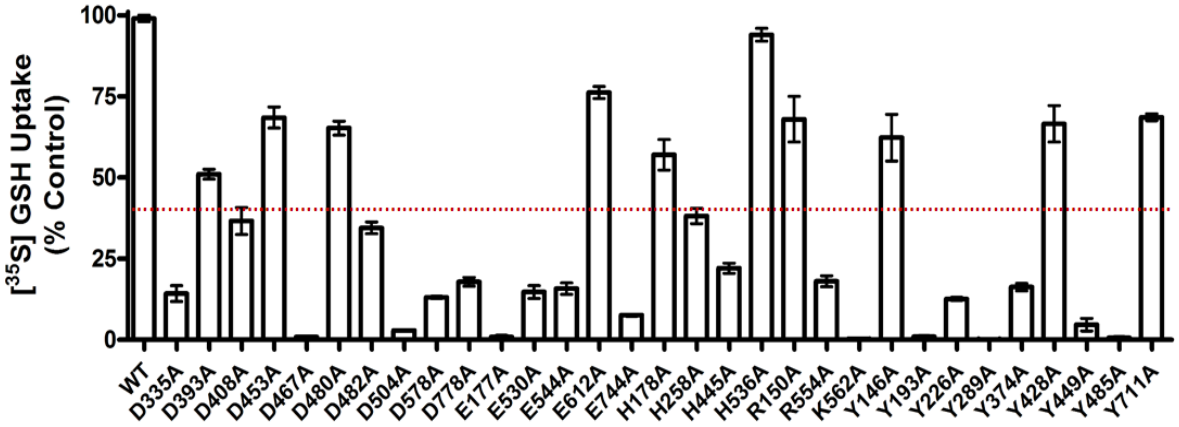

FIGURE 5.5D: Comparative uptake of [^{35}S] GSH by alanine mutants of Hgt1p: The initial rate of [^{35}S] GSH uptake was measured in ABC 817 transformed with empty vector, WT or different alanine mutants under TEF promoter at pH 5.5, 30 °C. The cells were harvested at 1 min and 3 min time intervals. After subtracting the initial rates of glutathione uptake in WT and mutants from empty vector, the results were normalized to the rate of uptake measured for the WT Hgt1p and plotted as % of WT-HGT1 transport. The dotted line represents 40% of the Y-axis. The experiments were repeated with three independent transformations.

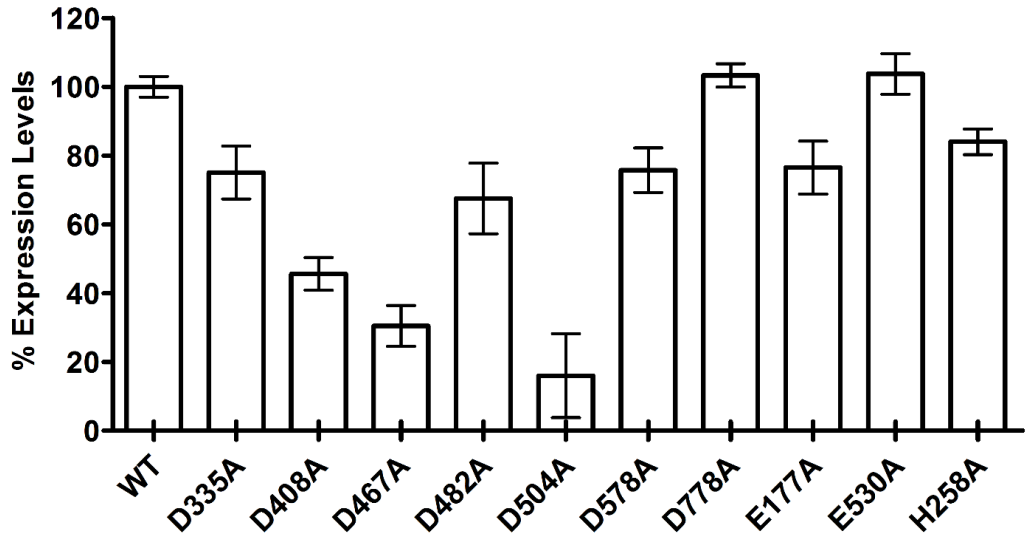

FIGURE 5.6A: Quantification of protein expression levels of the remaining severely or moderately defective mutants: Steady state protein expression levels were measured in ABC 817 yeast strain transformed with plasmids bearing WT or alanine mutants of HGT1 by immunoblotting. Equal amount of crude protein extracts were loaded onto SDS-PAGE gels, electroblotted to nitrocellulose membrane and probed with mouse anti-HA monoclonal antibody. Levels of protein were determined by densitometry analysis of unsaturated band signals. The data are expressed as the percentage protein expression compared with WT expression levels and are the mean ± SD of three independent experiments.

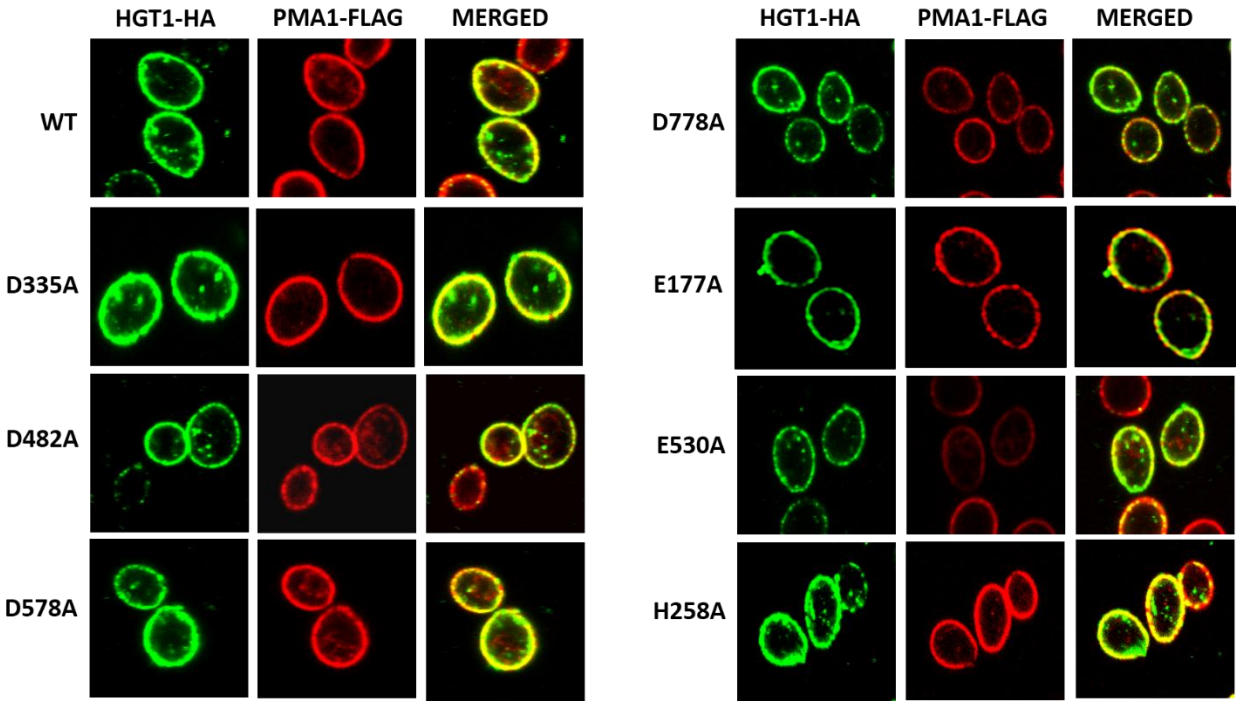

FIGURE 5.6B: Cell surface localization of mutants showing proper protein expression: BY4741 with PMA1 tagged with FLAG sequence at the C-terminus in the genome was transformed with plasmids bearing wild type (WT) or different alanine mutants of Hgt1p having a HA-tag at the C-terminus. The transformants were fixed, permeabilized and labelled by indirect immunofluorescence using rabbit anti-FLAG primary antibody and mouse anti-HA primary antibody followed by anti-rabbit IgG®647 and anti-mouse IgG Alexa® 488 conjugated secondary antibody and visualized using confocal microscopy, as described under "Chapter 2,section 2.18". PMA1 protein is a plasma membrane marker and localizes to the plasma membrane (red). For WT Hgt1p and the mutants a bright ring (green) at the cellular periphery was observed co-localizing (yellow) with the PMA1 suggesting proper localization on the plasma membrane. Experiment was repeated twice (n=4) using independent transformations and only fluorescence images have been shown.

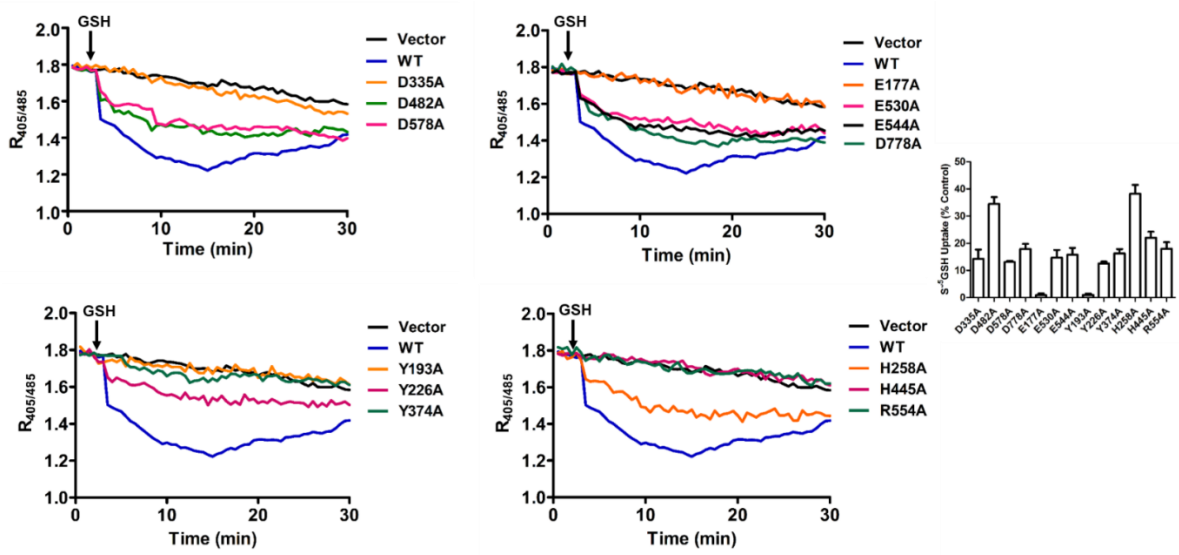

FIGURE 5.7: Cytosolic acidification monitoring of mutants using pHluorin: The yeast ABC 817 strain expressing pHluorin were transformed with WT or HGT1 mutant plasmid. The transformants were grown until they reached OD_{600} of 0.6-0.8. Cells were harvested, washed and finally resuspended (3.5 OD_{600}/ml) into resuspension buffer (20mM MES/KOH, 0.5mM CaCl2, 0.25mM MgCl2, 2% glucose pH 5.5). After a 10 min incubation at 30 °C, cell resuspension was transferred to cuvettes and fluorescence intensity was monitored for 30 min using FluoroMax 4 spectrofluorometer (Horiba Jobin Yvon Inc.) at 508 nm with excitation at 405 nm and 485 nm every 30 sec at 30 °C with constant stirring (1mM GSH was added after 3 min). Background signals (cells without pHluorin) were subtracted and the ratio of ex 405/ ex485 was calculated and plotted vs. time using GraphPad Prism 5 software. The experiment was repeated twice and the figure represents best of the data.

5.8. Effect of extracellular pH on transport mediated by mutants showing no acidification in response to GSH transport.

The mutants showing no acidification of the cytosol in response to GSH transport were further assessed for transport at different pH (5.0, 6.0, 7.0 and 8.0) (Fig 5.8). E177A and Y193A showed almost negligible amount of transport as compared to WT protein, at all the tested pH. Since all the residues tested in this study for their role in proton binding and transport is based on the conservation pattern in the PT clade, only E177 was conserved in the entire OPT family and present just outside predicted TMD3 (A179-A200) facing the extracellular side. Hence E177 is a strong candidate for being involved in the initial proton recognition/ substrate binding. In contrast, Y193A, also in TMD3 is predicted to be more towards the cytoplasmic side and hence cannot be the initial proton binding residue although they may be involved in its relay. Other mutants D335A, Y374A, H445A and R554A, showed pH dependent uptake similar to WT Hgt1p, although the transport rate was less in these mutants. This result suggests that the initial substrate binding is still proton-dependent, and these residues may come into force at latter stages of the proton translocation.

5.9. Saturation kinetics studies of mutants:

The analysis of protein expression levels and cell surface localization of the mutants (E177A, Y193A, D335A, Y374A, H445A and R554A) revealed that the mutations did not bear a significant effect on the protein expression or its cell surface localization. Further, these mutants showed no acidification of the cytosol in response to GSH transport suggesting a specific defect in proton-coupled glutathione uptake. To gain a better understanding of the possible roles of these residues in proton-coupled glutathione transport, we carried out the saturation kinetic analysis of the mutants by measuring the initial rates of [^{35}S] GSH uptake over a range of GSH concentrations (Fig 5.9). The apparent *Km* and *Vmax* of WT Hgt1p was estimated to be 27.8 ± 1.2 µM and 57 ± 0.8 nmol of glutathione.mg of protein^{-1}.min^{-1}. The kinetic characterization of other mutants revealed interesting insights into the role of these residues in the functional activity of the transporter (Table 5.2). The *Km* for D335A and H445A did not change significantly as compared to WT, but there was a decrease in *Vmax*. The corrected *Vmax* values (adjusted to protein expression levels) for D335A was found to be 12.6 ± 0.3 and for H445A was 25.2 ± 0.7 suggesting that the

mutation did not affect the substrate binding but a marked decrease (2-5 fold) in the carrier translocation rate. Y374A displayed an approximately two-fold increase in *Km* (55.0 ± 5.2) value and a four-fold reduction in *Vmax* (12.9 ± 1.2) suggesting its possible role in both substrate binding and controlling the translocation rate (Chapter 4). Further Kinetic analysis of R554A showed a drastic six-fold increase in *Km* (193.7 ± 43.7) value and a two-fold reduction in *Vmax* (23.9 ± 2.5) value. The decreased *Vmax* values obtained for these residues, which could not be attributed to the decreased protein levels for the mutants, suggest that these residues might play some critical role in the proton transport or conformational changes associated with translocation of the substrate by the protein.

5.10. Mapping of residues important for proton coupled transport in the *ab initio* Hgt1p model:

In the previous chapter an *ab initio* model of Hgt1p was developed for the TMDs based on the mutagenesis data of the all the thirteen predicted TMDs. This model suggested TMD3, TMD4, TMD5, TMD6, TMD7, TMD9 and TMD13 as the pore lining helices. We mapped the residues that are probably important for proton dependent transport by Hgt1p, on this model and found that the residues, Y193 (TMD3), Y374 (TMD6) and H445 (TMD7) were present in the predicted TMDs that were suggested to line the translocation pathway (Fig 5.10). The side chain of Y374 was found to be facing the transmembrane pore whereas for Y193 and H445, the side chains were found to be facing away from the translocation channel. In addition the residues D335 and R554 were present in the cytosolic loops connecting the TMDs and E177 is present in the extracellular loop, located just outside the predicted TMD3. In contrast the residues E135 (TMD2) and N710 (TMD12) which were found to be important for pH sensitivity and not for proton transport where found to present away from the translocation channel.

5.11. Discussion

Since Hgt1p transports glutathione using the inwardly directed proton gradient, identification of the residues that bind and translocate protons is crucial for the understanding of how Hgt1p actively transports glutathione. Here, we have taken multiple approaches to identify these residues.

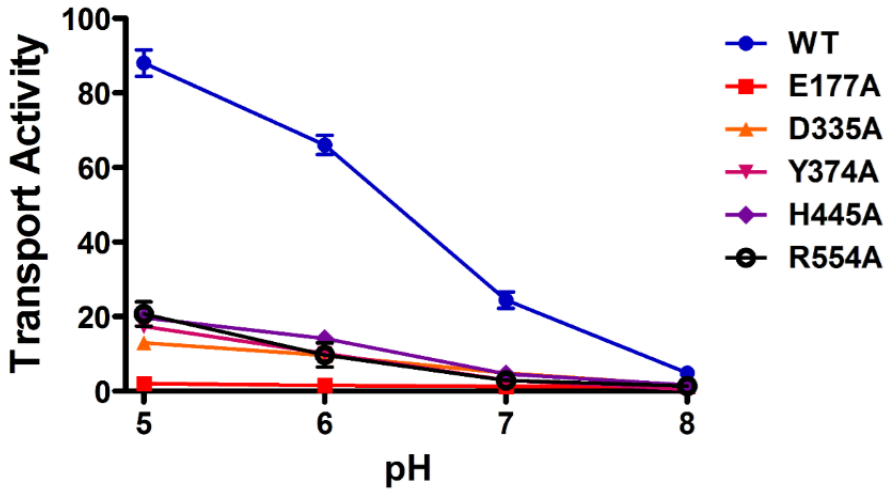

FIGURE 5.8: pH dependence of [^{35}S] GSH uptake by Hgt1p and mutants showing no cytosolic acidification in response to GSH transport: Initial rates of [^{35}S] glutathione uptake was measured at different pH in ABC 817 transformed with TEF-HGT1 and mutants (E177A, D335A, Y374A, H445A and R554A) showing no cytosolic acidification in response to GSH transport at different pH. The pH was maintained using 20 mM MES/KOH (pH 5.0 and 6.0) or 20 mM HEPES/KOH (pH 7.0 and 8.0). In each case buffer contained 0.5 mM CaCl2, 0.25 mM MgCl2 and 2% glucose. The data represents the mean ± SD of three independent experiments.

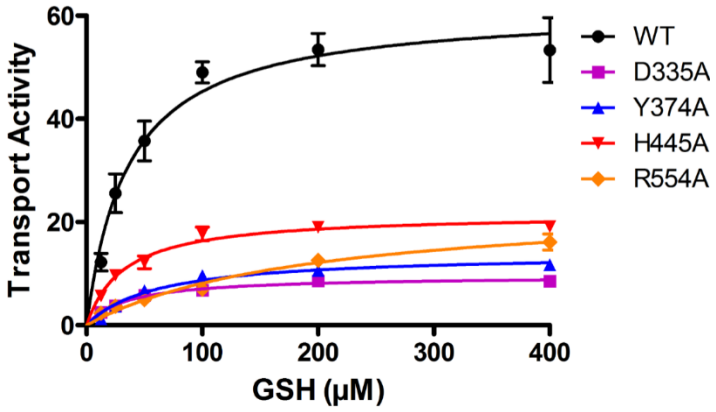

FIGURE 5.9: Kinetic analysis of [^{35}S] GSH uptake for WT-HGT1 and mutants showing no cytosolic acidification in response to GSH transport: The initial rate of glutathione uptake were measured in ABC 817 yeast strain transformed with empty vector, WT or different mutants (D335A, Y374A, H445A and R554A) of Hgt1p under TEF promoter at glutathione concentrations ranging from 12.5 to 400 µM at 1 min and 3 min time intervals. After subtracting the initial rates of glutathione uptake in WT-HGT1 and mutants from empty vector, Michaelis-Menten curve was drawn using GraphPad Prism 5.0 software. The data shown are the mean of values ± SD of the initial rate of uptake at each glutathione concentration, obtained in three different experiments.

Table 5.2: Kinetic characterization WT-HGT1 and mutants showing no cytosolic acidification in response to GSH transport. *Km* (µM) and *Vmax* (nmol of glutathione. mg of protein^{-1} .min^{-1}). *Vmax* was corrected to the protein expression levels:

Mutants	Km	Corrected Vmax
WT	27.8 ± 1.2	57.0 ± 0.8
D335A (IC5)	30.6 ± 4.1	12.6 ± 0.3
Y374A (TMD6)	55.0 ± 5.2	12.9 ± 1.2
H445A (TMD7)	29.3 ± 4.3	25.2 ± 0.7
R554A (IC9)	193.7 ± 43.7	23.9 ± 2.5

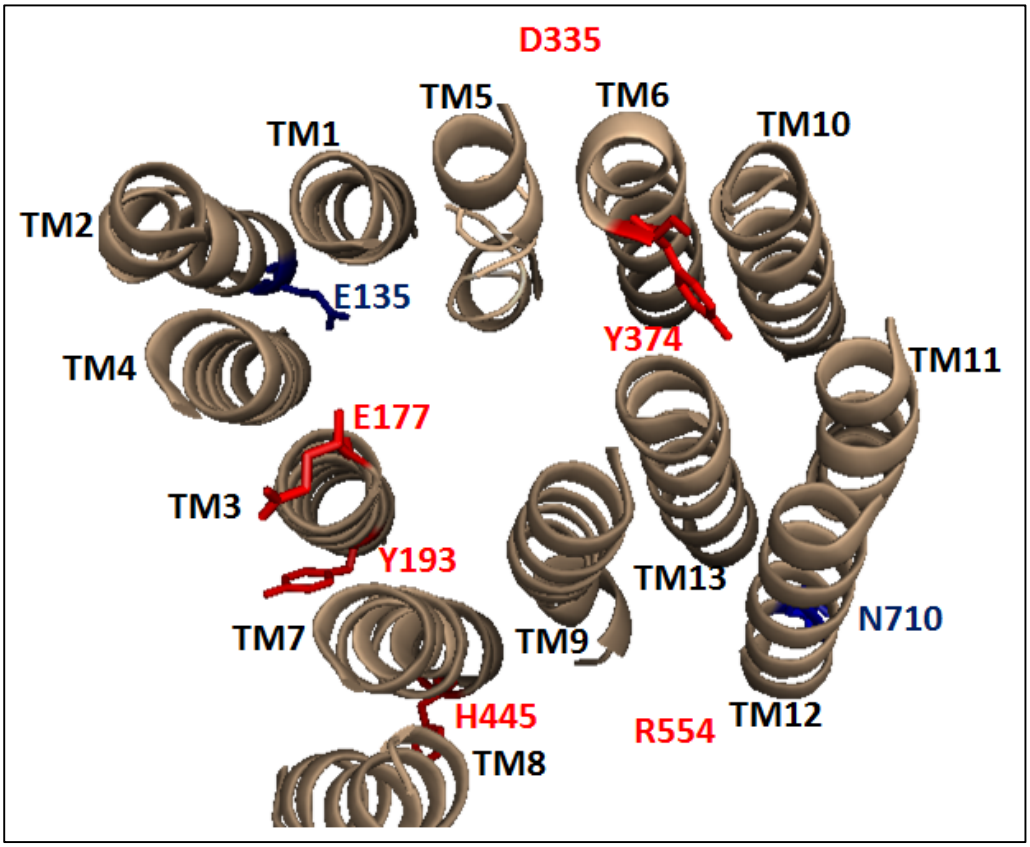

FIGURE 5.10: Mapping of residues important for proton coupled transport in the *ab initio* Hgt1p model: Periplasmic view of the Hgt1p *ab initio* model where **t**he TMD helices are numbered 1-13 and specific amino acid side chains are highlighted and labelled. Residues found to be important for proton binding are coloured in red while residues important for pH sensitive transport are highlighted in blue. For clarity, the loops connecting the TMDs are omitted and the important residues in the loops (D335 and R554) are depicted as single letter amino acid code followed by residue number with arbitrary location. Structure in this figure was generated using PyMol.

We first evaluated all alanine mutants of 13 predicted TMDs comprising of 269 mutants of Hgt1p to isolate functional mutants which were able to grow a pH 8.0. Using this screen, we identified E135A and N710A to be important for pH-dependent transport. Since this screen was restricted to TMDs and to alanine mutants, we then performed hydroxylamine based *in vitro* random mutagenesis on this transporter which also identified E135 position to be important for pH-dependent transport by Hgt1p. Biochemical characterization of these mutants showed increased uptake of glutathione at higher pH as compared to the WT Hgt1p, but the transport was not completely pH independent. Further to check for the possibility of the mutants for involvement in proton dependent transport, we used yeast cells expressing pHluorin in the cytosol to check cellular acidification in response to GSH transport by these mutants and found that substrate transport by E135 and N710 mutants are not proton independent, although they showed pH independent growth phenotype and transport at higher pH.

In the case of prokaryotes and eukaryotes, several transporters couple the movement of protons in the cell to drive the uphill transport of substrates in the same direction. The proton movement across the membrane by these proteins are carried out through networks of hydrogen bonds that is formed by the side chains of selected amino acids lining the permeation pathway (Unal *et al.* 2009). These residues are usually either Asp, Glu or His residues as they have low pKa values and hence can rapidly undergo protonation and deprotonation in these carriers. In addition to this positively charged, Arg and Lys residues have been suggested to participate in proton movement through the transporter by charge pairing with other negatively charged residues to facilitate deprotonation of carboxylic acid during turnover (Sahin-Tóth & Kaback 2001). Apart from these residues Tyr residues has also been suggested to be important for substrate proton coupling in EmrE (Adam *et al.* 2007). Based on these reports we targeted selective amino acid residues (Asp, Glu, His, Arg, Lys, or Tyr) depending on their conservation pattern and their location in the predicted topology model.

The strategy was successful and we were able to identify D335A (ICL5), Y374A (TMD6), H445A (TMD7) and R554 (ICL9) specifically defective in proton transport as no cytoplasmic acidification was observed in response to GSH transport even at high substrate concentration (1mM) or increased time intervals (1 hour) as compared

to mutants showing similar or low levels of transport suggesting uncoupling of substrate-proton transport. In bacterial Mnt1, a similar observation was made with Asp34 mutant that is involved in the coupling of metal-proton symport using pHluorin based measurement of proton transport. Mutation of Asp34 to Gly resulted in dose-dependent Cd^{2+} uptake, but Cd^{2+} induced proton uptake was not observed even at high concentrations of substrate (Courville *et al.* 2008). In Hgt1p, for E177A and Y193A mutants no acidification was observed as the initial rate of glutathione uptake was less than 2% of the WT although they showed proper expression and cell surface localization. Hence these residues clearly have a role in glutathione uptake and are also strong candidates for being involved in proton-coupled substrate transport by Hgt1p.

The mechanism of transport by all membrane transporter may be represented by the "alternating access model" where the substrate binding site(s) is alternatively exposed to either side of the membrane (Jardetzky 1966; Yan 2013). This mechanism of transport has been suggested for secondary active transporters and supported by numerous biochemical, kinetics and biophysical studies of a variety of transporters from different families. LacY, a lactose-proton symporter, belonging to the MFS superfamily has served as a paradigm for the study of alternating access (Unal *et al.* 2009; Forrest *et al.* 2011; Yan 2013; Kaback 2015). In these proton coupled symporters, the binding of proton is obligatory and several lines of evidence have suggested that the protonation may precede the substrate binding (Dang *et al.* 2010; Smirnova *et al.* 2012).

Crystal structure is not yet available for Hgt1p or any member of the OPT family. Nevertheless, based on the information obtained from the mutational studies and their kinetic analysis, one is tempted to put forward an alternating access model of transport as a possible mechanism of transport for Hgt1p. Residues D335A, Y374A and H445A, which showed no significant change in the *Km* compared to WT Hgt1p, were severely compromised in the translocation rate suggesting that the mutant transporters are possibly protonated. This would enable the substrate to bind with high affinity and hence these residues may not be involved in direct protonation but are probably required for its release. The mutant R554A showed a drastic increase in the *Km* with two-fold decrease in the *Vmax*. This is predicted to be present in the long interconnecting loop, facing the cytoplasm and thus is unlikely to be directly involved

in binding of a proton. This residue is either affecting initial proton binding, or they may have long range secondary effects on substrate or proton binding. However these suggested roles may need more detailed studies on the purified protein and/or crystal structure determination.

Mapping of the important residues from this study on to the previously generated *ab initio* model of Hgt1p suggested that the residues Y193 (TMD3), Y374 (TMD6) and H445 (TMD7) are present in the transmembrane domains predicted to be lining the translocation channel. Whereas E177, D335 and R554 was found to be in the loops connecting the TMDs. However, except Y374, whose side chain was found to be facing the transmembrane pore, Y193 and H445 was found to be facing away from the translocation channel. This model is based on the experimental data without any structural validation. In addition, only the TMDs were modelled and the loops connecting the TMDs were not considered. Hence additional biochemical and biophysical studies are required to confirm the orientation of the TMDs and loops in this *ab initio* model of Hgt1p.

In summary, this study has allowed us to extend the structure-function studies on the proton-coupled high affinity glutathione transporter Hgt1p, which belongs to a poorly characterized OPT family. We have identified D335, H445, Y374 and R554 to be probably involved in the proton translocation through Hgt1p. In addition we have also identified E135 and N710 to be important for pH-dependent substrate transport. However, the identity of the primary proton binding residue is still not definitive. We hope to identify this essential residue which will allow us to build an experimental based model of the mechanism of symport by this transporter.

Bibliography

Abramson J., Iwata S. & Kaback H.R. (2004) Lactose permease as a paradigm for membrane transport proteins (Review). *Molecular membrane biology* 21, 227-36.

Abramson J., Smirnova I., Kasho V., Verner G., Kaback H.R. & Iwata S. (2003) Structure and mechanism of the lactose permease of Escherichia coli. *Science* 301, 610-5.

Adam Y., Tayer N., Rotem D., Schreiber G. & Schuldiner S. (2007) The fast release of sticky protons: kinetics of substrate binding and proton release in a multidrug transporter. *Proceedings of the National Academy of Sciences* 104, 17989-94.

Adamczak R., Porollo A. & Meller J. (2004) Accurate prediction of solvent accessibility using neural networks-based regression. *Proteins* 56, 753-67.

Adamczak R., Porollo A. & Meller J. (2005) Combining prediction of secondary structure and solvent accessibility in proteins. *Proteins* 59, 467-75.

Adang A.E., Brussee J., van der Gen A. & Mulder G.J. (1990) The glutathione-binding site in glutathione S-transferases. Investigation of the cysteinyl, glycyl and gamma-glutamyl domains. *Biochem J* 269, 47-54.

Aggarwal M. & Mondal A.K. (2006) Role of N-terminal hydrophobic region in modulating the subcellular localization and enzyme activity of the bisphosphate nucleotidase from Debaryomyces hansenii. *Eukaryot Cell* 5, 262-71.

Aller I., Rouhier N. & Meyer A.J. (2015) Development of roGFP2-derived redox probes for measurement of the glutathione redox potential in the cytosol of severely glutathione-deficient rml1 seedlings. *Functional Imaging in living Plants-Cell Biology meets Physiology*, 43.

Andersson M., Bondar A.-N., Freites J.A., Tobias D.J., Kaback H.R. & White S.H. (2012) Proton-coupled dynamics in lactose permease. *Structure* 20, 1893-904.

Aouida M., Khodami-Pour A. & Ramotar D. (2009) Novel role for the Saccharomyces cerevisiae oligopeptide transporter Opt2 in drug detoxification In memory of Ghassan Belhadj. *Biochemistry and Cell Biology* 87, 653-61.

Arrigo A.-P. (1999) Gene expression and the thiol redox state. *Free Radical Biology and Medicine* 27, 936-44.

Bachhawat A.K., Thakur A., Kaur J. & Zulkifli M. (2013) Glutathione transporters. *Biochim Biophys Acta* 1830, 3154-64.

Baek Y.-U., Kim Y.-R., Yim H.-S. & Kang S.-O. (2004) Disruption of γ-glutamylcysteine synthetase results in absolute glutathione auxotrophy and apoptosis in Candida albicans. *FEBS letters* 556, 47-52.

Bai J., Lai L., Yeo H.C., Goh B.C. & Tan T.M. (2004) Multidrug resistance protein 4 (MRP4/ABCC4) mediates efflux of bimane-glutathione. *The international journal of biochemistry & cell biology* 36, 247-57.

Bakos E., Evers R., Szakács G., Tusnády G.E., Welker E., Szabó K., de Haas M., van Deemter L., Borst P. & Váradi A. (1998) Functional multidrug resistance protein (MRP1) lacking the N-terminal transmembrane domain. *Journal of Biological Chemistry* 273, 32167-75.

Ballatori N., Krance S.M., Marchan R. & Hammond C.L. (2009) Plasma membrane glutathione transporters and their roles in cell physiology and pathophysiology. *Molecular aspects of medicine* 30, 13-28.

Barth P., Schonbrun J. & Baker D. (2007) Toward high-resolution prediction and design of transmembrane helical protein structures. *Proc Natl Acad Sci U S A* 104, 15682-7.

Bekri S., Kispal G., Lange H., Fitzsimons E., Tolmie J., Lill R. & Bishop D.F. (2000) Human ABC7 transporter: gene structure and mutation causing X-linked sideroblastic anemia with ataxia with disruption of cytosolic iron-sulfur protein maturation. *Blood* 96, 3256-64.

Bernsel A., Viklund H., Falk J., Lindahl E., von Heijne G. & Elofsson A. (2008) Prediction of membrane-protein topology from first principles. *Proc Natl Acad Sci U S A* 105, 7177-81.

Birk J., Meyer M., Aller I., Hansen H.G., Odermatt A., Dick T.P., Meyer A.J. & Appenzeller-Herzog C. (2013) Endoplasmic reticulum: reduced and oxidized glutathione revisited. *J Cell Sci* 126, 1604-17.

Björnberg O., Østergaard H. & Winther J.R. (2006) Measuring intracellular redox conditions using GFP-based sensors. *Antioxidants & redox signaling* 8, 354-61.

Bogs J., Bourbouloux A., Cagnac O., Wachter A., Rausch T. & Delrot S. (2003) Functional characterization and expression analysis of a glutathione transporter, BjGT1, from Brassica juncea: evidence for regulation by heavy metal exposure. *Plant, Cell & Environment* 26, 1703-11.

Booty L.M., King M.S., Thangaratnarajah C., Majd H., James A.M., Kunji E.R. & Murphy M.P. (2015) The mitochondrial dicarboxylate and 2-oxoglutarate carriers do not transport glutathione. *FEBS letters* 589, 621-8.

Bourbouloux A., Shahi P., Chakladar A., Delrot S. & Bachhawat A.K. (2000) Hgt1p, a high affinity glutathione transporter from the yeast Saccharomyces cerevisiae. *J Biol Chem* 275, 13259-65.

Bradford M.M. (1976) A rapid and sensitive method for the quantitation of microgram quantities of protein utilizing the principle of protein-dye binding. *Anal Biochem* 72, 248-54.

Brechbuhl H.M., Gould N., Kachadourian R., Riekhof W.R., Voelker D.R. & Day B.J. (2010) Glutathione transport is a unique function of the ATP-binding cassette protein ABCG2. *Journal of Biological Chemistry* 285, 16582-7.

Cagnac O., Bourbouloux A., Chakrabarty D., Zhang M.-Y. & Delrot S. (2004) AtOPT6 transports glutathione derivatives and is induced by primisulfuron. *Plant Physiology* 135, 1378-87.

Cairns N.G., Pasternak M., Wachter A., Cobbett C.S. & Meyer A.J. (2006) Maturation of arabidopsis seeds is dependent on glutathione biosynthesis within the embryo. *Plant Physiol* 141, 446-55.

Campbell J.D., Koike K., Moreau C., Sansom M.S., Deeley R.G. & Cole S.P. (2004) Molecular modeling correctly predicts the functional importance of Phe594 in transmembrane helix 11 of the multidrug resistance protein, MRP1 (ABCC1). *Journal of Biological Chemistry* 279, 463-8.

Chan C.-Y., Prudom C., Raines S.M., Charkhzarrin S., Melman S.D., De Haro L.P., Allen C., Lee S.A., Sklar L.A. & Parra K.J. (2012) Inhibitors of V-ATPase proton transport reveal uncoupling functions of tether linking cytosolic and membrane domains of V0 subunit a (Vph1p). *Journal of Biological Chemistry* 287, 10236-50.

Chaudhuri B., Ingavale S. & Bachhawat A.K. (1997) apd1+, a gene required for red pigment formation in ade6 mutants of Schizosaccharomyces pombe, encodes an enzyme required for glutathione biosynthesis: a role for glutathione and a glutathione-conjugate pump. *Genetics* 145, 75-83.

Chen Z.-S., Lee K. & Kruh G.D. (2001) Transport of cyclic nucleotides and estradiol 17-β-D-glucuronide by multidrug resistance protein 4 resistance to 6-mercaptopurine and 6-thioguanine. *Journal of Biological Chemistry* 276, 33747-54.

Chen Z. & Lash L.H. (1998) Evidence for mitochondrial uptake of glutathione by dicarboxylate and 2-oxoglutarate carriers. *Journal of Pharmacology and Experimental Therapeutics* 285, 608-18.

Chen Z., Putt D.A. & Lash L.H. (2000) Enrichment and functional reconstitution of glutathione transport activity from rabbit kidney mitochondria: further evidence for the role of the dicarboxylate and 2-oxoglutarate carriers in mitochondrial glutathione transport. *Archives of biochemistry and biophysics* 373, 193-202.

CIaros M.G. & von Heijne G. (1994) Cabios applications notes.

Circu M.L. & Yee Aw T. (2008) Glutathione and apoptosis. *Free radical research* 42, 689-706.

Cole S.P. & Deeley R.G. (2006a) Transport of glutathione and glutathione conjugates by MRP1. *Trends Pharmacol Sci* 27, 438-46.

Cole S.P. & Deeley R.G. (2006b) Transport of glutathione and glutathione conjugates by MRP1. *Trends in pharmacological sciences* 27, 438-46.

Cordes F.S., Bright J.N. & Sansom M.S. (2002) Proline-induced distortions of transmembrane helices. *J Mol Biol* 323, 951-60.

Courville P., Urbankova E., Rensing C., Chaloupka R., Quick M. & Cellier M.F. (2008) Solute carrier 11 cation symport requires distinct residues in transmembrane helices 1 and 6. *Journal of Biological Chemistry* 283, 9651-8.

Csere P., Lill R. & Kispal G. (1998) Identification of a human mitochondrial ABC transporter, the functional orthologue of yeast Atm1p. *FEBS letters* 441, 266-70.

Cummins I., Dixon D.P., Freitag-Pohl S., Skipsey M. & Edwards R. (2011) Multiple roles for plant glutathione transferases in xenobiotic detoxification. *Drug metabolism reviews* 43, 266-80.

Curie C., Panaviene Z., Loulergue C., Dellaporta S.L., Briat J.-F. & Walker E.L. (2001) Maize yellow stripe1 encodes a membrane protein directly involved in Fe (III) uptake. *Nature* 409, 346-9.

Dalton T.P., Dieter M.Z., Yang Y., Shertzer H.G. & Nebert D.W. (2000) Knockout of the mouse glutamate cysteine ligase catalytic subunit (Gclc) gene: embryonic lethal when

homozygous, and proposed model for moderate glutathione deficiency when heterozygous. *Biochemical and biophysical research communications* 279, 324-9.

Dang S., Sun L., Huang Y., Lu F., Liu Y., Gong H., Wang J. & Yan N. (2010) Structure of a fucose transporter in an outward-open conformation. *Nature* 467, 734-8.

Davidson A.L., Dassa E., Orelle C. & Chen J. (2008) Structure, function, and evolution of bacterial ATP-binding cassette systems. *Microbiology and Molecular Biology Reviews* 72, 317-64.

DeGorter M.K., Conseil G., Deeley R.G., Campbell R.L. & Cole S.P. (2008) Molecular modeling of the human multidrug resistance protein 1 (MRP1/ABCC1). *Biochemical and biophysical research communications* 365, 29-34.

Desai P.R., Thakur A., Ganguli D., Paul S., Morschhauser J. & Bachhawat A.K. (2011) Glutathione utilization by Candida albicans requires a functional glutathione degradation (DUG) pathway and OPT7, an unusual member of the oligopeptide transporter family. *J Biol Chem* 286, 41183-94.

Dhaoui M., Auchere F., Blaiseau P.L., Lesuisse E., Landoulsi A., Camadro J.M., Haguenauer-Tsapis R. & Belgareh-Touze N. (2011) Gex1 is a yeast glutathione exchanger that interferes with pH and redox homeostasis. *Mol Biol Cell* 22, 2054-67.

DiDonato R.J., Jr., Roberts L.A., Sanderson T., Eisley R.B. & Walker E.L. (2004) Arabidopsis Yellow Stripe-Like2 (YSL2): a metal-regulated gene encoding a plasma membrane transporter of nicotianamine-metal complexes. *Plant J* 39, 403-14.

Doki S., Kato H.E., Solcan N., Iwaki M., Koyama M., Hattori M., Iwase N., Tsukazaki T., Sugita Y. & Kandori H. (2013) Structural basis for dynamic mechanism of proton-coupled symport by the peptide transporter POT. *Proceedings of the National Academy of Sciences* 110, 11343-8.

Dworeck T., Wolf K. & Zimmermann M. (2009) SpOPT1, a member of the oligopeptide family (OPT) of the fission yeast Schizosaccharomyces pombe, is involved in the transport of glutathione through the outer membrane of the cell. *Yeast* 26, 67-73.

Edgar R.C. (2004) MUSCLE: multiple sequence alignment with high accuracy and high throughput. *Nucleic Acids Res* 32, 1792-7.

El-Sheikh A.A., van den Heuvel J.J., Krieger E., Russel F.G. & Koenderink J.B. (2008) Functional role of arginine 375 in transmembrane helix 6 of multidrug resistance protein 4 (MRP4/ABCC4). *Molecular pharmacology* 74, 964-71.

Elbaz-Alon Y., Morgan B., Clancy A., Amoako T.N., Zalckvar E., Dick T.P., Schwappach B. & Schuldiner M. (2014) The yeast oligopeptide transporter Opt2 is localized to peroxisomes and affects glutathione redox homeostasis. *FEMS Yeast Res* 14, 1055-67.

Elskens M.T., Jaspers C.J. & Penninckx M.J. (1991) Glutathione as an endogenous sulphur source in the yeast Saccharomyces cerevisiae. *Microbiology* 137, 637-44.

Falcón-Pérez J.M., Martínez-Burgos M., Molano J., Mazón M.a.J. & Eraso P. (2001) Domain interactions in the yeast ATP binding cassette transporter Ycf1p: intragenic suppressor analysis of mutations in the nucleotide binding domains. *J Bacteriol* 183, 4761-70.

Falcón-Pérez J.M., Mazón M.a.J., Molano J. & Eraso P. (1999) Functional domain analysis of the yeast ABC transporter Ycf1p by site-directed mutagenesis. *Journal of Biological Chemistry* 274, 23584-90.

Forrest L.R., Krämer R. & Ziegler C. (2011) The structural basis of secondary active transport mechanisms. *Biochimica et Biophysica Acta (BBA)-Bioenergetics* 1807, 167-88.

Foyer C.H., Theodoulou F.L. & Delrot S. (2001) The functions of inter-and intracellular glutathione transport systems in plants. *Trends in plant science* 6, 486-92.

Franco R., DeHaven W.I., Sifre M.I., Bortner C.D. & Cidlowski J.A. (2008) Glutathione depletion and disruption of intracellular ionic homeostasis regulate lymphoid cell apoptosis. *Journal of Biological Chemistry* 283, 36071-87.

Fratelli M., Goodwin L.O., Ørom U.A., Lombardi S., Tonelli R., Mengozzi M. & Ghezzi P. (2005) Gene expression profiling reveals a signaling role of glutathione in redox regulation. *Proc Natl Acad Sci U S A* 102, 13998-4003.

Frey I.M., Rubio-Aliaga I., Siewert A., Sailer D., Drobyshev A., Beckers J., De Angelis M.H., Aubert J., Hen A.B. & Fiehn O. (2007) Profiling at mRNA, protein, and metabolite levels reveals alterations in renal amino acid handling and glutathione metabolism in kidney tissue of Pept2−/− mice. *Physiological genomics* 28, 301-10.

Gomolplitinant K.M. & Saier Jr M.H. (2011) Evolution of the oligopeptide transporter family. *The Journal of membrane biology* 240, 89-110.

Gopal S., Borovok I., Ofer A., Yanku M., Cohen G., Goebel W., Kreft J. & Aharonowitz Y. (2005) A multidomain fusion protein in Listeria monocytogenes catalyzes the two primary activities for glutathione biosynthesis. *J Bacteriol* 187, 3839-47.

Grant D., Long W.F., Mackintosh G. & Williamson F.B. (1996) The antioxidant activity of heparins. *Biochem Soc Trans* 24, 194S.

Green R.M., Graham M., O'Donovan M.R., Chipman J.K. & Hodges N.J. (2006) Subcellular compartmentalization of glutathione: correlations with parameters of oxidative stress related to genotoxicity. *Mutagenesis* 21, 383-90.

Green R.M., Seth A. & Connell N.D. (2000) A peptide permease mutant of Mycobacterium bovis BCG resistant to the toxic peptides glutathione and S-nitrosoglutathione. *Infect Immun* 68, 429-36.

Griffith O.W. & Meister A. (1985) Origin and turnover of mitochondrial glutathione. *Proc Natl Acad Sci U S A* 82, 4668.

Griffith O.W. & Mulcahy R.T. (1999) The enzymes of glutathione synthesis: gamma-glutamylcysteine synthetase. *Adv Enzymol Relat Areas Mol Biol* 73, 209-67, xii.

Guan L. & Kaback H.R. (2006) Lessons from lactose permease. *Annual review of biophysics and biomolecular structure* 35, 67.

Guan L. & Kaback H.R. (2007) Site-directed alkylation of cysteine to test solvent accessibility of membrane proteins. *Nature protocols* 2, 2012-7.

Guthrie C. & Fink G.R. (1991) Guide to yeast genetics and molecular biology. . *Methods Enzymol.* 194, 3-37.

Gutscher M., Pauleau A.-L., Marty L., Brach T., Wabnitz G.H., Samstag Y., Meyer A.J. & Dick T.P. (2008) Real-time imaging of the intracellular glutathione redox potential. *Nature methods* 5, 553-9.

Hagenbuch B. & Meier P. (2003) The superfamily of organic anion transporting polypeptides. *Biochimica et Biophysica Acta (BBA)-Biomembranes* 1609, 1-18.

Haimeur A., Conseil G., Deeley R.G. & Cole S.P. (2004) Mutations of charged amino acids in or near the transmembrane helices of the second membrane spanning domain differentially affect the substrate specificity and transport activity of the multidrug resistance protein MRP1 (ABCC1). *Molecular pharmacology* 65, 1375-85.

Haimeur A., Deeley R.G. & Cole S.P. (2002) Charged amino acids in the sixth transmembrane helix of multidrug resistance protein 1 (MRP1/ABCC1) are critical determinants of transport activity. *Journal of Biological Chemistry* 277, 41326-33.

Hardwick L., Velamakanni S. & Veen H. (2007) The emerging pharmacotherapeutic significance of the breast cancer resistance protein (ABCG2). *British journal of pharmacology* 151, 163-74.

Hauser M., Donhardt A.M., Barnes D., Naider F. & Becker J.M. (2000) Enkephalins are transported by a novel eukaryotic peptide uptake system. *J Biol Chem* 275, 3037-41.

He S.-M., Li R., R Kanwar J. & Zhou S.-F. (2011) Structural and functional properties of human multidrug resistance protein 1 (MRP1/ABCC1). *Current medicinal chemistry* 18, 439-81.

Henriksen U., Fog J.U., Litman T. & Gether U. (2005) Identification of intra-and intermolecular disulfide bridges in the multidrug resistance transporter ABCG2. *Journal of Biological Chemistry* 280, 36926-34.

Ito H., Fukuda Y., Murata K. & Kimura A. (1983a) Transformation of intact yeast cells treated with alkali cations. *J Bacteriol* 153, 163-8.

Ito H., Fukuda Y., Murata K. & Kimura A. (1983b) Transformation of intact yeast cells treated with alkali cations. *J Bacteriol* 153, 163-8.

Jardetzky O. (1966) Simple allosteric model for membrane pumps.

Jaruga E., Lapshina E.A., Biliński T., Płonka A. & Bartosz G. (1995) Resistance to ionizing radiation and antioxidative defence in yeasts. Are antioxidant-deficient cells permanently stressed? *Biochemistry and molecular biology international* 37, 467-73.

Jedlitschky G., Burchell B. & Keppler D. (2000) The multidrug resistance protein 5 functions as an ATP-dependent export pump for cyclic nucleotides. *Journal of Biological Chemistry* 275, 30069-74.

Jessop C.E. & Bulleid N.J. (2004) Glutathione directly reduces an oxidoreductase in the endoplasmic reticulum of mammalian cells. *Journal of Biological Chemistry* 279, 55341-7.

Jones D., Taylor W. & Thornton J. (1994) A model recognition approach to the prediction of all-helical membrane protein structure and topology. *Biochemistry* 33, 3038-49.

Jones D.T. (2007) Improving the accuracy of transmembrane protein topology prediction using evolutionary information. *Bioinformatics* 23, 538-44.

Kaback H.R. (2005) Structure and mechanism of the lactose permease. *Comptes rendus biologies* 328, 557-67.

Kaback H.R. (2015) A chemiosmotic mechanism of symport. *Proceedings of the National Academy of Sciences* 112, 1259-64.

Kaback H.R., Sahin-Tóth M. & Weinglass A.B. (2001) The kamikaze approach to membrane transport. *Nature reviews Molecular cell biology* 2, 610-20.

Kaiser C., Michaelis S. & Mitchell A. (1994) Methods in yeast genetics.

Kall L., Krogh A. & Sonnhammer E.L. (2005) An HMM posterior decoder for sequence feature prediction that includes homology information. *Bioinformatics* 21 Suppl 1, i251-7.

Kall L., Krogh A. & Sonnhammer E.L. (2007) Advantages of combined transmembrane topology and signal peptide prediction—the Phobius web server. *Nucleic Acids Research* 35, W429-W32.

Kaluzna K.G. & Bartosz G. (1997) Transport of glutathione S-conjugates in Escherichia coli. . *Mol Biol Int* 43, 161–71

Kaur J. & Bachhawat A.K. (2009a) Gln-222 in transmembrane domain 4 and Gln-526 in transmembrane domain 9 are critical for substrate recognition in the yeast high affinity glutathione transporter, Hgt1p. *J Biol Chem* 284, 23872-84.

Kaur J. & Bachhawat A.K. (2009b) A modified Western blot protocol for enhanced sensitivity in the detection of a membrane protein. *Anal Biochem* 384, 348-9.

Kaur J., Srikanth C.V. & Bachhawat A.K. (2009) Differential roles played by the native cysteine residues of the yeast glutathione transporter, Hgt1p. *FEMS Yeast Res* 9, 849-66.

Kim D.E., Chivian D. & Baker D. (2004) Protein structure prediction and analysis using the Robetta server. *Nucleic Acids Res* 32, W526-31.

Kiriyama K., Hara K.Y. & Kondo A. (2012) Extracellular glutathione fermentation using engineered Saccharomyces cerevisiae expressing a novel glutathione exporter. *Applied microbiology and biotechnology* 96, 1021-7.

Kispal G., Csere P., Prohl C. & Lill R. (1999) The mitochondrial proteins Atm1p and Nfs1p are essential for biogenesis of cytosolic Fe/S proteins. *The EMBO journal* 18, 3981-9.

Klein M., Burla B. & Martinoia E. (2006) The multidrug resistance-associated protein (MRP/ABCC) subfamily of ATP-binding cassette transporters in plants. *FEBS letters* 580, 1112-22.

Koffler B.E., Bloem E., Zellnig G. & Zechmann B. (2013) High resolution imaging of subcellular glutathione concentrations by quantitative immunoelectron microscopy in different leaf areas of Arabidopsis. *Micron* 45, 119-28.

Koh S., Wiles A.M., Sharp J.S., Naider F.R., Becker J.M. & Stacey G. (2002) An oligopeptide transporter gene family in Arabidopsis. *Plant Physiol* 128, 21-9.

König J., Cui Y., Nies A.T. & Keppler D. (2000) Localization and genomic organization of a new hepatocellular organic anion transporting polypeptide. *Journal of Biological Chemistry* 275, 23161-8.

Krems B., Charizanis C. & Entian K.-D. (1995) Mutants of Saccharomyces cerevisiae sensitive to oxidative and osmotic stress. *Current genetics* 27, 427-34.

Krogh A., Larsson B., Von Heijne G. & Sonnhammer E.L. (2001a) Predicting transmembrane protein topology with a hidden Markov model: application to complete genomes. *Journal of molecular biology* 305, 567-80.

Krogh A., Larsson B., von Heijne G. & Sonnhammer E.L. (2001b) Predicting transmembrane protein topology with a hidden Markov model: application to complete genomes. *J Mol Biol* 305, 567-80.

Kuhnke G., Neumann K., Mühlenhoff U. & Lill R. (2006) Stimulation of the ATPase activity of the yeast mitochondrial ABC transporter Atm1p by thiol compounds. *Molecular membrane biology* 23, 173-84.

Kumar C., Igbaria A., D'Autreaux B., Planson A.G., Junot C., Godat E., Bachhawat A.K., Delaunay-Moisan A. & Toledano M.B. (2011) Glutathione revisited: a vital function in iron metabolism and ancillary role in thiol-redox control. *EMBO J* 30, 2044-56.

Kumar H., Kasho V., Smirnova I., Finer-Moore J.S., Kaback H.R. & Stroud R.M. (2014) Structure of sugar-bound LacY. *Proceedings of the National Academy of Sciences* 111, 1784-8.

Lash L.H. (2005) Role of glutathione transport processes in kidney function. *Toxicology and applied pharmacology* 204, 329-42.

Lash L.H. (2006) Mitochondrial glutathione transport: physiological, pathological and toxicological implications. *Chemico-biological interactions* 163, 54-67.

Lash L.H. (2009) Renal glutathione transport: Identification of carriers, physiological functions, and controversies. *BioFactors* 35, 500-8.

Lash L.H. (2015) Mitochondrial glutathione in diabetic nephropathy. *Journal of clinical medicine* 4, 1428-47.

Lautier D., Canitrot Y., Deeley R.G. & Cole S.P. (1996) Multidrug resistance mediated by the multidrug resistance protein (MRP) gene. *Biochemical pharmacology* 52, 967-77.

Lee J.Y., Yang J.G., Zhitnitsky D., Lewinson O. & Rees D.C. (2014) Structural basis for heavy metal detoxification by an Atm1-type ABC exporter. *Science* 343, 1133-6.

Leslie E.M., Bowers R.J., Deeley R.G. & Cole S.P. (2003) Structural requirements for functional interaction of glutathione tripeptide analogs with the human multidrug resistance protein 1 (MRP1). *J Pharmacol Exp Ther* 304, 643-53.

Li Z.-S., Szczypka M., Lu Y.-P., Thiele D.J. & Rea P.A. (1996a) The yeast cadmium factor protein (YCF1) is a vacuolar glutathione S-conjugate pump. *Journal of Biological Chemistry* 271, 6509-17.

Li Z.S., Szczypka M., Lu Y.P., Thiele D.J. & Rea P.A. (1996b) The yeast cadmium factor protein (YCF1) is a vacuolar glutathione S-conjugate pump. *J Biol Chem* 271, 6509-17.

Liqi L. & Theresa M. (2002) Role of glutathione in the multidrug resistance protein 4 (MRP4/ABCC4)-mediated efflux of cAMP and resistance to purine analogues. *Biochemical Journal* 361, 497-503.

Liu G., Sánchez-Fernández R.o., Li Z.-S. & Rea P.A. (2001) Enhanced multispecificity of Arabidopsis vacuolar multidrug resistance-associated protein-type ATP-binding cassette transporter, AtMRP2. *Journal of Biological Chemistry* 276, 8648-56.

Lohman J.R. & Remington S.J. (2008) Development of a Family of Redox-Sensitive Green Fluorescent Protein Indicators for Use in Relatively Oxidizing Subcellular Environments†‡. *Biochemistry* 47, 8678-88.

Lorico A., Rappa G., Finch R.A., Yang D., Flavell R.A. & Sartorelli A.C. (1997) Disruption of the murine MRP (multidrug resistance protein) gene leads to increased sensitivity to etoposide (VP-16) and increased levels of glutathione. *Cancer research* 57, 5238-42.

Lubkowitz M. (2006) The OPT family functions in long-distance peptide and metal transport in plants. *Genet Eng (N Y)* 27, 35-55.

Lubkowitz M. (2011) The oligopeptide transporters: a small gene family with a diverse group of substrates and functions? *Mol Plant* 4, 407-15.

Lubkowitz M.A., Hauser L., Breslav M., Naider F. & Becker J.M. (1997) An oligopeptide transport gene from Candida albicans. *Microbiology* 143 (Pt 2), 387-96.

Mahagita C., Grassl S.M., Piyachaturawat P. & Ballatori N. (2007) Human organic anion transporter 1B1 and 1B3 function as bidirectional carriers and do not mediate GSH-bile acid cotransport. *American Journal of Physiology-Gastrointestinal and Liver Physiology* 293, G271-G8.

Mao Q., Deeley R.G. & Cole S.P. (2000) Functional reconstitution of substrate transport by purified multidrug resistance protein MRP1 (ABCC1) in phospholipid vesicles. *Journal of Biological Chemistry* 275, 34166-72.

Maresova L., Hoskova B., Urbankova E., Chaloupka R. & Sychrova H. (2010) New applications of pHluorin--measuring intracellular pH of prototrophic yeasts and determining changes in the buffering capacity of strains with affected potassium homeostasis. *Yeast* 27, 317-25.

Marí M., Morales A., Colell A., García-Ruiz C., Kaplowitz N. & Fernández-Checa J.C. (2013) Mitochondrial glutathione: features, regulation and role in disease. *Biochimica et Biophysica Acta (BBA)-General Subjects* 1830, 3317-28.

Markovic J., Borrás C., Ortega Á., Sastre J., Viña J. & Pallardó F.V. (2007) Glutathione is recruited into the nucleus in early phases of cell proliferation. *Journal of Biological Chemistry* 282, 20416-24.

Markovic J., García-Gimenez J.L., Gimeno A., Viña J. & Pallardó F.V. (2010) Role of glutathione in cell nucleus. *Free radical research* 44, 721-33.

Maughan S.C., Pasternak M., Cairns N., Kiddle G., Brach T., Jarvis R., Haas F., Nieuwland J., Lim B., Muller C., Salcedo-Sora E., Kruse C., Orsel M., Hell R., Miller A.J., Bray P., Foyer C.H., Murray J.A., Meyer A.J. & Cobbett C.S. (2010) Plant homologs of the Plasmodium falciparum chloroquine-resistance transporter, PfCRT, are required for glutathione homeostasis and stress responses. *Proc Natl Acad Sci U S A* 107, 2331-6.

Mehdi K. & Penninckx M.J. (1997) An important role for glutathione and γ-glutamyltranspeptidase in the supply of growth requirements during nitrogen starvation of the yeast Saccharomyces cerevisiae. *Microbiology* 143, 1885-9.

Meister A. & Anderson M.E. (1983) Glutathione. *Annu Rev Biochem* 52, 711-60.

Meister A. & Tate S.S. (1976) Glutathione and related γ-glutamyl compounds: biosynthesis and utilization. *Annual review of biochemistry* 45, 559-604.

Mendoza-Cózatl D.G., Xie Q., Akmakjian G.Z., Jobe T.O., Patel A., Stacey M.G., Song L., Demoin D.W., Jurisson S.S. & Stacey G. (2014) OPT3 is a component of the iron-signaling network between leaves and roots and misregulation of OPT3 leads to an over-accumulation of cadmium in seeds. *Mol Plant* 7, 1455-69.

Meyer A.J. & Dick T.P. (2010) Fluorescent protein-based redox probes. *Antioxidants & redox signaling* 13, 621-50.

Meyer A.J. & Hell R. (2005) Glutathione homeostasis and redox-regulation by sulfhydryl groups. *Photosynthesis Research* 86, 435-57.

Michelet L., Zaffagnini M., Massot V., Keryer E., Vanacker H., Miginiac-Maslow M., Issakidis-Bourguet E. & Lemaire S.D. (2006) Thioredoxins, glutaredoxins, and glutathionylation: new crosstalks to explore. *Photosynthesis Research* 89, 225-45.

Miguel V., Otero J.A., García-Villalba R., Tomás-Barberán F., Espín J.C., Merino G. & Álvarez A.I. (2014) Role of ABCG2 in transport of the mammalian lignan enterolactone and its secretion into milk in Abcg2 knockout mice. *Drug Metabolism and Disposition* 42, 943-6.

Mikolay A. & Nies D.H. (2009) The ABC-transporter AtmA is involved in nickel and cobalt resistance of Cupriavidus metallidurans strain CH34. *Antonie van Leeuwenhoek* 96, 183-91.

Mirza O., Guan L., Verner G., Iwata S. & Kaback H.R. (2006) Structural evidence for induced fit and a mechanism for sugar/H+ symport in LacY. *The EMBO journal* 25, 1177-83.

Miyake T., Hazu T., Yoshida S., Kanayama M., Tomochika K., Shinoda S. & Ono B. (1998) Glutathione transport systems of the budding yeast Saccharomyces cerevisiae. *Biosci Biotechnol Biochem* 62, 1858-64.

Miyake T., Hiraishi H., Sammoto H. & Ono B.-I. (2003) Involvement of the VDE homing endonuclease and rapamycin in regulation of the Saccharomyces cerevisiae GSH11 gene encoding the high affinity glutathione transporter. *Journal of Biological Chemistry* 278, 39632-6.

Mohsenzadeh S., Esmaeili M., Moosavi F., Shahrtash M., Saffari B. & Mohabatkar H. (2011) Plant glutathione S-transferase classification, structure and evolution. *African Journal of Biotechnology* 10, 8160-5.

Montero D., Tachibana C., Winther J.R. & Appenzeller-Herzog C. (2013) Intracellular glutathione pools are heterogeneously concentrated. *Redox biology* 1, 508-13.

Moon C., Zhang W., Ren A., Arora K., Sinha C., Yarlagadda S., Woodrooffe K., Schuetz J.D., Valasani K.R. & de Jonge H.R. (2015) Compartmentalized accumulation of cAMP near complexes of multidrug resistance protein 4 (MRP4) and cystic fibrosis transmembrane conductance regulator (CFTR) contributes to drug-induced diarrhea. *Journal of Biological Chemistry* 290, 11246-57.

Morgan B., Ezeriņa D., Amoako T.N., Riemer J., Seedorf M. & Dick T.P. (2013) Multiple glutathione disulfide removal pathways mediate cytosolic redox homeostasis. *Nature chemical biology* 9, 119-25.

Morth J.P., Pedersen B.P., Buch-Pedersen M.J., Andersen J.P., Vilsen B., Palmgren M.G. & Nissen P. (2011) A structural overview of the plasma membrane Na+, K+-ATPase and H+-ATPase ion pumps. *Nature reviews Molecular cell biology* 12, 60-70.

Mühlenhoff U., Gerber J., Richhardt N. & Lill R. (2003) Components involved in assembly and dislocation of iron–sulfur clusters on the scaffold protein Isu1p. *The EMBO journal* 22, 4815-25.

Mumberg D., Muller R. & Funk M. (1995) Yeast vectors for the controlled expression of heterologous proteins in different genetic backgrounds. *Gene* 156, 119-22.

Murata Y., Ma J.F., Yamaji N., Ueno D., Nomoto K. & Iwashita T. (2006) A specific transporter for iron(III)-phytosiderophore in barley roots. *Plant J* 46, 563-72.

Newstead S., Drew D., Cameron A.D., Postis V.L., Xia X., Fowler P.W., Ingram J.C., Carpenter E.P., Sansom M.S. & McPherson M.J. (2011) Crystal structure of a prokaryotic homologue of the mammalian oligopeptide–proton symporters, PepT1 and PepT2. *The EMBO journal* 30, 417-26.

Ni Z., Bikadi Z., Shuster D.L., Zhao C., Rosenberg M.F. & Mao Q. (2011) Identification of proline residues in or near the transmembrane helices of the human breast cancer resistance protein (BCRP/ABCG2) that are important for transport activity and substrate specificity. *Biochemistry* 50, 8057-66.

Noctor G., Gomez L., Vanacker H. & Foyer C.H. (2002) Interactions between biosynthesis, compartmentation and transport in the control of glutathione homeostasis and signalling. *J Exp Bot* 53, 1283-304.

Nozawa T., Imai K., Nezu J.-I., Tsuji A. & Tamai I. (2004) Functional characterization of pH-sensitive organic anion transporting polypeptide OATP-B in human. *Journal of Pharmacology and Experimental Therapeutics* 308, 438-45.

Nugent T. & Jones D.T. (2009) Transmembrane protein topology prediction using support vector machines. *BMC Bioinformatics* 10, 159.

Oldham M.L., Davidson A.L. & Chen J. (2008) Structural insights into ABC transporter mechanism. *Current opinion in structural biology* 18, 726-33.

Osawa H., Stacey G. & Gassmann W. (2006) ScOPT1 and AtOPT4 function as proton-coupled oligopeptide transporters with broad but distinct substrate specificities. *Biochem J* 393, 267-75.

Østergaard H., Henriksen A., Hansen F.G. & Winther J.R. (2001) Shedding light on disulfide bond formation: engineering a redox switch in green fluorescent protein. *The EMBO journal* 20, 5853-62.

Østergaard H., Tachibana C. & Winther J.R. (2004) Monitoring disulfide bond formation in the eukaryotic cytosol. *The Journal of cell biology* 166, 337-45.

Palmgren M.G. & Nissen P. (2011) P-type ATPases. *Annual review of biophysics* 40, 243-66.

Pang S., Li X.-F., Liu Z. & Wang C.-J. (2010) ZmGT1 transports glutathione conjugates and its expression is induced by herbicide atrazine. *Prog Biochem Biophys* 37, 1120-7.

Pao S.S., Paulsen I.T. & Saier M.H. (1998) Major facilitator superfamily. *Microbiology and Molecular Biology Reviews* 62, 1-34.

Paulusma C.C., Evers R., Heijn M., Ottenhoff R., Borst P. & Elferink R.P.O. (1999) Canalicular multispecific organic anion transporter/multidrug resistance protein 2 mediates low-affinity transport of reduced glutathione. *Biochemical Journal* 338, 393-401.

Pittman M.S., Robinson H.C. & Poole R.K. (2005) A bacterial glutathione transporter (Escherichia coli CydDC) exports reductant to the periplasm. *J Biol Chem* 280, 32254-61.

Prasad K. (2014) Rationale for using multiple antioxidants in protecting humans against low doses of ionizing radiation. *The British journal of radiology*.

Quistgaard E.M., Löw C., Moberg P., Trésaugues L. & Nordlund P. (2013) Structural basis for substrate transport in the GLUT-homology family of monosaccharide transporters. *Nature structural & molecular biology* 20, 766-8.

Rappa G., Finch R.A., Sartorelli A.C. & Lorico A. (1999) New insights into the biology and pharmacology of the multidrug resistance protein (MRP) from gene knockout models. *Biochem Pharmacol* 58, 557-62.

Rea P.A. (1999) MRP subfamily ABC transporters from plants and yeast. *J Exp Bot* 50, 895-913.

Rebbeor J.F., Connolly G.C. & Ballatori N. (2002) Inhibition of Mrp2-and Ycf1p-mediated transport by reducing agents: evidence for GSH transport on rat Mrp2. *Biochimica et Biophysica Acta (BBA)-Biomembranes* 1559, 171-8.

Rebbeor J.F., Connolly G.C., Dumont M.E. & Ballatori N. (1998a) ATP-dependent transport of reduced glutathione in yeast secretory vesicles. *Biochem J* 334 (Pt 3), 723-9.

Rebbeor J.F., Gregory C.C., Dumont M.E. & Ballatori N. (1998b) ATP-dependent transport of reduced glutathione on YCF1, the yeast orthologue of mammalian multidrug resistance associated proteins. *Journal of Biological Chemistry* 273, 33449-54.

Reddy V.S., Shlykov M.A., Castillo R., Sun E.I. & Saier M.H. (2012) The major facilitator superfamily (MFS) revisited. *FEBS Journal* 279, 2022-35.

Rees D.C., Johnson E. & Lewinson O. (2009) ABC transporters: the power to change. *Nature reviews Molecular cell biology* 10, 218-27.

Reuß O. & Morschhäuser J. (2006) A family of oligopeptide transporters is required for growth of Candida albicans on proteins. *Mol Microbiol* 60, 795-812.

Rius M., Hummel-Eisenbeiss J., Hofmann A.F. & Keppler D. (2006) Substrate specificity of human ABCC4 (MRP4)-mediated cotransport of bile acids and reduced glutathione. *American Journal of Physiology-Gastrointestinal and Liver Physiology* 290, G640-G9.

Rius M., Nies A.T., Hummel-Eisenbeiss J., Jedlitschky G. & Keppler D. (2003) Cotransport of reduced glutathione with bile salts by MRP4 (ABCC4) localized to the basolateral hepatocyte membrane. *Hepatology* 38, 374-84.

Rose M.D. & Fink G.R. (1987) KAR1, a gene required for function of both intranuclear and extranuclear microtubules in yeast. *Cell* 48, 1047-60.

Rost B. (1996) [31] PHD: Predicting one-dimensional protein structure by profile-based neural networks. *Methods in enzymology* 266, 525-39.

Rost B., Fariselli P. & Casadio R. (1996) Topology prediction for helical transmembrane proteins at 86% accuracy. *Protein Sci* 5, 1704-18.

Rouhier N., Lemaire S.D. & Jacquot J.-P. (2008) The role of glutathione in photosynthetic organisms: emerging functions for glutaredoxins and glutathionylation. *Annu. Rev. Plant Biol.* 59, 143-66.

Ryu S., Kawabe T., Nada S. & Yamaguchi A. (2000) Identification of basic residues involved in drug export function of human multidrug resistance-associated protein 2. *Journal of Biological Chemistry* 275, 39617-24.

Sahin-Tóth M. & Kaback H.R. (2001) Arg-302 facilitates deprotonation of Glu-325 in the transport mechanism of the lactose permease from Escherichia coli. *Proceedings of the National Academy of Sciences* 98, 6068-73.

Sambrook J., Fritsch E. F. and Maniatis T. (1989a) *Molecular Cloning: A Laboratory Manual*. Cold Spring Harbor Press, Cold Spring Harbor, New York.

Sambrook J., Fritsch, E. F., and Maniatis, T. (1989b) Molecular Cloning: A Laboratory Manual, 2nd Ed., Cold Spring Harbor Laboratory, Cold Spring Harbor, NY.

Schaedler T.A., Thornton J.D., Kruse I., Schwarzlander M., Meyer A.J., van Veen H.W. & Balk J. (2014) A conserved mitochondrial ATP-binding cassette transporter exports glutathione polysulfide for cytosolic metal cofactor assembly. *J Biol Chem* 289, 23264-74.

Serrano R., Kielland-Brandt M.C. & Fink G.R. (1986) Yeast plasma membrane ATPase is essential for growth and has homology with (Na+ + K+), K+- and Ca2+-ATPases. *Nature* 319, 689-93.

Shackelford R.E., Heinloth A.N., Heard S.C. & Paules R.S. (2005) Cellular and molecular targets of protein S-glutathiolation. *Antioxidants & redox signaling* 7, 940-50.

Sharma K.G., Mason D.L., Liu G., Rea P.A., Bachhawat A.K. & Michaelis S. (2002) Localization, regulation, and substrate transport properties of Bpt1p, a Saccharomyces cerevisiae MRP-type ABC transporter. *Eukaryotic Cell* 1, 391-400.

Sherrill C. & Fahey R.C. (1998) Import and Metabolism of Glutathione byStreptococcus mutans. *J Bacteriol* 180, 1454-9.

Shi Y. (2013) Common folds and transport mechanisms of secondary active transporters. *Annual review of biophysics* 42, 51-72.

Shi Z.-Z., Osei-Frimpong J., Kala G., Kala S.V., Barrios R.J., Habib G.M., Lukin D.J., Danney C.M., Matzuk M.M. & Lieberman M.W. (2000) Glutathione synthesis is essential for mouse development but not for cell growth in culture. *Proceedings of the National Academy of Sciences* 97, 5101-6.

Shimada Y., Okuno S., Kawai A., Shinomiya H., Saito A., Suzuki M., Omori Y., Nishino N., Kanemoto N. & Fujiwara T. (1998) Cloning and chromosomal mapping of a novel ABC transporter gene (hABC7), a candidate for X-linked sideroblastic anemia with spinocerebellar ataxia. *Journal of human genetics* 43, 115-22.

Slotboom D.J. (2014) Structural and mechanistic insights into prokaryotic energy-coupling factor transporters. *Nature Reviews Microbiology* 12, 79-87.

Smirnova G., Krasnykh T. & Oktyabrsky O. (2001) Role of glutathione in the response of Escherichia coli to osmotic stress. *Biochemistry (Moscow)* 66, 973-8.

Smirnova I., Kasho V. & Kaback H.R. (2011) Lactose permease and the alternating access mechanism. *Biochemistry* 50, 9684-93.

Smirnova I., Kasho V., Sugihara J., Choe J.-Y. & Kaback H.R. (2009) Residues in the H+ translocation site define the p K a for sugar binding to LacY. *Biochemistry* 48, 8852-60.

Smirnova I., Kasho V., Sugihara J., Vázquez-Ibar J.L. & Kaback H.R. (2012) Role of protons in sugar binding to LacY. *Proceedings of the National Academy of Sciences* 109, 16835-40.

Smirnova I.N., Kasho V. & Kaback H.R. (2008) Protonation and sugar binding to LacY. *Proceedings of the National Academy of Sciences* 105, 8896-901.

Söderdahl T., Enoksson M., Lundberg M., Holmgren A., Ottersen O.P., Orrenius S., Bolcsfoldi G. & Cotgreave I.A. (2003) Visualization of the compartmentalization of glutathione and protein-glutathione mixed disulfides in cultured cells. *The FASEB Journal* 17, 124-6.

Solcan N., Kwok J., Fowler P.W., Cameron A.D., Drew D., Iwata S. & Newstead S. (2012) Alternating access mechanism in the POT family of oligopeptide transporters. *The EMBO journal* 31, 3411-21.

Sonnhammer E.L., von Heijne G. & Krogh A. (1998) A hidden Markov model for predicting transmembrane helices in protein sequences. *Proc Int Conf Intell Syst Mol Biol* 6, 175-82.

Srikanth C.V., Vats P., Bourbouloux A., Delrot S. & Bachhawat A.K. (2005) Multiple cis-regulatory elements and the yeast sulphur regulatory network are required for the regulation of the yeast glutathione transporter, Hgt1p. *Curr Genet* 47, 345-58.

Srinivasan V., Pierik A.J. & Lill R. (2014) Crystal structures of nucleotide-free and glutathione-bound mitochondrial ABC transporter Atm1. *Science* 343, 1137-40.

Stephen D.W. & Jamieson D.J. (1996) Glutathione is an important antioxidant molecule in the yeast Saccharomyces cerevisiae. *FEMS microbiology letters* 141, 207-12.

Sugiyama k.-i., Kawamura A., Izawa S. & Inoue Y. (2000) Role of glutathione in heat-shock-induced cell death of Saccharomyces cerevisiae. *Biochemical Journal* 352, 71-8.

Suzuki H., Koyanagi T., Izuka S., Onishi A. & Kumagai H. (2005) The yliA, -B, -C, and -D genes of Escherichia coli K-12 encode a novel glutathione importer with an ATP-binding cassette. *J Bacteriol* 187, 5861-7.

Szczypka M.S., Wemmie J.A., Moye-Rowley W.S. & Thiele D.J. (1994) A yeast metal resistance protein similar to human cystic fibrosis transmembrane conductance regulator (CFTR) and multidrug resistance-associated protein. *Journal of Biological Chemistry* 269, 22853-7.

Sze H., Li X. & Palmgren M.G. (1999) Energization of plant cell membranes by H+-pumping ATPases: regulation and biosynthesis. *The Plant Cell* 11, 677-89.

Tamura A., Watanabe M., Saito H., Nakagawa H., Kamachi T., Okura I. & Ishikawa T. (2006) Functional validation of the genetic polymorphisms of human ATP-binding cassette (ABC) transporter ABCG2: identification of alleles that are defective in porphyrin transport. *Molecular pharmacology* 70, 287-96.

Tanford C. (1982) Simple model for the chemical potential change of a transported ion in active transport. *Proceedings of the National Academy of Sciences* 79, 2882-4.

Thakur A. & Bachhawat A.K. (2010) The role of transmembrane domain 9 in substrate recognition by the fungal high-affinity glutathione transporters. *Biochem J* 429, 593-602.

Thakur A. & Bachhawat A.K. (2013) Mutations in the N-terminal region of the Schizosaccharomyces pombe glutathione transporter pgt1+ allows functional expression in Saccharomyces cerevisiae. *Yeast* 30, 45-54.

Thakur A., Kaur J. & Bachhawat A.K. (2008) Pgt1, a glutathione transporter from the fission yeast Schizosaccharomyces pombe. *FEMS Yeast Res* 8, 916-29.

Thomas E.L. (1984) Disulfide reduction and sulfhydryl uptake by Streptococcus mutans. *J Bacteriol* 157, 240-6.

Tsirigos K.D., Peters C., Shu N., Kall L. & Elofsson A. (2015) The TOPCONS web server for consensus prediction of membrane protein topology and signal peptides. *Nucleic Acids Res* 43, W401-7.

Tusnady G.E. & Simon I. (2001a) The HMMTOP transmembrane topology prediction server. *Bioinformatics* 17, 849-50.

Tusnady G.E. & Simon I. (2001b) The HMMTOP transmembrane topology prediction server. *Bioinformatics* 17, 849-50.

Unal E.S., Zhao R. & Goldman I.D. (2009) Role of the glutamate 185 residue in proton translocation mediated by the proton-coupled folate transporter SLC46A1. *American Journal of Physiology-Cell Physiology* 297, C66-C74.

van Aubel R.A., Smeets P.H., Peters J.G., Bindels R.J. & Russel F.G. (2002) The MRP4/ABCC4 gene encodes a novel apical organic anion transporter in human kidney proximal tubules: putative efflux pump for urinary cAMP and cGMP. *Journal of the American Society of Nephrology* 13, 595-603.

Vasconcelos M.W., Li G.W., Lubkowitz M.A. & Grusak M.A. (2008) Characterization of the PT Clade of Oligopeptide Transporters in Rice. *The Plant Genome* 1, 77-88.

Vergauwen B., Elegheert J., Dansercoer A., Devreese B. & Savvides S.N. (2010) Glutathione import in Haemophilus influenzae Rd is primed by the periplasmic heme-binding protein HbpA. *Proc Natl Acad Sci U S A* 107, 13270-5.

Vergauwen B., Verstraete K., Senadheera D.B., Dansercoer A., Cvitkovitch D.G., Guédon E. & Savvides S.N. (2013) Molecular and structural basis of glutathione import in Gram-positive bacteria via GshT and the cystine ABC importer TcyBC of Streptococcus mutans. *Mol Microbiol* 89, 288-303.

Viklund H. & Elofsson A. (2004) Best alpha-helical transmembrane protein topology predictions are achieved using hidden Markov models and evolutionary information. *Protein Sci* 13, 1908-17.

Viklund H. & Elofsson A. (2008) OCTOPUS: improving topology prediction by two-track ANN-based preference scores and an extended topological grammar. *Bioinformatics* 24, 1662-8.

Vilsen B., Andersen J.P., Clarke D.M. & MacLennan D.H. (1989) Functional consequences of proline mutations in the cytoplasmic and transmembrane sectors of the Ca2(+)-ATPase of sarcoplasmic reticulum. *J Biol Chem* 264, 21024-30.

Vivancos P.D., Dong Y., Ziegler K., Markovic J., Pallardó F.V., Pellny T.K., Verrier P.J. & Foyer C.H. (2010) Recruitment of glutathione into the nucleus during cell proliferation adjusts whole-cell redox homeostasis in Arabidopsis thaliana and lowers the oxidative defence shield. *The Plant Journal* 64, 825-38.

von Heijne G. (1992) Membrane protein structure prediction. Hydrophobicity analysis and the positive-inside rule. *J Mol Biol* 225, 487-94.

Wachter A., Wolf S., Steininger H., Bogs J. & Rausch T. (2005) Differential targeting of GSH1 and GSH2 is achieved by multiple transcription initiation: implications for the compartmentation of glutathione biosynthesis in the Brassicaceae. *The Plant Journal* 41, 15-30.

Wang T., Lu W., Lu S. & Kong J. (2015) Protective role of glutathione against oxidative stress in Streptococcus thermophilus. *International Dairy Journal* 45, 41-7.

Wanke D. & Üner Kolukisaoglu H. (2010) An update on the ABCC transporter family in plants: many genes, many proteins, but how many functions? *Plant Biology* 12, 15-25.

Wemmie J.A. & Moye-Rowley W.S. (1997) Mutational analysis of the Saccharomyces cerevisiae ATP-binding cassette transporter protein Ycf1p. *Mol Microbiol* 25, 683-94.

Wielinga P.R., van der Heijden I., Reid G., Beijnen J.H., Wijnholds J. & Borst P. (2003) Characterization of the MRP4-and MRP5-mediated transport of cyclic nucleotides from intact cells. *Journal of Biological Chemistry* 278, 17664-71.

Wijnholds J., Mol C.A., van Deemter L., de Haas M., Scheffer G.L., Baas F., Beijnen J.H., Scheper R.J., Hatse S. & De Clercq E. (2000) Multidrug-resistance protein 5 is a multispecific organic anion transporter able to transport nucleotide analogs. *Proceedings of the National Academy of Sciences* 97, 7476-81.

Wiles A.M., Cai H., Naider F. & Becker J.M. (2006a) Nutrient regulation of oligopeptide transport in Saccharomyces cerevisiae. *Microbiology* 152, 3133-45.

Wiles A.M., Naider F. & Becker J.M. (2006b) Transmembrane domain prediction and consensus sequence identification of the oligopeptide transport family. *Res Microbiol* 157, 395-406.

Williams K.A. & Deber C.M. (1991) Proline residues in transmembrane helices: structural or dynamic role? *Biochemistry* 30, 8919-23.

Winther J.R. & Jakob U. (2013) Redox control: a black hole for oxidized glutathione. *Nature chemical biology* 9, 69-70.

Wintz H., Fox T., Wu Y.Y., Feng V., Chen W., Chang H.S., Zhu T. & Vulpe C. (2003) Expression profiles of Arabidopsis thaliana in mineral deficiencies reveal novel transporters involved in metal homeostasis. *J Biol Chem* 278, 47644-53.

Wisedchaisri G., Park M.-S., Iadanza M.G., Zheng H. & Gonen T. (2014) Proton-coupled sugar transport in the prototypical major facilitator superfamily protein XylE. *Nature communications* 5.

Wu A.L. & Moye-Rowley W.S. (1994) GSH1, which encodes gamma-glutamylcysteine synthetase, is a target gene for yAP-1 transcriptional regulation. *Mol Cell Biol* 14, 5832-9.

Wu G., Fang Y.-Z., Yang S., Lupton J.R. & Turner N.D. (2004) Glutathione metabolism and its implications for health. *The Journal of nutrition* 134, 489-92.

Xiang C. & Oliver D.J. (1998) Glutathione metabolic genes coordinately respond to heavy metals and jasmonic acid in Arabidopsis. *The Plant Cell* 10, 1539-50.

Xu J., Liu Y., Yang Y., Bates S. & Zhang J.-T. (2004) Characterization of oligomeric human half-ABC transporter ATP-binding cassette G2. *Journal of Biological Chemistry* 279, 19781-9.

Yachdav G., Kloppmann E., Kajan L., Hecht M., Goldberg T., Hamp T., Honigschmid P., Schafferhans A., Roos M., Bernhofer M., Richter L., Ashkenazy H., Punta M., Schlessinger A., Bromberg Y., Schneider R., Vriend G., Sander C., Ben-Tal N. & Rost B. (2014) PredictProtein--an open resource for online prediction of protein structural and functional features. *Nucleic Acids Res* 42, W337-43.

Yadav A.K., Desai P.R., Rai M.N., Kaur R., Ganesan K. & Bachhawat A.K. (2011) Glutathione biosynthesis in the yeast pathogens Candida glabrata and Candida albicans: essential in C. glabrata, and essential for virulence in C. albicans. *Microbiology* 157, 484-95.

Yadav S. (2014) A Mutational Study Of The Transmembrane Domains Of The Yeast Glutathione Transporter, Hgt1p Of Saccharomyces cerevisiae. In: *Department of*

Biological Sciences, p. MS dissertation thesis Indian Institute of Science Education and Research (IISER), Mohali.

Yamauchi S., Obara K., Uchibori K., Kamimura A., Azumi K. & Kihara A. (2015) Opt2 mediates the exposure of phospholipids during cellular adaptation to altered lipid asymmetry. *J Cell Sci* 128, 61-9.

Yan H., Huang W., Yan C., Gong X., Jiang S., Zhao Y., Wang J. & Shi Y. (2013) Structure and mechanism of a nitrate transporter. *Cell reports* 3, 716-23.

Yan N. (2013) Structural advances for the major facilitator superfamily (MFS) transporters. *Trends in biochemical sciences* 38, 151-9.

Yan N. (2015) Structural biology of the major facilitator superfamily transporters. *Annual review of biophysics* 44, 257-83.

Yarov-Yarovoy V., Schonbrun J. & Baker D. (2006) Multipass membrane protein structure prediction using Rosetta. *Proteins* 62, 1010-25.

Yen M.R., Tseng Y.H. & Saier M.H., Jr. (2001) Maize Yellow Stripe1, an iron-phytosiderophore uptake transporter, is a member of the oligopeptide transporter (OPT) family. *Microbiology* 147, 2881-3.

Yerushalmi H. & Schuldiner S. (2000) A common binding site for substrates and protons in EmrE, an ion-coupled multidrug transporter. *FEBS letters* 476, 93-7.

Zaman G., Lankelma J., vAN Tellingen O., Beijnen J., Dekker H., Paulusma C., Elferink R.O., Baas F. & Borst P. (1995) Role of glutathione in the export of compounds from cells by the multidrug-resistance-associated protein. *Proceedings of the National Academy of Sciences* 92, 7690-4.

Zelcer N., Huisman M.T., Reid G., Wielinga P., Breedveld P., Kuil A., Knipscheer P., Schellens J.H., Schinkel A.H. & Borst P. (2003) Evidence for two interacting ligand binding sites in human multidrug resistance protein 2 (ATP binding cassette C2). *Journal of Biological Chemistry* 278, 23538-44.

Zhai Y. & Saier Jr M.H. (2001) A web-based program for the prediction of average hydropathy, average amphipathicity and average similarity of multiply aligned homologous proteins. *Journal of molecular microbiology and biotechnology* 3, 285-6.

Zhai Y. & Saier M. (2001) A web-based program (WHAT) for the simultaneous prediction of hydropathy, amphipathicity, secondary structure and transmembrane topology for a single protein sequence. *Journal of molecular microbiology and biotechnology* 3, 501-2.

Zhang M.-Y., Bourbouloux A., Cagnac O., Srikanth C.V., Rentsch D., Bachhawat A.K. & Delrot S. (2004) A novel family of transporters mediating the transport of glutathione derivatives in plants. *Plant Physiology* 134, 482-91.

Zhang Z., Xie Q., Jobe T.O., Kau A.R., Wang C., Li Y., Qiu B., Wang Q., Mendoza-Cózatl D.G. & Schroeder J.I. (2016) Identification of AtOPT4 as a Plant Glutathione Transporter. *Mol Plant* 9, 481-4.

Zhong Q., Putt D.A., Xu F. & Lash L.H. (2008) Hepatic mitochondrial transport of glutathione: studies in isolated rat liver mitochondria and H4IIE rat hepatoma cells. *Archives of biochemistry and biophysics* 474, 119-27.